RESEARCH NEEDS RELATED TO THE PRE-APPLICATION ACTIVITIES OF IRIS

M. D. Carelli, S. E. Ritterbusch, C. B. Brinkman
Westinghouse Electric Co.

ABSTRACT

This paper focuses on the immediate research needs for pursuing the licensing pre-application for IRIS, an integral modular reactor with output capability up to 300 MWe. After a brief introduction of the IRIS program, a review is provided of the safety-by-design and the maintenance application approaches - since they have a direct bearing on the pre-licensing activities. A brief background on risk-informed regulation is provided since IRIS will be licensed using a risk-informed approach. Discussed in detail are the two immediate licensing research needs:
1. Out-of-pile scaled models testing to prove the predicted performance of IRIS innovative engineering
2. Application and implementation of risk-informed regulation in the IRIS licensing process
Also discussed is the IRIS goal of eventually demonstrating that there is no need for off-site emergency response actions, thanks to the superb safety characteristics of the IRIS design which are backed by experimental verification and risk-informed evaluation.

1. INTRODUCTION

IRIS (International Reactor Innovative and Secure) is a new generation advanced light water reactor which addresses the Generation IV objectives (enhanced safety, non-proliferation, improved economics, waste minimization) on an accelerated schedule. It is being developed by an international consortium led by Westinghouse and comprising over 20 organizations from nine countries (see Table I). The conceptual design (see Ref 1 for a detailed summary of the conceptual design activities) was completed and the project is now proceeding with the preliminary design phase, to be completed by the end of 2002. The projected schedule calls for starting construction of the IRIS First-Of-A-Kind plant by 2009, with deployment by 2012. The licensing process will start with a limited pre-application in 2002, progressing to SAR submittal by 2006 with the ultimate goal of obtaining design certification by 2008.

IRIS does not require new technology development since it is grounded on well-proven LWR technology. It is, however, a new design with novel engineering solutions (see Refs 1-7 for details). IRIS has an integral configuration (see Fig. 1) where all primary system components (pumps, steam generator, pressurizer) are enclosed within the reactor vessel. Also, internal shields positioned between the core and the vessel reduce the radiation field at the vessel outer surface to practically zero. Other major innovative characteristics of IRIS are: straight-burn long-life (4 to 5 years) core with no fuel shuffling or partial refueling; at least 48 months interval for maintenance shutdowns (which coupled with the long-life core gives very high capacity factors and reduced Operation and Maintenance (O&M) costs; and safety-by-design approach where certain major basis accidents are physically eliminated by design or, at least, their probability of occurring is substantially lessened and consequences are reduced.

Table I
IRIS Consortium Membership

Industry (7+2)		Universities (6)	
Westinghouse	(USA)	Polytechnic of Milano	(Italy)
BNFL	(UK)	U. California Berkeley	(USA)
MHI	(Japan)	MIT	(USA)
Bechtel	(USA)	Tokyo Institute of Technology	(Japan)
Ansaldo	(Italy)	University of Pisa	(Italy)
NUCLEP	(Brazil)	University of Zagreb	(Croatia)
ENSA	(Spain)		
* Washington Group	(USA)		
* OKBM (Experimental Design Bureau of Machine Building)	(Russia)		

Utilities (1+2)		R & D (3)	
JAPC	(Japan)	National Institute Nuclear Studies	(Mexico)
* TVA	(USA)	CNEN, Nuclear Energy Commission	(Brazil)
* Eletronuclear	(Brazil)	Oak Ridge National Laboratory	(USA)

+ Associates (5)

University of Tennessee	(USA)
Ohio State University	(USA)
Iowa State University	(USA)
University of Michigan	(USA)
Ames Laboratory	(USA)

* Membership pending.
+ Associates cooperate in specific parts of the IRIS project, but are not full consortium members.

The straight-burn long-life core is implemented to partially satisfy Generation IV non-proliferation objectives, by minimizing fuel handling and storage. It does not present any outstanding licensing issues, since the fuel enrichment is 4.95%, within current fabrication capabilities, and the projected average burnup is of the order of 40,000 MWd/MtU, also well within the current data base.

The extended maintenance and the safety-by-design approaches have licensing implications and are briefly discussed next. Also, briefly discussed will be risk-informed regulation, since IRIS will be licensed using a risk-informed approach.

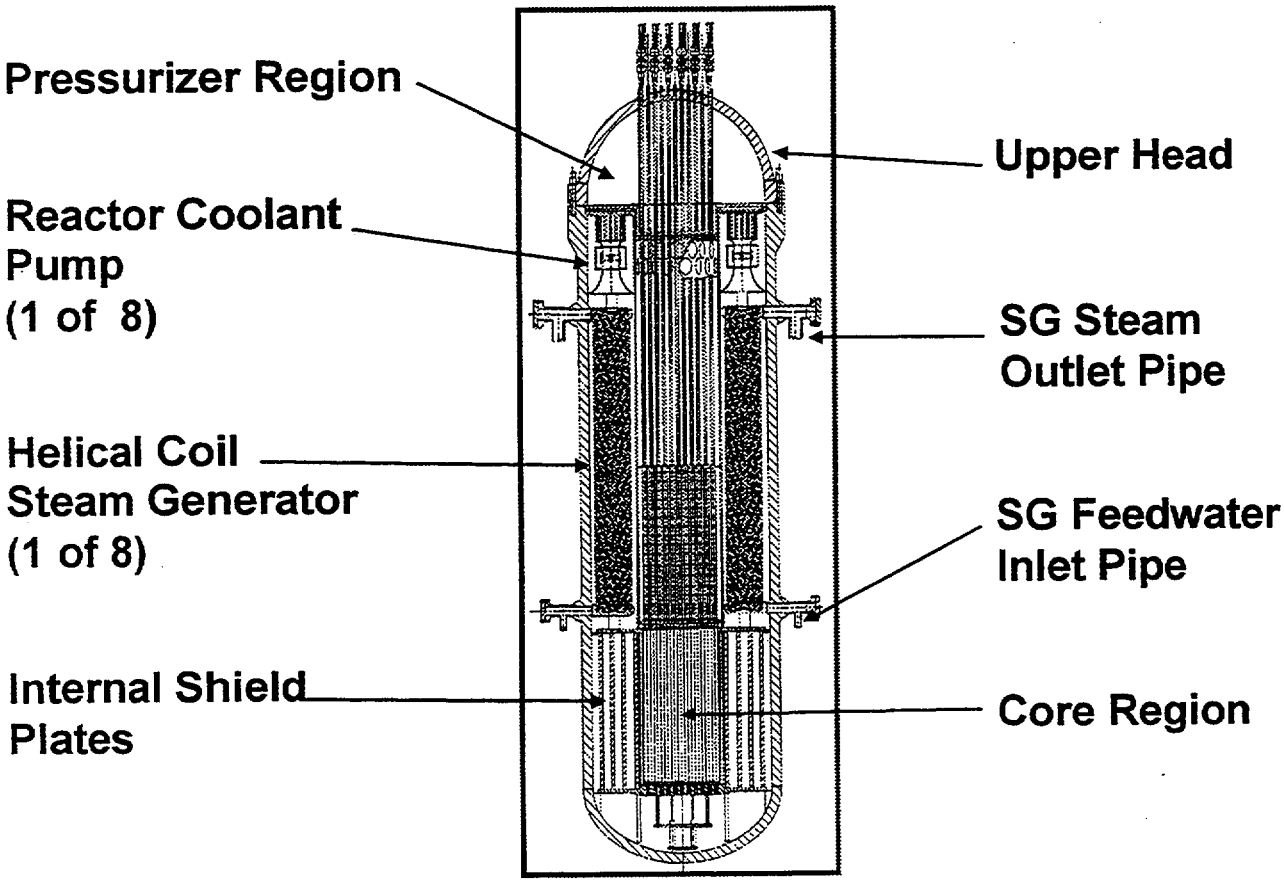

Figure 1 IRIS Integral Primary System Configuration

2. IRIS DESIGN CHARACTERISTICS DIRECTLY IMPACTING LICENSING

2.1 Optimized Maintenance

Both non-proliferation and economic Generation IV objectives suggest an optimized maintenance approach with extended intervals between shutdowns, the logical complement of the long core life. From the non-proliferation standpoint, it minimizes access to the reactor and reactor fuel. From the economic standpoint, it allows uninterrupted power generation for extended periods of time, yielding capacity factors in the high 90's and substantially reduced O & M costs.

An early study (Ref 8) completed by IRIS team member MIT in 1996 investigated what was necessary to extend the maintenance interval in LWRs from the current 18-month to a 48-month cycle. A total of 3743 maintenance items (on-line and off-line) were identified. They were examined as candidates for deferral to 48 months or for being performed on-line. Six hundred twenty-five items were recategorized from off-line to on-line, and eventually only 54 maintenance items were left unresolved. Building on the results of this study, MIT further examined (Ref 9) whether the LWR unresolved maintenance items did really apply to IRIS or could be dispensed by the difference in design; for example, items like pump oil lubrication do not apply to the IRIS internal, water-lubricated spool pumps. Only 7 maintenance items were identified as still needing resolution for attaining the 48 months intervals in IRIS and they are presently being addressed by the appropriate consortium members. From the licensing standpoint, it will be necessary to review the maintenance related regulations and determine whether they are actually applicable to the IRIS design and its 48 months extended maintenance approach.

2.2 Safety-by-Design

The IRIS safety philosophy exploits to the fullest what is offered by its design characteristics (chiefly, integral configuration and long-life core) to:

- physically eliminate the possibility for some accident(s) to occur;
- decrease the possibility of occurrence of most of the remaining scenarios; and
- lessen the consequences if an accident actually occurs.

The safety-by-design approach is not new; it is good engineering practice, which is the goal of all reactor designers. However, the case for IRIS is quite different because the integral configuration, if properly exploited, allows the implementation of the safety-by-design approach to an extent which is not possible in traditional loop LWRs. The most obvious implication is that large loss-of-coolant accidents (LOCAs) cannot occur since there are no primary system components outside the reactor vessel. Large LOCAs are, however, only the most obvious example. Other accident scenarios such as loss-of-flow accidents (LOFAs), steam and feed line breaks, steam generator tube ruptures, and losses of off-site power can be eliminated or downgraded. Table II reports how the safety-by-design is implemented in IRIS (for a more detailed discussion see Refs 1, 3 and 6). The result, as shown in Table III, is that out of those Class IV accidents typically considered for a PWR, 7 can be eliminated or reclassified to Class III or lower, and the only one remaining (refueling accident) is at a significantly lower probability.

Table II
Implementation of IRIS Safety by Design

Design Characteristic	Safety Implication	Related Accident	Disposition
Integral reactor configuration	No external loop piping	Large LOCAs	Eliminated
Tall vessel with elevated steam generators	Can accommodate internal control rod drives	Reactivity insertion due to control rod ejection	Can be eliminated
	High degree of natural circulation	Loss-of-all-flow events (e.g. loss of offsite power)	High partial natural circulation mitigates consequences/reduces required pump inertia
Low pressure drop flow path and multiple RCPs	Core flow remains above DNB limit with sudden loss of one pump	LOFAs (e.g., pump seizure or shaft break)	Reduced consequences - no core damage occurs
Large water inventory inside vessel	Slows transient evolution helps to keep core covered	Small-medium LOCAs	Core remains covered even with no safety injection assumed
Reduced size, higher pressure containment	Reduced driving force through primary opening		
Inside the vessel heat removal			
High pressure steam generator system	Primary system cannot over-pressure secondary system	SGTR	Reduced consequences – accident terminated quickly by simple automatic isolation
	No SG safety valves required	Steam and feed line breaks	Reduced probability and reduced consequences
Once through SG design	Low water inventory		
Long life core	No partial refueling	Refueling accidents	Reduced probability

Table III
Typical PWR Class IV Accidents and Their Resolution in IRIS Design

	Accident	IRIS Safety by Design	IRIS Resolution
1.	Steam system piping failure (major)	Reduced probability Reduced consequences	Can be reclassified as Class III
2.	Feedwater system pipe break		
3.	Reactor coolant pump shaft seizure or locked rotor	Minimal consequences	Eliminated as safety concern
4.	Reactor coolant pump shaft break		
5.	Spectrum of RCCA ejection accidents	Can be eliminated	Not applicable (with internal CRDMs)
6.	Steam generator tube rupture	Reduced consequences	Can be reclassified as Class III
7.	Large LOCAs	Eliminated	Not applicable
8.	Design basis fuel handling accidents	Reduced probability	Still Class IV, but significantly lower probability

A unique IRIS feature is the thermohydraulic coupling of the vessel with a small spherical containment. Besides fulfilling the usual containment functions, the IRIS containment, in concert with the integral vessel, practically eliminates small and medium LOCAs as a safety concern. The underlying principle is quite simple: during an accident, the pressure differential across the break decreases quickly and becomes very close to zero, thus choking the egress flow. This is possible because the vessel pressure decreases due to the internal heat removal by the steam generators, while the containment pressure is higher than in traditional LWR containments. In fact, other parameters being equal, the IRIS containment can sustain a peak pressure 4 times the value of LWR containments (factor of 2 due to spherical vs. cylindrical; an additional factor of 2 because the diameter of the IRIS containment is half that of a typical LWR).

Consequently the core remains covered for an extended period of time (several days and possibly weeks, depending on the heat removal rate on the containment surface) without any emergency water injection or core makeup (see Fig. 2). Therefore, IRIS requires no Emergency Core Cooling System (ECCS). There are, however, suppression pools for limiting the containment peak pressure, which can also double as core makeup in a unforeseen emergency. IRIS has four (three independent) decay heat removal systems: steam generators, natural circulation driven heat exchangers located outside the containment, air and water heat removal from the containment surface.

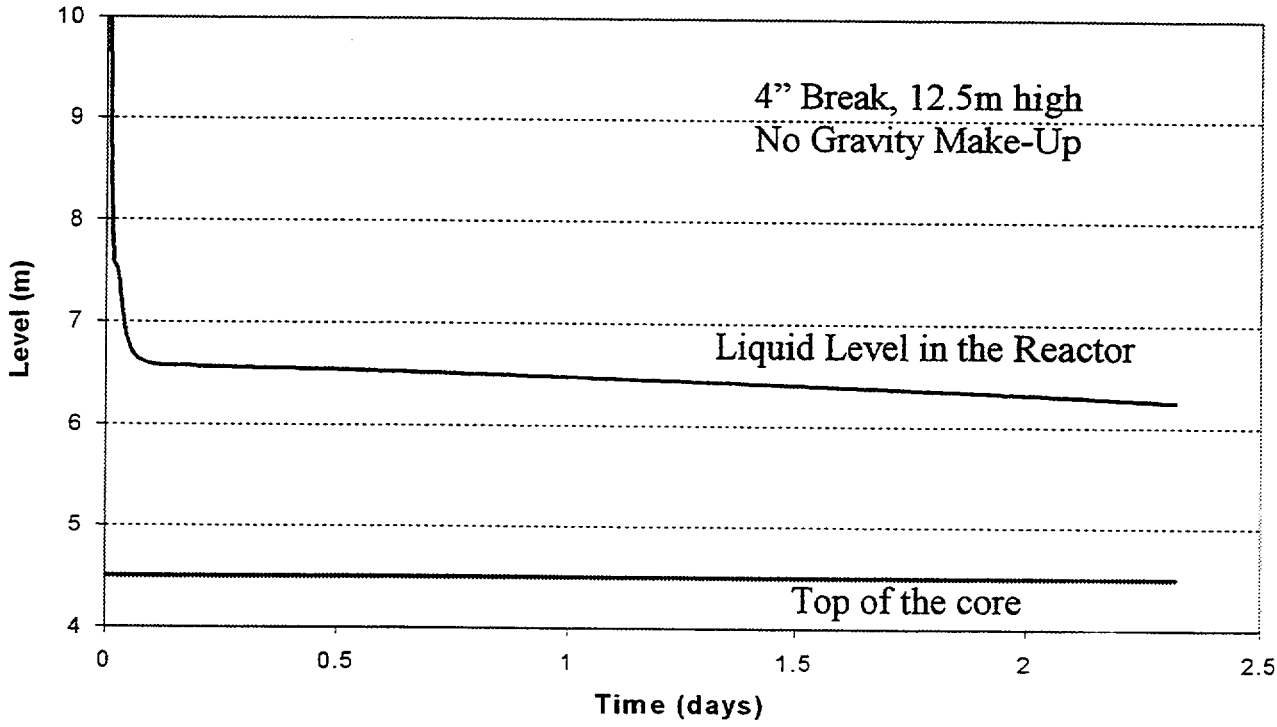

Figure 2 The IRIS core still remains under 2 meters of water after 2 days in the worst small-to-medium LOCA Accident

In terms of licensing, many traditional LWR accident sequences, starting with LOCAs, are not credible in the IRIS design. Thus, existing regulatory requirements written for traditional LWRs need to be reviewed for their applicability to IRIS. A substantial streamlining of regulatory requirements is expected, once it is accepted by the NRC that IRIS has, indeed, a lower number of possible accident sequences. On the other hand, because of novel engineering features, extensive testing will be performed; this will be discussed in detail in Section 3.1.

2.3 Risk-Informed Design and Regulation

While risk-informed regulation is not new to the nuclear industry, the manner in which it will be implemented for the IRIS project is significantly different from current practice. IRIS will adopt the new "risk-informed design and regulatory process" being developed under a DOE Nuclear Energy Research Initiative (NERI) project, reported elsewhere in this conference (Ref 10). The elements of the historic design and regulatory process are used also in the new risk-informed process, but they are implemented in the context of a Probabilistic Risk Assessment (PRA) as an over-arching integrated evaluation method. It is important to note that this method is applied to both the design and regulatory functions. In the new risk-informed process, the designer develops a design using risk-informed methods. Then the design is submitted for regulatory review, during which regulatory issues are resolved and some changes to the design may be made. While some basic design and safety criteria may be established at the beginning of the process in a risk-informed licensing process, most of the detailed design and regulatory criteria would be established during the actual design and regulatory review work.

In our new risk-informed process, all significant design features and deterministic analysis results are reflected in the PRA. This means that the designer must learn to iterate between deterministic design and evaluation tasks and PRA evaluations early in the design process. This requires that probabilistic design criteria be established and that many previously deterministic decisions must now be made only after considering and incorporating the PRA results. Any design margin and subjective judgments made by the designer must be incorporated into the PRA, and corresponding design and safety decisions made consistent with the PRA result (i.e., a design or operational requirement would not be adopted unless an appropriate degree of benefit were demonstrated by the PRA).

When the designer is satisfied with the design at each stage of development (preliminary, detailed, final), the design documentation is submitted to the regulator for regulatory input and safety review. One of the more difficult aspects of the new design and regulatory process will be the stating of regulatory issues in terms of the PRA, rather than in terms of prescriptive review guidance such as the current Standard Review Plan (NUREG-0800). The stating of regulatory issues in the context of the PRA includes not only proposed regulatory acceptance criteria, but also the regulator's desire for increased design margin and defense-in-depth.

DOE's current NERI project on risk-informed design and regulation (Ref 10) has demonstrated the feasibility of implementing the new process for the design of a new nuclear reactor. As reported in Reference 10, the new risk-informed approach has been applied to both LWR and gas reactor examples. Importantly, it has been shown that it is feasible to address regulatory issues and conduct safety negotiations using the new methods. Notwithstanding the progress to-date, much work remains to be done. The three main areas of needed research are: (1) development of methods for handling all types of uncertainties that would be incurred in a new design especially those previously addressed by the inclusion of deterministic design margin and subjective judgments; (2) development of probabilistic design criteria and the means for selecting probabilistic regulatory criteria; and (3) development of

procedures for conducting the regulatory negotiation, including appeals procedures in the event closure cannot be reached using the new risk-informed process.

The best way to conduct this research is to apply the new process to a "real" design and licensing project, with emphasis on identification and development of procedures that can be applied generically. A real project, such as IRIS, has the advantage of unique design features and safety issues that will force designers and regulators alike to face new issues and resolve them using the new proposed methods. In other words, using the new process on a new design will make it less likely that the designers and regulators will fall back to previous experience simply for the purpose of expediency.

3. RESEARCH NEEDS

Aside from the previously mentioned streamlining of existing regulations due to the extended maintenance period and the elimination of accident scenarios, the two most immediate research needs for IRIS are out-of-pile testing and application of risk-informed regulation, as will be discussed in the following sections.

3.1 Out-of-pile Testing

It is the position of the IRIS project that a prototype plant is not needed to obtain design certification. But, extensive out-of-pile testing will be performed for pre-certification and during safety analysis report (SAR) preparation. It is the intention of the IRIS project to test the significant differences from loop PWRs; this will include both the individual components as well as their integral behavior. These tests will be conducted on properly scaled models; therefore, the first activity will be a rigorous similitude analysis. Past experience has amply proved that time and money spent on achieving proper similitude and test planning have a many-fold return on hardware, testing and redesign savings.

Key individual components to be tested are the internal helical steam generators and the internal "spool" pumps. Both individual performance and interactive effects (e.g., flow effects due to positioning of the pumps on top of the steam generators) will be investigated. Scaled mockups in thermal-hydraulic similitude will be used. Since water is the coolant in both model and prototype (same Prandtl number), thermal similitude is not a major concern; thus modeling can be focused on hydraulic and structural (vibrational) similitude. Testing of the steam generator's characteristics has already been performed by IRIS team member Ansaldo on a 20 MWt scaled mockup in the early 90s (Ansaldo had developed the helical steam generator for their ISIS reactor design, which is in many aspects a precursor of IRIS). Similarly, prospective team member Washington Group has already conducted tests of the spool pumps.

The other major class of tests includes a set of transients to confirm the safety analyses results. In this context, interaction effects such as the thermal-hydraulic coupling of vessel and containment are of primary importance. This will require demonstrating temporal as well as thermal-hydraulic similitude. It will be impossible to simulate the entire transient behavior in any scaled model, short of a full scale mock-up. One possible approach is to "segment" the transient and simulate, with proper boundary conditions, only selected portions of the overall transient. Different models will be needed for the various portions in order to properly reproduce boundary conditions and transient behavior. But first, analyses will be needed to confirm the adequacy of this approach in satisfactorily reproducing the transient behavior and its economic advantage over a full-scale mock-up in the event that several different models are required.

The availability of suitable testing facilities is critical to the success of the IRIS pre-certification application project. Many of the IRIS team members have specific test facilities that could be utilized for separate-effects and integral-effects testing. For example, prospective team member OKBM was the main designer of integral PWRs for the Russian submarine Navy. At the end of the 1980s, OKBM had developed a land-based version for commercial operation. Not only is OKBM the only organization in the world with experience in designing and building IRIS type reactors, but it also has an experimental facility where integral effects can be examined.

3.2 Implementation of Risk-informed Regulations

Implementation of the new risk-informed design and regulatory process will require that new PRA models be developed to reflect unique IRIS design and safety features such as the interaction between the reactor vessel and containment during a small-to-medium LOCA. As in the current PRA method, the success paths are established based on deterministic analyses. However, the event sequences controlling the design are based on the PRA results, not on "arbitrary" past experience. While this process may produce enough information to allow the establishment of design basis events for other new reactors of a very similar design, the use of a specific set of deterministic design basis events (as currently done for "Chapter 15" safety analyses) is not envisioned as a required part of the new risk-informed design and regulatory process.

The extensive testing campaign to be conducted for IRIS as discussed in Section 3.1 will provide the IRIS specific data base necessary to quantitatively support the risk-informed methodology. Additionally, where applicable, IRIS will draw upon the extensive data base from existing LWRs. In the IRIS project, we will have to reflect the "safety-by-design" features, performance testing, and uncertainties in the PRA and make corresponding design decisions. This means that design features may have to be added to meet the safety and operational criteria. This use of the PRA as an over-arching evaluation and decision-making tool also means that design features would not be adopted, if they do not produce a significant benefit to plant safety or performance. As the IRIS project proceeds, it will provide a level of design detail appropriate for the particular design stage. That is, in the early stages of design, less design detail is available, but less is needed since the designers and regulators would emphasize only the major design features and regulatory issues. When these major features and issues are resolved, more design detail would be developed and a more detailed level of regulatory issues can be addressed. In this multiple-stage process, detailed regulatory criteria cannot be imposed prematurely (assuming that the designers and regulators are rigorously following the new risk-informed process) because the corresponding level of design detail is not available.

While much work remains to be done, expectations are that implementation of risk-informed methods will provide an integrated method for evaluating the design and resolving regulatory issues, without reverting to arbitrary judgments, which have a significant impact on the viability of the design. For example, a very detailed evaluation of offsite release sequences (both their frequency and magnitude) is expected to provide an impartial evaluation of the necessity for offsite emergency planning. Consistent with one of DOE's objectives for Generation IV reactors, our early judgment is that it may be demonstrated for IRIS that offsite emergency planning in not required.

This judgment is based on the fact that, to start with, the safety-by-design approach that exploits the integral configuration characteristics provides a very strong, deterministic, starting basis. As shown in Section 2.2, almost all sequences leading to Class IV accident scenarios in loop PWRs are no longer applicable in IRIS. On the other hand, application of risk-informed methodology to the System 80+

design indicated (Ref 10) that the probability of the considered accident sequence can be substantially reduced, even by a decade with respect to "traditional" evaluations. Thus, when risk-informed regulation is applied to the significantly more benign IRIS accident scenarios, it might be expected to demonstrate a reduction in the overall release probability sufficient to show that there is no need for off-site emergency response.

The newness of the IRIS design also provides a good opportunity to develop generic methods for other new nuclear plant designs (Generation IV) based on a reasonable combination of experience (proven LWR) and new challenges (e.g., development of probabilistic safety criteria, addressing the issue of no required emergency planning). It is believed that the implementation of risk-informed research for IRIS and the interactions with the NRC on the development and implementation on new methods for regulatory negotiations during the IRIS licensing process will allow the industry to establish new risk-informed design and regulatory methods and procedures for Generation IV reactor designs in general.

4. CONCLUSIONS AND FUTURE DEVELOPMENTS

The IRIS design is characterized by superb safety characteristics that will be demonstrated by an extensive testing campaign to confirm the analytical predictions. IRIS will undergo the licensing process under a risk-informed regulatory framework, with the objective of ultimately eliminating the need for off-site emergency response planning.

Pre-licensing activities with the NRC are planned to start in 2002 with a review of the consortium approach to similitude analysis, test planning, and facilities selection. This will be the first scheduled licensing activity, since testing lies on the critical path to design certification. PRA analyses are currently being conducted by a few IRIS team members and their incorporation in the overall risk-informed regulation framework will be the second pre-licensing activity, preliminarily scheduled for the latter part of FY02.

5. REFERENCES

1. Carelli, M. D., L. E. Conway, B. Petrovic, D. V. Paramonov, M. Galvin, N. E. Todreas, C. V. Lombardi, F. Maldari, M. E. Ricotti, L. Cinotti, "IRIS Reactor Conceptual Design", *Global* 2001, Paris, France, September 9-13, 2001

2. Carelli, M. D., D. V. Paramonov, K. Miller, C. V. Lombardi, M. E. Ricotti, N. E. Todreas, E. Greenspan, K. Yamamoto, A Nagano, H. Ninokata, J. Robertson and F. Oriolo, "IRIS Reactor Development," *Proceedings of the 9th International Conference on Nuclear Engineering,* Nice, France, April 8-12, 2001.

3. Conway, L. E., C. V. Lombardi, M. Ricotti and L. Oriani, "Simplified Safety and Containment Systems for the IRIS Reactor," *Proceedings of the 9th International Conference on Nuclear Engineering,* Nice, France, April 8-12, 2001.

4. Oriani, L., C. V. Lombardi, M. E. Ricotti, D. V. Paramonov, M. D. Carelli and L. E. Conway, "Thermal Hydraulic Tradeoffs in the Design of the IRIS Primary Circuit," *Proceedings of the 9th International Conference on Nuclear Engineering,* Nice, France, April 8-12, 2001.

5. Carelli, M. D., B Perovic, D. V. Paramonov, T. Moore, C. V. Lombardi, M. E. Ricotti, E. Greenspan, J. Vujic, N. E. Todreas, M. Galvin, K. Miller, A. Nagano, K. Yamamoto, H. Ninokata, J. Robertson, F. Oriolo, G. Proto, G. Alonso and M. M. Moraes, "IRIS: An Integrated International Approach to Design And Deploy A New Generation Reactor," *IAEA International Seminar on Status and Prospects for Small and Medium Sized Reactors*, Cairo, Egypt, May 27-31, 2001.

6. Carelli, M. D., L. E. Conway, G. L. Fiorini, C. V. Lombardi, M. E. Ricotti, L. Oriani, F. Berra and N. E. Todreas, "Safety by Design: A New Approach to Accident Management in the IRIS Reactor," *IAEA International Seminar on Status and Prospects for Small and Medium sized Reactors*, Cairo, Egypt, May 27-31, 2001.

7. Carelli, M. D., B. Petrovic, H. D. Garkisch, D. V. Paramonov, C. V. Lombardi, L. Oriani, M. E. Ricotti, E. Greenspan and T. Lou (2001), "Trade-Off Studies for Defining the Characteristics of the IRIS Reactor Core", *16th International Conference on Structural Mechanics in Reactor Technology*, Washington, DC, USA, August 12-17, 2001.

8. McHenry, R. S., T. J. Moore, J. H. Maurer, and N. E. Todreas, "Surveillance Strategy for an Extended Operating Cycle in Commercial Nuclear Reactors," *The Fifth International Topical Meeting on Nuclear Thermal Hydraulics, Operations and Safety (Nuthos-5)*, April 1997, Beijing, China.

9. Galvin, M. R. and N. E. Todreas, "Maintenance Cycle Extension in Advanced Light Water Reactor Design," MIT-NSP-TR-004, October 2001.

10. Apostolakis, G. E., M. W. Golay, A. L. Camp, F. A. Duran, D. J. Finnicum, S. E. Ritterbusch, "A New Risk-Informed Design and Regulatory Process," *NRC's Nuclear Safety Research Conference*, October 22-24, 2001, Washington, D.C.

ACKNOWLEDGEMENTS

The financial support of the IRIS program (NERI project 99-0027) and of the risk-informed assessment (NERI project 99-0058) by the US DOE is gratefully acknowledged. Contributions by the IRIS consortium members were invaluable to the progress of the project.

THE PACKAGE PERFORMANCE STUDY: A STUDY OF SPENT FUEL TRANSPORTATION

Andrew J. Murphy and Robert J. Lewis
U.S. Nuclear Regulatory Commission
Washington, D.C. 20555, USA 301-415/6011

Jeremy L. Sprung and Ken Sorenson
Sandia National Laboratories
Albuquerque, NM, 87185, USA 505/844-0134

ABSTRACT

The U.S. Nuclear Regulatory Commission's (NRC's) responsibilities in the transport of spent nuclear fuel include certification of transport packaging designs, approval of transport package Quality Assurance programs, issuance of general licenses authorizing licensees to offer material to carriers for transport, and establishment of physical protection requirements for spent fuel in transit. The Commission has been studying safety in the transport of spent nuclear fuel under its regulations for nearly 25 years. In December 1977, when the Commission adopted the generic environmental impact statement for transportation, it directed that regulatory policy concerning transportation be subject to close and continuing review.

The spent fuel transportation Package Performance Study (PPS) investigates the performance of casks and behavior of fuel when subjected to thermal and impact forces that exceed the hypothetical accident conditions specified in 10 CFR Part 71. Issues related to the probability and consequences of severe transport accidents will be examined. The objective of PPS is to verify models, through combinations of detailed analysis and physical testing, used to predict accident risk associated with transportation of spent fuel in NRC certified casks. PPS is a follow-on project to NUREG/CR-6672, "Reexamination of Spent Fuel Shipment Risk Estimates," which was published in March 2000. An enhanced public participatory process has been used in developing the PPS issues for study and the conceptual testing and analysis plans.

This paper will first review the studies of the safety of the transportation that the NRC has conducted over the last three decades and summarize the results obtained as an introduction to the PPS. Next the paper will outline the objectives and scope of the PPS.

INTRODUCTION

The U.S. Nuclear Regulatory Commission's (NRC's) responsibilities in the transport of spent nuclear fuel include certification of transport packaging designs, approval of transport package Quality Assurance programs, issuance of general licenses authorizing licensees to offer material to carriers for transport, and establishment of physical protection requirements for spent fuel in transit. Pertinent NRC regulations are contained in 10 CFR Part 71, "Packaging and Transportation of Radioactive Material," and in 10 CFR 73.37, "Requirements for Irradiated Reactor Fuel in Transit."

The Commission has been studying safety in the transport of spent nuclear fuel under its regulations for nearly 25 years. In December 1977, when the Commission adopted the generic environmental impact statement for transportation, it directed that regulatory policy concerning transportation be subject to close and continuing review. NRC's studies have shown that the risk of release of radioactive material from transport is low. Moreover, NRC's transportation regulations are based on those developed through consensus at the International Atomic Energy Agency (IAEA), and the experience derived from the shipment of spent fuel by IAEA Member States who have corroborated NRC's safety results.

Nevertheless, public concern over spent fuel shipments is high. As an example, when shipment of less than 10 individual spent fuel rods (less than one assembly) from PECO Energy's Limerick reactor to the General Electric facility in Vallecitos, California, was announced, questions from local government and media representatives about shipment safety and security began to arise, particularly in the San Francisco Bay area. NRC staff held a public meeting during October 1999, in Alameda County, California, to address concerns about the shipment and facility operations at General Electric. Days before the shipment departure, the State of Ohio Turnpike Authority advised the NRC that it was denying access to the shipment, resulting in a last-minute re-routing of the shipment through Maryland and West Virginia. The State of Illinois also expressed concerns about the shipment route. The Limerick shipment contained 10 spent fuel assembly rods, or a little over 20 kg of 2.8 percent enriched uranium. As large-scale shipment campaigns approach, with much greater quantities of spent fuel going from NRC-licensed facilities to storage and disposal facilities, public interest is expected to increase substantially.

OVERVIEW OF PAST STUDIES

The NRC first evaluated the impact on public health and safety resulting from regulated transportation activities in NUREG-0170, "Final Environmental Statement on the Transportation of Radioactive Material by Air and Other Modes" (Vols. I and II, December 1977). NUREG-0170 examined impacts from all licensed material by land, air, and sea transport modes under both incident-free and accident conditions. Spent fuel was one of 25 radioactive materials studied. The report contains an assessment of spent fuel shipment risk using the 1975 level of shipments, and a projection of risks for 1985, based on the assumption of a reprocessing fuel

cycle. Sandia National Laboratories conducted the risk assessment for NRC, and developed the RADTRAN I radioactive material transport risk code, to perform the related dose calculations. NUREG-0170 was issued for public comment; Volume II contains the comments and responses.

Considering the information developed and received, and the safety record associated with the transportation of radioactive material, the Commission determined in 1984 that the regulations then in place were adequate to protect the public against unreasonable risk from the transport of radioactive materials, and that no immediate changes in the regulations were needed to improve safety (46 FR 21619). The U.S. Department of Transportation also relied on NUREG-0170 to assess the impact of radioactive material transportation under its "Hazardous Materials Regulations" (49 CFR Subchapter C, Parts 171-180). However, the Commission concluded that prudence dictated that regulatory policy concerning transportation of radioactive materials be subject to close and continuing review.

In the mid-1980s, several spent fuel shipment campaigns were initiated to return spent fuel from the West Valley facility in western New York to the originating utilities. These campaigns drew considerable public interest, and questions focused on the difficulty in comparing NRC's spent fuel cask accident standards with actual accident conditions. The standards are expressed as a series of hypothetical tests and acceptance criteria that are contained in 10 CFR 71.73. Because the NUREG-0170 spent fuel accident source terms were not derived from response of spent fuel and spent fuel casks to severe accident conditions, NRC sponsored an examination of the response of generic steel-lead-steel truck and rail spent fuel casks to collision and fire accident conditions, using finite element impact and thermal heat transport calculations. This effort, frequently referred to as the "Modal Study," was conducted by Lawrence Livermore National Laboratory ("Shipping Container Response to Severe Highway and Railway Accident Conditions," NUREG/CR-4829, Volumes I and II, February 1987). Probabilities and forces associated with severe transportation accidents were also assessed. Although the Modal Study did not perform dose consequence calculations, comparison of the probabilities and magnitudes of the accident source terms developed for that study to those developed for NUREG-0170 allowed the authors of the Modal Study to conclude that the risks per spent fuel shipment for shipments by both truck and rail were "at least 3 times lower that those documented in NUREG-0170." The NRC staff concluded from the Modal Study that NUREG-0170 clearly bounded spent fuel shipment risks, which reaffirmed the Commission's 1984 decision that there was no need to reconsider the transportation regulations to improve safety.

REEXAMINATION OF SPENT NUCLEAR FUEL RISK ESTIMATES

In 1996, NRC decided to reexamine the risks associated with the shipment of spent fuel by truck and rail. The reexamination was initiated (1) because a significant increase in the number of spent fuel shipments is likely during the next few decades, (2) because these shipments will be made to facilities along routes and in casks not previously examined in risk studies, and (3) because the risks associated with these shipments can be estimated using new data and improved methods of analysis. The report, "Reexamination of Spent Nuclear Fuel Risk Estimates,"

NUREG/CR-6672, May 2000, documents the results of this study performed by Sandia National Laboratories.

The purpose of the reexamination was to assess the characteristics of large-scale spent-fuel shipment campaigns currently anticipated and, using the results of the "Modal Study" and the most recent risk assessment code (RADTRAN 5), to determine whether the original NUREG-0170 risk estimates bounded those for the anticipated shipment campaigns. Like NUREG-0170, this study calculates the risks for spent fuel shipments under both incident-free and accident conditions, but unlike that study, takes into account such factors as the design, enrichment, burn-up, and cooling time of fuel currently anticipated to be shipped in the U.S.; the capacity and designs of newer casks; and current population densities along road and rail routes.

In addition, for the first time in an NRC sponsored transportation risk study, NUREG/CR-6672 explicitly treated variability of RADTRAN 5 input parameters. For the "more important" input parameters (e.g., route lengths, population densities, accident rates, durations of truck stops, and cask surface dose rates), distributions of parameter values were constructed that reflected the likely real-world range and frequency of occurrence of the value of each parameter. Next, 200 sets of parameter values were constructed by sampling these distributions using a structured Monte Carlo sampling technique called Latin Hypercube Sampling (LHS). This procedure generated one set of 200 parameter values for spent fuel transportation by truck and a second set for transportation by rail. Each set included parameter values for 200 representative highway or railway routes that traversed the length and breadth of the continental United States but had no specific origins or destinations. Central (best) estimate values were selected for each of the parameters that have less impact on risk calculations (e.g., breathing rate).

For source term parameters, review of studies of transportation accidents, in particular the Modal Study, allowed representative sets of truck and train accidents and their impact and fire environments to be defined. This analysis developed 19 representative truck accidents and 21 representative train accidents. Severity fraction and release fraction values were estimated for each representative accident. Severity fractions specify the fraction of all possible accidents that are represented by each of the representative accidents. Severity fraction values were estimated by review of the accident event trees, accident speed distributions, and accident fire distributions that were developed for the Modal Study. Because only impact onto a very hard surface can result in the release of radioactive materials during a collision accident, new event tree frequencies of occurrence of route wayside surfaces (e.g., hard rock; concrete, soft rock, and hard soil; soft soil; water) were developed using U.S. Department of Agriculture data [15] and Geographic Information System (GIS) methods [16].

Release fractions were estimated as the product of (a) the fraction of the rods in the cask that are failed by the severe accident, (b) the fraction of each class of radioactive materials (e.g., noble gases, volatiles, particulates) that might escape from a failed spent fuel rod to the cask interior, and (c) the fraction of the amount of each radioactive material released to the cask interior that is expected to escape from the cask to the environment. Rod failure during high speed collision accidents was estimated by scaling rod strains calculated for relatively low speed impacts and

then comparing the scaled rod strains to a strain failure criterion [17]. Heating of the cask by a hot long duration fire to rod burst rupture temperatures was assumed to fail all rods (i.e., those not failed by collision impact). Rod-to-cask release fractions were estimated by review of literature data, especially the experimental results of Lorenz [18, 19, 20]. Cask-to-environment release fractions were based on MELCOR [21] fission product transport calculations [22] that estimated the dependence of these release fractions on the cross-sectional area of the cask leak path through which the release to the environment occurs.

Specifications for generic steel-lead-steel truck and rail casks and for a generic steel-DU-steel truck cask and a generic monolithic steel rail cask were developed from literature data [23]. The response of these generic casks to severe collisions (e.g., seal leak areas) was examined by performing three-dimensional finite element calculations for impacts onto an unyielding surface at various impact speeds. Unyielding surface impact speeds were converted to equivalent impact speeds onto yielding surfaces (e.g., soft rock) by considering the energy that would be absorbed by the yielding surface, increasing the energy of the unyielding surface calculation by that amount, and converting the new total energy to an initial impact speed for a yielding surface. Seal degradation and rod burst rupture temperatures due to heating during fires were estimated from literature data. The durations of engulfing, optically dense fires needed to produce seal leakage and rod burst rupture were estimated by performing one-dimensional heat transport calculations.

The reexamination attempts to provide a best estimate of accident risk, by extending the Modal Study methodology to examine the response of the cask closure mechanism to mechanical and thermal loads. The Reexamination contains the results of two analyses, one based on Modal Study cask response and release information, and another based on newer cask response and release information developed in the Reexamination study. Results using the Modal Study cask information, coupled with the data representative of anticipated shipments, continue to show that accident risk estimates are less than those in NUREG-0170. The best-estimate spent-fuel shipment risks from the reexamination appear to be less than the Modal Study based estimates, by as much as 2 orders of magnitude. This is also much less than the NUREG-0170 estimates. To support NRC's efforts on improving risk communication and public confidence, a plain English summary of the Reexamination Study is being prepared in addition to Sandia's technical report.

PACKAGE PERFORMANCE STUDY

The most recent NRC initiative in the transportation area is the "Package Performance Study." This study should take approximately 5-7 years and was begun in 1999. The objective of the Package Performance Study is to address remaining spent fuel transportation issues from the Modal Study and the Reexamination of Spent Fuel Transportation Risk Estimates, using a public-participation approach to solicit public and stakeholder interests in developing the study's scope and parameters for review. Further, whereas the preceding studies have all been analytical in nature, the Package Performance Study will consider the use of physical testing to address

issues, where appropriate. Risk insights obtained using current analysis techniques, using physical testing, and through interaction with stakeholders and the public, will support NRC's ongoing efforts to assure that its regulatory actions are risk-informed and effective. The staff is using an enhanced public participation process throughout the Package Performance Study, to establish clear expectations and both help design and conduct the study.

Sandia has completed the first phase of the Package Performance Study, which was a scoping study. Two sets of roundtable public meetings, in Maryland and Nevada have already been held on the Package Performance Study. A World Wide Web site, ttp://ttd.sandia.gov/nrc/modal.htm, has been established to facilitate interactions on the project. Ongoing public interactions throughout this project will help ensure that public concerns are effectively identified and understood, and that the study design considers these issues. The product of this scoping phase of the study was an "Issues and Resolutions Option Report," (Issues Report) released by letter report in June 2000. NRC also plans to compile the report and comments received on it for publication as a NUREG-series report.

The Issues Report documented the issues and concerns that were raised at public meetings and by questions and comments submitted to the NRC as a result of those meetings. The report considered five topical areas: (1) package performance during collisions, (2) package performance during fires, (3) spent nuclear fuel behavior during accidents, (4) highway and railway accident conditions and probabilities, and (5) other transportation safety issues. A technical merit score was recommended in the report by the Sandia authors, for each issue and associate resolution options.

With the close of the scooping phase of the Package Performance Study, the confirmatory research phase began in mid-2001. Likely areas on which the study may focus include:

- demonstrating the validity of cask finite element package collision damage predictions by comparison to test results,
- demonstrating the validity of thermal analysis predictions of package heating rates in fires by comparison to test results,
- determining response of CRUD1, fuel pellets, fuel rods, and fuel assemblies to severe impact environments by experiments and computations, and
- reconstructing the Modal Study truck and train accident event trees and the parameter distributions associated with these trees using recent industry practices and accident data.

Cask damage due to impact onto hard surfaces could be estimated by performing finite element impact calculations based on actual cask designs, in greater detail than has been done in NUREG/CR-6672 for generic casks. In this way behavior of the closure-seal system, including

1 CRUD is an acronym for Chalk River Unidentified Deposits; these deposits on nuclear fuel are formed due to water chemistry. Specifically, chemical reactions in the water that circulates through the core of a nuclear power plant cause deposits to form on the surfaces of the fuel rods. For PWRs, the deposits are typically nickel iron oxides; the non-radioactive nickel in the deposits is converted to radioactive cobalt by neutron bombardment.

bolts, can be modeled to better calculate details of leak pathway creation in severe impacts. A test plan will be developed for an extra-regulatory impact test of an actual certified cask design, including crushed or intact impact limiters and a fuel canister, against an essentially unyielding target. It is anticipated that the test specimen will be propelled with sufficient velocity that it will sustain permanent/plastic deformation that is readily visible and measurable. The test plan will also discuss the feasibility and benefits of performing a regulatory test (impact equivalent to a 30' drop onto an unyielding surface in the most damaging orientation) on the test specimen, before the high-velocity test.

Cask damage due to exposure to fires could be estimated by performing three dimensional heat transport calculations. In order to demonstrate that these computational methods are able to credibly predict the results of hypothetical severe cask accidents, pretest computational predictions could be compared to the results of crash and fire tests that employ a sub-scale or a full-scale test article.

The behavior of spent fuel rods, CRUD, and fuel pellets when subjected to impact loads could be examined by performing bench-scale experiments that examine rod failure, fracturing of CRUD and fuel pellets, formation of particle beds due to fracturing of fuel, and filtering of respirable particles by particle beds.

The Modal Study truck and rail accident event trees may be updated by developing new branch point probabilities and new wayside surface hardness frequencies. NRC expects the need for alternative event trees will be determined, with justification, based on the current accident database and carrier practices (e.g., use of dedicated freight service). In addition, NRC expects to construct a barge/inland vessel event tree, with conditional probabilities. Distributions of bridge heights, embankment heights, accident speeds (both initiating speeds and speeds at impact), and fire durations (based on historic data and on inferences derived from quantities of shipped combustibles) will be constructed. NRC staff is also interested in developing a methodology and capability to link any specific route to the representative route characteristics. Finally, NRC expects to develop a method to map selected historically severe, real transportation accidents into cask structural-thermal response regimes.

Stakeholder and public participation will continue through the confirmatory research phase of the package performance study. As a next step, detailed test and analysis plans will be developed that clearly state the objectives, procedures, success definitions, and limitations of possible research to be performed. These test and analysis plans will be issued for public comment and will include plain-language explanations. In addition NRC expects that these plans will be peer reviewed, possibly by a committee of the National Academy of Sciences. Each of the test plans will describe options for follow-on testing or analysis, however, NRC will not make a decision on particulars until public comments and peer review activities are completed. NRC staff expects to base decisions to proceed value-benefit assessments in the context of NRC's four performance goals: (1) maintaining safety, (2) decreasing unnecessary regulatory burden, (3) increasing public confidence, and (4) improving regulatory effectiveness and efficiency.

CONCLUSION

The shipment of SNF in NRC-certified packages has an excellent safety record. Since spent fuel transportation occurs in the public domain, shipments have, and will continue, to raise considerable interest, particularly as the series of new large-scale shipments approaches. The Commission studied public interest issues associated with spent fuel shipments ("Case Histories of West Valley Spent Fuel Shipments," NUREG/CR-4847, January 1987), as a way to identify effective measures to help address public concerns before commencement of spent fuel shipment campaigns. That study found that the development and implementation of comprehensive public information (and educational) programs that explain the technical, operational, safety, and physical protection aspects of spent fuel transport in layman's terms improve public confidence in spent fuel shipping campaigns. The NRC is implementing this lesson learned in its transportation risk study plans.

The transportation risk studies described here provide a technical basis for determining that current regulations are sufficient to prevent releases of radioactive material during transport. The most recent Package Performance Study provides a process for public involvement in the decision making process for further studies.

A RISK ANALYSIS OF DRY CASK STORAGE

Christopher Ryder, Edward Rodrick, Lee Abramson
Office of Nuclear Regulatory Research
Jack Guttmann
Office of Nuclear Materials Safety and Safeguards
U.S. Nuclear Regulatory Commission, Washington, DC

Abstract

The spent fuel pools of commercial nuclear power plants are becoming filled with spent fuel assemblies. To avoid having to cease operations when the pools are full, many utilities have been removing fuel from the pools and storing it in dry casks on site. The NRC Office of Nuclear Materials Safety and Safeguards (NMSS), which licenses these casks, wants to quantify the risk of dry storage of spent nuclear fuel. The NRC Office of Nuclear Regulatory Research is performing a pilot probabilistic risk assessment (PRA) of a spent fuel dry cask storage system, the Holtec International HI-STORM 100. This cask is being studied at a specific BWR site where the operations can be observed and modeled. Event tree and fault tree methods are used to develop logic models of plausible accident sequences. Engineering analyses are used to determine the probability of a cask failing when subjected to postulated accident conditions. The goals of this study are to determine the risk of radionuclide releases to the environment and the dominant factors that contribute to the risk.

1 Statement of the Problem

Few PRAs have been done on dry cask storage systems. In Reference 1, the relative risk of four storage concepts, pool, cask, caisson, and vault was determined. The study was of conceptual designs, not of a specific storage system. The results of the dry cask PRA will be used for considering options for risk-informing 10 CFR 72 regulatory requirements (including inspection programs), considering various options for safety goal development, enhancing public confidence, increasing regulatory efficiency and effectiveness, reducing unnecessary regulatory burden, and assessing the extent to which data on the performance of the casks in the field need to be improved. The tasks are to apply PRA methods to study a specific design of a cask at a specific site and determine the risk of radionuclide releases to the environment. Event trees and faults trees are used to delineate the responses of the cask to initiating events. Engineering analyses are used to ascertain the responses of the cask to postulated mechanical and thermal loads.

2 Subject of the PRA

The subject of the PRA is the Holtec International HI-STORM 100 cask at a BWR site. The cask consists of three major components, a multi-purpose canister (MPC) that confines the fuel, a transfer cask shields the MPC while being moved inside the plant, and an overpack that protects and shields the MPC during storage. The cask is illustrated in Figure 1. Panel (A)

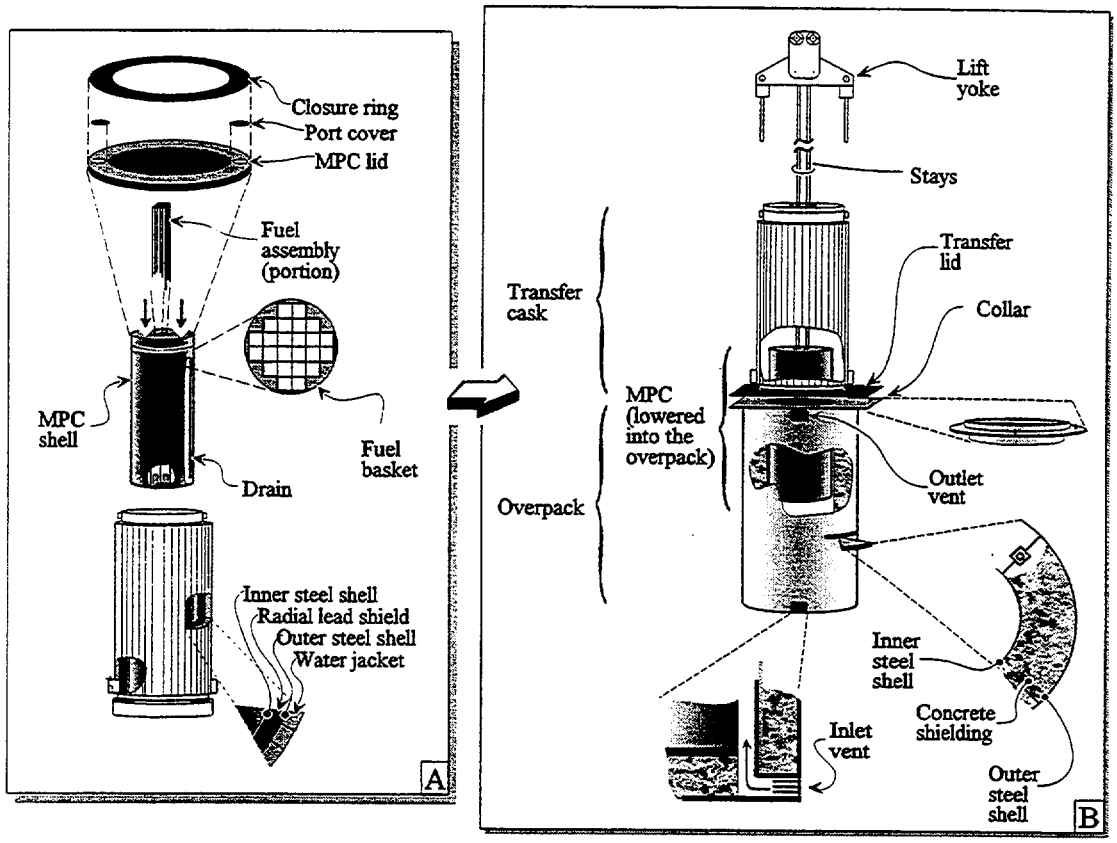

Figure 1 Holtec International dry cask system. Panel (A): Multi-purpose canister (MPC) and the transfer cask. Panel (B): MPC and the overpack.

shows the MPC and the transfer cask. Panel (B) shows the MPC and the overpack.

The operations of dry cask storage are shown in Figure 2. The multi-purpose canister is inserted into the transfer cask, filled with water, and lowered into an alcove of the spent fuel pool. Fuel assemblies are removed from racks in the pool and placed in a fuel basket inside the MPC. The lid of the MPC is placed on the MPC before the transfer cask is lifted out of the pool with the MPC inside. The lid on the top and the transfer cask on the sides and bottom shield workers from radiation. The transfer cask is brought to a preparation area where the MPC is dried, filled with helium, and sealed. In Panel (B) of Figure 1, the MPC is lowered by long stays through the transfer cask into the overpack. After the lid of the overpack is bolted into place, the cask is brought to the storage pad with a specially designed vehicle referred to as a transfer vehicle or crawler. The cask is licensed for 20 years of storage.

The study is of internal and external events during onsite operations and spent fuel storage that may lead to the release of radionuclides to the environment. Offsite transport and storage in a permanent repository are outside the scope of this study. The fabrication of the cask is also beyond the scope of the study; the cask is considered to be built as designed, following accepted quality assurance procedures, and contain flaws in welds within ASME acceptance criteria.

Though the risk to workers is also beyond the scope of the study, the methods can be applied to make such estimates.

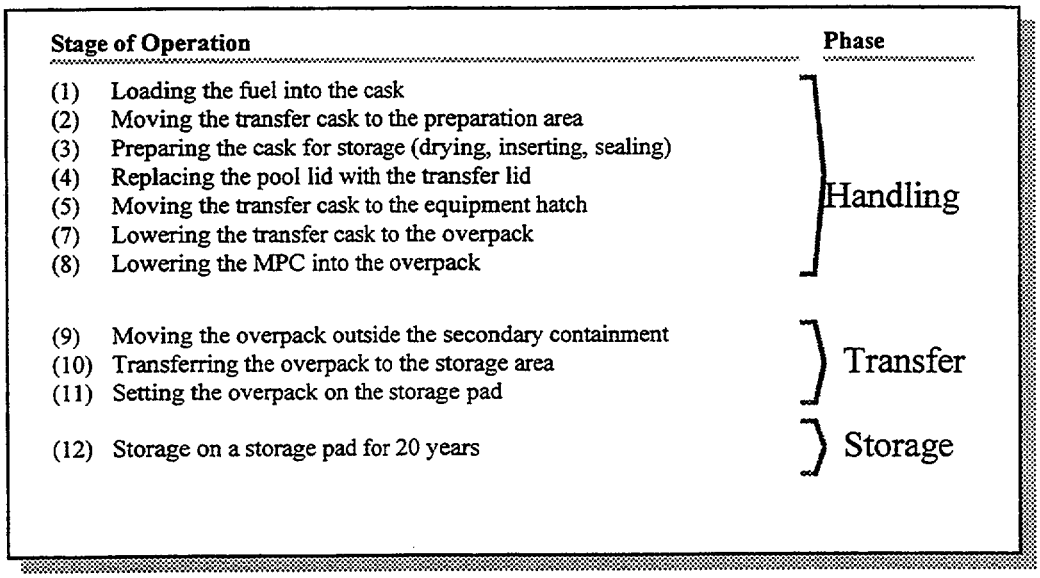

Figure 2. Dry cask storage operation.

3 PRA Approach

The list of initiating events used in the PRA began with the external events at operating nuclear power plants described in Reference 2. Additional events were added to the list as the understanding of the cask and the plant operations increased. The list was reviewed by NMSS for additional insights. Figure 3 is a summary of the initiating events.

With a comprehensive list of initiating events, two approaches are possible. The first approach is to retain all initiating events to calculate risk, no matter how low their frequency. The second approach is to perform a screening analysis where events can be eliminated based on a screening threshold. A screening analysis serves the purpose of focusing limited resources on potentially significant accident scenarios. The second approach, the screening analysis, is used to conduct the study. In PRAs of nuclear power plants, the screening threshold is the frequency of sequences that are excluded from further analysis. In such PRAs, the threshold is chosen to make the analyses manageable; a lower threshold increases the number of sequences that are included in the PRA, making the time of risk calculations prohibitive. But in the PRA of dry cask storage, the event trees and fault trees are much simpler. Although far fewer sequences are included in the PRA, the uncertainties and inaccuracies in the PRA model become progressively larger at low sequence frequencies. For this PRA, the threshold is initially be set a low value. If only a few sequences remain, the threshold may be lowered to identify dominant sequences.

Events were eliminated from consideration based on the following criteria:

- The events were irrelevant to the subject site. For example, the site is not subject to tsunamis or volcanic activity. Also, the storage pad was found to be above the maximum

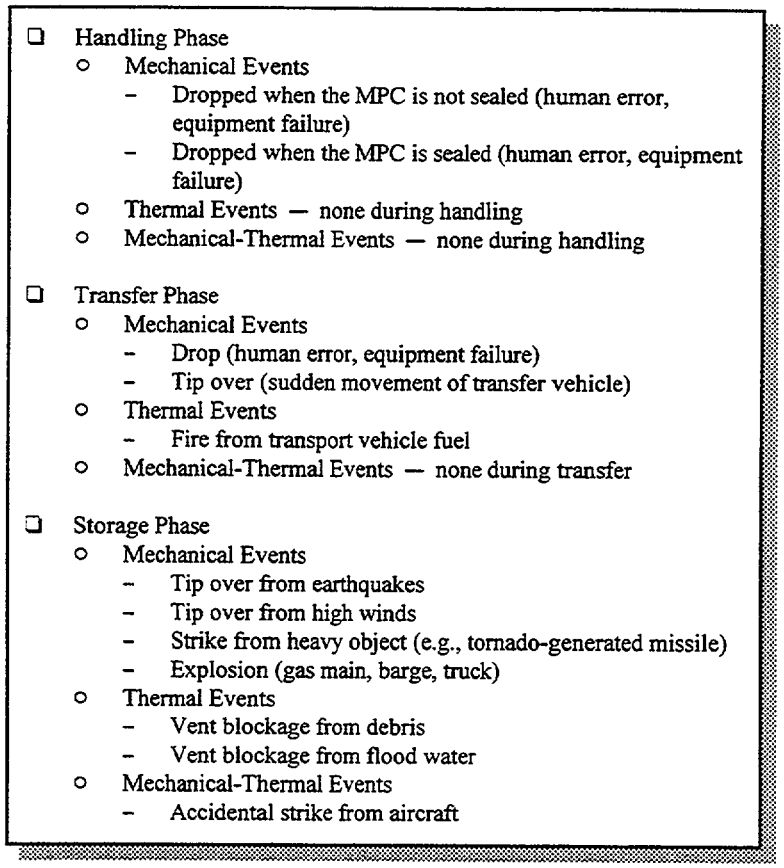

Figure 3 Initiating events.

flood level which could conceivably affect the site.

- The events did not affect the cask. For example, high winds could not achieve the speeds that would be necessary to slide and tip the cask. Though there is no known physical limit to wind speed, the maximum observed wind speed of tornadoes is about 300 mph. Wind speeds in excess of 400 mph are needed to slide the cask and winds in excess of 600 mph are needed to tip the cask.

- When an initiating event could not be screened out based on low frequency, sometimes it could be eliminated because their consequences are found to be low. For example, though lightning can strike the cask with relatively high frequency, the large amount of energy delivered to the cask may be conducted thorough the overpack, to the ground, and not impact the MPC.

4 Method of Analysis

The models used to estimate risk are event trees and fault trees. Event trees are used to model the response of the cask to initiating events. Fault trees are used to determine the probability of

accidents caused by human error or equipment failure during cask operations, such as when the cask is moved while inside the secondary containment. Engineering analyses are used to determine the stresses that would be imposed by the postulated events. Fracture mechanics is used to determine the probability of a cask failing when subjected to the stresses from postulated accident conditions.

The risk analysis of dry cask storage has similarities to and differences from the risk analysis of a nuclear power plant. A detailed study of a power plant is typically done in three phases, called levels. Level 1 is an analysis of the progression of accidents. Level 2 is an analysis of the containment systems that mitigate accidents. Level 3 is an analysis of consequences. In the PRA of dry cask storage, the complexity of the Level 1 is greatly reduced, consisting of an initiating event and sometimes one event following the initiating event. The Level 2 analysis, which is the response of the cask to the initiating event, is analogous to that of the containment at

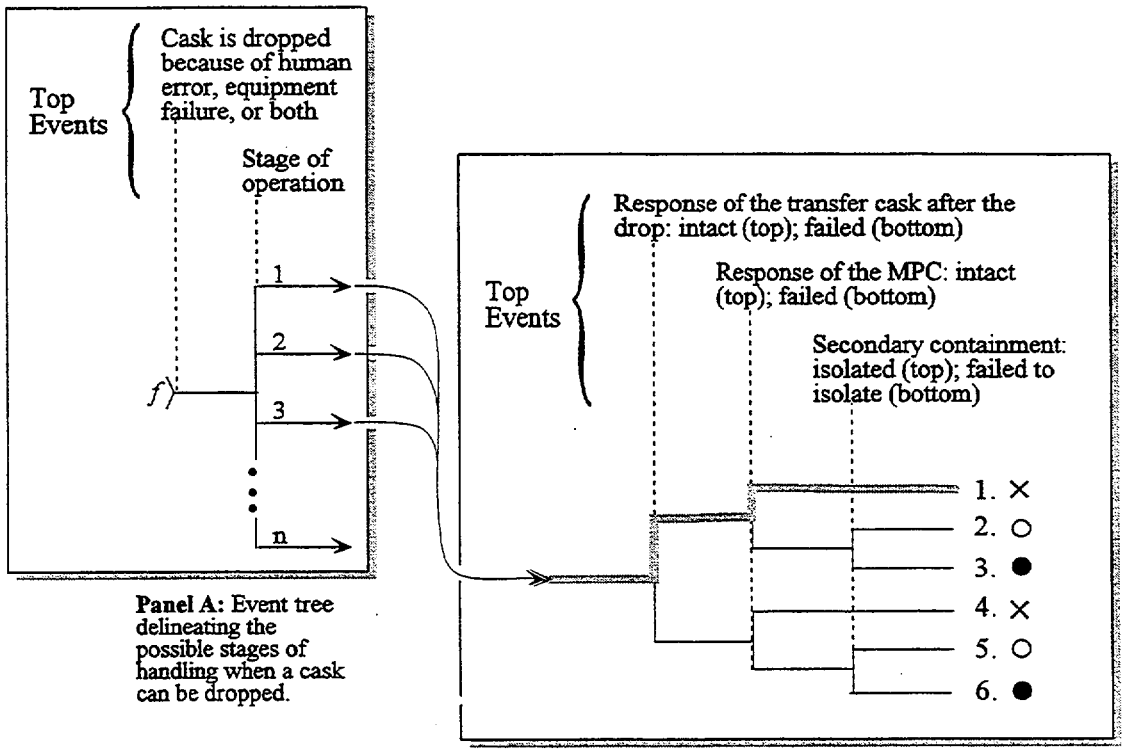

Figure 4 Stylized event tree of dropping a sealed cask inside the secondary containment. LEGEND: × denotes no consequences. ○ denotes smaller consequences. ● denotes larger consequences. The highlighted sequence is discussed in the text.

a power plant. The Level 3 analysis of dry cask storage is different in that the radionuclide inventory is lower and the releases are less energetic. The event trees of the dry cask PRA are simpler compared to the PRA of a nuclear power plant. In a PRA of a power plant, the event tees contain between 5 and 100 top events, depending on the use and the size of the fault trees. In the PRA of dry cask storage, the top events are few (e.g., four top events) and typically do not require fault trees.

An event tree modeling the drop of a cask inside the secondary containment is illustrated in Figure 4. The event tree is stylized to illustrate the concepts. Simple fault trees are used to determine the probability of human errors and equipment failures. Panel A shows the event tree with the initiating event. Panel B shows the event tree of the responses of a cask to the drop.

In Panel A, the event tree begins with a drop of a cask, which is characterized by its frequency. After the drop, the first top event is the handling stage that a cask is in, given that it is dropped, and is characterized by its probability. The initiating event is the first event of a sequence. Both the initiating event and subsequent events are referred to as top events as shown in Figure 2. The stages to move a cask from the spent fuel pool and place it in storage are shown in Figure 2. Each sequence in Panel A transfers to the event tree in Panel B.

In Panel B, the general structure of the event tree modeling the responses of the cask to the drop at given stages is shown. This event tree is the same for each stage; the stages differ from each other in the probabilities at the branch points and the consequences. The first top event is the response of the transfer cask to the drop. Though the transfer cask is not a confinement boundary as is the MPC, its close fit around the MPC could affect the release path if the MPC fractures.

The second top event is the response of the MPC. The MPC is the confinement boundary. When this boundary is intact, there is no release of radioactive material, and hence, there are no consequences as indicated by the ×. When radiation is detected in the secondary containment, the containment is supposed to isolate. Even with the containment isolated, minuscule amounts of radionuclides can leak from the building; consequences are small as indicated by the open circles at the ends of the sequences. If the containment fails to isolate, larger releases to the environment occur; consequences are larger as indicated by the filled circles.

The risk that is calculated with the event trees is given by Equation 1.

$$R = \sum_j f_j \sum_k P_{j,k} C_{j,k} \qquad (1)$$

where R = risk (consequences/time)
f_j = frequency of the initiating event
$P_{j,k}$ = conditional probability of a consequence given an initiating event
$C_{j,k}$ = consequences
j denotes the j^{th} initiating event
k denotes the k^{th} sequence

The units of risk are in consequences per year. Consequences can be expressed in many ways, such as the number of early fatalities or number of latent fatalities.

The total risk of storing spent fuel in a dry cask is the risk incurred during the three operational phases. A consideration in determining the risk of dry cask storage is that the risk of handling and transfer is demand-related while the risk of storage is time-related. The risks of the phases must be expressed in such a way as to permit them to be added together. Consider one cask in the first year of use. During the first year, the cask passes through the handling and transfer phases and begins the storage phase.

The handling phase is treated as a demand-related activity because of its characteristics and duration. The movement of the cask during the lift occurs over a relatively short period; during this period, external initiating events are unlikely to occur that challenge the crane or the integrity of the cask. For example, during lifting, which takes about an hour, an earthquake is unlikely to occur. If, instead, the cask were to be lifted over a much longer period (e.g., month), the probability of external events, such as an earthquake, might not be negligible. Hence, only the demand-related risk is considered. The cask is not subject to other events, such as high winds or floods, because the handling is done inside the secondary containment on the refueling floor.

The risk in the handling phase is given by Equation 2. In order to express the handling risk in units consistent with the storage risk, the frequency of the lifts is expressed as the number of lifts during the first year of service life (i.e., the number of lifts during the handling phase).

$$R_H = \sum f_L \Pr\{D|L\} \Pr\{F|D\} \Pr\{I|F\} [C_H|I] \qquad (2)$$

where R_H = handling risk
f_L = frequency of lifts per year
$\Pr\{D|L\}$ = probability of dropping a cask during a lift
$\Pr\{F|D\}$ = probability of a cask failing given a drop
$\Pr\{I|F\}$ = probability of failure of secondary containment isolation if a cask fails
$[C_H|I]$ = consequences if a cask fails and the secondary containment failures to isolate

The summation is over all sequences. The handling risk is in the units of consequences per year.

The transfer phase is analogous to the handling phase. Hence, it too is demand related. Although the transfer phase occurs outside of the refueling building, where time-related external events such as high winds and floods can occur, the transfer phase is done only under favorable conditions. An earthquake is unlikely to occur during the brief period. The time-related risk is negligible relative to the demand-related risk.

The risk of the transfer phase is given by Equation 3.

$$R_T = \sum f_T \Pr\{D|T\} \Pr\{F|D\} [C_T|F] \qquad (3)$$

where R_T = transfer risk
f_T = frequency of transfers in the first year
$Pr\{D|T\}$ = probability of dropping a cask during a transfer
$Pr\{F|D\}$ = probability of a cask failing given that it is dropped
$[C_T|F]$ = consequences given that a cask fails

The summation is over all sequences. The units of the transfer risk are in consequences per year.

Storage risk is time-related. During the storage period, the cask is in a normal state where it is subject to events (e.g. earthquakes, high winds) that could challenge the integrity of the cask. The longer that the cask is on the storage pad, the longer it is subject to events that can affect it. Hence, the risk is time-related. The risk of the first year of storage is given by Equation 4.

$$R_S = \sum f_S \, Pr\{F|E\}[C_s|F] \qquad (4)$$

where R_S = storage risk
f_S = frequency of events during storage
$Pr\{F|E\}$ = probability of a failure given an initiating event
$[C_s|F]$ = consequences given that a cask fails

The summation is over all sequences. The units of risk are in consequences per year.

During the first year of operation, the cask passes through the handling and transfer phases into the storage phase. The handling and storage phases last a small fraction of a year, so that the cask is in storage for almost a full year. Accordingly, the risk of a cask for the first year of its service life is given by Equation 5.

$$R\{1\} = R_H + R_T + R_S \qquad (5)$$

where $R\{1\}$ = risk during the first year of use
R_H = risk from handling a cask
R_T = risk from transferring a cask
R_S = risk from storing a cask

The units of total risk are in consequences/year.

After the first year of operation, the cask is no longer handled or transferred. Only the storage risk is incurred for the remainder of the 19 years of its service life. Equation 6 gives the total risk of dry cask storage during 20 years.

$$\begin{aligned} R\{20\}_{Total} &= (1 year) R\{1\} + (19 years) R_S \\ &= R_H + R_T + 20 R_S \end{aligned} \qquad (6)$$

The total risk for the service life is in units of consequences.

At the end of the storage period, the cask may be transferred to another area where it is prepared for transport to a permanent repository. Post-storage activities are beyond the scope of this study.

5. Conclusion

PRA methods are being successfully applied to determine the risk of dry cask storage. Preliminary indications are that a PRA of dry cask storage needs to be specific to the design features of a cask, the characteristics of a site, operations at the plant, and characteristics of the plant. The design of the cask determines its response to initiating events. Site-specific characteristics determine relevant initiating events that can potentially challenge a cask. Plant-specific equipment influence the frequency of dropping a cask inside the containment and the capability of the containment to mitigate an accident. Plant-specific operations influence reliability of human actions.

The PRA is progressing. Event tree models are being revised. Load analyses and fracture mechanics analyses are continuing to determine the response of the MPC and the fuel to mechanical and thermal loads. Source term and consequence are being determined. At the completion of these analyses, risk estimates will be obtained, along with the dominant contributors of risk. Preliminary results are expected in mid-2002.

6 References

1. "Review of Proposed Dry-Storage Concepts Using Probabilistic Risk Assessment," Electric Power Research Institute, EPRI NP-3365, February 1984.

2. J.W. Hickman, "PRA Procedures Guide," NUREG/CR-2300, Volumes 1 and 2, NRC, January 1983.

Seismic Behavior of Spent Fuel Dry Cask Storage Systems

S. Khalid Shaukat, U.S. Nuclear Regulatory Commission, Washington, DC, USA
Vincent K. Luk, Sandia National Laboratories, Albuquerque, NM, USA

ABSTRACT

The U. S. Nuclear Regulatory Commission (NRC) is conducting a research program to investigate technical issues concerning the dry storage of spent nuclear fuel by conducting confirmatory research for establishing criteria and review guidelines for the seismic behavior of these systems. The program focuses on developing 3-D finite element analysis models that address the dynamic coupling of a module/cask, a flexible concrete pad, and an underlying soil/rock foundation, in particular, the soil-structure-interaction. Parametric analyses of the coupled models are performed to include variations in module/cask geometry, site seismicity, underlying soil properties, and cask/pad interface friction. The analyses performed and planned to be performed include:

1) a rectangular dry cask module typical of Transnuclear West design at a site in Western USA where high seismicity is expected;

2) a cylindrical dry cask typical of Holtec design at a site in Eastern USA where low seismicity is expected; and

3) a cylindrical dry cask typical of Holtec design at a site in Western USA with medium high seismicity.

The paper includes assumptions made in seismic analyses performed to date, results, and conclusions.

INTRODUCTION

A simple type of Independent Spent Fuel Storage Installations (ISFSI) licensed under 10 CFR Part 72 [1] consists of array(s) of freestanding dry cask storage systems resting on a concrete pad constructed on a natural sub-grade or engineered fill. The cask stability is a high priority issue to evaluate the seismic safety of these systems. The current Standard Review Plan for Dry Cask Storage System, NUREG-1536 [2] calls for the use of a safety margin of 1.1 as the review criterion against cask sliding and overturning during a postulated design earthquake; that is, the cask is not allowed to move or tip. However, in an earthquake event of medium to high magnitude, the casks may slide and wobble in many different ways. In the safety review process, there is no guidance in the current review criteria to address the important issues of simultaneous sliding, wobbling, and tipping of casks, potential impact of casks hitting neighboring casks, and structural integrity of their internals. In addition, the SRP states that the tip-over and cask-to-cask impact in an earthquake are considered to be accidents and should be analyzed regardless of the likelihood of occurrence. The consequences of these occurrences have not been fully assessed by the NRC beyond the requirements that the licensing basis of the cask and the storage site must not be violated.

This paper provides some insight on the results from analyses of coupled finite element models involving rectangular concrete cask modules with steel horizontal casks and cylindrical casks. The rectangular cask module consists of a tie-together unit of at least three modules. The cylindrical casks are separately freestanding on concrete pad. The analyses performed and planned to be performed include:

1) a rectangular dry cask module typical of Transnuclear West design at a site in Western USA where high seismicity is expected;

2) a cylindrical dry cask typical of Holtec design at a site in Eastern USA where low seismicity is expected; and

3) a cylindrical dry cask typical of Holtec design at a site in Western USA with medium high seismicity.

The analysis results will be used to generate nomograms, tables, charts, etc. that would provide the NRC staff tools to evaluate the license applications for dry cask storage systems.

Rectangular Dry Cask Module at Western USA Site

Analyses Model:

A three-dimensional coupled finite element model consisting of the three-module assembly of rectangular modules/casks, a flexible concrete pad, and an underlying soil foundation was developed and analyzed using the ABAQUS/Explicit code, Version 5-8.19 [3]. The coupled modeling approach allows an in-depth evaluation of the nonlinear dynamic seismic behavior of the module/cask with the soil-structure-interaction (SSI) effect. The model development effort involved two analysis groups who used independent modeling approaches to develop the coupled model. This modeling arrangement with separate efforts provided a better check-and-balance and a much-improved solution of the seismic response of the modules/casks. It will not be possible to otherwise validate the analysis results due to lack of relevant test data. There were considerable differences in the analysis results produced from the two approaches. Most of the identified discrepancies were eventually resolved to arrive at a final model with all desirable features.

The modules/casks and their internals were modeled as elastic bodies and the three modules were assumed to be tied together in the model. In the coupled model, the base of the concrete pad was assumed rigidly bonded to the top surface of the soil foundation. At the interface between the module and the pad, a sliding contact condition was assumed with assigned friction coefficients of 0.3, 0.5, or 0.75. The top of the pad was designated to be the "master" surface and the underside of the module to be the "slave" surface to prevent any portion of the module from entering the pad. The four vertical sides of the soil foundation were represented by edge columns that allow horizontal shear deformation only in order to simulate infinite boundary conditions. The input motions of seismic accelerations were applied at the base of the soil foundation. The following data for the module/cask assembly was used:

- Weight = 213,207 kg (470,041 lbs).
- Width = 7.70 m (25' - 3") (for a three-module assembly)
- Length = 6.00 m (19' - 7")
- Height = 5.64 m (18' - 6") (with shield block)
- Cask Height = 2.58 m (8' - 5.7")
- Height of combined center of gravity above pad = 3.08 m (10' - 1.13")

The concrete pad model covers the area directly underneath the three-module assembly plus 3.04-m (10-foot) clearance on its all four sides.

- Thickness = 0.91 m (3')
- Width = 13.79 m (45' - 3")
- Length = 12.07 m (39' - 7")

Per US Corps of Engineers soil-structure-interaction modeling guidelines [4], the selected width and length of the soil foundation should be seven times the corresponding dimensions of the pad. Therefore, the soil foundation was dimensioned with width = 96.55 m (316' - 9") and length = 84.46 m (277' - 1"). In addition, the depth of the soil foundation was selected to be 30.48 m (100' - 0") that is more than twice the width of the assembly.

The module/cask assembly and the concrete pad were assumed to behave elastically when subjected to the seismic excitations. The internal details of the assembly were not represented and the concrete pad would not crack in the coupled model. Table 1 provides their elastic material properties selected in the model.

Table 1. Elastic Material Properties of Module/cask and Pad

Structural Element	Young's Modulus, E (MPa) (x 10^3)	Poisson's Ratio, ν	Density, ρ (kg/m^3)
Pad	24.856	0.2	2403
Shield Wall	27.789	0.2	2403
Module (Zone 1)*	27.789	0.2	1416 (from base to 1.57 m above pad)
Module (Zone 2)*	27.789	0.2	2349 (from 1.57 m above pad to top)

* This arrangement puts the center of gravity of the assembly at the correct elevation.

The material properties of the soil foundation, which varies with depth, was developed according to the specific soil profile data at the chosen site. The soil profile data indicate that this site has a soft soil foundation. Since the seismic input amplification was found to be rather sensitive to the choice of soil properties, and in addition, preliminary analyses with the softest soil assumption ("large-strain" properties) produced rather nonconservative cask response results, the "low-strain" properties were used for the analyses documented herein. The 30.48-

m (100' - 0") depth of the soil foundation was subdivided into six sub-regions. Using these gradations, the "low-strain" soil properties were averaged for these six sub-regions. The density of the soil foundation is 2082 kg/m^3 (130 lb/ft^3).

Soil Damping

In the ABAQUS/Explicit code, the material damping is represented by Rayleigh damping, which usually involves two damping factors to account for stiffness and mass proportional damping. The final analyses used the mass proportional damping, ξ_n for each layer such that

$$\xi_n = a_0 / 2\omega_n$$
where $a_0 = 2 \times \xi \times 2\Pi / T$

For shear wave propagation model of horizontal motion site response, site period T = 0.68 second.

Time Histories of Seismic Accelerations

Two sets of seismic excitations were used in the analyses: (1) the artificial seismic time histories, generated by the staff, whose response spectra were based on RG 1.60, and (2) the actual Tabas earthquake records [5]. The selected peak ground acceleration (PGA) level is 1.50 g and 1.00 g for the horizontal and vertical components of seismic accelerations, respectively. Two horizontal components and one vertical component of the seismic accelerations, which are "surface" motions, were applied simultaneously to the coupled model. The seismic response of the assembly was also investigated by switching the horizontal accelerations with respect to the module coordinate system for every analysis case.

Both sets of seismic time histories are defined at the free surface, but the earthquake excitations were applied at the base of the soil foundation in the coupled model. An appropriate frequency-domain deconvolution procedure was developed to adjust magnitudes and frequencies simultaneously. This procedure was used for deconvoluted accelerations.

Analyses Results:

The seismic analyses were performed using an artificial time history based on R.G. 1.60 (1.5g in each horizontal direction, and 1.0g in vertical direction) and also using time history for actual Tabas (Iran) earthquake records (1.5g in each horizontal direction, 1.0g in vertical direction). These analyses were 3-D coupled non-linear finite element analyses with cask, pad and soil underneath. A range of coefficient of friction (0.3 to 0.75) was applied. The worst coefficient of friction assumed was 0.3, although it is extremely conservative and non-realistic for concrete to concrete friction which is believed to be higher than 0.3. The conclusion was that the 3-cask module tied together may slide but the horizontal displacement will be less than half the clear distance between the neighboring modules or the edge distance of the pad. The cask will not slide off the pad, will not hit other cask modules, and will not tip over.

Cylindrical Dry Cask at Eastern USA Site

Analyses Model:

A three-dimensional coupled finite element model of a cylindrical HI-STORM 100 cask, a flexible concrete pad, and an underlying soil foundation was analyzed using the ABAQUS/Explicit code, Version 5-8.19 [3]. The cylindrical cask is partitioned into four horizontal sections with six rows of solid elements in each section and 64 elements around the outside perimeter. The density of solid elements in each horizontal section is calculated and distributed in such a manner that the center of gravity of the cask is located at the correct design position. The cask and its internals are modeled as elastic bodies.

In the coupled model, the base of the concrete pad was assumed rigidly bonded to the top surface of the soil foundation. At the cask/pad interface, a sliding contact condition was assumed with an assigned friction coefficient of 0.25, or 0.53. The top of the pad was designated to be the "master" surface and the underside of the module to be the "slave" surface to prevent any portion of the module from entering the pad. The four vertical sides of the soil foundation were represented by edge columns that allow horizontal shear deformation only in order to simulate infinite boundary conditions. The vendor provided earthquake excitation information was treated with a deconvolution procedure to produce a modified time history of deconvoluted accelerations with properly adjusted frequencies and magnitudes to be applied at the base of soil foundation. The concept of deconvolution is a mathematically rigorous solution process that applies the wave propagation equation of the free-field surface along with the boundary conditions. It has been proven that the solution would be unique and rigorously correct for a linear representation of the soil mass (that is, linear shear modulus and viscous damping model). The deconvolution procedure has been discussed by Idriss and Seed [6] and Schnabel, et al. [7]. The input motions of deconvoluted seismic accelerations were applied to all nodes at the base of the soil foundation. The following data for the HI-STORM 100 overpack with multi-purpose canister (MPC) fully loaded MPC-68 was used:

- Weight = 163,293 kg (360,000 lbs).
- Outside Diameter = 3.37 m (11' - 0.5")
- Height = 5.87 m (19' - 3.25")
- Height of center of gravity above pad = 3.00 m (9' - 10.38")

A section of the concrete pad that holds 4 (2x2) casks was selected as the optimal dimension for the pad in the coupled model, even though only one cask was simulated. The selected pad was 9.45 m (31' - 0") square. The pad thickness was 7.32 m (2' - 0").

The size of soil foundation submodel plays an important role in assessing the soil-structure-interaction (SSI) effect. Sensitivity studies on the submodel size were performed to demonstrate that its chosen model size could simulate the behavior of a semi-infinite soil foundation underneath the concrete pad. Three different lateral dimensions were selected in the studies having 1.0, 1.22, and 1.33 times a baseline lateral geometry of a square of 85 m (279 feet), which is nine times the pad dimension. It should be noted that the outside layer of elements on the four vertical sides of soil foundation submodel, with width equal to the pad

dimension of 9.45 m (31' - 0"), are represented by edge columns. This model setup indicates that the true model size is defined by the nodes at the inner row of the layer with degrees of freedom constrained to those at the outside row. Therefore, the baseline geometry of soil foundation submodel is only seven times the pad dimension. This selection of the lateral dimension of soil foundation submodel follows the US Corps of Engineers soil-structure-interaction modeling guidelines [4].

The sensitivity studies on the submodel sizes on the horizontal displacements of the cask base with respect to the pad showed closer displacement solutions for the cases of 1.22 and 1.33 times the baseline geometry, indicating that a convergence trend of soil foundation submodel sizes was observed. Therefore, the final soil foundation submodel, which was selected to be 1.22 times the baseline geometry, was a square with length of 103.94 m (341' - 0").
In addition, a depth of 56.39 m (185' - 0") which was partitioned into eight horizontal layers was selected for soil foundation submodel.

The cask and the concrete pad are assumed to behave elastically when subjected to seismic excitations. Therefore, their elastic material properties were chosen as shown in Table 2.

Table 2. Elastic Material Properties of Cask and Pad

Structural Element	Young's Modulus, E (MPa) (x 10^3)	Poisson's Ratio, ν	Density, ρ (kg/m^3)
Cask	27.789	0.2	3407 (Section 4)*
			2600 (Section 3)*
			2600 (Section 2)*
			6408 (Section 1)*
Pad	24.856	0.2	2403

* Geometry definition of horizontal sections:

Section 1: from cask base to 0.2 m (0' - 8") above base
Section 2: from 0.2 m (0' - 8") above base to 0.6 m (2' - 0") above base
Section 3: from 0.6 m (2' - 0") above base to 3 m (9' - 10.38") above base
Section 4: from 3 m (9' - 10.38") above base to cask top

The 56.39 m (185' - 0") depth of soil foundation submodel is partitioned into eight horizontal layers. The depth variation of soil properties such as shear wave velocity and damping profiles was developed to incorporate the site specific soil profiles provided by the vendor. The best-estimated strain-compatible soil properties were selected to be used in the seismic analyses. The weight density of the top 56.39 m (185' - 0") of soil foundation was estimated to be 2162 kg/m^3 (135 lb/ft^3).

Soil Damping

The final analyses used the mass proportional damping, ξ_n for each layer such that

$$\xi_n = a_0 / 2\omega_n$$

where $a_0 = 2 \times \xi \times 2\Pi / T$

For shear wave propagation model of horizontal motion site response, site period T is assumed as 0.53 second.
For compression wave propagation model of vertical motion site response, site period T is assumed as 0.33 second.

Time Histories of Seismic Accelerations

The time history utilized was the one used by the applicant for the design basis. The selected PGA level is 0.15 g for the two horizontal directions and 0.1 g for the vertical direction. Two horizontal components and one vertical component of the seismic accelerations, which are "surface" motions, were applied simultaneously to the coupled model. A frequency domain deconvolution procedure was applied to the time histories of seismic surface accelerations. This procedure uses the Fourier transforms to adjust simultaneously their magnitudes and frequency contents. The net outcome is that when deconvoluted seismic motions are applied at the base of soil foundation submodel, the dynamic characteristics of the original seismic motions is preserved and the desired surface shaking intensity can be achieved.

Analyses Results:

For seismic excitation analyzed with horizontal PGA of 0.15g, and vertical PGA of 0.1g using 3-D coupled non-linear finite element model of the cask, pad and soil underneath, the analyses show that the cask may slide less than 0.1" assuming lower bound coefficient of friction 0.25, and will not tip over with any coefficient of friction from 0.25 to 0.53.

Cylindrical Dry Cask at Western USA Site

Analyses Model:

Cylindrical cask similar to the one used at Eastern site is used in the analyses, but with a little more complicated model for a site in Western USA. The complication is due to an additional layer of soil cement between the pad and the soil underneath. This introduces additional variables such as the coefficient of friction between the pad and cement, and between cement and soil. The ground motion used is the one provided by the cask vendor (0.728g in one horizontal direction, 0.707g in the other horizontal direction, and 0.721g in vertical direction). In the coupled model, initially the coefficient of friction between cask and pad is to be assumed as 0.2 lower bound and 0.8 upper bound assuming the cement layer is fully bonded with the soil below. With the governing case of the two mentioned above, a third case was analyzed assuming 0.31 as the coefficient of friction between pad and cement and also between cement

and soil. The input motions of deconvoluted seismic accelerations is applied to all nodes at the base of the soil foundation. The same data mentioned above for the HI-STORM 100 overpack with multi-purpose canister (MPC) fully loaded MPC-68 is used:

Analyses Results:

In all the case analyzed for various coefficients of friction between the cask/pad interface, pad/soil-cement interface and soil-cement/soil interface, the cask horizontal displacement was less than 4 inches. It is observed that the horizontal displacement results are relatively insensitive to the assumed friction at the interfaces underneath the pad. This insensitivity is believed to be attributed to the confining effect provided by the soil-cement surrounding the pad.

Since the separation distance between neighboring casks is 47.50 inches and the horizontal displacement calculated for even the worst case is less than 4 inches, no cask collision will occur. In addition, the analysis results indicate that the cask undergoes very small tipping angles, and therefore casks will not tip-over.

Work to be done:

Additional work under way is the sensitivity analyses in the seismic behavior of the Holtec cylindrical dry cask by varying the following:

Friction coefficient between cask and pad
Friction coefficient between pad and cement layer
Friction coefficient between cement layer and soil
Soil properties
Use of a different time history (e.g., San Fernando Earthquake, Pacoima Dam record.)

A review panel of eight members (4 sponsored by the NRC, and 4 sponsored by EPRI was established at the beginning of this project to provide direction and guidelines on how the work should proceed. The 4 members sponsored by the NRC have now reduced to 3 staff members. The 4 members sponsored by EPRI include one from EPRI, one nationally recognized expert and two representatives from the Industry). A review panel meeting is expected after completing the above mentioned analyses. All the review panel members will be provided the information developed to seek guidance on the progress and direction of the work on generic applicability of these analyses. Generic review guidelines will be developed by evaluating a large number of cases with varying friction coefficients, soil properties, and seismic excitation levels. The end product is expected to be in the form of nomograms, charts, and/or tables that could be used as a tool for NRC review of licensee applications.

The schedule for completion of these efforts is Mid 2003.

References:

1. Title 10, The Code of Federal Regulation, January 1, 1997.

2. Standard Review Plan for Dry Cask storage System, NUREG-1536, January 1, 1997.

3. ABAQUS/Explicit: User's Manual, Version 5.8-19, 1998, Pawtucket, RI, Hibbitt, Karlsson, and Sorensen, Inc.

4. US Army Corps of Engineers, Engineer Technical Letter No. 1110-2-339, March 1993.

5. J. Shoja-Taheri and J. G. Anderson, "The 1978 Tabas, Iran, Earthquake: An Interpretation of the Strong Motion Records," Bulletin of the Seismological Society of America, Vol. 78, No. 1, pp. 142-171, February 1988.

6. Idriss, I. M. and Seed, H. B., "Seismic Response of Horizontal Layers," Journal of the Soil Mechanics and Foundation Division, ASCE, Vol. 94, No. SM 4, July 1968.

7. Schnabel, P. B., Lysmer, J., and Seed H. B., "SHAKE: A computer Program for Earthquake Response Analysis of Horizontally Layered Sites," Report No. UCB/EERC-72/12, Earthquake Engineering Research Center, University of California, Berkeley, December 1972, 102p.

An Analysis of a Spent Fuel Transportation Cask Under Rail Tunnel Fire Conditions

Christopher S. Bajwa
Spent Fuel Project Office
Office of Nuclear Material Safety and Safeguards
U.S. Nuclear Regulatory Commission,
Rockville, MD

Abstract

The U.S. Nuclear Regulatory Commission has established Title 10 of the Code of Federal Regulations Part 71 section 73(c)(4), (10 CFR 71.73(c)(4)) which requires radioactive material transportation packages to resist a consuming 30 minute fire in order to prevent a release of radioactive material to the environment. Transportation package designs must be evaluated to ensure survivability in the case of a fire accident. This paper presents the study of a spent fuel transportation cask with a welded canister that was prompted by a severe fire that occurred in a Baltimore, Maryland railroad tunnel.

Introduction

Hazards in the transportation industry from rail shipments can result in accidents involving fire. Fire is a concern in the transportation of radioactive material, specifically that transportation accidents can cause ignition of flammable materials that could fully engulf a spent fuel transportation package, increasing the potential for release of radioactive material.

On July 18, 2001, a freight train derailed in a tunnel in Baltimore, Maryland. A fire involving hazardous materials occurred as a result of the derailment. According to reports, the fire burned for several days. Although a fire of the duration and intensity of the one that occurred in Baltimore would be an unlikely occurrence during rail shipment of spent nuclear fuel, fires do happen. Several questions have been raised with regards to how a spent fuel cask would perform if exposed to a fire for longer than 30 minutes. This analysis was prompted by the Baltimore railroad tunnel accident

This paper discusses the Baltimore tunnel fire, transportation of spent nuclear fuel, the analysis performed on a spent fuel cask under severe fire conditions, including the ANSYS® model that was developed for the analysis, and finally the preliminary results of the analysis including a discussion of the significance of those results.

The Baltimore Tunnel Fire

The CSX freight train involved in the accident traveled through the Howard Street Tunnel in Downtown Baltimore, Maryland. The details of the accident as recorded in this paper were derived from media reports concerning the accident, and press releases provided by the National Transportation Safety Board (NTSB).

The Howard Street Tunnel is single rail tunnel, 1.66 miles in length. It has a 1/10% upward grade from the entrance to the exit. The original tunnel was constructed in 1859, with additions being made to the original length to reach the current length of 1.66 miles. The tunnel is constructed of mostly concrete and refractory brick, and has no active ventilation system. The cross sectional dimensions of the tunnel vary along its length, but it is approximately 14 feet high by 32 feet wide.

The CSX freight train involved in the accident consisted of 3 locomotives and 60 cars. As the train traveled through the tunnel there was a derailment of 11 of the 60 rail cars, the cause of which is currently under investigation. A tanker car carrying Tripropylene was ruptured and caught fire during the derailment. Tripropylene carries a National Fire Protection Association (NFPA) hazards rating of 3 for flammability, which is the same as gasoline. This means that it can be ignited at ambient conditions.

The freight train was also transporting hydrochloric acid and other hazardous materials, which were not thought to have contributed to the fire. Media reports indicate that the Tripropylene tanker car burned for no more than 12 hours. It was reported that 24 hours after the fire began, firefighting personnel deemed it safe to enter the tunnel to remove the derailed cars and fight what remained of the fire.

Temperatures in the tunnel during the fire were reported by the media to be as high as 1500°F; however, the actual temperature versus time history of the fire is not known. The staff is currently working with the National Institute of Standards and Technology (NIST) to model the Baltimore tunnel fire to more accurately predict possible temperatures.

Transportation of Spent Nuclear Fuel

The occurrence of the Baltimore tunnel fire has raised questions about how a spent fuel transportation cask might perform, should a cask be involved in an accident and severe fire during transit. Current NRC regulations specify exposure of a cask to a fire accident for a period of no less than 30 minutes with an average flame temperature of no less that 1475°F (800°C). Transportation casks must be subjected to an open pool fire test or analyzed for a fire accident meeting the aforementioned criteria. Casks must maintain shielding and criticality control functions throughout the fire event and post-fire cool down in order to meet NRC requirements.

The analysis described below was conducted to determine the response of a spent fuel cask to a severe fire event. Because the conditions present in the Baltimore tunnel fire were not known, this analysis was considered a scoping analysis to characterize the behavior of a transportation cask in severe fire conditions. The analysis does not attempt to capture the conditions that were present in the Baltimore tunnel fire, but may be similar to what they were.

Description of Spent Fuel Transportation Cask

The spent fuel transportation cask used in this analysis is an NRC approved cask design that utilizes a welded canister, called a multi-purpose canister (MPC), to hold spent fuel. The MPC has an integrated fuel basket with space for 24 Pressurized Water Reactor (PWR) fuel assemblies. The spent fuel assemblies are placed within the fuel basket during loading. MPC loading usually occurs in the spent fuel pool of a nuclear reactor facility. After the MPC has been loaded with spent fuel, it is dried of all water and backfilled with helium gas to create an inert environment for the fuel and to aid with heat transfer away from the fuel assemblies. The lid is then welded in place and the MPC is tested to ensure that it has been properly sealed.

The MPC is placed within the steel "overpack," which has a bolted closure lid and a metallic o-ring seal. The overpack is then backfilled with helium gas, to aid with heat transfer away from the MPC. The outer shell of the overpack is fabricated of carbon steel and is 0.25" thick. The next layer is the neutron shield, a polymeric material, which is strengthened by a network of stainless steel stiffeners. The neutron shield and stiffeners are almost 4.5" thick. The next layer, the gamma shield layer, is actually 6 layers of carbon steel plates and is a total of 6.5" thick. The overpack inner shell is 2.5" thick and is stainless steel material. Impact limiters are affixed to the ends of the transportation overpack to prevent damage in case of a cask drop accident.

A diagram of the spent fuel cask (MPC and overpack) as well as a figure of the cask with impact limiters is provided (See Figure 1 and Figure 2 below).

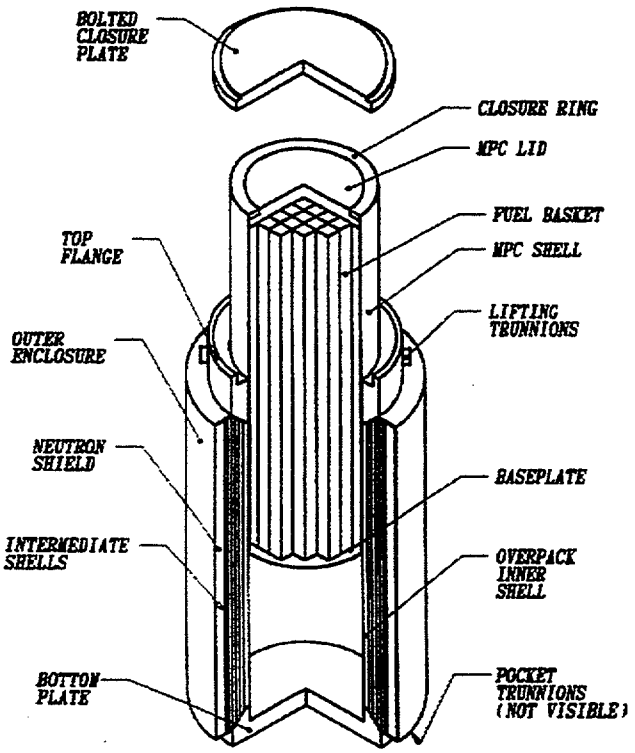

Spent Fuel Cask and Overpack

Figure 1

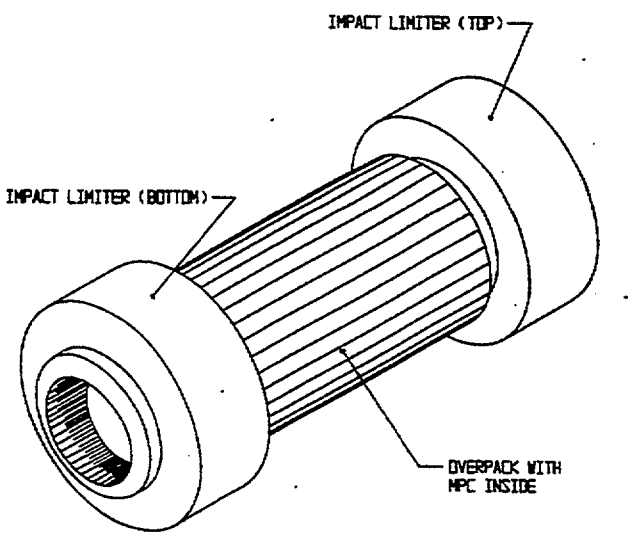

Spent Fuel Cask with Impact Limiters

Figure 2

Description of Cask Analysis Model

A model of the cask was developed in ANSYS® in order to analyze the performance of the cask when subjected to a severe fire. The thermal model is a 2-dimensional planar (circular) cross section of the cask, utilizing PLANE55 thermal elements for conduction and SURF151 surface effect elements for convection and radiation. The model consists of several layers as described above, and is shown in Figure-3. The model has approximately 7,500 elements.

The material properties used in the analysis were from the cask vendor's SAR. The neutron shield region is modeled as a composite of the neutron shield polymer material and the stainless steel stiffeners. This composite region is given an effective thermal conductivity and effective density to simplify the modeling process. Similarly, the analysis model utilizes two homogenized fuel "regions" rather than a detailed model of the fuel basket and individual fuel assemblies. The outer region represents the area between the outer fuel basket and the MPC shell.

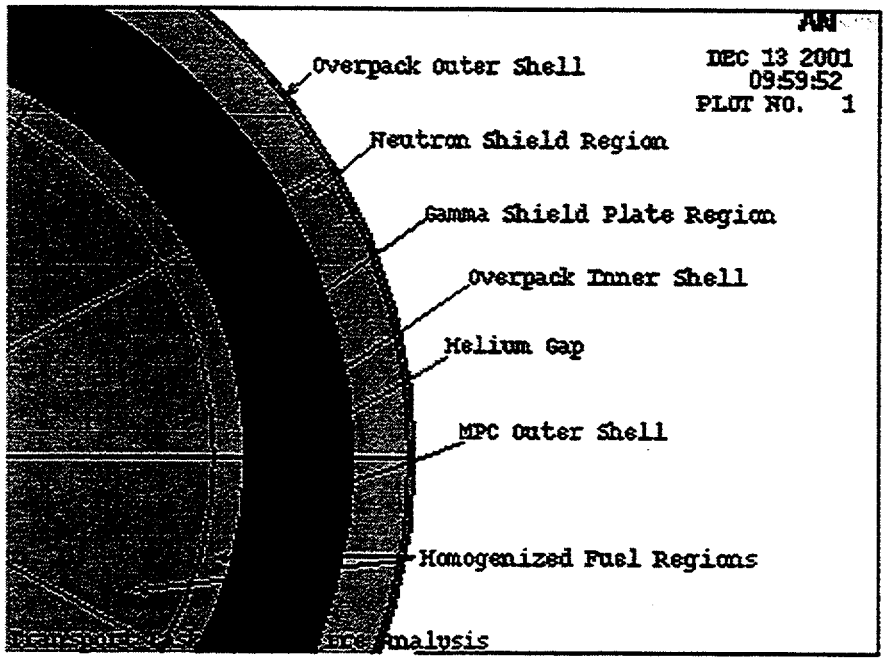

Figure 3

The inner region models the bulk of the fuel assemblies and fuel basket. Both fuel regions represent a homogenization of the fuel assemblies (fuel pellets, fuel rods, and rod fill gas), fuel basket, and helium fill gas within the MPC.

The homogenization for this analysis takes into account the main heat transfer mechanisms in the fuel basket region including conduction, radiation, and to a lesser degree, convection. The values used in this analysis were based on effective conductivity and average density and specific heat calculations performed by the vendor. The procedure the vendor used for determining the effective conductivity and density values is briefly described below.

First, a detailed model of a single fuel assembly (including fuel pellets, fuel cladding and rod fill gasses) was developed to account for all heat transfer mechanisms involved, including conduction, radiation, and convection. This model was verified against spent fuel temperature data to ensure that it provided an accurate fuel assembly temperature profile to work with.

Next the vendor solved the fuel assembly model to obtain a temperature difference across the assembly for a given heat generation. Using the calculated temperature difference and the geometry of the fuel assembly an effective conductivity for the fuel assembly region was calculated using an empirical relation.

Finally, the effective conductivity region was modeled to assure that the temperature profile closely matched that of the original detailed fuel model. The vendor further reduced the homogenized fuel assembly and fuel basket model to obtain two homogenized fuel regions. The effective conductivity values for these two regions were used in this analysis. Separate calculations were performed by the vendor for the fuel assembly and fuel basket region to obtain an average density and average heat capacity. The values for these were also used in the analysis.

Analysis of Spent Fuel Transportation Cask

Boundary Conditions

Federal Regulations in 10 CFR 71.71 describe normal conditions for transportation of spent fuel casks as an ambient of 100°F, with a specified insolation to account for heat flux from sunlight on the surface of the cask. It was assumed that the cask would be exposed to sunlight before the fire exposure. The surface of the cask was also radiating heat to the environment, and was given an emissivity value of 0.85 for the analysis. This is based on the emissivity value of the painted cask surface. Radiation is modeled using surface effect elements (SURF151). Convection is also applied to the surface of the cask using surface effect elements, and the convective heat transfer coefficient is given a value of 0.891 BTU/ft^2-hr-°F (5.1 W/m-°C). This value was derived from the cask vendor's analysis, and is roughly equivalent to natural convection.

Internally, heat generation was applied to the inner and outer fuel regions to simulate a 20kW internal heat loading. This internal heat loading was present for all parts of the analysis. Radial conduction was modeled through the cask wall, and the fuel region model accounts for radiation in the formation of an effective thermal conductivity value.

The normal (pre-fire) condition defined above is run to steady state to achieve a normal condition temperature distribution for the cask. This temperature distribution was checked against an analysis performed by the cask vendor, and was found to be in good agreement with the vendor's results. A plot of the normal condition temperatures for the cask is provided. (See Figure 4)

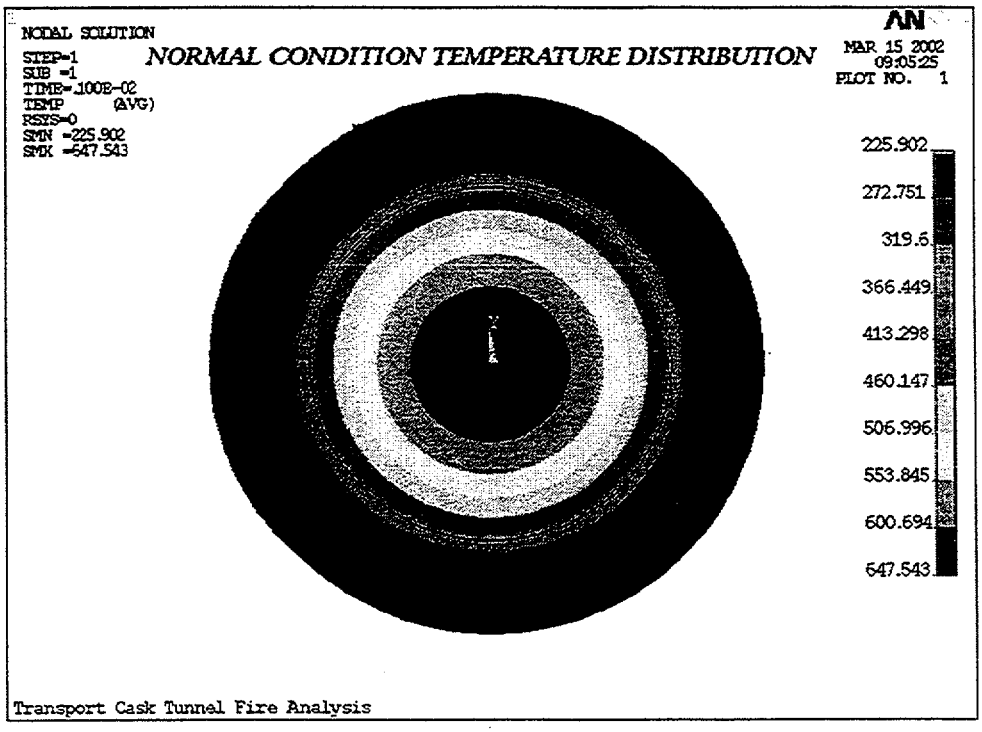

Figure 4

The cask was then subjected to a fire transient which consisted of the following conditions: an ambient of 1500°F (815.5°C), no solar heat flux (insolation), and an external convective coefficient of 2.5 BTU/ ft^2-hr-°F (14.2 W/m-°C). The convective coefficient is based upon the temperature and velocity of gasses in an open pool fire. Gas velocities in a pool fire can range from 13 feet/sec. (4 m/sec) to almost 40 feet/sec (12 m/sec)[9]. The convective coefficient used in the analysis is based on a gas velocity of over 40 feet/sec and serves to simulate the turbulent nature of the fire environment. The fire condition described above was run until the fuel region approached the fuel clad temperature limits described in the next section.

Following the fire transient, the cask was returned to normal conditions for 20 hours. For this post-fire transient, no solar heat flux (insolation) was applied. The ambient temperature was once again 100°F (38°C).

Analysis Results & Discussion

The results of the analysis show a maximum fuel region temperature of 1015°F (546°C), which occurred at 19.7 hours into the transient. The temperature distribution of the cask at the end of the fire (7 hours) is provided. (See Figure 5) A graph depicting the temperature rise of the cask skin, outer fuel region and fuel basket centerline is also provided. (See Figure 6) Due to the large mass of the cask, the maximum internal temperature of the MPC occurred over 12 hours after the end of the fire.

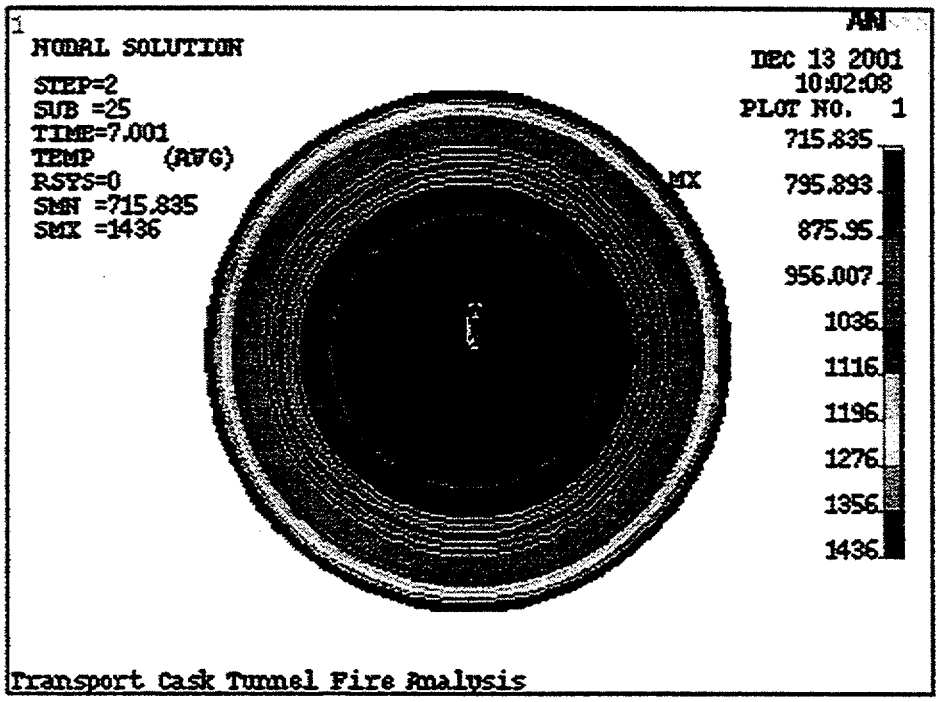

Figure 5

It should be noted that the maximum fuel region temperatures are not necessarily a precise indicator of what the maximum spent fuel cladding temperatures would be for this event. Spent fuel assemblies, when modeled accurately, will show a significant temperature gradient across the assembly, with the highest temperature (hottest fuel pin) usually near the center of the assembly. The gradient can be as much as 40°F from the coolest fuel pin to the hottest fuel pin in the assembly[10]. Fuel assembly homogenization tends to reduce the magnitude of the temperature gradient, producing an average temperature for the fuel assembly rather than a true maximum fuel temperature. Therefore, this analysis conservatively predicted that actual fuel cladding temperatures could be as much as 40 degrees (F) higher than the calculated maximum fuel region temperature.

The currently accepted short term fuel temperature limit for Zircalloy clad spent fuel is 1058°F (570°C)[4]. This limit is based on creep experiments done at this temperature. Two fuel cladding test samples held at 1058°F (570°C) remained undamaged (i.e., there was no significant observable damage) for times up to 30 and 71 days. These results indicate that in order for fuel cladding to be damaged, the 1058°F (570°C) limit would have to be exceeded continuously for more than 71 days. For a 7-hour fire and 20-hour cooldown, a conservative estimate of the maximum fuel cladding temperature would be 1055°F (568°C). (This number is reached by adding 40°F to the maximum fuel region temperature). This temperature would only be present for a short amount of time (less than 1 hour). Therefore, this analysis indicates that no cladding damage would have occurred due to this fire event.

The MPC, which contains the spent fuel, is a seal welded pressure vessel and is designed to American Society of Mechanical Engineers (ASME) Code, Section III, Subsection NB. In order for an external release of radioactive material to occur, the welds of the MPC would have to fail. The MPC has a maximum internal pressure limit of 125 psig (868 KPa) for accident conditions; however, this limit is only a fraction of the pressure that could possibly cause a seal weld failure. A pressure calculation was completed using the methodology provided in the cask vendor's SAR, and the pressure in the MPC at the highest cask internal temperature was found to be 95 psig (655.5 KPa).

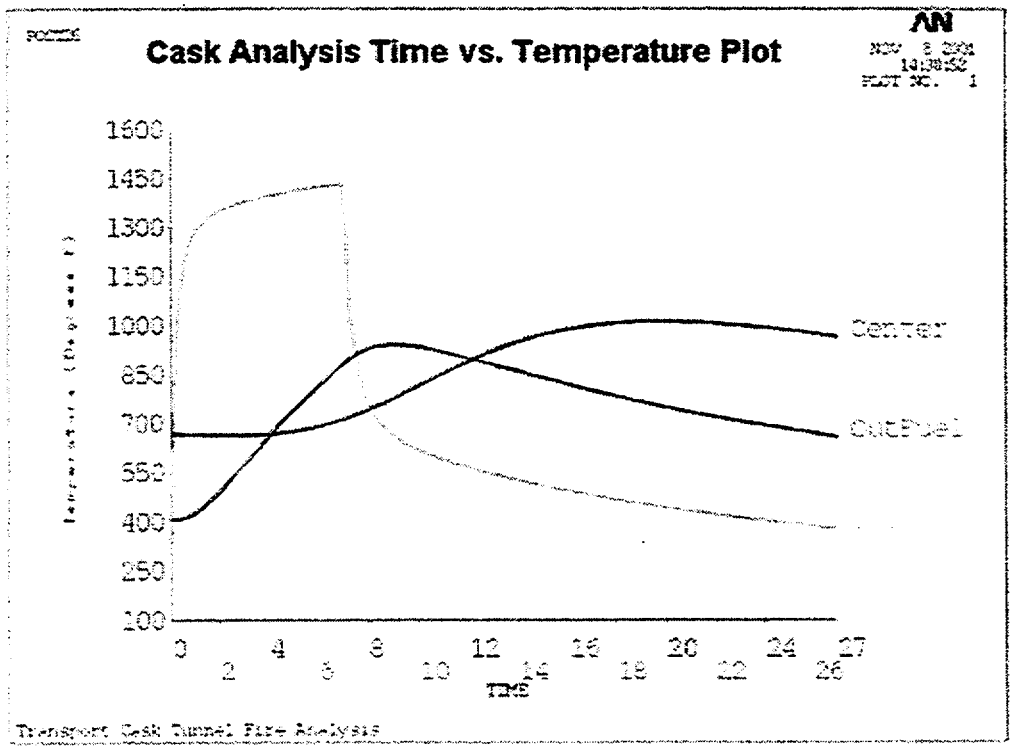

Figure 6

Conservatisms in the Transportation Cask Model

Several assumptions made in this analysis could be considered conservative. First, because the model was a 2-dimensional model, axial conduction is neglected. Therefore, temperatures obtained in the model will be higher than in an actual cask. Second, the rail car that would carry the cask for transport was not modeled. The transport railcar would prevent the spent fuel cask from being fully engulfed by a fire and would provide an additional heat sink. With the cask in place on the transport railcar, less heat would be directly absorbed by the cask, and cask temperatures would be lower. Third, natural convective cooling was assumed after the fire event. In reality, if a transport cask was involved in an accident and a fire ensued, there would be forced cooling (such as a hose-stream or a cooling fan) provided to the surface of the cask from emergency responders. This would reduce the internal

temperature rise of the cask. Finally, the internal heat load for the cask was the maximum allowed for the cask design (20 kW). It is unlikely that a cask would be carrying fuel at the maximum design thermal load.

Conclusion

It is clear from the preliminary analysis described in this paper that this specific transportation cask design could endure an engulfing fire of 1500°F (815.5°C) for 7 hours or more with no spent fuel cladding damage. The robust nature of such casks is clearly evident in the results of this analysis.

Current information indicates that the fire in Baltimore did not likely burn at full strength for the duration of the event, which means that if temperatures as high as 1500°F (815.5°C) were reached during the fire, it is unlikely that the temperature remained that high for a prolonged period of time.

As an extension of this study, the National Institute of Standards and Technology (NIST) will model the fire that occurred in the Baltimore tunnel to more accurately predict the temperatures that could have been reached during the fire.

With the new information provided by NIST, the staff will adjust the boundary conditions of this analysis to better simulate the actual conditions of the Baltimore tunnel fire and revise the analysis to include the effects of the cask transport rail car and the surrounding tunnel walls. This effort will provide additional insight into the performance of a spent fuel transportation cask in an actual tunnel fire event.

References

1) Title 10, Code of Federal Regulations, Part 71, *Packaging and Transportation of Radioactive Material*, Jan. 1, 2000, United States Government Printing Office, Washington, D.C.

2) Title 49, Code of Federal Regulations, Subchapter C, *Hazardous Materials Regulations*, Oct. 1, 2000, United States Government Printing Office, Washington, D.C.

3) National Transportation Safety Board Advisory, *Investigation into the Derailment of CSX Train L41216 in Howard Street Tunnel, Baltimore, Maryland*, August 7, 2001, Washington, D.C.

4) Johnson, A.B., Gilbert, E.R., *Technical Basis for Storage of Zircalloy-Clad Spent Fuel in Inert Gases*, Pacific Northwest Laboratory, PNL-4835, September 1983.

5) NRC Docket Number 72-1008, *Topical Safety Analysis Report for Holtec International Storage Transport and Repository Cask System* (HI-STAR 100 Cask System), Holtec Report HI-941184, Volumes I and II, Rev. 10

6) ANSYS, Inc., "ANSYS Users Guide for Revision 5.7.1," ANSYS, Inc., Canonsburg, PA, USA. 2001

7) Siegel, R. and Howell, J., 1992, Thermal Radiation Heat Transfer, 3rd ed., Hemisphere Publishing Co., p. 1040

8) ASME Boiler and Pressure Vessel Code, Section III, Subsection NB, American Society of Mechanical Engineers, 1995.

9) Nakos, J.T., and Keltner, N.R., *The Radiative-Convective Partitioning of Heat Transfer to Structures in Large Pool Fires*, Heat Transfer Phenomena in Radiation, Combustion, and Fires, ASME-HTD-Vol. 106, pp 381-387, 1989.

10) Creer, J.M., et. Al., "TN-24P PWR Spent Fuel Storage Cask: Testing and Analysis," EPRI NP-5128, Electric Power Research Institute, Palo Alto, California, 1987.

Stress Corrosion Cracking and Non-Destructive Examination of Dissimilar Metal Welds and Alloy 600

Deborah A. Jackson
Office of Nuclear Regulatory Research
United States Nuclear Regulatory Commission

ABSTRACT

The United States Nuclear Regulatory Commission (USNRC) has conducted research in the areas of assessment and reliability of Non-Destructive Examination (NDE) and environmentally assisted cracking since the 1977. Recent occurrences of cracking in Inconel (Alloy 82/182) welds and Alloy 600 base metal at several domestic and overseas plants have raised several issues. The occurrences of cracking have been identified through indirect means, specifically the discovery of boric acid deposits resulting from through-wall cracking in the primary system pressure boundary. Analyses indicate that the cracking has occurred due to primary water stress corrosion cracking (PWSCC) in Alloy 82/182 welds, in both hot leg nozzle-to-safe end welds and control rod drive mechanism (CRDM) nozzle welds. In addition, circumferential cracking of CRDM nozzles in Alloy 600 base metal originating from the outside diameter (OD) of the nozzle has been identified. The cracking associated with safe end welds is important due to the potential for a large loss of coolant inventory, and the cracking of CRDM nozzle welds and circumferential cracking of CRDM nozzle base metal is important due to the potential for control rod ejection and loss of coolant accident.

The industry response in the U.S. to this cracking is being coordinated through the Electric Power Research Institute (EPRI) Materials Reliability Project (MRP) in a comprehensive, multifaceted effort. Although the industry program is addressing many of the issues raised by these cracking occurrences, confirmatory research is necessary for the staff to evaluate the work conducted by industry groups. Several issues requiring additional consideration regarding the generic implications of these isolated events have been identified.

This paper will discuss significant events (i.e. at V.C Summer, Ringhals, and Oconee) of stress corrosion cracking (SCC); discuss the non-destructive examination (NDE) deficiencies in detecting SCC; discuss the NDE capabilities for control rod drive mechanisms, identify deficiencies in information available in this area such as crack initiation sites, crack growth rates; discuss United States Nuclear Regulatory Commission (USNRC) approach to address this issues; and the development of an international cooperative.

BACKGROUND

USNRC has conducted research in the areas of assessment and reliability of non-destructive examination (NDE) and environmentally assisted cracking since the 1977. Recent occurrences of cracking in Inconel (Alloy 82/182) welds and Alloy 600 base metal at several domestic and overseas plants have raised several issues. The occurrences of cracking have been identified through indirect means, specifically the discovery of boric acid deposits resulting from through-wall cracking in the primary system pressure boundary. Analyses indicate that the cracking has occurred due to primary water stress corrosion cracking (PWSCC) in Alloy 82/182 welds, in both hot leg nozzle-to-safe end welds and control rod drive mechanism (CRDM) nozzle welds. In addition, circumferential cracking of CRDM nozzles in Alloy 600 base metal originating from the outside diameter (OD) of the nozzle has been identified. The cracking associated with safe end welds is important due to the potential for a large loss of coolant inventory, and the cracking of CRDM nozzle welds and circumferential cracking of CRDM nozzle base metal is important due to the potential for control rod ejection and LOCA

One of the early incidences of reactor vessel head cracking was the incidence of cracking that occurred in France at Bugey Unit 3 in 1991. In December 1991 Electricite de France (EDF) undertook the task to replace all reactor vessel heads in France. EDF concluded that the cost to replace the heads was less than the cost to repair all reactor vessel heads.

DOMESTIC EVENTS

In 2000 and 2001 there were instances of significant cracking in Alloy 82/182 welds in commercial pressurized water reactors (PWRs). Confirmed cracking in the reactor vessel head penetrations and cracking in the primary system piping was identified in Oconee and V.C Summer, respectively. V.C. Summer, a Westinghouse 3 loop plant that went into commercial operation in January 1984, identified leakage in the "A" outlet nozzle-to-pipe weld of the primary system piping. In October 2000 approximately 300 pounds of boric acid was identified during a containment building walkdown during a refueling outage. The origin of the boric acid was identified as a small weep hole in the alloy 82/182 field weld. Initial NDE identified a circumferential crack. Additional NDE, eddy current testing (ET) with ultrasonic testing (UT), performed from the inner diameter (ID) confirmed a through wall axial crack in the A hot leg in the 182/82 weldmetal, extending to the basemetal on either side of the weld, in an area previously repaired during construction. The weld with this cracking was located approximately 3 feet from the reactor vessel. Additional examinations of the remaining five nozzle safe ends found crack indications, but no through-wall cracks. Figure 1 shows a schematic of the area of the axial crack.

Confirmed incidences of cracking in the control rod drive mechanism nozzles and housing seal welds were identified in all three of the Oconee units. Oconee Units 1, 2, and 3 are Babcock & Wilcox (B&W) PWRs. Unit 1, which went to into commercial operation in July 1973, identified boric acid deposits on the vessel head in November 2000. Axial cracking was confirmed in the alloy 600 nozzle base metal and the 182 nozzle weld metal. Oconee Unit 2 went into commercial operation in September 1974. Boric acid deposits on the vessel head of Unit 2, identified in May 2001, were the result of circumferential cracking in alloy 600 base metal and 182 weld metal. Unit 3 began commercial operation in December 1974 and identified boric acid

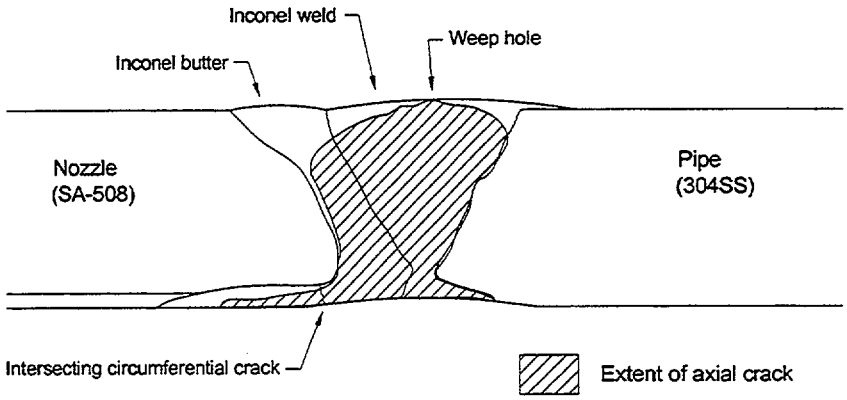

Figure 1 V.C. Summer A Hot Leg

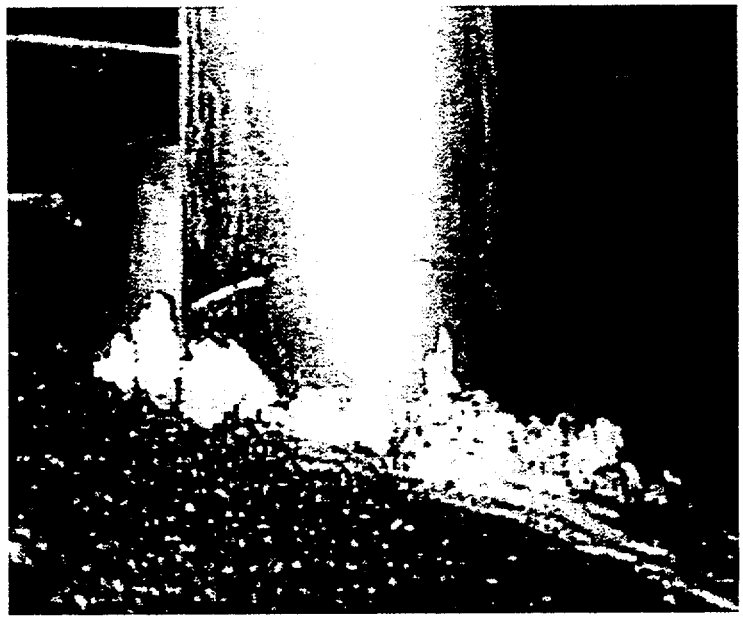

Figure 2. Boric Acid Deposits on Oconee Unit 1 Reactor Vessel Head

deposits on the vessel head in February 2001 from circumferential cracking in the alloy 600 base metal and 182 weld metal. Figure 2 shows boric acid deposits on Oconee Unit 1 reactor vessel head. Crystal River Unit 3, another B&W PWR, identified circumferential through wall cracking after boric acid deposits were identified during inspections of the vessel head.

At the end of 2001, the majority of the vessel head penetration indications were identified in B&W designs. North Anna Unit 1, a Westinghouse PWR that began commercial operation in 1974, identified boric acid deposits on the CRDM nozzles. The results of the North Anna Unit 1 examination as of this date were identified as CRDM housing leaks. The NRC recently issued Bulletin 2001-01 "Circumferential Cracking of Reactor Pressure Vessel Head Penetration Nozzles," that requests licensees to provide information related to the structural integrity of the reactor vessel head penetration nozzles. The mechanism which caused the cracking in previously discussed events was PWSCC.

FOREIGN EVENTS

Electricite de France's (EDF) Bugey Unit 3 was one of the first identified occurrences of reactor vessel head cracking. In September 1991 axial cracking of CRDM nozzles IDs was confirmed and the decision to replace all reactor vessel heads was made in December of the same year. Studies of repair versus replacement concluded that replacement was the more cost effective decision. The control rod drive mechanisms in the replaced reactor vessel heads are constructed with alloy 690 base metal with alloy 152 weldmetal. Presently, NDE is performed using liquid penetrant, UT, ET, and visual testing. No defects have been found to date and EDF has concluded that the consequences of VC Summer and Oconee incidents are not applicable to plants in France

Ringhals Unit 3 in Sweden is a Westinghouse 3 loop PWR that went into commercial operation in 1981. In October 2001, NDE (ET and UT) identified two indications in a vessel nozzle safe-end that were initially evaluated as sub-surface planar flaws. Re-evaluation of these results, subsequent to more significant findings at Ringhals 4, revealed that cracks were initially undersized and were larger than qualification targets.

Ringhals Unit 4, also a Westinghouse 3 loop PWR, went into commercial operation in 1983. NDE (ET and UT) identified several indications in a vessel nozzle safe-end which were evaluated as volumetric defects in a repaired area. Of the defects, three were identified as sub-surface planar flaw and one as a surface breaking planar flaw larger than qualification targets. Further destructive examination revealed that two cracks were undersized and all were surface breaking flaws.

It is interesting to note that Ringhals Unit 4 had extensive weld repairs but Unit 3 had no repaired areas. Similar to V.C. Summer, Ringhals Unit 4 had extensive ID weld repair. There are concerns as to why the cracks are so tight and what must be done to adequately simulate these cracks for inspection qualification processes which will results in meaningful ISI in the future.

NDE CHALLENGES

The NDE challenges associated with the dissimilar metal welds and alloy 600 cracking issue have made it clear that additional long term solutions must be developed. Complex grain structure, geometry, and grain growth patterns all contribute to the difficulty in detecting and sizing indications. Some locations are inaccessible. Limiting radiation exposure during these

examinations is another factor that requires efficient examinations. Visual examinations from the top of a surface such as the vessel head are the most cost effective method of identifying leaks.

The V.C Summer and Ringhals events were identified as PWSCC of large butt welds leading to primary system leaks. The PWSCC in both plants were predominantly axial indications with significant branching that included cracks with small circumferential components. Circumferential flaws in primary system butt welds are of concern as they could lead to pipe breaks. Since the length of axial flaws was limited to the width of the weld, axial flaws pose less of a safety concern. The specific challenges with the butt weld configuration is detecting flaws initiating from the ID due to the weld geometry. Transducer lift-off affects flaw detection and in field welds is more of a problem than in shop welds. There is also limited crack growth data for alloy 600 material which presents problems for flaw evaluation to determine acceptable intervals between ISI examinations.

The NDE challenges in identifying PWSCC in CRDM nozzles are related to the fact that current programs have focused on flaws initiated on the nozzle ID and current techniques for OD initiated flaws are not qualified. Volumetric examinations of CRDM nozzle tubes and welds are also unqualified at this time. Due to various plant designs there is no uniform method to perform effective visual examinations of the vessel head. For effective visual examinations (VT-2) to be performed on the CRDM penetration, the entire area surrounding the CRDM penetration must be visible. This requires removal of the insulation or in cases where clearances exist, performing remote inspections between the insulation and the vessel head. Additional challenges are presented by reactor vessel heads that have insulation glued to the surface. Access to the vessel head is not possible with insulation that is adhered to the head. In addition, leak detection should not be relied upon as a substitute for an effective visual examination since leak rates may be very low. There must be adequate access to the reactor vessel head in order to perform a reliable inspection of the CRDM penetrations.

INDUSTRY INITIATIVES

The recent industry events of cracking are re-setting priorities for the development of adequate NDE and demonstration activities. Industry has been extremely proactive in responding to this issue and has developed a comprehensive, multifaceted program to address this issue. The industry program addressing PWSCC in reactor vessel head penetrations is being coordinated by the Electric Power Research Institute's (EPRI) Material Reliability Program (MRP) in cooperation with Nuclear Energy Institute (NEI) and various NDE vendors and owners groups.

American Society of Mechanical Engineers (ASME) Boiler and Pressure Vessel Code, Section XI, formed a task group on alloy 600/182 cracking which has the responsibility for developing and proposing Code revisions and Code cases concerning Alloy 600/182. The task group held its initial meeting at the ASME Section XI meeting in August 2001. The task group will develop changes to ASME Section XI that address examination, repair, and replacement requirements of Alloy 600/182 used in pressure boundary applications. The task group will also evaluate the need for changes in the examination of other alloy 600/182 components.

NRC RESEARCH INITIATIVES

The Office of Nuclear Regulatory Research (RES) has identified areas that will require additional research and development in order to fully understand the mechanisms of PWSCC and the root causes. Presently, industry is developing short-term solutions which will address the near term problem. Additional research must be completed to make certain that all uncertainties associated with PWSCC, including NDE and crack growth data are adequately addressed. Reliable NDE methods and systems must be developed and their performance must be demonstrated.

The Office of Nuclear Regulatory Research formed an independent group of experts to review the technical aspects of the reactor vessel head penetration cracking problem. Crack growth rates and volumetric examinations were two of the areas in which the panel provided recommendations. For crack growth rates the panel noted that, due to the possibility of the concentration of aggressive chemical species in the annulus between reactor vessel head penetrations and the reactor vessel head, it is probable that crack growth rates for OD cracking may be higher than expected for SCC in Alloy 600. The panel also reviewed NDE, specifically concentrating on the reliability and effectiveness of volumetric examinations. An extensive literature review was completed, dating back to the early 1990s after Bugey Unit 3 vessel head cracking was observed in France. Results of the independent evaluation of the reactor vessel head penetration cracking identified the need for volumetric examinations for plants with known cracking and that volumetric examinations would be the preferred method for plants with a high susceptibility to PWSCC. The expert group noted that given the nature of the observed cracking, a limited volumetric inspection in a sampling basis would not be adequate to deal with the uncertainties. NDE vendors currently have equipment capabilities but the inspection methods are not yet qualified. In addition, it was concluded that inspections could be effective if adequate pre-qualifications can be performed. Existing research programs are being modified and new programs being developed as necessary to address the short-term and long-term needs of NDE, crack growth rates studies related to the issue of PWSCC. Developing improvements for the use of various UT techniques such as phased-array and SAFT-UT are being studied as part of the USNRC research programs at Pacific Northwest National Laboratory (PNNL).

An International Research Cooperative on Inconel cracking is being developed in RES to address the issue of PWSCC. The objectives of the research cooperative are to compile a knowledge base on all cracking in Inconel; to identify the mechanisms that cause cracking in Inconel develop NDE methods to adequately detect, size and characterize tight cracks such as PWSCC; and develop adequate mockups and training aids with artificial cracks to simulate tight PWSCC indications. With the incidences of reactor vessel head cracking occurring in PWRs and mostly in B&W plants, there are additional questions that arise. Is this a generic problem for PWR as IGSCC was a generic problem for BWRs? If so, what factor or factors would eliminate PWSCC as a generic problem for Inconel and how many NSSS vendors worldwide have identified this problem with PWSCC. The research cooperative will attempt to address each of these issues and provide answers to the previously discussed questions.

CONCLUSIONS

The most recent events of stress corrosion cracking are resulting in new priorities for NDE development, including performance demonstration activities. The generic implications of the cracking mechanism are not fully understood. Because the generic implications are not fully understood, confirmatory research needs to be performed in conjunction with industry initiatives to address this issue of "Stress Corrosion Cracking and Non-Destructive Examination of Dissimilar Metal Welds and Alloy 600".

REFERENCES

USNRC memorandum from J. Strosnider/M. Mayfield to S. Collins/ A. Thadani " Results of Independent Evaluation of Recent Reactor Vessel Head Penetration Cracking" Sept 7, 2001 ADAMS Accession No. ML012550290

"Circumferential Cracking of Reactor Pressure Vessel Head Penetration Nozzles," NRC Bulletin 2001-01, August 3, 2001

"Crack in Weld Area of Reactor Coolant System Hot Leg Piping at V.C. Summer," Information Notice 2000-17, October 18, 2000

"Crack in Weld Area of Reactor Coolant System Hot Leg Piping at V.C. Summer, " Information Notice 2000-17, Supplement 1, November 16, 2000

"Aging Evaluation of Cables in Japan"

Atsunori Yamaguchi
Tsurumi Research and Development Center
Japan Power Engineering and Inspection Corporation

Abstract

Cables used in the nuclear power plants which had been operated for 30 years were technically evaluated and the functional capabilities of cables throughout the plant service life, including the extended life, were ensured.

Many new findings obtained in Japan are introduced. As for radiation aging, the oxygen penetrating length (La), which controls the degree of radiation induced oxidation degradation, is formulated and made clear to depend on both the dose rate and the oxygen pressure on the polymer. Synergistic effects of thermal aging and radiation aging are also formulated, which shows the influence of combined and sequential environmental conditions. The value of activation energy, Ea, which controls the temperature sensitivity of the degradation rate by thermal aging, was experimentally shown not to be constant over the whole temperature domain around 373K.

Based on the new findings mentioned above, Environmental Qualification Methods of cables will be improved near future in Japan.

1.Introduction

30 years have already passed since the commercial nuclear power plants started operation in Japan. 51 plants are operated now, and among them, Tsuruga power Plant Unit-1, Mihama Power Plant Unit-1 and Fukushima No.1 Nuclear Power Unit-1 have been operated over 30 years.

Under these circumstances, the Ministry of International Trade and Industry (MITI, now METI) issued "Basic Policy on Aged Nuclear Power Plants" in April, 1996. According to the MITI report, electric utility companies performed the detailed technical evaluations of nuclear power plant components when they reached 30 years of service life and established the detailed long-term maintenance schedules thereafter.

The final reports concerning the technical evaluations conducted by the three electric utility companies on 3 nuclear powers plant mentioned above were issued in February 1999. Aging of cables were evaluated in these reports, because polymer materials used as insulating materials of cables were known to be degrated by thermal aging and radiation aging.

2. Technical Evaluation of Cable Aging[1)]

Safety-related cables installed within the containment vessels of nuclear power plants were classified according to the types (high voltage cable, low voltage cable, co-axial cable) and insulating materials. Technical evaluations were performed for the representative cables of each groups in accordance with "Recommendation methods on environmental qualification tests and tests for fire prevention of electric cables used in nuclear power plants " (The Japanese Electrotechnical Committee technical report (II) No.139) based on IEEE Std. 323 & 343. Tests were performed under the conditions which enveloped the normal operating conditions, including extended life. Examples of test conditions for high voltage cables are shown in the following table.

For Cables, which must fulfill the function during LOCA, tests were performed adding the LOCA conditions. Mandrel bend tests were done for the aged test samples and no loss of insulation resistance occurred. The functional capabilities of cables throughout the plant service life, including

the extended life, were ensured by these test results.

3. Japanese R&D activities on aging evaluation of cables

By the way, the Recommendation methods mentioned above was issued in 1982. Since then, researches in the aging evaluation of cables have been performed and the following new findings have been obtained in Japan.

(1) Aging mechanism and accelerated radiation aging[2)]

Polymer materials for insulators are degraded by irradiation under the existence of oxygen because of the radiation-induced oxidation.

When a polymer film is irradiated, active sites are produced on the polymer chains. The sites combine each other to form cross-linking, or react with oxygen molecules to form oxidative products as follows.

$$P(\text{polymer}) \xrightarrow{\Phi I} P\cdot \text{ (active site)} \quad (1)$$

$$P\cdot + P\cdot \xrightarrow{k_1} P-P \text{ (cross-linking)} \quad (2)$$

$$P\cdot + O_2 \xrightarrow{k_2} PO_2 \text{(oxidative product)} \quad (3)$$

From mass balances of the active site and oxygen, the following equations are obtained.

$$d[P\cdot]/dt = \Phi I - k_1[P\cdot]^2 - k_2[P\cdot]C \quad (4)$$

$$\partial C/\partial t = D\partial^2 C/\partial \chi^2 - k_2[P\cdot]C \quad (5)$$

where $[P\cdot]$ is the concentration of active site, Φ the specific rate constant of active site formation, I the dose rate, k_1, k_2 the rate constants for the combination and oxidation of active sites, C the oxygen concentration in the film, D the diffusion coefficient of oxygen in the film and χ the distance from the center of the film cross section.

By numerical calculation of the above equations, the oxygen penetrating length, La, from the film surface is expressed approximately by the following equation.

$$La = (2DC_0/\Phi I)^{1/2} = (2DSP/\Phi I)^{1/2} \quad (6)$$

where C_0 is the oxygen concentration at the film surface, S the solubility constant of oxygen and P the oxygen pressure on the film. As seen in the above equation, La increases with decreasing dose rate at constant oxygen pressure at constant or increasing oxygen pressure at constant dose rate.

Polyethylene (PE) and ethylene-propylene rubber (EPR) were irradiated under vacuum and the gel fractions were measured. Figure 1 shows that the gel fraction decreases linearly with the square root of oxygen pressure, and the slope of the straight line depends on the film thickness and the dose rate.

If the gel fraction is formed only in the non-oxidation region, the gel fraction of the whole film (gel_t) is expressed by the following equation.

$$gel_t = gel_{vac}(1-2La/L) = gel_{vac}\{1-2(2DSP/\Phi I)^{1/2}/L\} \quad (7)$$

where gel_{vac} is the gel fraction in the non-oxidation region and is equal to that of the film irradiated under vacuum, L the film thickness.

The slope of the straight line of Fig.1 is equal to $2(2DS/\Phi I)^{1/2}/L$ in equation (7). $(DS/\Phi)^{1/2}$ were calculated using equation (7) and compared with the ones obtained from the slopes of the straight lines in Fig.1. Table 2 shows that the calculated values agree well with the experimental ones.

(2) Synergistic effects of thermal aging and radiation aging[3)]

Cables in the nuclear power plants sustain thermal aging and radiation aging simultaneously. It is known that there is synergism on organic polymer degradation in combined radiation and

The index of degradation, D(r-ox), by radiation-induced oxidation is expressed in eq. (8).

$$dD(r\text{-}ox)/dt = \alpha I \quad (8)$$

where α is a constant, I the dose rate and t the irradiation time. The index of thermal degradation, D(T), is expressed using Arrhenius equation in eq. (9).

$$dD(T)/dt = K_0 \exp(-E/RT) \quad (9)$$

where K_0 is a constant, E the activation energy, R the gas constant and T the aging temperature. The synergistic effects are seen in the simultaneous exposure to the radiation and the elevated temperature, and the pre-irradiated dose dependency on the thermal degradation can be expressed in eq. (10).

$$dD(r \longrightarrow T)/dt = 2\beta I K_0 \exp(-E/RT) \quad (10)$$

where β is a factor of radiation thermal combined aging or the coefficient of synergism. The radiation thermal simultaneous oxidative degradation, D(r,T), can be derived by integrating and summing eqs. (8), (9), (10).

$$D(r,T) = \alpha I t + K_0 (1 + \beta I t)\, t K_0 \exp(-E/RT) \quad (11)$$

The synergistic effects of thermal aging and radiation aging are shown as follows, by combining the above eqs.(8), (9), (10), (11).

radiation followed by thermal aging { D(r-ox)+ D(T)+D(r⟶T) }

>simultaneous aging by radiation and high temperature { D(r,T) }

>thermal aging followed by radiation { D(T)+D(r-ox) }

(3) Accelerated thermal aging technique

Arrhenius's law is often used as a physical model for life time prediction during thermal aging. It assumes that the rate of the thermal aging decreases with the inverse of the temperature. A plot of the reaction rate on a log scale against 1/T should yield a straight line whose slope is determined by the activation energy Ea. The activation energy, Ea, controls the temperature sensitivity of the degradation rate.

But the experimental results[4),5)], carried out over a large range of temperature, showed the "break point"s in the plots. An example of this effect in a polymer is shown in Fig.2[4)], where change in slope is observed. It was observed that thermal oxidation occurred nearly uniform over the cross section of insulating material in the lower temperature range, though thermal oxidation occurred mainly near the outer surface region in the higher temperature range[5)]. This phenomenon seems to be one of the reasons why the "break point" in the plot occurs.

In such condition, an extrapolation based on the data measured at high temperature would give an underestimation of the aging at lower temperature. So, the value of activation energy, which is used for acceleration tests, is of major importance in obtaining representative data.

4.Summary

Cables used in the nuclear power plants which had been operated for 30 years were technically evaluated according to the "Recommendation methods on environmental qualification" issued by the Japanese Electrotechnical Committee, and the functional capabilities of cables throughout the plant service life, including the extended life, were ensured.

Since the issue of "Recommendation methods", many new findings have been obtained in Japan. As for radiation aging, the oxygen penetrating length (La), which controls the degree of radiation induced oxidation degradation, is formulated and made clear to depend on both the dose rate and the oxygen pressure on the polymer. Synergistic effects of thermal aging and radiation aging are also formulated, which showed the influence of combined and sequential

environmental conditions. The value of activation energy, Ea, which controls the temperature sensitivity of the degradation rate by thermal aging, was experimentally shown not to be constant over the whole temperature domain around 373K.

Based on the new findings mentioned above, Environmental Qualification Methods of cables will be improved near future in Japan.

Reference

1) Technical Evaluation Report of Aging Countermeasures for nuclear power plants: Tsuruga Unit-1 (JAPC), Mihama Unit-1 (KEPCO) and Fukushima No.1 Unit-1 (TEPCO), February, 1999

2)T.Seguchi, S.Hashimoto, K.Arakawa, N.Hayakawa, W.Kawakami and I.Kuriyama,"RADIATION INDUCED OXIDATIVE DEGRADATION OF POLYMERS- I , OXIDATION REGION IN POLYMER FILMS IRRADIATED IN OXYGEN UNDER PRESSURE " Radiat. Phys. Chem. Vol. 17 pp.195-201 1981

3)T.Seguchi "ANALYSIS OF DOSE RATE DEPENDENCE ON RADIATION THERMAL COMBINED AGEING OF POLYMER MATERIALS" Proceeding of the International Topical Meeting on Operability of Nuclear Power System in Normal and Adverse Environments, Albuquerque, Sep. 29- Oct.3, 1986

4)S.Nakanishi, K.Mito, K.Kikuchi, M.Konishi, S.Suzuki, T.Yamamoto, "EVALUATION OF THE ENVIRONMENTAL QUALITY OF CABLES AT PWR PLANTS IN JAPAN" ICONE-9 April 2001

5)M.Sugiyama, T.Seguchi, et al., The Japanese Electrotechnical Committee Research Memo, DEI-94-88, 1994

Table 1 : Test conditions for technical evaluation of cables [1]

Test conditions	Tsuruga Unit-1	Mihama Unit-1	Fukushima No.1 Unit-1
Temperature -exposured day	394K-7days	418K-32days	394K-7days
Total dose	500kGy	450kGy	500kGy

Table 2 : $(DS/\Phi)^{1/2}$ obtained by calculation and experiment[2]

	Film thickness (mm)	Dose rate (Gy/h)	$(DS/\Phi)^{1/2}$ caluculation	$(DS/\Phi)^{1/2}$ experiment
PE	1.0	950	0.29	0.29

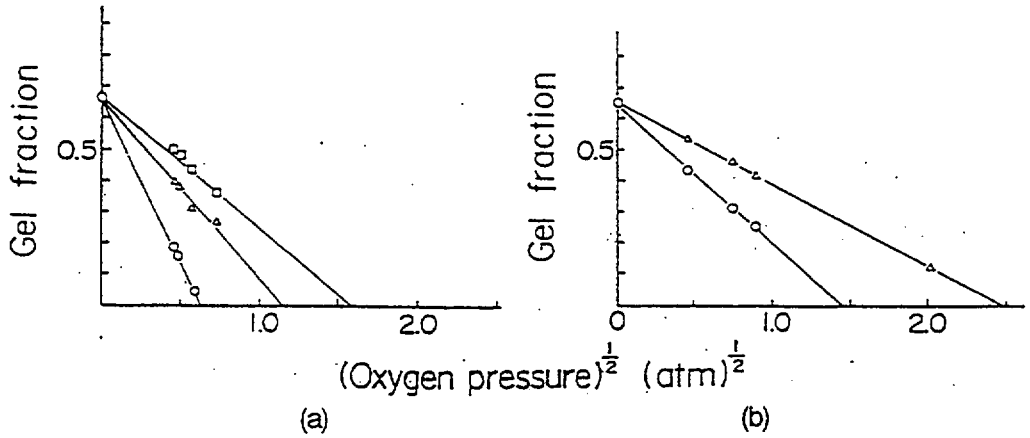

Fig.1 Relation between gel fraction and square root of oxygen pressure in radiation-induced oxidation of polyethylene film at room temperature and dose rates of (a) 950kGy/h and (b) 5kGy/h[2]

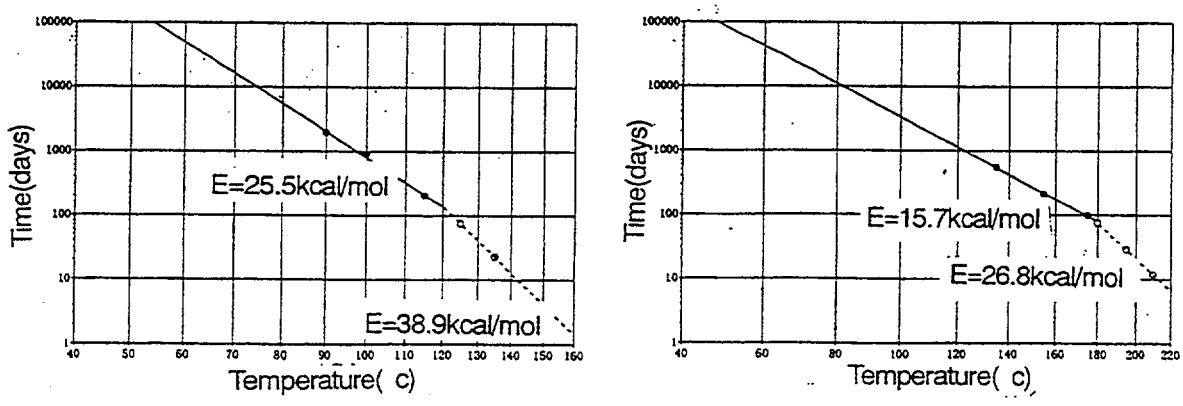

Fig.2 Arrhenius plot of (a) EP rubber, (b) Silicon rubber [4]

METHODS TO INTEGRATE AGING EFFECTS INTO PROBABILISTIC RISK ASSESSMENTS

Arthur Buslik
Division of Risk Analysis and Applications
Probabilistic Risk Analysis Branch
U.S. Nuclear Regulatory Commission
Washington, DC 20555

Abstract

This paper describes a method for integrating cable aging effects into probabilistic risk assessments. The method uses reliability physics models to estimate the cable failure probabilities. Essentially, deterministic lifetime prediction models are modified by introducing an initial resource, or capacity, which has randomness associated with it, and by introducing uncertainty distributions on the parameters of the lifetime prediction model. The initial step in the method is a screening analysis, to see which cable failures may be neglected. This step is used because the evaluation of the failure probabilities of cables by reliability physics models can be labor intensive. The final step, the use of the cable failure probabilities in the fault trees and event trees, is relatively straightforward, but the evaluation of the probability of operator actions when the operator is presented with erroneous or missing information from failed instrumentation can present difficulties.

Introduction

The inclusion of the aging of systems, structures, and components in probabilistic risk assessments (PRAs) is important (1) to gain additional confidence that the risk from aging is acceptable, (2) to determine the most risk significant structures, systems, and components (SSCs) from the viewpoint of aging, and (3) to reduce, if necessary, the risk by, for example, inspection, testing, and condition monitoring of risk significant components and by taking appropriate action depending on the condition of the SSC. The work in this area has recently focused on passive SSCs; other SSCs are overhauled/replaced on a schedule which is expected to control the effects of their aging. The work presented in this paper will describe a method to incorporate cable aging into PRA. The scope of the paper is limited to instrumentation and control (I & C) cables inside containment. Cables inside containment are liable to a potential common mode failure mechanism, since cables associated with redundant trains of a system are exposed to the same or similar harsh environment after a loss of coolant accident (LOCA). Hence they may potentially be an important source of risk. Instrumentation and control cables may be relatively more important than power cables, because leakage currents could cause misleading operation indications, and failure of automatic actuation of equipment. Relatively small leakage currents in power cables would likely not affect their function. The current study will not consider cable terminations or connectors, or the possible effects of condition monitoring of cables on the risk. The emphasis will be on effects of cable aging on the core damage frequency, although much of the method may be useful for determining the effects of cable aging on other risk measures, such as large early release frequency, or expected offsite consequences.

One difficulty with the incorporation of the aging of passive SSCs into PRA is that failure data are sparse. This difficulty is even greater for I & C cables inside containment, since there is little or no data on the failure of in-containment I & C cables during the harsh environment of a LOCA. The risk of common mode failure of in-containment cables during a LOCA is thought to be controlled by the use of environmental qualification techniques involving accelerated aging, but it is desirable to verify this.

One approach to the problem of sparse data is to use reliability physics models to estimate the failure probabilities. Prior work in this area was performed at INEEL by Smith et al. (Ref. 1). In this prior study, the example of flow accelerated corrosion in secondary system piping was chosen.

Because of the resource-intensive nature of the use of reliability physics models, the first step in the method is the use of screening methods to select those cables for which detailed reliability physics methods must be used; the effect on the risk of other cables will be neglected, or treated by bounding calculations. The screening is performed by the use of risk importance methods. After the cable failure probabilities, as a function of cable age are calculated, they are inserted into PRA calculations (event-tree/fault-tree calculations) to estimate the effect on the core damage frequency of the cables, as a function of plant age.

Screening Method

The cable failures of concern are those that occur after an initiating event [loss of coolant accident (LOCA) or transient-induced LOCA] which causes a harsh environment in containment. Since the harsh environment has the potential to cause failure of cables in redundant trains, it is not appropriate to use single component importance measures. Instead one uses measures of importance of the joint failures of cables in redundant trains.

Let X = Event that the I & C cables in redundant trains of some system are failed

Consider:

$$I(t)=\sum_{E_I} f(E_I)(pr\{C|X,E_I\}-pr\{C|\bar{X},E_I\})pr\{X|E_I,t\}, \quad (1)$$

where:

C = event that core damage has taken place
E_I = initiating event; $f(E_I)$ = frequency of E_I
t = cable age, assumed the same as plant age
I(t)= contribution to core damage frequency from event X, in the sense that the core damage frequency would be reduced by the amount I(t) if X never happened.

The above equation for I(t) does not explicitly express the fact that the cable failures X may have a greater effect on the core damage frequency (or the core damage probability given an initiating event E_I) if the cable failures occur early in the accident instead of later. For example, at Surry, for a small break LOCA, it may be necessary to have operation of the containment sprays early in the recirculation period, to remove decay heat from the containment. However, later in the accident, when decay heat levels are less, sufficient heat removal may occur through the steam generators, or the residual heat removal system

may be put into service. Thus, if cables associated with containment pressure sensors fail early in the accident, and the operator does not manually initiate containment sprays, core damage may occur. However, if the cables fail later in the accident, core damage may be averted, even if the containment sprays are stopped because of faulty information being supplied to the operator as to containment pressure. In general, component failures occurring late in an accident are considered to have lesser risk significance than those occurring earlier (see Ref. 2, p. 21).

The effect of the time at which the cables fail on the value of I(t) may be included explicitly in Eq. (1) by writing

$$pr\{C|X,E_I\} = \int_0^\infty pr\{C|E_I,t_a\} f(t_a|E_I) dt_a \quad . \tag{2}$$

where t_a = time during accident that the failure event occurs, and $f(t_a|E_I)dt_a$ is the probability that the cable failures X will occur between t_a and t_a+dt_a, given that the failure occurs.

It is possible to use I(t) as a guide for screening. Evaluate $pr\{C|X,E_I\}$ assuming X occurs early in the accident. If, even with the probability of cable failure, $pr\{X|E_I\}$, equal to unity, the value of I(t) is small, one can screen out the cable failures X. In other words, if the Birnbaum importance,

$$\sum_{E_I} f(E_I)(pr\{C|X,E_I\} - pr\{C|\bar{X},E_I\}) \quad , \tag{3}$$

is small, then X can be screened out. There is a difficulty with this approach. The quantity $pr\{C|X,E_I\}$ represents the probability of core damage, given the cable failures X and the initiating event E_I. But the cable failures X are associated with instrumentation and control cables. If the cables are instrumentation cables, then the evaluation of $pr\{C|X,E_I\}$ involves evaluating the probability of a human recovery action given failure of instrumentation. This can be a difficult probability to evaluate. For example, suppose, in the given accident sequence, it is necessary for the containment sprays to actuate, in order to avoid core damage. If the containment sprays do not actuate, because of failure of cables associated with containment pressure sensors, then one has to estimate the probability of manual actuation of the containment sprays, given failure of containment pressure indication in the control room. It therefore seems best, at this point, to evaluate the probability of human recovery conservatively, and not try to obtain a realistic estimate. If one cannot screen out the failures X with a conservative human error estimate, one continues further with the evaluation of the probability of the cable failures.

Cable Failure Probabilities

We assume that the cable has an initial capacity (or resource) h_0 which is degraded by aging stressors such as temperature T and dose rate D. If the rate of degradation is R(T,D), for fixed T, D, then at time t the capacity h is given by

$$h=h_0-tR(T,D). \tag{4}$$

When the resource h falls below some value, failure occurs, for a given set of environmental conditions. The set of environmental conditions we are considering are those for a LOCA, including the humidity conditions of a LOCA. We will consider the environmental conditions of the LOCA as more or less

fixed, analogous to a fixed stress in a strength-stress reliability model. The model we are using is the simple wear model given in Chapter 8 of Ref. 3. In general, the value of h_0 will be considered to be a random variable, corresponding to a certain randomness in the initial capacity of the particular segment of cable we are considering. Also, there is uncertainty in the value of R(T,D). The degree of degradation is determined by the value of h. If, for two different sets of (t, T, D) the values of h are the same, then the two different sets of (t,T,D) correspond to equivalent degrees of degradation. Suppose that, for two segments of cable made of the same material, it is possible to assume, for the case at hand, that the values of h_0 are the same, to an adequate degree of approximation. Suppose that radiation dose effects are negligible, and the rate of degradation due to temperature is given by an Arrhenius expression. Then the times to equivalent degradation (i.e, times to equivalent values of h) are given at temperatures T_1, T_2 by the values t_1, t_2 related to each other by

$$e^{-\frac{E}{RT_1}t_1}=e^{-\frac{E}{RT_2}t_2} \tag{5}$$

where E is the activation energy, and R is the molar gas constant. This suggests that if cables are qualified for, say, a lifetime of t_1 years at a temperature T_1, and if the temperature T_2 during normal operation at the location of the cables is considerably less than T_1, so that t_2 is considerably longer than the plant lifetime, then one may neglect the cable failures under consideration. This assumes that radiation dose effects can be neglected, and that any uncertainties associated with the similarity of the cable undergoing the qualification test and the cable in the plant are sufficiently small as to not affect the results. For example, the activation energies for the cable undergoing qualification testing and the cable in the plant must be sufficiently close, and the values of the initial resource h_0 for the two cables must be sufficiently close.

Let us now consider the more general case where radiation dose effects cannot be neglected. In Ref. 4, on p. 79 of vol. II, empirical relationships are given which relate the time to equivalent degradation for two cables, one exposed to a dose rate D at some reference temperature T, and the other at the same reference temperature, but at zero dose rate. If we denote t_1 as the time to some given degradation at the reference temperature with zero dose rate, and t_2 as the time to the same level of degradation at the same temperature with dose rate D, then

$$t_2=\frac{t_1}{1+k(T)D^n} \tag{6}$$

where k(T) and n are empirical constants, with k possibly depending on temperature. This equation is valid for all degradation levels. In terms of h, one has

$$h(T,0,t_1)=h(T,D,t_2)$$

Taking derivatives with respect to t_1 one has

$$\frac{dh(T,0,t_1)}{dt_1}=\frac{dh(T,D,t_2)}{dt_2}\frac{dt_2}{dt_1}=\frac{dh(T,D,t_2)}{dt_2}\frac{1}{1+k(T)D^n}$$

or, writing the rate $dh(T,0,t_1)/dt_1$ as $R(T,0)$ and $dh(T,D,t_2)/dt_2$ as $R(T,D)$,

$$R(T,D)=R(T,0)(1+k(T)D^n) \tag{7}$$

In other words, the rates of degradation, as given by Eq. (7), are inversely proportional to the times to equivalent degradation, as given by Eq. (6).

If one uses an Arrhenius form for R(T,0) one obtains

$$R(T,D)=Ae^{-E/RT}(1+k(T)D^n) \tag{8}$$

where the molar gas constant R is to be distinguished from the degradation rate R(T,D).

Suppose a resource level h_1 during normal operation is taken as a surrogate for cable failure, so that if a LOCA occurs when the resource level is less than h_1, then failure is assumed to occur. For example, the resource level corresponding to a relative elongation at break of 50% for the cable insulation may be taken as corresponding to cable failure. Then the time to failure t_{f1}, for a cable at temperature T_1, D_1 during normal operation is given by

$$h_1= h_0-t_{f1}R(T_1,D_1) \tag{9}$$

That is to say, if the cable age is t_{f1} or greater, and a LOCA occurs, the cable will fail. As already noted, the resource (or capacity) level h_0 is a random variable. (The model where the initial resource level is a random variable is suggested in Ref. 3.) Since it appears that an extreme value distribution is suitable, corresponding to a chain is as strong as its weakest link model, a Weibull distribution for h_o appears suitable. That is to say, there is assumed to be random variation of the material properties of the cable along its length, and failure will occur at its weakest point.

Then, solving the above equation for t_{f1},

$$t_{f1}= (h_0-h_1)/R(T_1,D_1) \tag{10}$$

Thus t_{f1} also has a Weibull distribution. By writing an equation similar to the above equation at a different T_2, D_2, and dividing the two equations one gets

$$t_{f1}/t_{f2} = R(T_2,D_2)/R(T_1,D_1) \tag{11}$$

Suppose that the conditions T_2, D_2 correspond to accelerated testing conditions, and that repeated samples are used, so that a sample distribution of values of t_{f2} are obtained, and that this sample distribution can be fitted to a Weibull distribution. Because of the above equation, one can obtain the Weibull parameters for the distribution of t_{f1}. In particular, if the probability P_2 the cable is failed for a LOCA occurring at cable age t, for conditions T_2, D_2, is given by

$$P_2 = 1 - e^{-(\frac{t-c}{a})^b}, \tag{12}$$

where a is the scale factor, b the shape factor, and c the location parameter of the Weibull distribution, then for conditions T_1,D_1 the probability the cable is failed for a LOCA occurring at cable age t is given by the same formula, but with the scale factor and location parameter multiplied by

$$\frac{R(T_2,D_2)}{R(T_1,D_1)} \tag{13}$$

If, during accelerated testing with temperature and dose rate (T_2, D_2) the cable has a probability of failure at t of P, then, at conditions T_1, D_1 the cable will have the same probability of failure P at time t_1 given by

$$t_1 = \frac{R(T_2,D_2)}{R(T_1,D_1)} t \tag{14}$$

Thus, for any time t, during plant operation, one can estimate the probability of failure of the cable, if a LOCA occurs at that time.

Note that if a Weibull distribution is used for t_{f1}, then the failure probability for a given time t will depend on the length of the cable considered. At a given time t, if the probability of survival is P for a ten foot length of cable, then the probability of survival for a twenty foot length of cable will be P^2. The Weibull shape parameter for the twenty foot length of cable will be the same as for the ten foot length, but the scale parameter will differ.

The variability expressed by the Weibull distribution is aleatory. But there are also epistemic (or state of knowledge) uncertainties. The parameters appearing in R(T, D) are uncertain and should have state of knowledge uncertainty distributions associated with them. In the example we are considering, the uncertain parameters are the activation energy E, and the parameters k, n which appear in the expression for the rate of degradation due to aging. Also, there is uncertainty in the parameters of the Weibull distribution, since these are obtained from limited data. What this means is that the probability P of cable failure at time t is an uncertain quantity with a state of knowledge distribution. One sometimes talks of a probability of frequency representation of results. The probability P is then termed a frequency, because it refers to the fraction of failures in a large number of trials. The uncertainty in the frequency is described by a (Bayesian) probability. Reference 1 discusses the aleatory and epistemic uncertainties, as applied to the flow accelerated corrosion problem.

Up until this point, we have considered a surrogate measure of failure probability, such as 50% relative elongation at break during normal operation, which did not consider the time during the LOCA at which failure occurred. If one uses such a surrogate measure, then one has no information as to when during the LOCA that failure occurs, and in order to avoid making optimistic estimates it would appear that one would have to assume that the failure occurred early in the LOCA, when the failures are most risk significant.

It would therefore be desirable to be able to predict the probability of failure of the cable as a function of time after the LOCA starts. Gardner and Meyer (see Ref. 5, p. 850) indicate that the aging effects of sustained high-level, design-basis events are simply an acceleration of normal aging. One might therefore try a model where, first, one takes a resource level h_2 appropriate to a failure probability occurring a time t_a after a LOCA. For example one could say that if relative elongation at break of the insulation were less than 10% at the time t_a after the LOCA begins, the cable would be failed at time t_a. The rate of degradation would be given by R(T(t),D(t)), both before the LOCA and during the LOCA, where R(T,D) is given by Eq. (7). Then one would integrate the rate over time, use this quantity instead of tR(T,D). In other words, one would replace Eq. (9) by

$$h_2 = h_0 - tR(T_1, D_1) - \int_0^{t_a} R(T(t'), D(t'))dt', \tag{15}$$

for the resource level after a time t_a of the LOCA, for a LOCA occurring at cable age t. Here T_1, D_1, refer to the temperature and dose rate during normal operation, and T(t'), D(t') refer to the temperature and dose rate during the LOCA. The development of the method for predicting the probability of failure of the cable at time t_a would then be analogous to the development given in Eqs. (9) through (14). But there is a problem with this approach. It is known that the radiation dose occurring before thermal aging increases the aging during the time of elevated temperature. This is discussed, for example, in Ref. 6.

One possible way of approaching this difficulty is to limit oneself to estimating the effects of cable failures on the core damage frequency only, and not the frequencies of various radioactive releases. Then one is interested only in the behavior of the cables under the elevated temperature of a LOCA, but the radiation dose occurring during the LOCA will be minimal, since core damage has not occurred, and the reactor is shut down, so that the gamma radiation is reduced. Clough and Gillen, in Ref. 6, discuss the mechanism by which previous radiation accelerates thermal aging. Peroxides are formed by the radiation. Thermally-induced breakdown of the peroxides yield free radicals which react with oxygen. It seems therefore that, phenomenologically, one can consider the degradation during the elevated temperature of the LOCA to be proportional to the concentration of peroxides and of oxygen, with a rate constant which depends on temperature. Because the peroxide concentration depends on the dose rate prior to the LOCA, one might try a modification of Eq. (15) where the dose rate during the LOCA is replaced, in R(T(t'), D(t')) by the dose rate D_1 before the LOCA, but the temperature dependent constants are appropriate to the elevated temperature of the LOCA. That is to say, Eq. (15) is replaced by

$$h_2 = h_0 - te^{-\frac{E}{RT_1}}(1 + k(T_1)D_1^n) - \int_0^{t_a} e^{-\frac{E}{RT(t)}}(1 + k(T(t))D_1^n)dt \tag{16}$$

Because we are using the dose rate before the LOCA in the integral, one would expect this equation to be valid for only a limited time after the LOCA begins. But the most risk significant time period is the first few days after the LOCA, so this is acceptable. Although this approach appears to qualitatively account for the phenomenon of enhanced thermal degradation occurring after irradiation, it would have to be tested quantitatively; it has not as yet been tested quantitatively. If one writes Eq. (16) in the form

$$h_2 = h_0 - Q(t,t_a)$$

then $Q(t,t_a)$ will have a Weibull distribution, so that for any values of t, t_a one could determine the probability of cable failure. The parameters of the Weibull distribution could be determined by accelerated aging tests. If, at the accelerated aging test conditions, a given value of Q corresponds to a given cable failure probability, this value of Q will correspond to the same cable failure probability for the plant conditions. Again, for this method to be viable, one must quantitatively evaluate the method described above for including the synergistic effects of prior radiation on thermal degradation. Otherwise, one must use the method which essentially assumes that, if the cable fails, it fails early in the LOCA, and takes a surrogate for failure of, say, 50% elongation at break at the time the LOCA occurs.

Incorporation of the Cable Failure Probabilities into the PRA Calculation

This is a relatively straightforward calculation. The cable failures are modeled in the fault trees. For the cables where it is judged important to do so, the time during the LOCA at which the cable fails can be modeled. At a given time in plant life, the event tree/fault tree models can be evaluated quantitatively, using the cable failure probabilities appropriate to that time in plant life. The calculations can be repeated during the plant life. If it turns out that the cable failures have a significant contribution to the core damage frequency using conservative estimates of human error probability, or of the probability of operator recovery actions, more realistic methods of estimating these probabilities must be used. This method cannot really take into account the case where the cables are replaced because of the results of condition monitoring. One would have to know in advance the times at which the cables are replaced, if they are replaced at all.

Summary

A method for integrating cable aging effects into PRA was described. The method uses reliability physics models to estimate the cable failure probabilities. Essentially, deterministic lifetime prediction models are modified by introducing an initial resource, or capacity, which has randomness associated with it, and by introducing uncertainty distributions on the parameters of the lifetime prediction model. The initial step in the method is a screening analysis, to see which cable failures may be neglected. This step is used because the evaluation of the failure probabilities of cables by reliability physics models can be labor intensive. The final step, the use of the cable failure probabilities in the fault trees and event trees, is relatively straightforward, but the evaluation of the probability of operator actions when the operator is presented with erroneous or missing information from failed instrumentation can present difficulties.

References

1. C.L. Smith, V.N. Shah, T. Kao, and G. Apostolakis, "Incorporating Aging Effects into Probabilistic Risk Assessment -- A Feasibility Study Utilizing Reliability Physics Models, NUREG/CR-5632, August 2001.

2. L.D. Bustard, J. Clark, G.T. Medford, and A.M. Kolaczkowski, "Equipment Qualification (EQ) -- Risk Scoping Study, NUREG/CR-5313, January 1989.

3. S.P. Carfagno and R.J. Gibson, "A Review of Equipment Aging Theory and Technology", EPRI NP-1558, September 1980.

4. "Assessment and Management of Ageing of Major Nuclear Power Plant Components Important to Safety: In-containment Instrumentation and Control Cables", IAEA-TECDOC-1188, December 2000.

5. J.B. Gardner and L.C. Meyer, "Light Water Reactor Cables and Connections in Containment" in *Aging and Life Extension of Major Light Water Reactor Components,* edited by V.N. Shah and P.E. MacDonald, Elsevier, 1993.

6. R.L. Clough and K.T. Gillen, "Radiation-Thermal Degradation of PE and PVC: Mechanism of Synergism and Dose Rate Effects", NUREG/CR-2156, June 1981.

AGE-RELATED DEGRADATION OF STRUCTURES AND PASSIVE COMPONENTS AT NUCLEAR POWER PLANTS

J.I. Braverman, C.A. Miller, C.H. Hofmayer - Brookhaven National Laboratory, Upton NY
B.R. Ellingwood - Georgia Institute of Technology, Atlanta GA
D.J. Naus - Oak Ridge National Laboratory, Oak Ridge TN
T.Y. Chang - United States Nuclear Regulatory Commission

ABSTRACT

This paper describes a multi-year research program to assess age-related degradation of structures and passive components important to the safe operation of nuclear power plants (NPPs). The purpose of the research effort is to develop the technical basis for the validation and improvement of analytical methods and acceptance criteria which can be used to make risk-informed decisions and to address technical issues related to degradation of structures and passive components. The approach adopted for this research program consists of two Phases. In Phase I, specific degradation occurrences at plants were collected and evaluated, existing technical information on aging was reviewed, and a scoping study was performed to identify which structures and components should be studied in the subsequent phases of the research program. Based on the results of the Phase I effort, selected structures and passive components are evaluated in Phase II to assess the effects of age-related degradation using existing and enhanced analytical methods. Fragility analyses are performed for undegraded and degraded structures and passive components to determine the effect of degradation on their fragility. These results can then be used to assess the potential impact of degradation on overall plant risk. The Phase II effort also utilizes the results of the analyses to develop probabilistic degradation acceptance criteria for the structures and passive components studied. These research activities provide useful tools to support the current goals of developing risk-informed and performance-based regulation in the nuclear industry.

1. INTRODUCTION

1.1 Objective

To ensure the safe operation of nuclear power plants in the United States, it is essential to assess the effects of age-related degradation of plant structures, systems, and components. This concern becomes even more important in view of the submittals of license renewal applications to the NRC under 10 CFR Part 54. Such applications will extend nuclear plant operation for an additional 20 years beyond the current 40 year limit.

Since substantial research has already been performed by other NRC and industry programs on active components, the research effort described in this paper focuses on structures and passive components. To achieve the goal of assessing the effects of age-related degradation, it is first necessary to understand which structures and passive components have experienced aging

degradation, the predominant/applicable aging mechanisms and their effects, the physical manifestations of degradation, and the importance of these components to plant safety. With this information, the research effort can focus on achieving the objective to develop the technical basis for the validation and improvement of analytical methods and acceptance criteria which can be used in making risk-informed decisions regarding degradation of structures and passive components.

The approach adopted for this research project consists of two phases. The Phase I effort includes data collection, review of existing technical information, and a scoping study. Phase II consists of assessing the effects of age-related degradation and improvement of available analysis techniques to evaluate degradation. This effort includes calculating how varying levels of degradation affects the fragility of structures and passive components, how this reduction in fragility might impact plant risk, and what probability-based degradation acceptance criteria could be developed to assess observed degradations at a plant site.

1.2 Background

The NRC has sponsored many programs in the past to address concerns related to aging of nuclear power plants (NPPs) in the United States. Most of these programs studied the effects of age-related degradation of active components. However, cases of degradation of safety-related structures and passive components in operating NPPs have been identified in recent decades, and such occurrences are expected to increase as plants continue to age. A better understanding of the behavior of age-degraded structures and passive components is clearly needed to ensure that the degradation can be adequately managed for the continued safe operation of NPPs.

Currently, there are 103 operating NPPs in the United States producing approximately 20 percent of the Nation's total electric power generation. As of 2001, approximately 60 percent of the NPPs in the United States received their construction permits over 30 years ago. Although the performance of safety-related structures and passive components at these plants has been good, the number of occurrences of age-related degradation has been increasing as NPPs age. Examples of age-related degradation of structures and passive components in NPPs have been reported in NUREG-1522 and Naus et al., 1999. Most of the information presented in NUREG-1522 was obtained from actual walkdowns of structures and components at six representative NPPs licensed before 1977. Common degradation occurrences were identified in intake structures/pumphouses, service water piping, tendon galleries, masonry walls, anchorages, containments, and other concrete structures.

If properly designed and constructed, civil structures generally have substantial safety margins. However, the available margins for degraded structures have not been established. In addition, how age-related degradation may affect the dynamic properties (stiffness, frequency, and damping), structural response, structural resistance/capacity, failure mode, and location of failure initiation is not well understood. A better knowledge of the effect of aging degradation on structures and passive components is essential to ensure that the current licensing basis is maintained under all loading conditions.

Based on risk evaluation research programs conducted by the NRC, such as the Individual Plant Examination of External Events (IPEEE) program, external events such as earthquakes, high

winds, and tornadoes can be significant contributors to core damage frequency. In some cases, structures and passive components have been found to be significant contributors to plant risk when subjected to these external events. As structures and components age, the effect of age-related degradation will become a more significant factor in assessing risk.

1.3 Scope

The research effort included all structures and passive components normally found in NPPs in the United States. Structures in the context of this research include steel and reinforced concrete buildings, masonry walls, canals, embankments, underground structures, and stacks. Passive components consist of equipment which do not move or change their state to perform their intended function. Examples of passive components are tanks, cable tray systems, conduit systems, and HVAC ducts/supports. A more complete definition of the specific structures and passive components included within the scope of this project is presented in Section 2.1.

2. Phase I

2.1 Collection and Review of Degradation Occurrences

The initial effort under Phase I consisted of collecting and reviewing age-related degradation occurrences of structures and passive components at NPPs. For the purpose of this research project the term "degradation occurrence" is defined as age-related degradation which was reported in NRC generic correspondence, Licensee Event Reports (LERs), NUREGs, and other publicly referenced documents.

Structures and Passive Components Reviewed

The structures and passive components included in this research effort were those that fall within the scope of the NRC License Renewal Rule - 10 CFR Part 54 and the Maintenance Rule - 10 CFR 50.65. The structures and passive components reviewed are those: (1) that are safety-related, (2) whose failure could affect safety-related functions, and (3) that meet several other criteria defined within the scope of the license renewal rule and the maintenance rule.

All structures and components identified to be within the scope of review were placed into one of eighteen categories. A complete listing of the eighteen categories is presented in Table 1. Each of the eighteen categories contains a number of components which define specific types of structures and passive components included. As an example, the category "anchorages" includes embedded anchors, expansion anchors, undercut anchors, drop-in anchors, embedded studs, and the grout beneath baseplates. For certain structures and components, the NRC and industry already have been studying and addressing issues related to aging degradation. Thus, it was decided to eliminate such items from subsequent phases of this research effort; these items are noted in Table 1.

Table 1 Categories of Structures and Passive Components

1	Anchorages	Anchors - embedded, expansion, undercut, drop-in, embedded studs and grout; for all components including equipment
2	Cable Tray Systems	Electrical cable trays, tray supports, junction boxes
3	Concrete	Reinf. conc. bldgs.; water intake structures; underground structures; concrete – walls, floors, ceilings, mat foundations, canals, pools, pits, pedestals, prestressed, & manholes; and masonry
4	Conduit Systems	Electrical conduits, conduit supports
5	Containment	Shell – steel & concrete, prestressing system, penetrations*, torus, bellows, liners, and supports
6	Cooling Tower	
7	Electrical Conductors*	Cable/wires, including insulation, bus duct
8	Exchangers	Steam generator, heat exchanger, condenser (including ice) and supports
9	Filters	Mechanical & HVAC – screen, separator, strainer, adsorber, supports, housing. Only material type degradation;exclude regular maintenance items
10	HVAC Duct	Duct and duct supports
11	Insulation/seal	Pipe insulation*, containment insulation, ceramic insulators, floor seals, and flood protection seals
12	Piping System	Piping*, fittings*, small bore piping* & tubing*, sleeves*, pipe supports (excluding hydraulic & mechanical assembly of snubbers), buried piping
13	RPV	Shell, internals, CRD (passive components only), supports
14	Structural Seismic Gap	
15	Structural Steel	Frames, trusses, platforms, supports, bolts, studs, fasteners, liners, doors, covers, hatches, support to all types of equipment
16	Tanks	
17	Vessels	Pressurizer, other pressurized vessels, and supports
18	Water-Control Structures	Dams, embankments, spray ponds

* These items removed from further review due to other existing/past programs

Sources for Degradation Occurrences

Various publicly available sources of information were investigated to identify instances of age-related degradation of structures and passive components. These sources primarily consist of LERs, NRC generic correspondence, NUREGs, and industry reports.

LERs were obtained from the Sequence Coding & Search System (SCSS) maintained by the Oak Ridge National Laboratory (ORNL). The SCSS database was developed by the NRC's Office for Analysis and Evaluation of Operating Data through the Nuclear Operations Analysis Center at ORNL. The SCSS is an electronic database developed to allow users to retrieve commercial nuclear plant operating experience data from LERs. The database contains over 35,000 LERs from 1980 to the present time. Because of the very large number of LERs, the initial review of LERs was conducted for the period 1990 to 1997. Then, the search was expanded to include LERs extending back to 1985. Thus, the total period reviewed covered 1985 to 1997.

NRC generic correspondence includes Inspection and Enforcement Bulletins (IEs), Generic Letters (GLs), and Information Notices (INs). Correspondence contained in the Generic Correspondence Library on the Fedworld Information Network (Internet) was investigated. The selection of the applicable documents was performed by reviewing all of the generic correspondence titles. Those that apply to structures and passive components or those that may

be related in some manner were identified and retrieved for review. If instances of age-related degradation were noted then that occurrence was recorded for use in this research project.

Degradation Occurrence Database

To document and evaluate the enormous amount of data collected, a computerized database entitled Degradation Occurrence Database (DOD) was created. The advantages of this computerized database are: 1) simple entry and update of degradation data, 2) sorting and organizing of data in a meaningful way, 3) quickly locating desired information, 4) creation of tabulated listings or reports, and 5) sharing of data with other authorized users and programs in the system.

A number of tables were created as part of the DOD to fully describe the age-related degradation of structures and passive components. The tables that are included in the DOD are: Structures and Passive Components, Degradation Occurrences, Aging Effects and Mechanisms, System Definition Codes, and Stress Corrosion Codes.

The Structures and Passive Components Table identifies the various types of structures and passive components included in the scope-of-work. The list of structures and components in this table corresponds to the items in Table 1.

The most important table in the DOD is the Degradation Occurrence Table (DOT) which contains all of the degradation occurrences identified as applicable under this research project. A total of 492 degradation occurrences were included in the DOT. It should be noted that there are many more occurrences of degradation than were identified and reported in this DOT. However, if they were not reported in LERs or other publicly available documents then they would not be included in this database. For example, some degradation occurrences may not be reported in LERs if the event or condition does not seriously affect the plant or result in an unanalyzed condition that significantly compromised plant safety.

A representative copy of a portion of the data from the DOT is presented in Table 2. The "Component" and "Subcomponent" entries identify the type of structure or passive component as listed in Table 1. The "System" refers to the plant system such as service water system or containment system. The "Aging Effect" and corresponding "Aging Mechanism" entries are obtained from the various sources of information discussed earlier.

The "Plant" entry identifies the nuclear power plant where the age-related degradation occurred. All nuclear power plants were included; operating plants, plants that have been shut down, and plants that have been or are going through a decommissioning process. The entry for the Month, Date, and Year corresponds to the date that the degradation occurrence was identified.

The next three columns in the DOT describe how the degradation was identified, evaluated, and repaired. Identification methods include visual, inspection, leaking, alarm, test, low flow and other methods. The evaluation methods indicate how the degradation was investigated/reviewed. These methods generally consisted of visual examinations; tests such as leak rate tests, ultrasonic tests, and eddy current tests; and engineering judgment. For repair methods, designations such as repair, replacement, monitoring, tightening, and cleaning were noted. As with any of the other entries in the database, if the required information is not given or is insufficient then an "NA", meaning not available, is noted.

Table 2 Degradation Occurrence Table (DOT) - Sample

COMPONENT	SUBCOMPONENT	SYSTEM	AGING EFFECTS	AGING MECHANI	PLANT	M	DA	YR	HOW IDENT	EVALN METH	REPAIR MEAS	DKT	REF DOC	REF NO
ANCHORAGES	ANCHOR BOLTS - STRAINER	SERVICE WATER	DETERIORATION	N. A.	ROBINSON 2			95*	VISUAL	N. A.	N. A.	261	NUREG	1522
ANCHORAGES	EXPANSION ANCHOR	ERCSW	FAILURE	CORROSION	MILLSTONE 2	4	29	86	VISUAL	VISUAL	N. A.	336	LER	860100
ANCHORAGES	EXPANSION ANCHOR - NUTS	ERCSW	LOOSENING	VIBRATION	QUAD CITIES 1	5	8	87	N. A.	VISUAL	REPLACEMENT	254	LER	870801
ANCHORAGES	GROUT & BASEPLATES	N. A.	DETERIORATION	CORROSION	BEAVER VALLEY 1			95*	VISUAL	N. A.	N. A.	334	NUREG	1522
ANCHORAGES	GROUT- EQUIPMT. SUPPORT	PUMPHOUSE	CRACKING DETERIORATION	MOISTURE	POINT BEACH 2			95*	VISUAL	N. A.	N. A.	301	NUREG	1522
ANCHORAGES	GROUT- EQUIPMT. SUPPORT	PUMPHOUSE	CRACKING DETERIORATION	MOISTURE	POINT BEACH 1			95*	VISUAL	N. A.	N. A.	266	NUREG	1522
ANCHORAGES	N. A.	SEVERAL	DETERIORATION	N. A.	COOPER			95*	VISUAL	N. A.	N. A.	298	NUREG	1522
ANCHORAGES	STUDS - EMBEDDED	N. A.	FAILURE	MECHANICAL LOADS	INDIAN POINT 2	2	12	91	VISUAL	VISUAL	REPAIR	247	LER	910401
CABLE TRAY SYSTEM	ELECTRICAL CABLE TRAY-SEAL	CBEAF	DETERIORATION	N. A.	BRUNSWICK 1	10	25	95	TEST	N. A.	REPAIR	325	LER	952001
CONCRETE	CEILING	FHB	CRACKING DETERIORATION	MOISTURE	TURKEY POINT 3			95*	N. A.	N. A.	N. A.	250	NUREG	1522
CONCRETE	CEILING/ FOUNDATION	SECONDARY CONTMT.	DETERIORATION	N. A.	DRESDEN 2	4	7	89	TEST	N. A.	REPAIR	237	LER	891400
CONCRETE	FLOORS, WALLS, FOUNDATION	VARIOUS STRUCTURES	CRACKING SPALLING	N. A.	COOPER			95*	VISUAL	N. A.	N. A.	298	NUREG	1522
CONCRETE	INTAKE STRUCT. - BEAMS	CIRCULAT. WATER	CRACKING	CORROSION - EMBED. STL.	TURKEY POINT 4			89	N. A.	N. A.	REPAIR	251	NUREG	1522
CONCRETE	INTAKE STRUCT. - BEAMS	CIRCULAT. WATER	CRACKING	CORROSION - EMBED. STL.	TURKEY POINT 3			89	N. A.	N. A.	REPAIR	250	NUREG	1522

Degradation Analysis and Trending

All 492 degradation occurrences that were identified in the DOD were evaluated. A tabulation of the total number of degradation occurrences for each structure/component category was made.

With the entry of the data into a computerized database program, the information can also be searched, sorted, and tabulated in a number of different ways. For example, the degradation occurrences can be easily sorted by types of components, types of degradation, causes of degradation, plant names, dates, or systems. To evaluate the degradation occurrences the data was filtered and sorted to obtain trending information. Trending data were developed for distributions by:

1. Components/Subcomponents
2. Year (1985-1997)
3. Age of Plant
4. Steel Degradation Aging Effects
5. Concrete Degradation Aging Effects
6. Aging Mechanisms of Degradation
7. Types of Cracking Induced by Corrosion
8. Subcomponents for Structural Steel
9. Subcomponents for Concrete
10. Subcomponents for Containment
11. Subcomponents for Filters
12. Subcomponents for RPV
13. Systems
14. Methods of Identification

The distribution of degradation by types of components/subcomponents, shown in Figure 1, was obtained by compiling the number of occurrences for each of the components listed in Table 1. Where a subcomponent had an extremely large number of occurrences such as piping and steam generators, it was included as a separate item on the bar chart in Figure 1. Where a component had no occurrences identified such as structural seismic gap and vessels (other than RPVs and steam generators) it was not included on the bar chart.

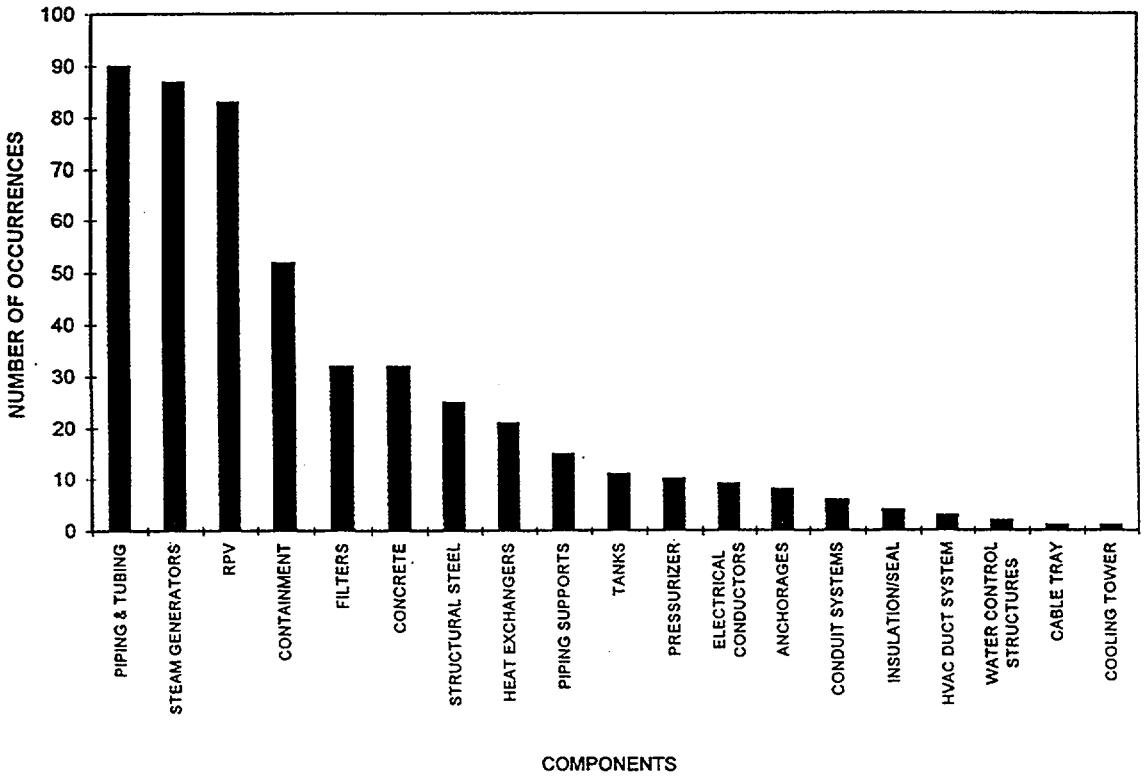

Fig. 1 Degradation Occurrences - Distribution by Components/Subcomponents

From this distribution of degradation by types of components/subcomponents, it is evident that piping & tubing, steam generators, RPVs, and containments have the largest number of degradation occurrences. This is not surprising since it has been known in the industry that these structures and components have had numerous instances of degradation. Following these, the structures and passive components with the greatest number of occurrences in descending order are filters, concrete, structural steel, heat exchangers, piping supports, tanks, pressurizers, electrical conductors, and anchorages. All of the remaining items have six or less occurrences.

Degradation concerns related to piping (other than buried piping and piping supports), steam generators, RPVs, and containments, were eliminated from the subsequent phases of this research project because other NRC and industry programs have been studying and addressing aging issues related to these components.

Figure 2 shows the distribution of degradation occurrences by age of plant. The graph represents the average number of occurrences per plant per year for different plant vintages. This

was developed by categorizing all U.S. nuclear power plants by age (1997 minus year of construction permit). Then the total number of occurrences for each group of plants in a given age category was divided by the number of plants in that age category and the age of the plants in that category. Although the actual number of occurrences are not high, this curve demonstrates that as the age of plants increase, the number of occurrences per plant per year also increases. The complete DOD and trending data as well as a description of the entire Phase I effort are included in NUREG/CR-6679.

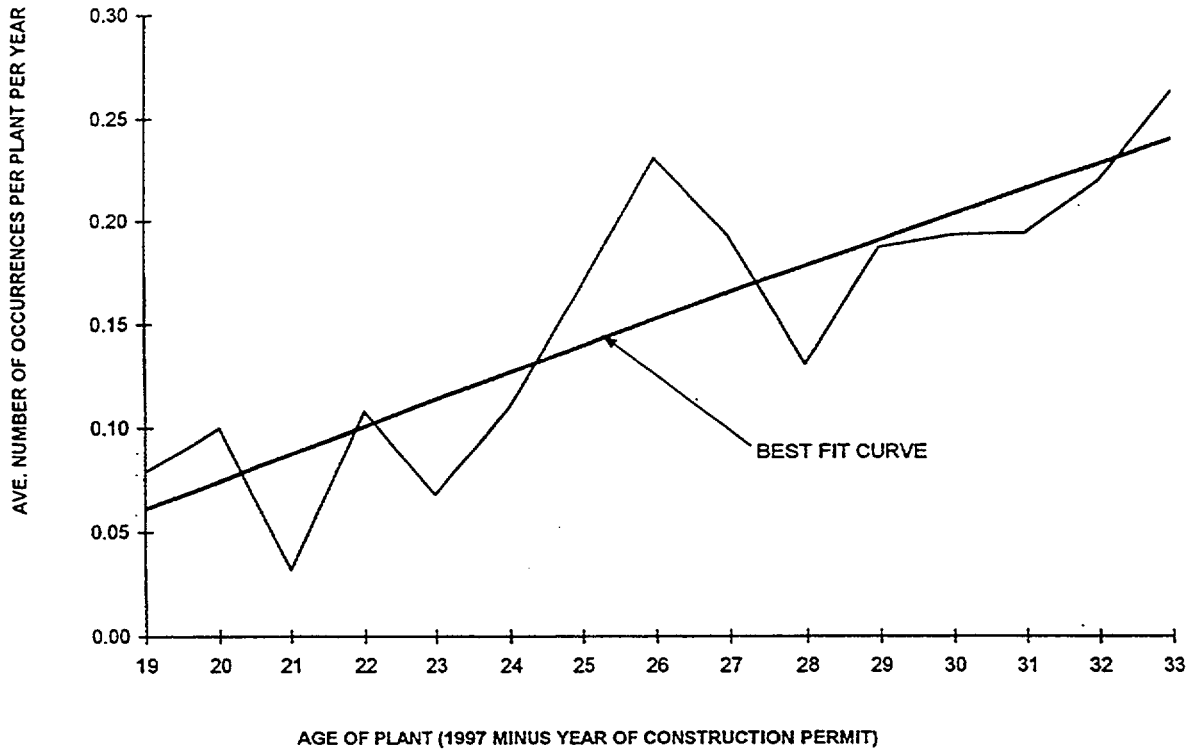

Fig. 2 Degradation Occurrences - Distribution by Age of Plant

2.2 Age-Related Degradation Technology Information

Existing technical information was collected and reviewed to provide input into the research effort. Information from NRC programs and industry programs regarding inspection, testing, assessment, and repair techniques were identified and reviewed. In addition, information related to aging/degradation mechanisms and effects on material properties/strengths was also reviewed.

To aid the process of collecting and reviewing the various documents related to aging degradation of structures and passive components a Degradation Reference Database (DRD) was created. The DRD includes the codes, industry standards and guidelines, NUREG reports, technical papers, presentations (at conferences), regulatory documents, and other reports that were collected and reviewed in Phase I of this research project. The regulatory documents include

Title 10 CFRs; NRC generic correspondences such as IEs, INs, GLs, etc.; NRC inspection reports; NRC regulatory guides; and NRC SECY papers.

All of the information obtained from these documents was entered into a computerized database. Currently there are over 180 documents in the database which can be sorted in any manner or specific documents can be located by identifying a subject of interest. A copy of this database is included in the NUREG/CR-6679 report.

The information contained in the database consists of the type of document, the identification or ID (document no.), title of the document, date of publication, author/organization, a summary description, types of components covered, and potential aging issues identified in the document.

2.3 Risk Significance of Aging Effects

In the past two decades, seismic probabilistic risk assessment (PRA) studies have been carried out on a large number of NPP's, including the recent studies conducted as part of the independent plant examination of external events (IPEEE) (NUREG-1407). Surveys on the seismic fragility values used in the past seismic PRA's are also available in numerous publications (e.g., NUREG/CR-4334, Campbell 1988, NUREG/CR-3558, and Park 1998). Based on a survey of a large number of past seismic PRA's (including those of IPEEE) and surveys of seismic fragilities, the structures and passive components that were determined to be the most frequently observed weak links are:

- Anchorage and supports of equipment
- Flat-bottom storage tanks
- Critical reinforced concrete members
- Concrete block walls
- Interconnecting pipes (e.g. buried piping)
- Cable trays
- Dams

The information from the surveys described above contributed to the determination of the priority ranking of structures and passive components, which is described in the next section.

2.4 Technology Needs and Priority Ranking of Structures and Passive Components

Technology Needs

In order to gain an understanding as to the technology needs and which structures and components require further assessments, a review was conducted of what NRC and industry programs exist and how well they are addressing aging degradation. The programs reviewed covered NRC and industry requirements, as well as NRC and industry research related to aging degradation of structures and components at NPPs.

To facilitate this review and presentation of the results, a table was developed in matrix form for each category such as anchorages, tanks, and reinforced concrete structures. From the original eighteen categories shown in Table 1, eight structures and passive components were selected for this assessment of technology needs. The other ten categories were eliminated

because there were either very few degradation occurrences identified in the Degradation Occurrence Database (DOD) or there are existing programs that adequately address aging concerns for these items.

The eight types of structures and passive components that were assessed are: masonry walls, tanks, anchorages, concrete structures, buried piping, supports for equipment and systems, concrete containments, and steel containments. For each of the structures and components, the NRC and/or Industry program that relates or addresses aging concerns was tabulated along with a summary of whether the programs adequately address aging. While this tabulation may not list every single program, it does capture the major requirements, research programs, and industry programs that address aging. The tabulation for the eight structures and passive components is presented in NUREG/CR-6679.

Priority Ranking of Structures/Components

To identify which structures and components warrant further review in subsequent phases of the research project, it was decided to rank or prioritize them. The process of ranking the eight structures and passive components discussed above considered four key parameters: seismic risk significance, degradation occurrences, importance to current licensing basis/license renewal, and adequacy of existing NRC and industry programs. Then a final ranking was developed based on a compilation of all the information from these four key parameters.

Masonry walls (particularly unreinforced walls) and flat bottom steel tanks were rated as very high followed by anchorages, reinforced concrete, and buried piping which were rated as high. Supports for equipment and systems were rated as moderate and concrete and steel containments were rated as low. It should be noted that a low rating does not mean the structure or component is not important or does not experience age-related degradation, but rather that it is simply less important relative to the other structures and components. A lower ranking may occur because some key parameter(s) discussed above, such as seismic risk significance or adequacy of existing nuclear industry programs, results in its lower ranking. Containments were removed from further study because the aging effects of steel and concrete containments are being studied in other NRC sponsored research programs.

3. Phase II

From the results of the Phase I research effort, it has been concluded that Phase II should address: reinforced concrete structures (other than containments), masonry walls, flat bottom tanks, anchorages, and buried piping. The focus of the research will be on improving and developing methods to assess the effects of age-related degradation on the structural performance of structures and passive components, including fragility evaluations for use in PRA/seismic margin assessment (SMA) studies. The methodologies that will be developed to determine the structural performance can then be used to quantify the impact of age-related degradation of structures and passive components on overall plant risk. Phase II will also implement this methodology to develop probability-based degradation acceptance criteria. The aim is to provide confidence in the use of risk assessment as a tool in making risk-informed decisions for age-degraded structures.

The Phase II research effort consists of the following four activities:

- Evaluate existing degradation condition assessment techniques and identify the relationship between varying levels of degradation and observable manifestations of degradation.
- Improve and/or develop methodologies to predict the structural response of degraded structures and passive components.
- Develop fragility curves for degraded structures and passive components based on the results of analytical structural evaluations or tests of degraded structures and passive components, and assess their potential effect on overall plant risk.
- Develop probability-based degradation acceptance criteria for structures and passive components based on the above activities, existing codes, standards, NRC regulatory guides, and other NRC or industry reports.

The above activities have already been completed for one of the five structures and passive components – reinforced concrete elements. A summary of the research activities under Phase II for reinforced concrete members is described in the following section. Details of this research effort for reinforced concrete flexural members and shear walls are presented in NUREG/CR-6715.

3.1 Description of Evaluation for Degraded Reinforced Concrete Members

Concrete structural members, such as shear walls, slabs, beams and columns, that are found in the reactor building, control or auxiliary building, and other balance-of-plant facilities, are designed and constructed in accordance with criteria in ACI Standards 318, 349, and the NRC Standard Review Plan 3.8.4. Such components generally have substantial safety margins when properly designed and constructed; however, the available margins for aged or degraded concrete structures are not known. Aging can lead to changes in engineering properties and may affect the dynamic properties, structural resistance/capacity, failure mode, and location of failure initiation. Two common reinforced concrete members were selected for the structural assessments in this study: a propped cantilever beam and a low-rise shear wall. The research focused on degradation of the reinforced concrete members due to the two most predominant aging effects: loss of steel reinforcing area and loss of concrete area (cracking/spalling). Loss of steel area is typically caused by corrosion while cracking and spalling can be caused by corrosion of reinforcing steel, freeze-thaw, or aggressive chemical attack. Structural performance in the presence of uncertainties is depicted by a fragility (or conditional probability of failure). The fragility modeling procedures applied to degraded concrete members can be used to assess the effects of degradation on plant risk and can lead to the development of probability-based degradation acceptance limits.

Fragility Methodology

Degradation effects can be quantified with fragility curves developed for both undegraded and degraded components. Fragility analysis is a technique for assessing, in probabilistic terms, the capability of an engineered system to withstand a specified event. Fragility modeling requires a focus on the behavior of the system as a whole and, specifically, on things that can go wrong with the system. The fragility modeling process leads to a median-centered (or likely) estimate of

system performance, coupled with an estimate of the variability or uncertainty in performance. The fragility concept has found widespread usage in the nuclear industry, where it has been used in seismic probabilistic safety and/or margin assessments of safety-related plant systems (e.g., Kennedy and Ravindra, 1984).

The lognormal cumulative distribution function (CDF), is the most common model used in previous structural fragility analysis. If the structural capacity is described as the product of statistically independent random variables, the central limit theorem provides some justification for the lognormal model. The lognormal CDF is described by,

$$F_R(x) = \Phi[\ln(x/m_C)/\beta_C] \quad (1)$$

in which $F_R(x)$ is the probability of failure for an applied load equal to x, $\Phi[\,]$ = standard normal probability integral, m_C = median capacity, and β_C = logarithmic standard deviation, approximately equal to the coefficient of variation, V_C, when $V_C < 0.3$. It should be emphasized that all sources of uncertainty known to impact structural performance should be included in this model. These would include aleatory uncertainties, β_R (inherent variability in strength of concrete and reinforcing steel, dimensions, etc) and epistemic uncertainties, β_U (simplifying assumptions regarding structural mechanics, approximate methods of analysis, limitations in data). There are a number of ways to distinguish between these sources of uncertainty in the fragility assessment. In this study, we combine the aleatory and epistemic uncertainties as, $\beta_C = \sqrt{\beta_R^2 + \beta_U^2}$ in Eq. (1).

A summary of available statistical data to describe the strength of reinforced concrete flexural members (beams and slabs) and short concrete shear wall structures is provided in Tables 3 and 4, respectively. These are based on a comprehensive review of published literature (Ellingwood and Hwang, 1985; MacGregor et al., 1983) and additional data from specific NPPs. The limit state for the indeterminate beams considered herein is defined by the beam strength measured in terms of uniform load capacity. Deformation-based limit states (peak displacement, maximum rotations, or ductility) usually are not the limiting condition for flexural members in NPPs. Most loads acting on flexural members in power plants are static gravity loads, with dynamic seismic loads constituting a small portion of the total load. Thus, static rather than dynamic effects are considered for the beam. Since the principal loads acting on the flexural members are considered to be static, the steel and concrete strengths presented are static strengths in-situ, i.e., the strength when loading to failure takes approximately one hour. Mill tests of steel and concrete cylinder tests are conducted at a higher strain rate than is typical for static structural loading, and must be adjusted to static conditions. The principal loads acting on shear walls, however, are generally due to a seismic event so that dynamic concrete and steel properties are used. This accounts for the differences in the data in Tables 3 and 4. The in-situ strength of concrete requires additional corrections to account for differences between standard-cure cylinder strengths and field strengths that arise from field placement, consolidation, and curing conditions (MacGregor, et al., 1983). Thus, the concrete strength statistics reflect 28-day in-situ strength under static load conditions for the flexural members and under dynamic load conditions for the shear walls. There can be a significant gain in concrete strength beyond the 28-day strength used as the basis for design. Such increases have only a nominal effect on flexural strength of the under-reinforced beam, but may have a substantial impact on shear wall behavior, where the concrete strength is more important. For conservatism, this strength increase is ignored in the current study.

Table 3
Structural Resistance Statistics for Beams

Property	Mean	V_C	CDF
Concrete (4,000 psi)			
Comp. Strength	3,552 psi	0.16	N
Splitting strength	358 psi	0.18	N
Initial tangent modulus	3,800 ksi	0.18	N
Max comp. strain	0.004	0.20	N
Grade 60 reinforcement			
Yield strength	66 ksi	0.10	LN
Modulus of Elasticity	29,000 ksi	NA	NA
Placement of reinforcement			
Effective depth, d	d (in)	0.5/d	N
Analysis Flexure (B_f)	1.04	0.07	N

Table 4
Structural Resistance Statistics for Shear Walls

Property	Mean	V_C	CDF
Concrete (4,000 psi)			
Comp. Strength	4,400 psi	0.16	N
Splitting strength	475 psi	0.18	N
Initial tangent modulus	3,834 ksi	0.18	N
Max comp. strain	0.004	0.20	N
Grade 60 reinforcement			
Yield strength	71 ksi	0.10	LN
Modulus of Elasticity	29,000 ksi	NA	NA
Placement of reinforcement			
Effective depth, d	d (in)	0.5/d	N
Analysis Shear (B_{sh})	1.00	0.14	N

Note: 1 in. = 25.4 mm; 1 psi = 6.895 kPa; 1 ksi = 6.895 Mpa
N = normal distribution; LN = lognormal distribution; NA = not applicable

The factors B_f and B_{sh} account for epistemic uncertainty in the analysis itself. This uncertainty arises from idealizations of behavior in any analytical model of a structure. Refined structural models (e.g., nonlinear finite element analysis models) tend to be closer to reality than design code models, and in such cases the means of B_f or B_{sh} will be close to 1 (unbiased).

The uncertainties are propagated through the analyses of the structural components using Latin Hypercube sampling, a stratified sampling technique designed to reduce the variance in the estimator for small samples. Nineteen samples are used for each analysis to facilitate probability plotting within approximately the center 90% range of the fragility curve.

3.2 Fragility Evaluation of Degraded Flexural Members

Degradation effects on the behavior of indeterminate flexural reinforced concrete members are determined using a specific example of a propped cantilever beam. Fragility curves for the undegraded beam and the beam with degraded properties are calculated and compared for varying levels of degradation. Lognormal distributions for the important beam properties are developed both for the undegraded and degraded conditions. These properties are then used to evaluate the probability of failure for the beam. Extensive calculations are performed with an analytical model of the beam (as recommended in ACI 318) and these results are verified with a finite element model of the beam.

Beam Design and ACI Code Analysis

A propped cantilever beam with a 6.1 meter (20 ft) span is used as the sample problem. The beam is designed, using the procedures in ACI 318-99, for a dead load of 14.6 kN/m (1 kip/ft) and a live load of 43.8 kN/m (3 kips/ft). The resulting ultimate load on the beam (including load factors) is 94.9 kN/m (6.5 kips/ft). The design of the beam used compressive strength of concrete (f'_c) at 27.6 MPa (4,000 psi) and Grade 60 reinforcement [yield strength f_y = 414 MPa (60 ksi)]. Young's modulus for the concrete is 24.9 GPa (3,605 ksi). The design is shown in Fig. 4. The reinforcement ratios in the negative and positive moment regions are 0.0145 and 0.0087, respectively. The balanced reinforcement ratio is 0.0285 so that one expects the strength of the beam to be controlled by yielding of the reinforcement as required by the Code.

The load-deflection behavior of the beam is evaluated using the procedures defined in ACI 318. When the loading is small and before concrete cracking occurs, the stiffness of the beam is controlled by the gross section with negligible contribution from the reinforcement. The bending moment causing cracking (M_{cr}) is defined in the ACI code to occur when the tensile flexural stress is $f_r = 7.5 [f'_c]^{1/2} = 474$ psi (3.27 MPa). The value of M_{cr} is 66.8 kN-m (49.3 ft-kips). The maximum bending moment occurs at the fixed support and is equal to $w L^2 / 8$. Equating this moment to the cracking moment results in the cracking load [w_{cr} = 14.4 kN/m (0.986 kips/ft)]. The ultimate moment capacities of the beam, evaluated at the support and positive moment regions are M_u^- = 490 kN-m (361 ft-kips) and M_u^+ = 312 kN-m (230 ft-kips), respectively. The first plastic hinge occurs at the support when the loading equals 105 kN/m (7.22 kips/ft). The second plastic hinge occurs at 3.81 m (12.5 ft) from the fixed support when the load equals 114 kN/m (7.79 kips/ft). The magnitude of this load is:

$$w_u = 2 [M_u^- + M_u^+ L / (L - x)] / L x \qquad (2)$$

Finite Element Model

The results from the above closed form solutions are verified with a finite element model of the beam with solutions obtained using the ANSYS computer code. The model used for the beam is shown in Fig. 5. The concrete is modeled with element "SOLID65" of ANSYS. Cracking and crushing behavior of the concrete is considered in the solutions. The steel reinforcement is modeled discretely with spar elements having elastic-perfectly plastic material properties.

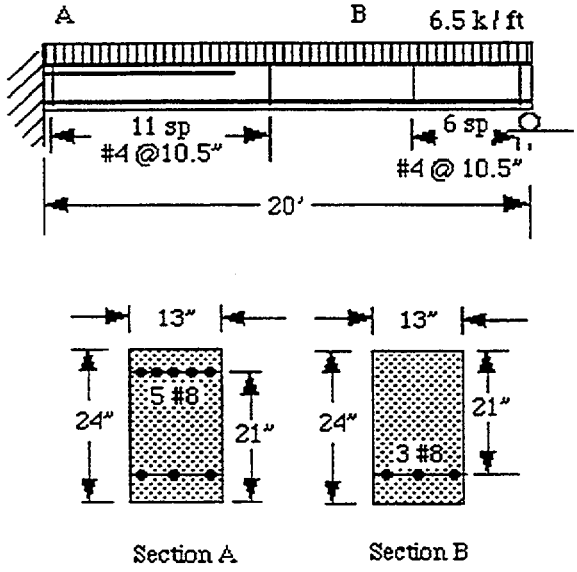

Fig. 4 Sample Beam Problem
(1 in. = 25.4 mm; 1 ft = 30.48 cm;
1 kip/ft = 14.6 kN/m)

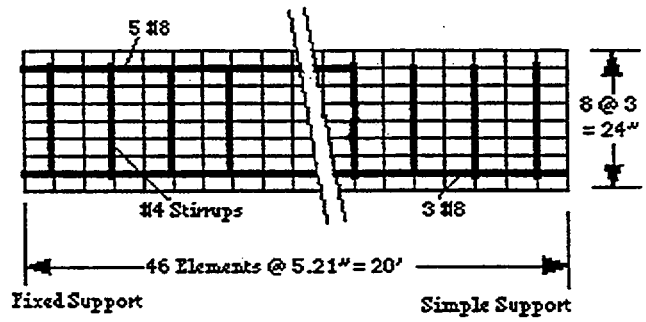

Fig. 5 ANSYS Beam Model
(1 in. = 25.4 mm; 1 ft = 30.48 cm)

The uniform load on the beam is increased until convergence of the ANSYS solutions can no longer be achieved. Cracking is calculated to occur at a load of 24.1 kN/m (1.65 kips/ft). The first plastic hinge (defined at the first yielding of the reinforcement) forms at 103 kN/m (7.05 kips/ft) and the second plastic hinge forms at 115 kN/m (7.88 kips/ft). It should be recalled that the corresponding ACI code calculated values are 14.4 kN/m (0.986 kips/ft) for cracking, 105 kN/m

(7.22 kips/ft) for the first plastic hinge, and 114 kN/m (7.79 kips/ft) for the second hinge. Plots of load versus deflection for the beam are shown in Fig. 6 for both the finite element and hand calculation models. It can be seen that the agreement between the two is quite good. Based on these results, the ACI 318 calculations are used to generate the beam fragility curves.

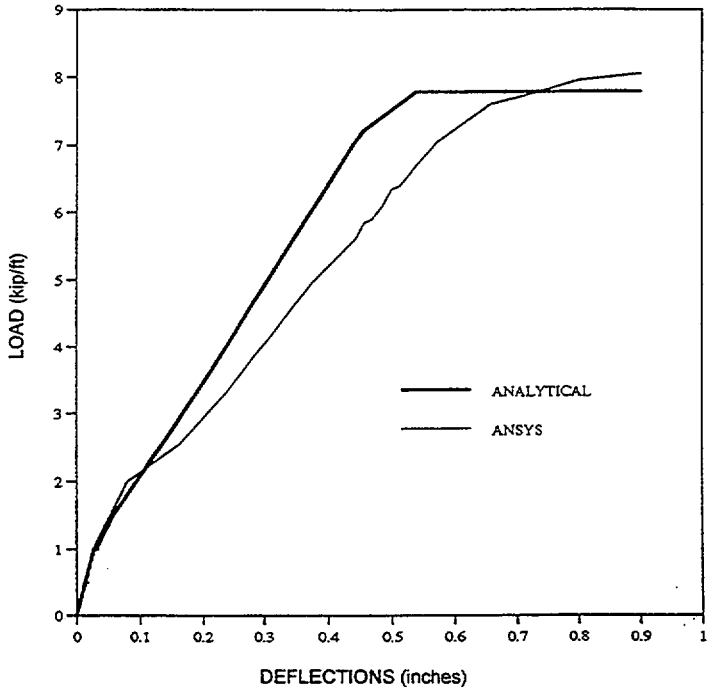

Fig. 6 Comparison of ANSYS and Analytical Beam Deflection
(in. = 25.4 mm; 1 kip/ft = 14.6 kN/m)

Fragility Results for Beams

Fragility curves are generated for the undegraded (benchmark case) and degraded beams. The data presented in Table 3 are used to develop the fragility of the undegraded beam. Equation (2) is used to evaluate the beam strength for each of 19 Latin Hypercube samples. A standard statistical package is used to evaluate the 19 samples and the resulting mean strength is found to be 126 kN/m (8.66 kips/ft) (compared to 114 kN/m (7.79 kips/ft) for the design case). The logarithmic standard deviation, V_C, is found to be 0.11.

Based on published data (Amleh and Mirza, 1999), several levels of corrosion were identified for crack widths observed in concrete members. It was found that crack widths (parallel to the reinforcement) on the order of 0.15 mm (0.0059 in.) correspond to the first stage of corrosion with essentially no reduction in steel area or bond strength, while crack widths on the order of 9 mm (0.354 in.) are associated with 20% loss in steel (cross-sectional) area and significant loss of bond strength. Since the 9 mm (0.354 in.) crack would be readily observable during an inspection and would afford the opportunity to make repairs, it was decided to consider steel area losses of 20% and 10% (treated as random variables).

In addition to loss of steel area, concrete spalling (resulting from either freeze thaw problems or steel corrosion) is also considered as a degradation mechanism. Spalls in concrete beams usually occur outside of the steel cage. This is modeled by reducing the effective depth of the

beam section by subtracting the cover from the depth. The cover is defined with a mean depth of 4.45 cm (1.75 in.) with a COV in depth equal to 0.36. Since corrosion can result in loss of steel and concrete spalling, the combined case of both effects are considered in addition to the individual effects.

The fragility parameters for the degraded beam for several postulated states of degradation are summarized in Table 5, and the fragilities are shown in Fig. 7. The results indicate that there is about ½% probability of failure at the design ultimate capacity of 94.9 kN/m (6.5 kips/ft). It can be seen (in the Table and Figure) that the V_c is about the same for all cases and thus the fragilities are nearly parallel to one another. The strength of the beam is reduced by less than 18% for the worst cases. The most severe cases result from a 20% loss of steel area. It should be noted that this mechanism is associated with severe cracking of the concrete section which could be readily observed during an inspection. It is believed that inspections of the facility would identify such problem areas before serious degradation of strength occurs. The results for the beam evaluation have been expanded to other beams and slabs and are presented in NUREG/CR-6715.

Table 5
Fragility Curve Statistics for Degraded and Undegraded Beam Case

Case	Mean Capacity		V_c
	kips/ft	kN/m	
Undegraded	8.66	126	0.11
Bottom Spall	8.23	120	0.12
Top Spall	8.06	118	0.12
Top and Bottom Spall	7.89	115	0.13
10% Loss of Top and Bottom Steel	7.81	114	0.12
20% Loss of Top and Bottom Steel	7.29	106	0.13
20% Loss of Steel & Spall, Both at Bottom	7.11	104	0.12
20% Loss of Steel & Spall, Both at Top	7.45	109	0.12

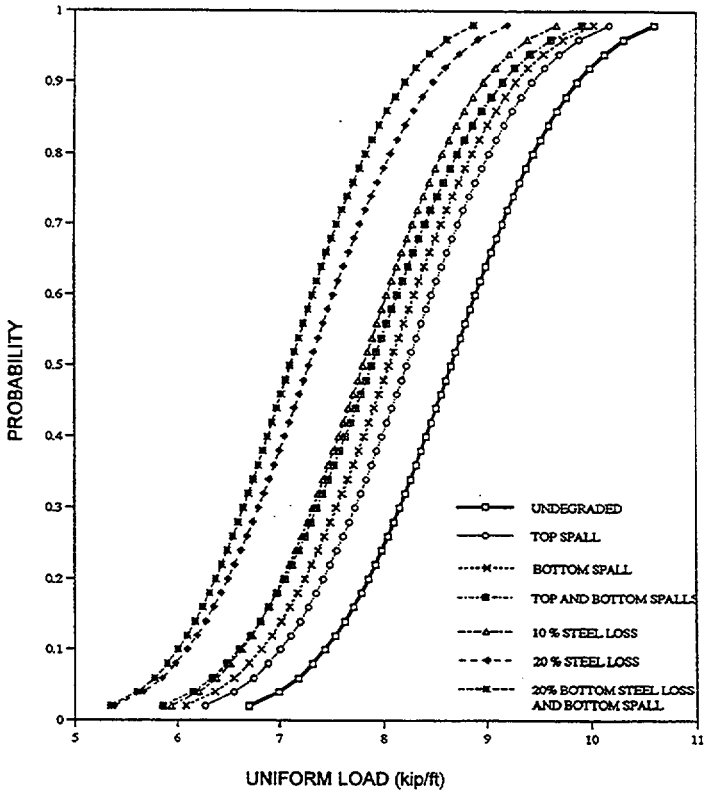

Fig. 7 - Fragility Curves For Various Beam Degradation Conditions (1 kip/ft = 14.6 kN/m)

3.3 Fragility Evaluation of Degraded Shear Walls

Validation of Analytical Code

A series of tests performed in Japan (Yamakawa, 1995) on shear walls are used to verify ANSYS models of shear walls. The walls are 950 mm (37.4 in.) high, 800 mm (31.5 in.) wide, and 80 mm (3.15 in.) thick. The reinforcement consists of two layers of 6 mm bars (0.236 in.) spaced

at 100 mm (3.94 in.) in each direction. Thick (essentially rigid) edge beams were placed at the top and bottom of the specimen. Static cyclic loading was applied to the specimens. Both undegraded and degraded (with various levels of steel corrosion) shear walls were tested; the verification is made for the undegraded case.

The ANSYS model used for this verification study utilizes the finite element "SOLID65" which includes both cracking and crushing of the concrete. The development of a crack at an integration point modifies the stress-strain relations by introducing a plane of weakness. The post-cracking behavior is represented using a shear transfer coefficient which consists of a shear strength reduction factor for subsequent loads which induce sliding (shear) across the crack face. The shear transfer coefficient can range from 0.0 to 1.0. A value of 0.5 was selected for this study and varied by ± 25% to evaluate its impact. The sensitivity analyses indicated that the response of the model was not significantly affected by variation in this parameter. The steel reinforcement is modeled with elastic-perfectly plastic spar elements.

A comparison of the load-deflection behavior and crack patterns from the test specimens and the ANSYS model demonstrated that the ANSYS finite element modeling approach is suitable for predicting the behavior of reinforced concrete shear walls for the purpose of this study.

Deterministic Analyses of a Representative Shear Wall

A specific shear wall with characteristics that are representative of those found in NPPs was selected to evaluate the effects of degradation on reinforced concrete walls. The wall is 6.1 m (20 ft) high by 6.1 m (20 ft) wide and is 61 cm (2 ft) thick. The reinforcement consists of 15.9 mm (#5) bars spaced at 21.6 cm (8.5 in.) at each face in each direction resulting in a horizontal and vertical reinforcing ratio equal to 0.003. The shear wall is assumed to be part of an enclosure of a square room having similar shear walls on all sides and a ceiling with similar dimensions. The walls normal to the shear wall under consideration act as flanges and provide moment resistance. The ceiling slab acts as a stiff member to distribute the shear load uniformly across the wall. A vertical load resulting from gravity loads in the building is included and selected to produce a uniform compressive stress in the wall equal to 2.07 MPa (300 psi). The specified concrete strength is taken as 27.6 MPa (4 ksi) and grade 60 reinforcement is used. Several analytical methods are used to calculate the ultimate capacities for comparison with the ANSYS solution.

ACI Design Code Methodology

Using ACI 318-99 the shear capacity of the wall can be calculated using the expression:

$$\phi V_n = \phi \, [3.3 \, (f'_c)^{1/2} \, h \, d + N_u \, d / 4 \, L_w + A_v \, f_y \, d / s_2] \qquad (3)$$

where, ϕ = capacity reduction factor, taken =1.0 (since true estimate of capacity is desired for fragility calculations)

h = wall thickness

d = 0.8 * wall width

A_v = area of horizontal steel within distance s_2

s_2 = spacing of horizontal reinforcement

N_u = axial load = 0.3 * h * L_w

L_w = wall width

The resulting design capacity of the wall in shear is calculated to be 2,150 kips (9.56MN).

Barda et al. Methodology

The ACI code is known to be conservative for low-rise walls. Barda et al. (1977) used experimental data (based on tests of low-rise shear walls) to develop the following equation for the concrete contribution to the wall shear strength:

$$V_{conc} = [8.3 (f'_c)^{1/2} - 3.4 (f'_c)^{1/2} (H / L_w - 0.5) + N_u /(4 h L_w)] h d; \quad (4)$$

where, H = wall height

For fragility analyses, in which the statistics of V_{conc} are required, the term $f_t / 6$ (where f_t = splitting strength) should be substituted for $(f'_c)^{½}$. This is necessary because the variability in the shear strength is incorrectly reduced when $(f'_c)^{½}$ is used in Eq. (4). To account for the contribution of vertical and horizontal reinforcement to wall strength, Wesley and Hashimoto (1981) developed the following equation for the shear strength developed from the horizontal and vertical reinforcement ratios (ρ_h and ρ_v):

$$V_{steel} = [a r_h + b r_v] f_y h d \quad (5)$$

where, $a = 1 - b$

$b = 1$ for $H / L_w < 0.5$; $= 2 (1-h / L_w)$ for $0.5 < H / L_w < 1$; $= 0$; for $H / Lw > 1$

The total shear wall capacity is calculated as the sum of equations (4) and (5). This results in a shear capacity of 3,170 kips (14.1 MN), which is about 50% higher than the ACI code predicted capacity.

Evaluation of Shear Wall (Design Case) Using Finite Element Method

The ANSYS model used to evaluate the load-deflection characteristics of the example wall is shown in Fig. 8. The same model characteristics are used as discussed above for the ANSYS validation except that the material properties reflect the design properties. The material properties used for this "design case" are f'_c = 27.6 MPa (4 ksi), f_t = 3.09 MPa (448 psi), E_{it} (initial tangent modulus) = 26.4 GPa (3,834 ksi), and f_y = 414 MPa (60 ksi). Sensitivity studies were made for various solution parameters (load step size, number of iterations, and convergence criteria) to confirm the accuracy of the selected values while minimizing the computer execution time. Several sensitivity studies were also conducted to determine the importance of certain design and analysis parameters. The studies included variations on the concrete tensile strength and the shear transfer coefficient used as input for the ANSYS finite element when cracking occurs.

A load-deflection plot derived from the ANSYS solution is shown in Fig. 9. Straight lines are fit to the elastic and inelastic portions of the design curve so that various characteristics of the curve may be established. This shows that the yield load is about 2,550 kips (11.3 MN) and the corresponding yield deflection is 0.075 in. (1.91 mm) (drift ratio = 0.03%). The ACI Code predicted strength is about 83% of the yield load while the Barda et al. methodology predicted a strength higher than the yield load, at a deflection equal to approximately 0.18 in. (4.57 mm) (2.3 times yield deflection). For this study, the limit state is defined by the point where the drift ratio exceeds four times the yield drift ratio, a point where significant damage to attachments and penetrations may occur. Similar limiting deformation levels have been assumed in previous seismic PRAs and margin studies of NPPs (e.g., Wesley and Hashimoto, 1981). For the "design case" shown in Fig. 9, the limit state is calculated to be 0.3 in. (7.62 mm).

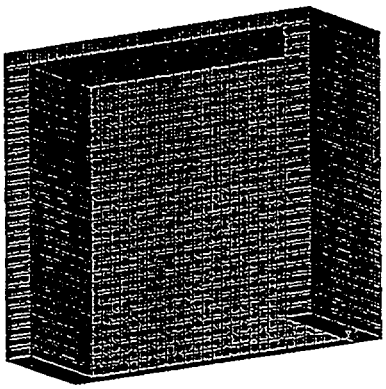

Fig. 8 Shear Wall Finite Element Model

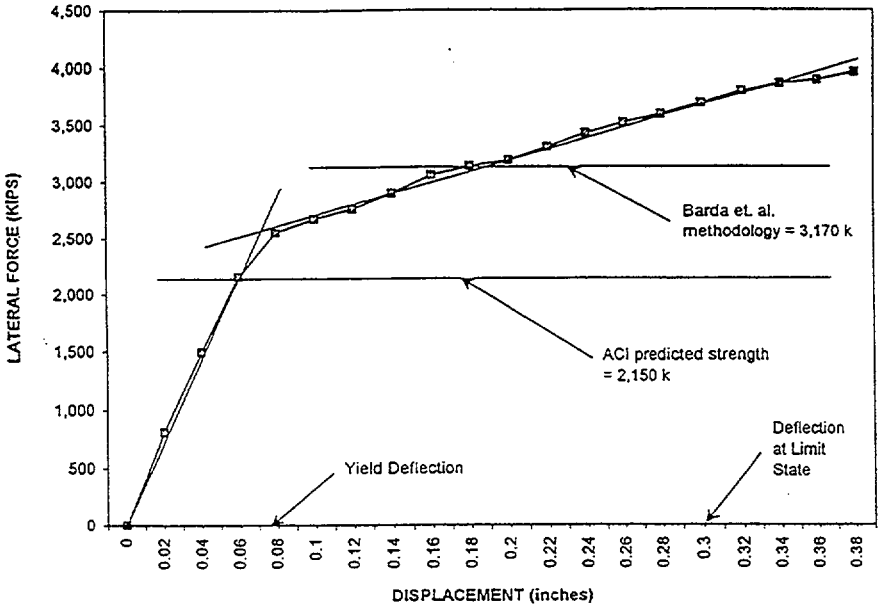

Fig. 9 Shear Wall Design Case, Undegraded, Load-Deflection Curve (1 in. = 25.4 mm; 1 kip = 4.45 kN)

Fragility Results for Shear Walls

The shear wall model shown in Fig. 8 is used to develop fragility curves for evaluation of the effect of degradation using the data shown in Table 4. A horizontal lateral (in plane) load is applied to the top of the wall for each case and increased until large plastic deformations occur. The wall is evaluated using an equivalent static lateral force method of analysis, making the process of evaluation of wall capacity similar to a nonlinear pushover analysis of the type often used in recent years to evaluate buildings for earthquake resistance. The objective of the study is to develop the relative fragilities for undegraded and degraded concrete members. It is likely that dynamic effects play similar roles in modifying the fragilities for both conditions, and therefore the ratio of the degraded to undegraded fragility would be about the same in either case. Load-deflection curves are calculated for the 19 Latin Hypercube data samples for the undegraded case and each degraded condition. For each curve, straight lines are fitted to the elastic and plastic portions of the curve (similar to those shown in Fig. 9 for the design case). Then the load corresponding to 4 times the design yield drift is read off the curve.

Solutions are obtained for both the undegraded wall and for degradation of the wall with a 20% loss of steel area and complete spalling of the concrete cover. The solutions for the undegraded case indicate a mean strength of 16.3 MN (3,655 kips) with a V_C of 0.15. Solutions for the 20% steel area loss indicate a mean strength of 16.2 MN (3,634 kips) with a V_C equal to 0.16. Considering a 20% loss of steel area in combination with concrete spalling, the mean strength is reduced further to 15.3 MN (3, 446 kips) with a coefficient of variation equal to 0.15. A plot of the fragility curves is given in Fig. 10. For this case, the 20% loss of steel area was considered only for the shear wall (i.e., not the flange walls).

To confirm the fragility results for the shear wall by analytical means is difficult. It is known that applying the ACI code methodology to low rise shear walls leads to very conservative (i.e. low)

estimates of ultimate shear load capacity. Therefore, the Barda et al. methodology is used to determine the effect of degradation on the ultimate capacity (not the deformation-related limit state as defined previously for this study). For the configuration and design discussed in this paper, the resulting mean strength (ultimate shear capacities) for the undegraded case is calculated to be 16.7 MN (3,751 kips). For the 20% loss of steel area, the mean strength is 15.8 MN (3,545 kips) and for the combined loss of steel area and concrete spalling the mean strength drops to 14.4 MN (3,244 kips). These results, as well as the finite element evaluation, indicate that the effect of degradation due to loss of steel (up to 20%) is small. This occurs because of the relatively low steel ratio for the sample shear wall problem. Evaluation of the wall for other variations in degradation and design parameters (e.g., different reinforcement ratios and aspect ratios) are presented in NUREG/CR-6715.

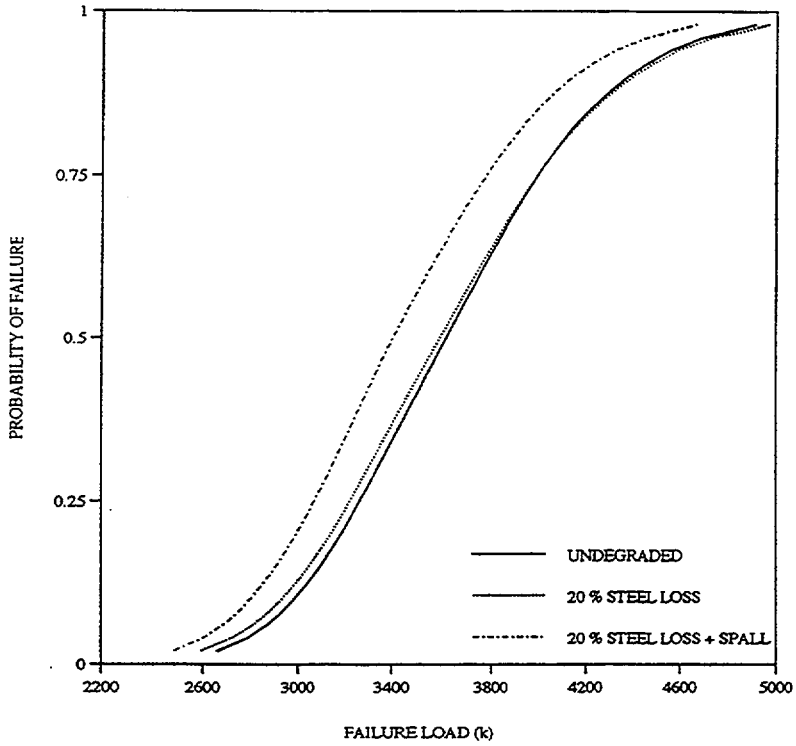

Fig. 10 Fragility Curves for Example Shear Wall (1 kip = 4.45 kN)

3.4 Development of Probability-Based Degradation Acceptance Limits

Probability-based degradation acceptance limits were developed based on levels of degradation that would have to occur to significantly increase plant risk. The potential impact of structural degradation on plant level HCLPF (High Confidence Level of Low Probability of Failure) and core damage frequency was based on a study of the Zion Plant (Ellingwood 1998). Based on conclusions reached from the Zion study, inferences on changes in core damage frequency at other plants were made. The criteria presented in Figure 3 of NRC Regulatory Guide 1.174 were used to define acceptable (i.e., small) changes in core damage frequency.

From the above effort, it was concluded that approximately a 20% reduction in fragility is a reasonable criteria to determine probability-based degradation acceptance limits. This level of reduction in fragility would result in changes in core damage frequency which would fall into "Region II" of Figure 3 in NRC Regulatory Guide 1.174. Changes within Region II are considered

to be "small" and cummulative impacts are to be "tracked." The next step was to relate observable levels of degradation to reduction in fragility. Two of the most common degradation effects, cracking and spalling, were considered. For cracking, experimental data (Alonso, C. et al., 1998) were utilized to obtain a relationship between crack size and loss of reinforcing steel area. This information was utilized to develop the probability-based degradation acceptance criteria for concrete members. Samples of the probability-based degradation acceptance criteria developed for beams and shear walls are presented in Tables 6 and 7, respectively.

Table 6 - Probability-Based Crack Acceptance Limits For Beams Considering Loss of Steel Area and Concrete Spalling

Interior Beams (1-1/2 in. Cover)

Minimum Beam Depth (in.)				Acceptable Crack Width (in.)
#4 Reinf	#5 & #6 Reinf	#7 & #8 Reinf	> #9 Reinf	
13	12.2	12	11.	1/32
20	15.2	13.	12.	1/16
*	29	19	14.	3/32
*	*	39	20	1/8
*	*	*	35	5/32

Table 7 - Probability-Based Crack Acceptance Limits For Shear Walls Considering Loss of Steel Area and Concrete Spalling

Bar Size	Acceptable Crack Width (in.)
#5 or Smaller	1/8
#6 and #7	5/32
#8 or larger	3/16

Note: Conditions for the use of the above criteria is presented in NUREG/CR-6715;
1 in. = 25.4 mm

4. Recommendations

The Phase II research effort is continuing with evaluation of the other four structures and passive components using a similar approach as described above for reinforced concrete members. Currently, buried piping is being evaluated which will be followed by anchorages, flat bottom steel tanks, and masonry walls. The analytical results and degradation acceptance criteria for all of these evaluations are being developed using a probabilistic risk assessment methodology which can be used to determine whether observed levels of degradation potentially have a significant effect on plant risk. Currently, probability-based methods cannot be utilized for NRC licensing activities such as license renewal under 10 CFR Part 54. Therefore, in addition to the research effort described in this paper, it is recommended that deterministic methods be utilized in order to develop degradation acceptance criteria that could be used as guidance for NRC licensing activities related to license renewal. This effort is deemed to be important because quantitative degradation acceptance criteria apparently is lacking in the design, inspection, and construction industry for a number of materials, structures and passive components.

5. Conclusions

The results of the Phase I research effort have led to the development of a degradation occurrence database. Trending analyses of the degradation occurrences has identified which structures and passive components were most susceptible to degradation at NPPs. This information along with seismic risk significance, importance to current licensing basis/license

renewal, and adequacy of existing NRC and industry programs on aging has identified five structures and passive components that warrant further detailed evaluation in the Phase II effort. The five structures and passive components are reinforced concrete members (other than containments), underground piping, masonry walls, flat bottom steel tanks, and anchorages. Details of the Phase I research effort are presented in NUREG/CR-6679.

Phase II evaluation for the first structure/passive component identified in the Phase I effort was performed for degraded reinforced concrete flexural members and shear walls. This evaluation has led to the following conclusions:

1. For a 20% loss of steel cross-sectional area (without concrete spalling) or complete spalling of concrete cover (without loss of steel area) the strength of degraded beams decreases by less than 20%. For the case of loss of steel area in combination with complete concrete spalling, the loss of steel area must be restricted to be less than 20% in order to maintain the same level of reduction in fragility curves.
2. Beam fragility curves shift to lower values of strength and remain almost parallel to each other as the beam properties degrade (i.e., concrete spalling and loss of steel area). This implies that the effects of degradation on beam strength at any given conditional probability of failure can be estimated, to first approximation, by considering the impact of degradation on its median capacity, determined by assuming all parameters take on their median values.
3. Finite element results for the shear wall, having an aspect ratio of 1.0 and a steel ratio of 0.003, indicate that the effect of a 20% loss of steel area in combination with spalling of concrete results in a reduction of the mean wall strength of approximately 6%. The effects of steel degradation increase for higher steel ratios and larger aspect ratios.
4. As in the case of flexural members, the wall fragility curves shift to lower values of strength and remain nearly parallel when degradation occurs. Therefore, the effects of degradation can be estimated, to first order, by determining the median wall capacity from the medians of the individual variables, and anchoring the reduced fragility curves at the 50^{th} percentile.
5. The research effort also assessed the potential effects of degradation on plant risk and developed probability-based degradation acceptance limits. The probability-based degradation limits provide quantitative guidance to determine whether observed levels of degradation potentially have a significant effect on plant risk. The criteria could be used during walkdowns to determine whether repairs are warranted or further evaluation/monitoring is needed.

Details of the Phase II research effort for evaluation of degraded reinforced concrete members are presented in NUREG/CR-6715.

6 REFERENCES

10 CFR Part 54, "Requirements for Renewal of Operating Licenses for Nuclear Power Plants."

10 CFR 50.65, "Requirements for Monitoring the Effectiveness of Maintenance at Nuclear Power Plants."

ACI 318, "Building Code Requirements for Reinforced Concrete," American Concrete Institute, Farmington Hills, MI.

ACI 349, "Code Requirements for Nuclear Safety Related Concrete Structures," American Concrete Institute, Farmington Hills, MI.

Alonso, C., Andrade, C., Rodriguez, J., and Diez, J. M. (1998), "Factors Controlling Cracking of Concrete Affected by Reinforcement Corrosion," Materials and Structures 31(211), pp. 435-441, RILEM, Cachan, France.

Amleh, I. and Mirza, S., "Corrosion Influence on Bond Between Steel and Concrete," ACI Structural Journal 96(3), 415-423, American Concrete Institute, Farmington Hills, Michigan, 1999.

ANSYS, Finite Element Computer Code, ANSYS Rev. 5.4, ANSYS, Inc., Canonsburg, PA.

Barda, F., Hanson, J. M., and Corley, W. G., "Shear Strength of Low-Rise Walls with Boundary Elements," Reinforced Concrete Structures in Seismic Zones, ACI SP-53, American Concrete Institute, 1977.

Campbell, R. D., Ravindra, M. K., and Murray, R. C., "Compilation of Fragility Information from Available Probabilistic Risk Assessments," LLNL, UCID-26071, Rev. 1, September 1988.

Ellingwood, B. R. and Hwang, H., (1985), "Probabilistic Descriptions of Resistance of Safety-Related Structures in Nuclear Plants," Nuclear Engineering and Design 88(2): 169-178.

Ellingwood, B. R., (1998), "Issues Related to Structural Aging in Probabilistic Risk Analysis of Nuclear Power Plants," Reliability Engineering and System Safety 62(3): 171-183.

Kennedy, R. P. and Ravindra, M., (1984), "Seismic Fragilities for Nuclear Power Plant Studies," Nuclear Engineering and Design 79(1): 47-68.

MacGregor, J. G., Mirza, S. A. and Ellingwood, B. R., (1983), "Statistical Analysis of Resistance of Reinforced and Prestressed Concrete Members," Journal American Concrete Institute 80 (3): 167-176.

Naus, D. J., Oland, C. B., Ellingwood, B. R., Hookham, C. J., and Graves, H. L., (1999), "Summary and Conclusions of a Program to Address Aging of Nuclear Power Plant Concrete Structures," Nuclear Engineering and Design,194, 1999: 73-96.

NRC "Standard Review Plan for the Review of Safety Analysis Reports for Nuclear Power Plants," NUREG-0800, U.S. Nuclear Regulatory Commission, Washington, D.C.

NRC Regulatory Guide 1.174, "An Approach for Using Probabilistic Risk Assessment in Risk-Informed Decisions on Plant-Specific Changes to the Licensing Basis," Nuclear Regulatory Commission, Washington, D.C., July 1998.

NUREG-1407, "Procedural and Submittal Guidance for the Individual Plant Examination of External Events (IPEEE) for Severe Accident Vulnerabilities," by Chen, J. T., Chokshi, N. C.,

Kenneally, R. M., Kelly, G. B., Beckner, W. D., McCracken, C. A., Murphy, J., Reiter, L., and Jeng, D., U.S. Nuclear Regulatory Commission, Washington, D.C., June 1991.

NUREG-1522, "Assessment of Inservice Conditions of Safety-Related Nuclear Plant Structures," by Ashar, H. and Bagchi, G., U.S. Nuclear Regulatory Commission, Washington, D.C., June 1995.

NUREG/CR-3558, "Handbook of Nuclear Power Plant Seismic Fragilities," by Cover, L. E., Bohn, M. P., Campbell, D. A., and Wesley, D. A., June 1985.

NUREG/CR-4334, "An Approach to the Qualification of Seismic Margins in Nuclear Power Plants," by Budnitz, R. J., Amico, P. J., Cornell, C. A., Hall, W. J., Kennedy, R. P., Reed, J. W., and Shinozuka, M., Lawrence Livermore National Laboratory, July 1985.

NUREG/CR-6679, "Assessment of Age-Related Degradation of Structures and Passive Components for U.S. Nuclear Power Plants," by Braverman, J. I., Hofmayer, C. H., Morante, R. J., Shteyngart, S., Bezler, P., Brookhaven National Laboratory, Upton, N.Y., August 2000.

NUREG/CR-6715, "Probability-Based Evaluation of Degraded Reinforced Concrete Components in Nuclear Power Plants," by Braverman, J. I., Miller, C. A., Ellingwood, B. R., Naus, D. J., Hofmayer, C. H., Shteyngart, S., Bezler, P., Brookhaven National Laboratory, Upton, N.Y., April 2001.

Park, Y. J., Hofmayer, C. H., and Chokshi, N. C., (1998), "Survey of Seismic Fragilities Used in PRA Studies of Nuclear Power Plants," *Reliability Engineering & System Safety*, v. 62, No. 3, pp. 185-195.

Wesley, D. A., and Hashimoto, P. S., "Seismic Structural Fragility Investigation for the Zion Nuclear Power Plant," NUREG/CR-2320, U.S. Nuclear Regulatory Commission, October 1981.

Yamakawa, T., (1995), "An Experimental Study on Deterioration of Aseismic Behavior of R/C Structural Walls Damaged by Electrolytic Corrosion Testing Method," Concrete Under Severe Conditions: Environment and Loading, Volume 2, Edited by K. Sakai, N. Banthia and O.E. Gjorv, E & FN Spon, London, England.

DISCLAIMER

This work was performed under the auspices of the U.S. Nuclear Regulatory Commission. This paper was prepared in part by an employee of the United States Nuclear Regulatory Commission. It presents information that does not currently represent an agreed-upon position. NRC has neither approved nor disapproved its technical content.

Study of High Burnup Fuel Behavior under LOCA Conditions at JAERI: *Hydrogen Effects on the Failure-bearing Capability of Cladding Tubes*

F. NAGASE and H. UETSUKA

Department of Reactor Safety Research
Japan Atomic Energy Research Institute
Tokai-mura, Ibaraki-ken, 319-1195, Japan

Abstract

This paper describes recent results from studies on high burnup fuel behavior under LOCA conditions at JAERI. The influence of pre-hydriding and restraint load on the failure-bearing capability of oxidized cladding tubes was evaluated by "Integral thermal shock tests." Maximum restraint load on a fuel rod upon quenching was estimated based on results from compression tests of control-rod guide tubes.

1. INTRODUCTION

The Japanese LOCA criteria on fuel safety, 15% cladding oxidation (ECR*) and 1200 °C peak cladding temperature, were established in 1975, based on the concept of zero ductility of cladding as in the U.S. After their establishment, the Japan Atomic Energy Research Institute (JAERI) found that inner surface oxidation of the cladding after rod-burst is accompanied by significant hydrogen absorption [1]. Ring compression tests were performed on specimens cut from the cladding that experienced rod-burst and double-sided oxidation to examine the embrittlement due to oxidation and hydrogen absorption. The ductility of the ring specimens fell down to the zero ductility range when the cladding was oxidized to several percent ECR, indicating that significant hydrogen absorption enhances cladding embrittlement [2]. Accordingly, JAERI conducted "integral thermal shock tests" to evaluate the failure-bearing capability of oxidized cladding under appropriately simulated LOCA conditions [3]. In the test, a short test rod was heated up, burst, oxidized in steam and quenched by flooding water, and it was completely restrained during quenching in order to conservatively simulate possible axial loading. Obtained results confirmed that the criterion of 15% ECR still had safety margin, and the LOCA criteria were revised in 1981 referring the results of the integral thermal shock tests. Therefore, the current Japanese LOCA criteria on fuel safety are not based on the concept of zero ductility of cladding, but on the failure threshold value determined in the integral thermal shock tests under restrained conditions. However, the current LOCA criteria are generally grounded on a database from the tests with non-irradiated cladding materials. Although burnup effect was generally taken into account for the revised criteria, the level of fuel burnup was rather low at that time. Therefore, high burnup fuel behavior under LOCA conditions is a subject of great concern; consequently, extensive research programs have been performed in France, the Unites States and Japan etc. [4-8]. A systematic research program is being conducted at JAERI with a view to

* ECR: Equivalent Cladding Reacted (Proportion of oxide layer thickness assuming that all of absorbed oxygen forms stoichiometric ZrO_2)

obtaining a wide range database for evaluating the influence of burnup extension on fuel behavior under LOCA conditions. The outline of the research program and recent results are described in this paper.

2. OUTLINE OF TEST PROGRAM

The research program consists of integral thermal shock tests and other separate tests including Zircaloy-steam oxidation tests, mechanical property tests of cladding, and tube burst tests. Several types of Zircaloy cladding samples are used for these tests to assess separate effects and to provide a wide range of basic data available for regulatory judgment. They are (a) as-received cladding tubes, (b) simulated high burnup fuel cladding tubes that are artificially pre-oxidized, pre-hydrided and/or neutron irradiated, and (c) high burnup PWR fuel cladding tubes [4]. The schedule of the present research program is shown in **Table 1**. The integral thermal shock tests, the oxidation tests, the mechanical tests have been performed with non-irradiated cladding tubes. Preparations for the tests with irradiated cladding tubes have been progressed in parallel. As a part of the program, a computer code is developed to analyze the fuel rod behavior under LOCA conditions including possible cladding failure on quenching. Data from the experiments will be incorporated into the computer code. The program will be once summarized in five years, then the tests will be continued targeting at the higher burnup range in the long-term research program of JAERI, Advanced LWR Fuel Performance and Safety Research Program (ALPS Program). High burnup UO_2 and MOX fuels will be shipped from European countries to JAERI, and subjected to the systematic fuel safety research, such as the NSRR tests and the LOCA experiments.

Table 1 Schedule of research program on high burnup fuel behavior under LOCA conditions

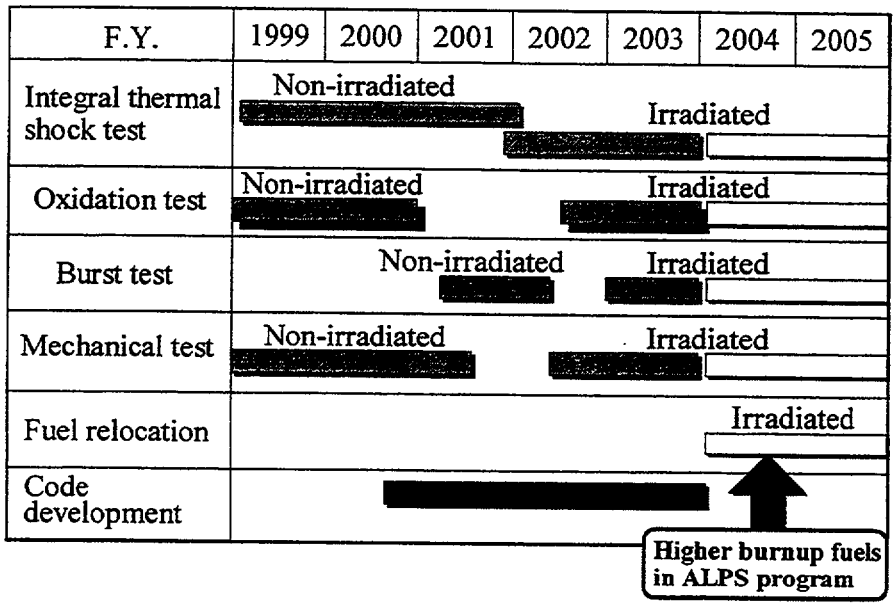

3. INTEGRAL THERMAL SHOCK TESTS

Non-irradiated low-tin (1.3wt%Sn) Zircaloy-4 cladding tube was used in the present study. It was the 17x17-type cladding tube currently used in the PWRs. The outer and inner diameters of the cladding

tube were 9.50 and 8.36 mm, respectively, and the thickness was 0.57mm. Initial hydrogen concentration was about 10wtppm. Key points for evaluating the failure-bearing capability of the high burnup fuel cladding are considered to be:

- Degradation of cladding ductility due to reduction of cladding wall thickness by waterside corrosion, hydrogen absorption, and neutron irradiation, and
- Axial constraint condition.

Considering the first point, the cladding tubes were mechanically thinned and pre-hydrided to simulate corrosion and hydrogen absorption in high burnup fuel cladding. About 10% reduction of initial cladding thickness and hydriding to 100 to 1200wtppm were adopted in the present study. A short test rod was assembled with 600-mm cladding tube, Alumina pellets, end plugs and Swagelok, and was filled with 5 MPa Ar gas at room temperature. **Figure 1** shows schematic drawing of the test apparatus. It is composed of an Instron type tensile test machine, a quartz-made reaction tube, upper and lower manifolds, an infrared image furnace, a steam generator and a water supply system for flooding. **Figure 2** shows an example of the temperature history in the tests. The rod was heated up at a rate of 10 K/s in a steam flow, and then isothermally oxidized for a pre-determined time. The steam flow rate was 1.1×10^2 g/m^2/s. The temperature was measured with Pt-Pt/13%Rh thermocouples spot-welded on the outer surface of the cladding at three axial locations. Rod burst took place at temperatures from 750 to 800°C during the heat up. In the present study, isothermal oxidation temperature and time ranged from 1000 to 1250°C and from 120 to 5500s, respectively. After the isothermal oxidation, the rod was slowly cooled down to about 700 °C and finally quenched with water flooding from the bottom. The reflooding rate was about 30 to 40 mm/s. During a LOCA transient, a fuel rod shall be axially expanded with temperature increase and then be shrunk with decrease in temperature. Oxide layer growth on the cladding surface might enhance the fuel rod expansion. The shrinkage of fuel rod could be restricted to some extent in a fuel assembly, though it is greatly dependent on the fuel design. Then, the test rod was axially restrained at the end of the isothermal oxidation to simulate the possible loading. Since complete constraint of both ends of the rods is

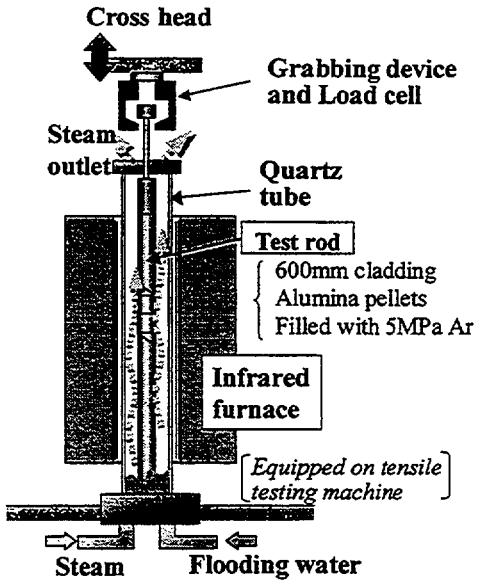

Fig.1 Schematic drawing of test apparatus

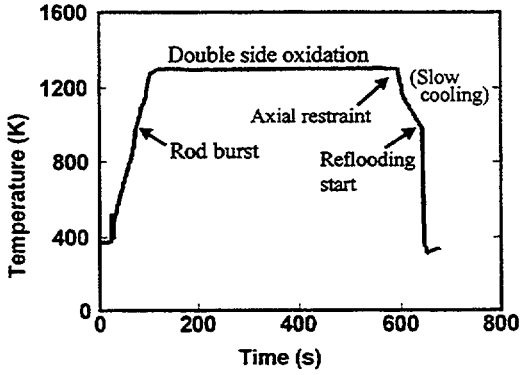

Fig.2 Example of temperature history

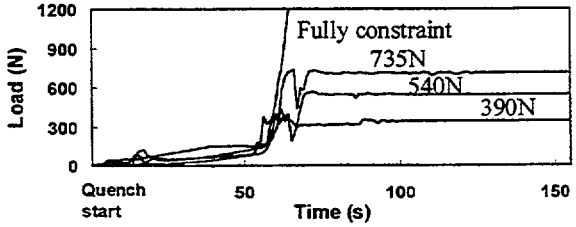

Fig.3 Tensile load control under restraint conditions

probably too conservative in terms of constraint condition, the tensile load was controlled and limited to three different levels of 390±50, 539±50, and 735±50N to realize intermediate constraint conditions, in addition to the fully restrained condition. **Figure 3** shows tensile load curves measured during quenching. The tensile load on the test rod was measured with the load cell, and the obtained load data were used to adjust the restraint load by displacing the crosshead of the tensile machine. The restraint load was successfully to limit the tensile load under the pre-determined levels as shown in the figure.

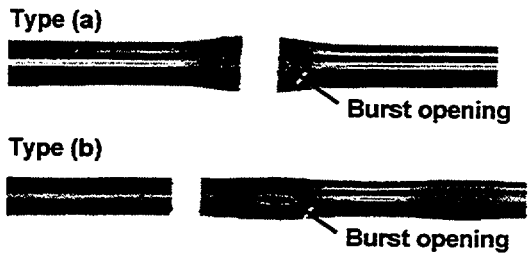

Fig.4 Typical post-test appearances of failed rods

Over 200 tests were conducted and 95 cladding failures were observed during quenching. Most failed claddings split into two parts with circumferential cracking, while fragmentation due to sever embrittlement was observed only in the claddings oxidized to very high ECR. Typical post-test appearances of failed rods are shown in **Fig.4**. Failure during quenching occurred at the ballooned and burst position (Type (a) in the figure) or 30 to 50mm apart from the burst position (Type (b)). Type (a) failure was observed in most of the tests (82 out of 95 tests), while Type (b) failure was observed only in some tests at higher ECR.

Failure maps obtained from the tests under the fully restrained condition are shown in **Fig.5**. The oxidation amount, ECR, of each data was calculated by the Baker-Just equation, and both reduction in cladding wall thickness due to ballooning and double-sided oxidation after cladding rupture were taken into account in the calculation. Open marks in the figure denote oxidation conditions of "survived", while closed marks denote "failed". Figure 5(a) indicates that the failure threshold is about 20%ECR for the tests with non-hydrided claddings. This result agrees very well with the previous data obtained in the experiment with 14×14 type cladding by authors [12]. On the other hand, the failure threshold decreases to about 10%ECR for pre-hydrided cladding tubes, as seen in Fig.5 (b), indicating the obvious influence of pre-hydriding on the failure threshold. Fig.5 (c) shows the failure map for the pre-hydrided cladding with thinner wall of 0.513mm. The threshold is nearly equal to that for 0.57mm-thick cladding tubes. Accordingly, that influence of wall thinning by 10% is negligible on the failure threshold of

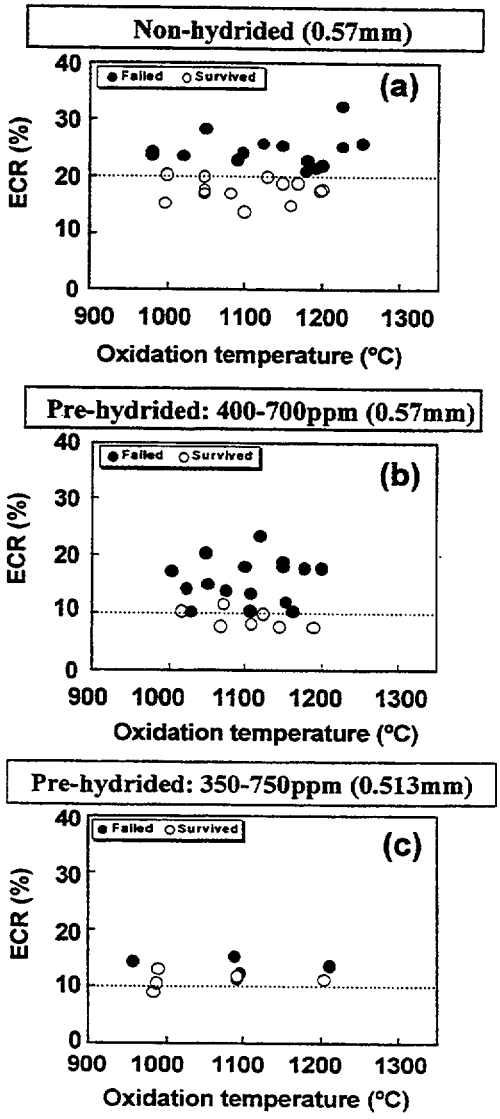

Fig.5 Failure maps relative to oxidation amount and oxidation temperature based on the test results under fully restrained condition; (a) as-received, (b) pre-hydrided cladding tubes (0.57mm thick) and (c) pre-hydrided (0.513mm thick)

oxidized cladding on quenching.

Figure 6 shows fracture loads measured in the tests of thinned and pre-hydrided cladding tubes under the fully restrained conditions. The fracture load ranges almost between 800 and 1800N. Realistic restraint load conditions are probably between the non-restrained and the fully restrained conditions. Based on these data on fracture load, the axial tensile load during quenching was controlled and limit to the three load levels of 390, 540, and 735N. **Figure 7** shows failure maps in the correlation between ECR and the axial tensile load for three different levels of hydrogen concentration. The initial wall thickness is 0.513mm in those cladding tubes. Maximum load during quenching is used for a survived sample and fracture load is used for a failed sample. The figures reveal that the failure threshold generally increases with the decrease of axial tensile load. Comparison of three plots shows that the failure threshold decreases with the increase of hydrogen concentration both in the intermediate and the fully restrained conditions. Consequently, it can be estimated to be higher than 20% ECR, when the tensile load is below about 600N, for the hydrogen concentration range that was examined.

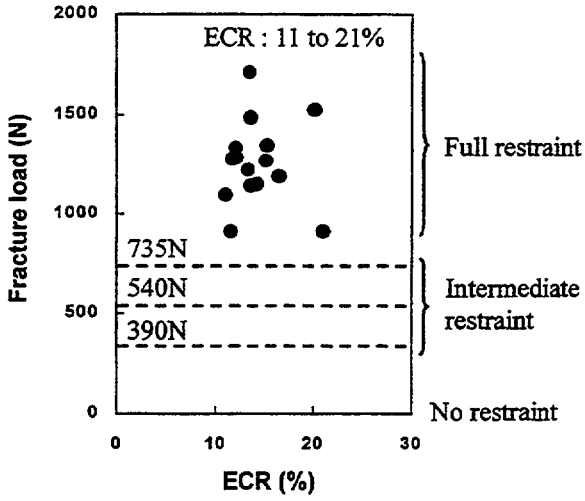

Fig. 6 Fracture loads measured in the tests under fully restrained conditions

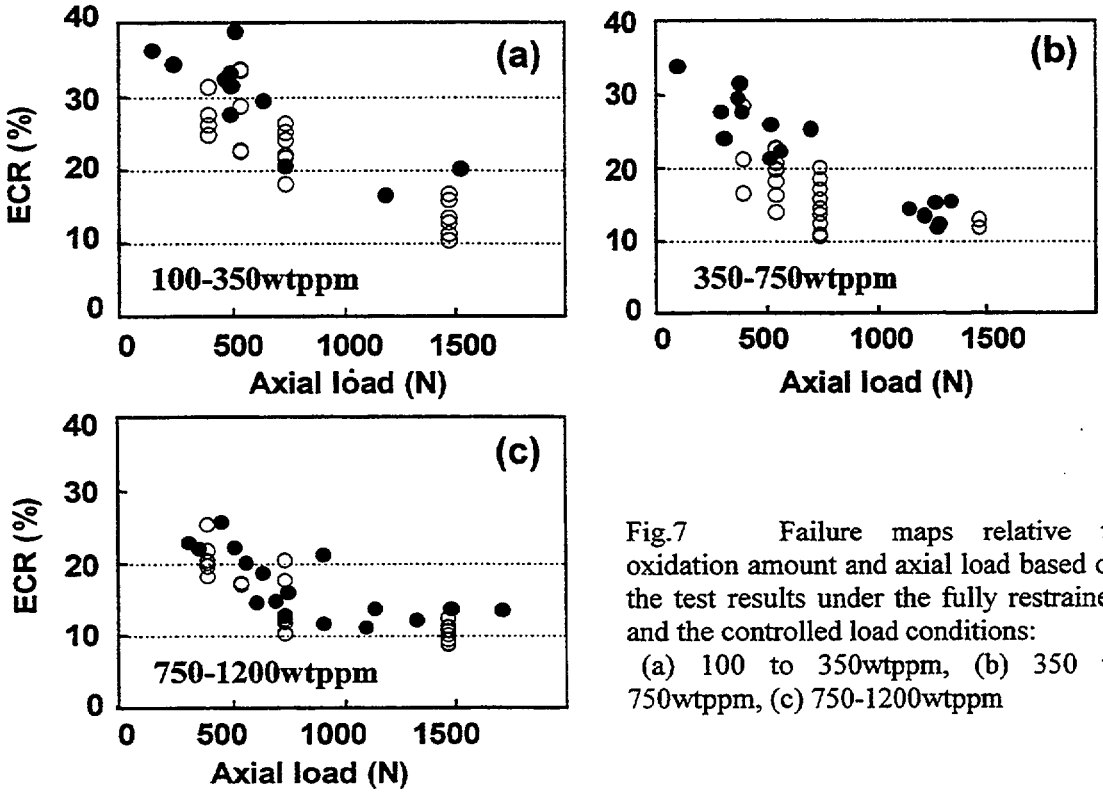

Fig.7 Failure maps relative to oxidation amount and axial load based on the test results under the fully restrained and the controlled load conditions:
(a) 100 to 350wtppm, (b) 350 to 750wtppm, (c) 750-1200wtppm

4. Evaluation of restraint load

The influence of the restraint load on the failure threshold is large as described above. Therefore, it is also required to estimate the realistic range of the restraint load, and analytical and experimental studies have been performed [9-11]. These studied are based on FEM analysis for 2-D fuel bundle model, measurement of load to pull out deformed or reacted cladding tubes through the spacer grid, and calculation of the radial temperature distribution in a fuel assembly. The obtained results depend on assumed mechanism and bundle design as well as estimation method, and reported values varied from 0 to 430N.

Estimation of the restraint load on the fuel rod during quenching was attempted also in the present study taking a different approach. In the LOCA sequences, axial expansion and shrinkage take place with temperature changes and oxide layer growth not only in the fuel rod but also in the control-rod guide tube. Since the guide tube does not contain fuel pellets, temperature increase in the guide tube is smaller than in the fuel rod. The higher temperature in the fuel rod causes higher extent of axial expansion and shrinkage. Therefore, tensile load is generated in the fuel rod during quenching if the shrinkage is restrained. Possible maximum tensile load generated by this mechanism is estimated below. It is assumed that, at the initiation of quench, (a) the guide tube is already cooled down while the fuel rod is still hot, and that (b) the guide tubes and the fuel rods are completely fixed with the spacer grid. These two conditions can be much more conservative than the actuality. By quenching the fuel bundle, tensile load is generated on the fuel rod, while compressive load is generated on the guide tube. Since the number ratio of the guide tubes to the fuel rods is very small, the load per rod is much higher on the guide tube than on the fuel rod. Therefore, the guide tube may be buckled earlier and the maximum tensile load in the fuel rod is limited to the buckling of the guide tube.

Compression tests were performed to estimate the buckling load of the Zircaloy guide tube. The outer diameter and thickness of the used guide tube were 12.2 and 0.41mm, respectively. The length of the tube specimen is about 550mm. As-fabricated specimens and oxidized and quenched specimens were subjected to the compression tests. Oxidation temperatures ranged 1000 to 1200°C and times ranged 150 to 1800s. Proportion of oxide layer in the tubes thickness is estimated to be from 13 to 24% by calculation with the Baker-Just equation. The tubes were quenched from about 700°C after slow cooling from the oxidation temperatures. Compression test were performed at room temperature and the displacement rate of the crosshead was 10mm/min.

Figure 8 shows load-displacement curves obtained in the tests for both as-fabricated and pre-oxidized specimens. The curves show the peaks in the load range from 1500 to 2000N for the as-fabricated tube specimens. The decrease of the load is attributed to bending of the specimen. Since the specimen deformed during the pre-oxidation, bending starts at lower loads for the oxidized specimen, which is indicated by the gentle slope above 500N. **Figure 9** shows typical post-test appearances of pre-oxidized specimens. The specimens oxidized to higher extent became brittle and they were broken into pieces at fracture. Consequently, obtained buckling loads of the pre-oxidized specimens are from 1000 to 1400N and they are obviously smaller than those of the

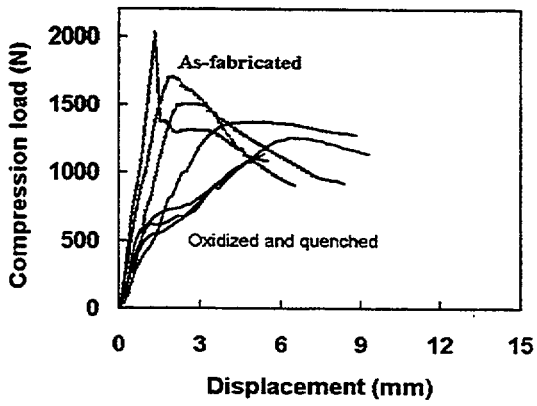

Fig.8 Load-displacement curves in compression tests for guide tube specimens

as-fabricated specimens.

To obtain a conservative result, the maximum buckling load obtained from the as-fabricated specimens, 2000N, is used in the present estimation of the tensile load in a fuel rod. The number ration of guide tube to fuel rod is 1 to 11 in the 17x17 type PWR fuel bundle. It is again assumed that all the fuel rods and the guide tubes are fixed to the spacer grid and the temperature are the same in all the fuel rods. Thus, the tensile load per fuel rod is no larger than 190N when the guide tube buckles by the compressive load less than 2000N. As shown in Fig.7, the failure threshold of the oxidized cladding tube is very high at the load of 190N. However, it should be noted that the present estimation was obtained under some assumptions, and that the restraint load varies with changes in temperature difference among fuel rods, the number of the fuel rods and the guide tubes which are fixed to the spacer grids, the extent of embrittlement of the guide tube etc.

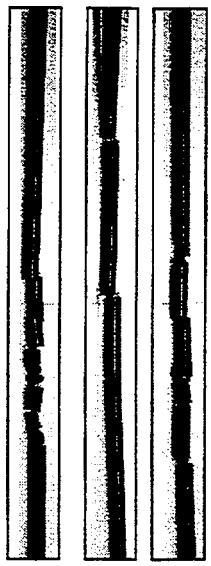

Fig.9 Post-test appearances of pre-oxidized guide tubes

5. Summary

A systematic research program on high burnup fuel behavior under a LOCA condition is being conducted at JAERI, aiming at a wide range database for evaluating the influence of burnup extension. In the program, the integral thermal shock tests to evaluate the failure-bearing capability of oxidized cladding on quenching were performed with non-irradiated Zircaloy-4 cladding tubes that were pre-hydrided to 1200wtppm. Axial tensile loads generated by restricting the cladding shrinkage are controlled to realize intermediate restraint conditions in addition to the fully restrained condition. As a result, variations of the failure threshold value were evaluated as functions of hydrogen concentration and restrained condition during quenching.

- The failure threshold generally decreased with the increases in axial tensile load.
- The influence of pre-hydriding was obviously seen on the failure threshold value under restraint conditions.
- The threshold of highly pre-hydrided claddings was as low as 10% ECR under the fully restrained condition which is the most conservative loading condition.
- It was estimated to be higher than 20% ECR when the axial tensile load was controlled below 600N, for the hydrogen concentration range that was examined.

The control-rod guide tube supports the restraint load on the fuel rod during quench. Then, compression tests of control-rod guide tubes were performed to estimate maximum restraint load on fuel rod. The present estimation under some assumptions suggested that the tensile load is smaller than 190N.

Acknowledgments

The integral thermal shock tests under controlled restraint loads were carried out as the collaboration program between JAERI and Japanese PWR utilities.

REFERENCE

1. H. Uetsuka et al., J. Nucl.Sci.& Tech. Vol.20, No.9, pp.705, 1981.
2. H. Uetsuka et al., report JAERI-M 9445, April, 1981 (Text in Japanese).
3. H. Uetsuka et al., J. Nucl.Sci.& Tech., Vol.20, No.11, pp 941, 1983.
4. F. Nagase et al., Proceedings of ANS topical meeting on LWR fuel performance, Park City (USA), April 10-13, 2000.
5. C. Grandjean et al.,. Proceedings of 24th Water Reactor Safety Information Meeting, UREG/CP-0157, Vol.1, October, 1996.
6. N. Waeckel et al., ibid.
7. M. Ozawa et al, Twelfth International Symposium on Zirconium in the Nuclear Industry, 1998.
8. M. Aomi et al, Proceeding of ANS topical meeting on LWR fuel performance, Park City (USA), April 10-13, 2000.
9. K. Honma et al., ANS Annual Meeting, Milwaukee, Wisconsin, June 17-21, 2001.
10. T. Murata et al., ANS Annual Meeting, Milwaukee, Wisconsin, June 17-21, 2001.
11. N. Waeckel et al, OECD/NEA SEG/FSM LOCA Meeting March 22-23, 2001, Aix-en-Province, March, 2001.
12. H. Uetsuka et al., J. Nucl. Sci.& Technol., Vol.18, No.9, pp 705-717, 1981.

OVERVIEW OF TEST RESULTS ON MECHANICAL PROPERTIES OF UNIRRADIATED AND IRRADIATED Zr-1%Nb (E110 ALLOY) CLADDING

L.Yegorova, K.Lioutov, E.Kaplar
Nuclear Safety Institute of Russian Research Centre "Kurchatov Institute", Moscow, Russian Federation

Abstract

Studies of commercial Zr-1%Nb cladding made of the E110 alloy were performed to reveal differences in the mechanical behavior of unirradiated and irradiated cladding under accident conditions. The research program included such types of mechanical tests as uniaxial tensile tests in transverse and axial directions, low temperature biaxial burst tests with and without axial loading, high temperature burst tests. The final data base with test results contains the mechanical properties (including anisotropy coefficients) burst parameters and parameters of the power law versus burnup (0, 48 MW d/kg U), temperature (20–1200°C), direction of loading, biaxiality ratio, and strain rate. Overview of these results is presented in the paper.

Introduction

Assessments of IGR, CABRI, and NSRR pulse reactor tests performed with high burnup fuel [1, 2, 3] show the need for research programs to study the mechanical behavior of irradiated cladding under accident conditions (reactivity-initiated accident [RIA] and loss-of-coolant accident [LOCA]). One of these programs to investigate Zr-1%Nb (E110 alloy) was initiated in 1997 by the Nuclear Safety Institute of the Russian Research Centre "Kurchatov Institute". This program was conducted in cooperation with the State Research Centre "Research Institute of Atomic Reactors" (Russian Federation) with the support of Ministry of Science and Technologies of Russian Federation, U.S. Nuclear Regulatory Commission, and Institute for Protection and Nuclear Safety (France).

The first part of this program carried out during 1997–2000 was focused on the major physical phenomena characterizing differences in the mechanical behavior of unirradiated and irradiated cladding under RIA and early stage of LOCA (up to the start of high temperature oxidation) conditions. The second part of the program, started this year, is focused on the mechanical behavior of high temperature oxidized cladding (late LOCA and reflooding). The goal of this paper is to present the major findings of the first part of the program.

As-received VVER cladding tubes of Zr-1%Nb (E110 alloy) and cladding specimens of VVER-1000 high burnup fuel rods irradiated at the 5th unit of the NovoVoronezh Nuclear Power Plant up to 48 MW d/kg U were used for this part of the program. Typical parameters of the irradiated Zr-1%Nb cladding are presented in Fig. 1. The approach to select the types of mechanical tests was based on the following set of the program tasks:

- to measure the basic mechanical properties of each type of the cladding versus the temperature and strain rate in the most representative direction (transverse direction);

- to reveal the comparative tendencies in the behavior of unirradiated and irradiated cladding versus the loading direction (transverse and axial), the type of loading (uniaxial and biaxial with different biaxiality ratio) and the temperature;
- to determine the burst parameters for the low temperature and high temperature failure;
- to estimate the anisotropy coefficients versus the temperature;
- to develop the power law in accordance with the MATPRO standard ($\sigma = K\,\varepsilon^{n}\left(\frac{\dot{\varepsilon}}{\dot{\varepsilon}_{o}}\right)^{m}$) [4].

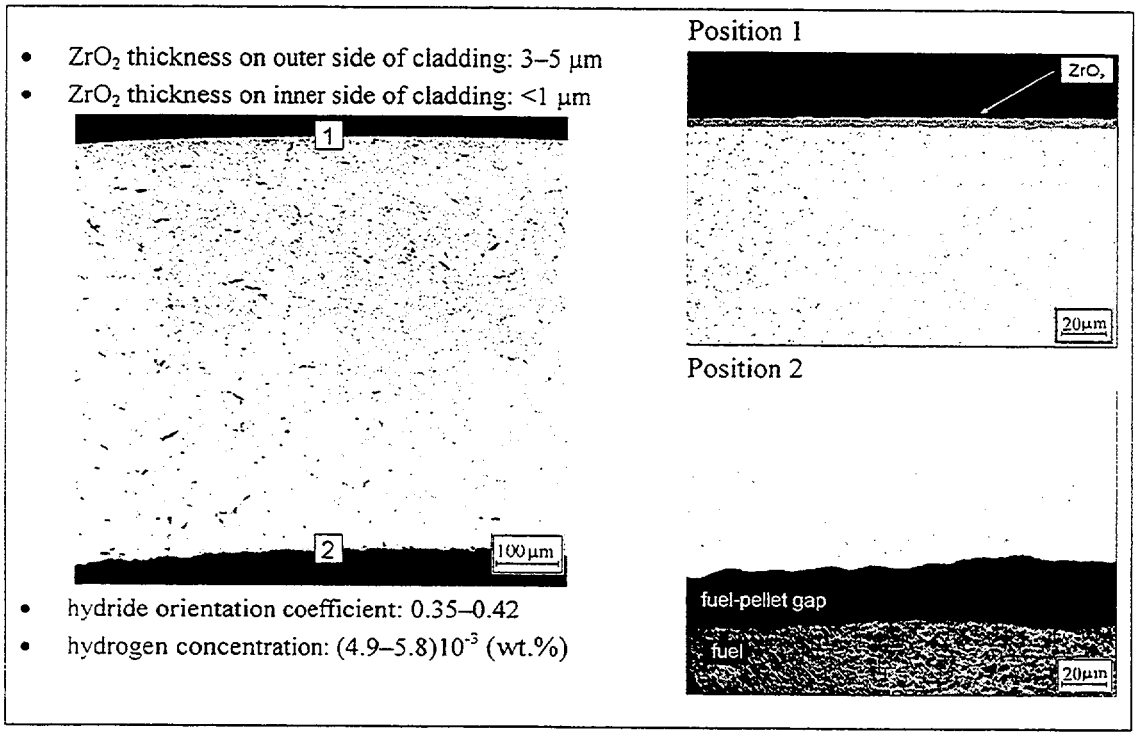

Fig. 1. Microstructure and some characteristics of the irradiated Zr-1%Nb cladding.

The final scope of the mechanical tests, used for this program, is presented in Fig. 2. Besides, the methodological aspects and results of tests are described in [5, 6, 7, 8].

Analysis of results of mechanical tests

As can be seen in Fig. 3, the irradiated Zr-1%Nb cladding is characterized by the higher strength and lower elongation than the unirradiated cladding in the low temperature range. However, the irradiated cladding retains a high level of ductility due to a low level of the oxidation and hydriding (see Fig. 1).

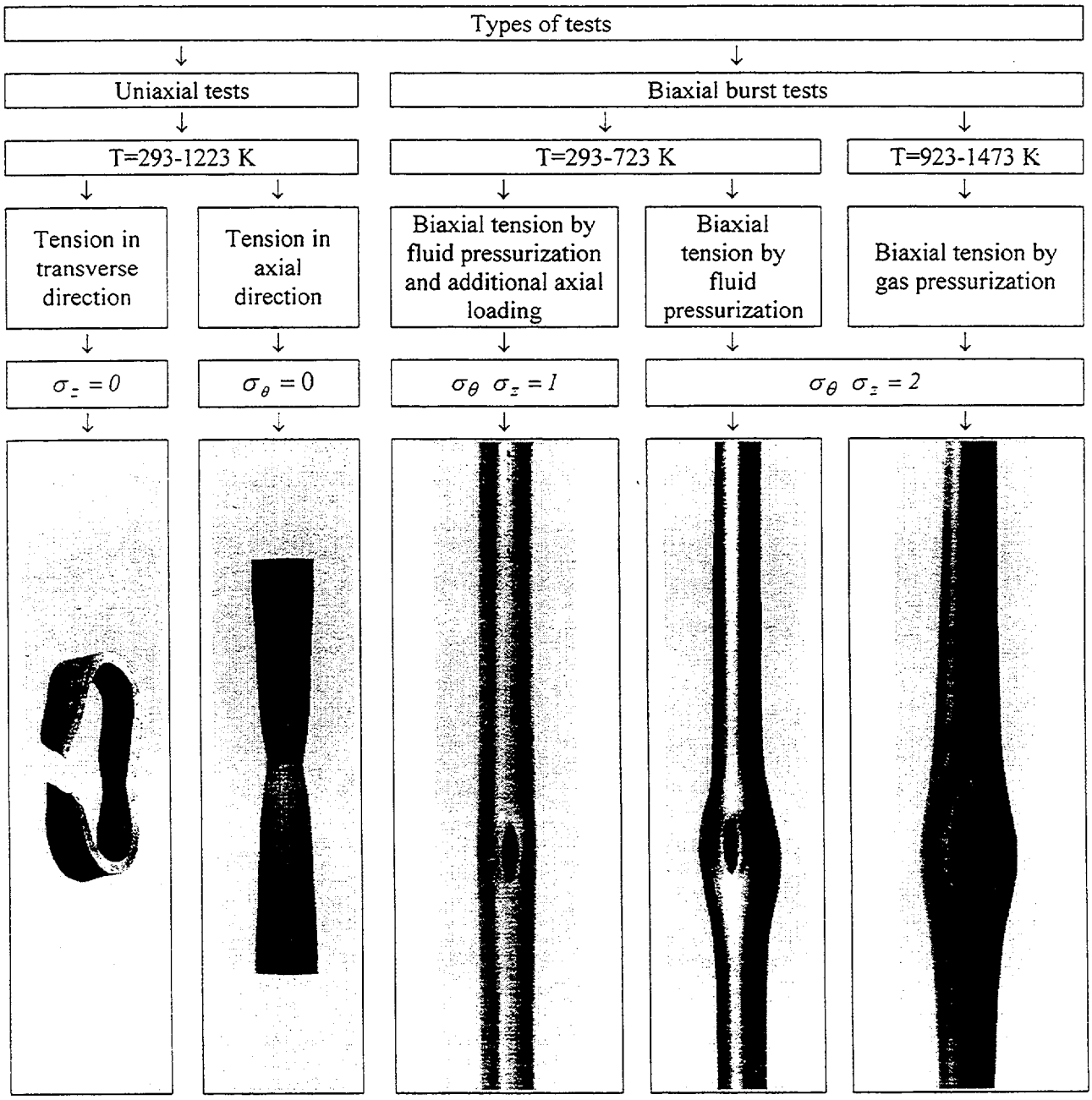

Fig. 2. The structure of mechanical tests with unirradiated and irradiated cladding.

This conclusion is satisfied with the monotonic decrease of differences between mechanical properties of two types of cladding in the temperature range 750-860 K. This is because the annealing of radiation damages is completed and the irradiated cladding has the same mechanical properties as the unirradiated one at the temperature higher than 860 K. Both cladding types have demonstrated that the highest elongation of the cladding material occurs at 1000 K (for the basic strain rate). This observation obtained in the uniaxial tensile tests correlates with results of high temperature biaxial tests (see Fig. 4).

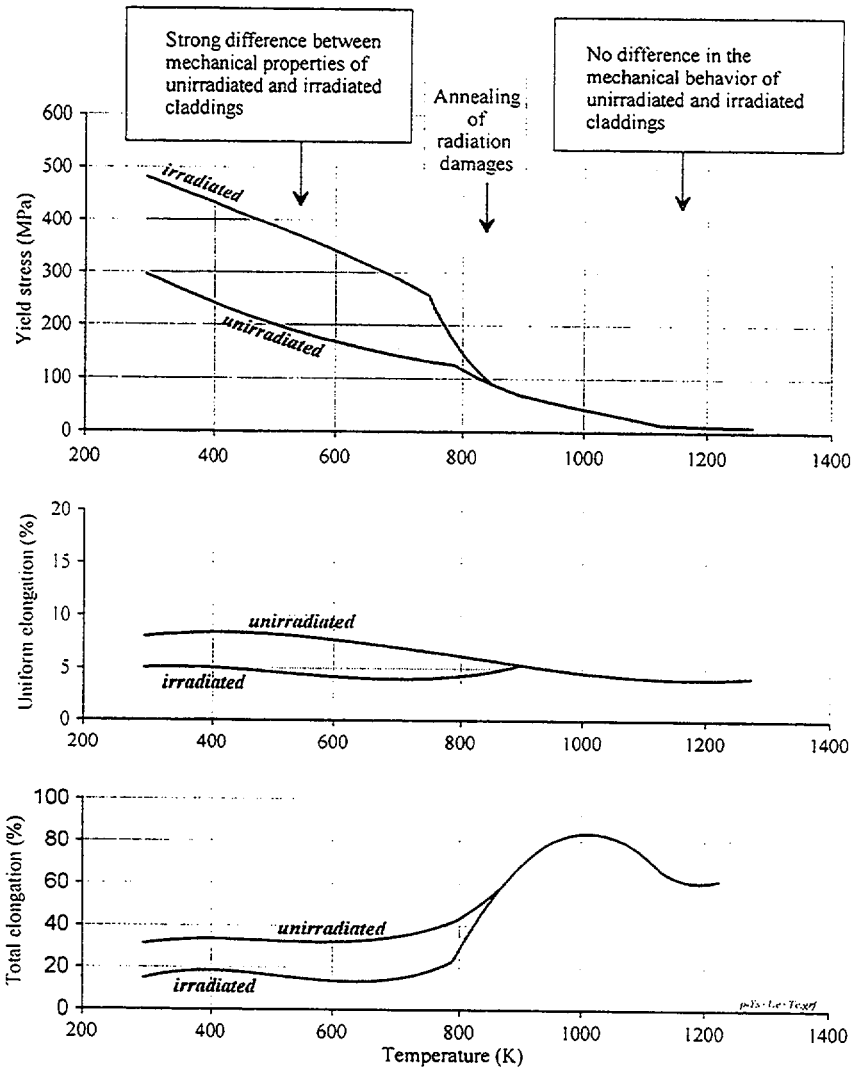

Fig. 3. Comparison of mechanical properties of unirradiated and irradiated Zr-1%Nb cladding vs. temperature.

The increase of the strain rate relocates the maximum of the cladding elongation to the higher temperature. The quantitative analysis of this effect is in progress now. Additional data to determine the sensitivity of the cladding strain to the irradiation and loading conditions was obtained on the basis of different biaxial tests performed in the low temperature range. Results of these tests presented in Fig. 5 show that the unirradiated cladding has a high sensitivity to the biaxiality ratio due to the anisotropy effect.

However, the irradiated cladding demonstrates a very low sensitivity to the biaxiality ratio. This fact testifies evidence that the irradiated cladding material becomes more isotropic. This conclusion is satisfied with results characterizing the strength of the irradiated cladding (see Fig. 6). Nevertheless, it should be noted that the strength parameters of the unirradiated cladding respond to the biaxiality ratio also insignificantly.

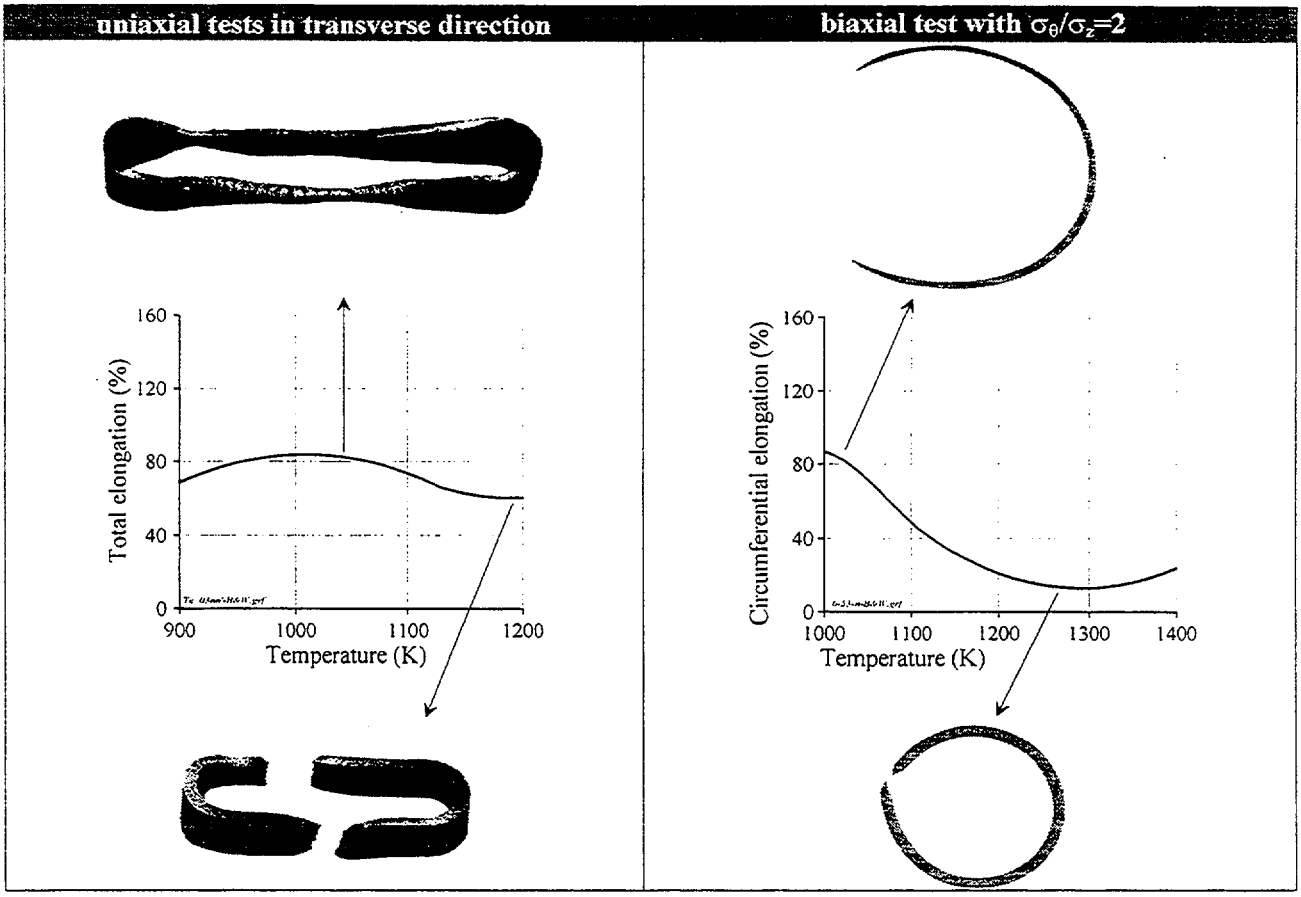

Fig. 4. Cladding strain vs. temperature and loading conditions.

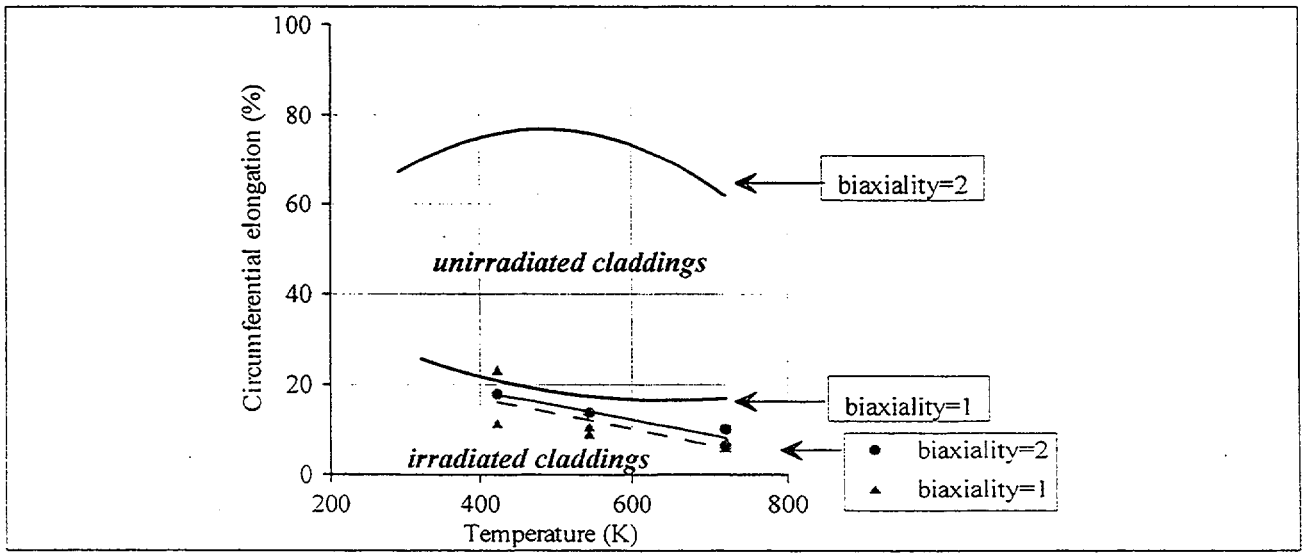

Fig. 5. Circumferential elongation of cladding vs. irradiation, temperature, and biaxiality ratio.

The final step in the estimation of the anisotropy effect of the irradiated cladding was made on the basis of the effective stress equation proposed by R.Hill [9] and on the results of four types of mechanical tests (see Fig. 7).

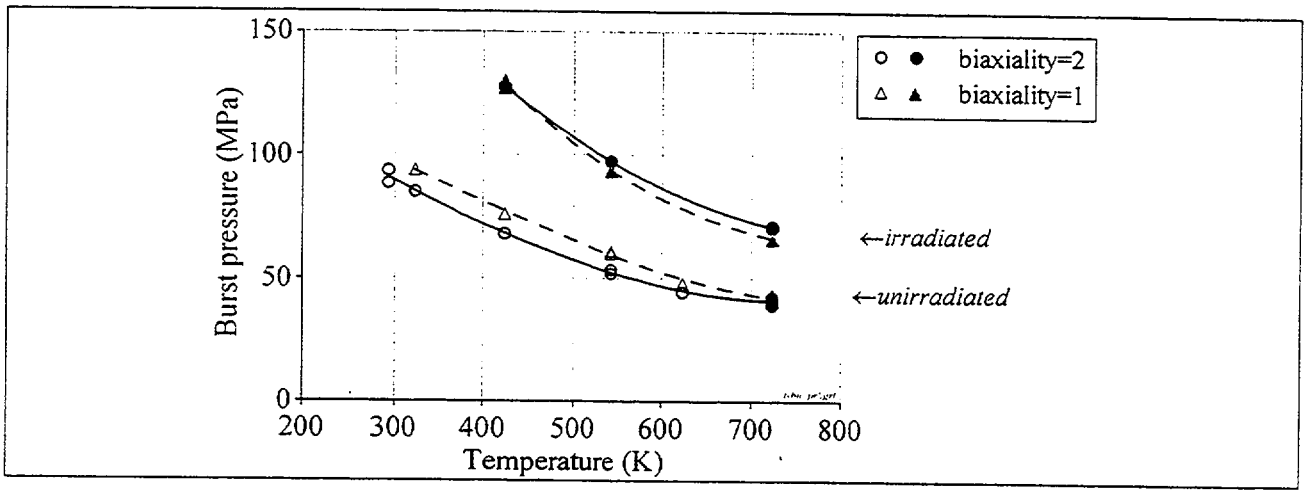

Fig. 6. Sensitivity of strength parameters of the unirradiated and irradiated cladding to the biaxiality ratio.

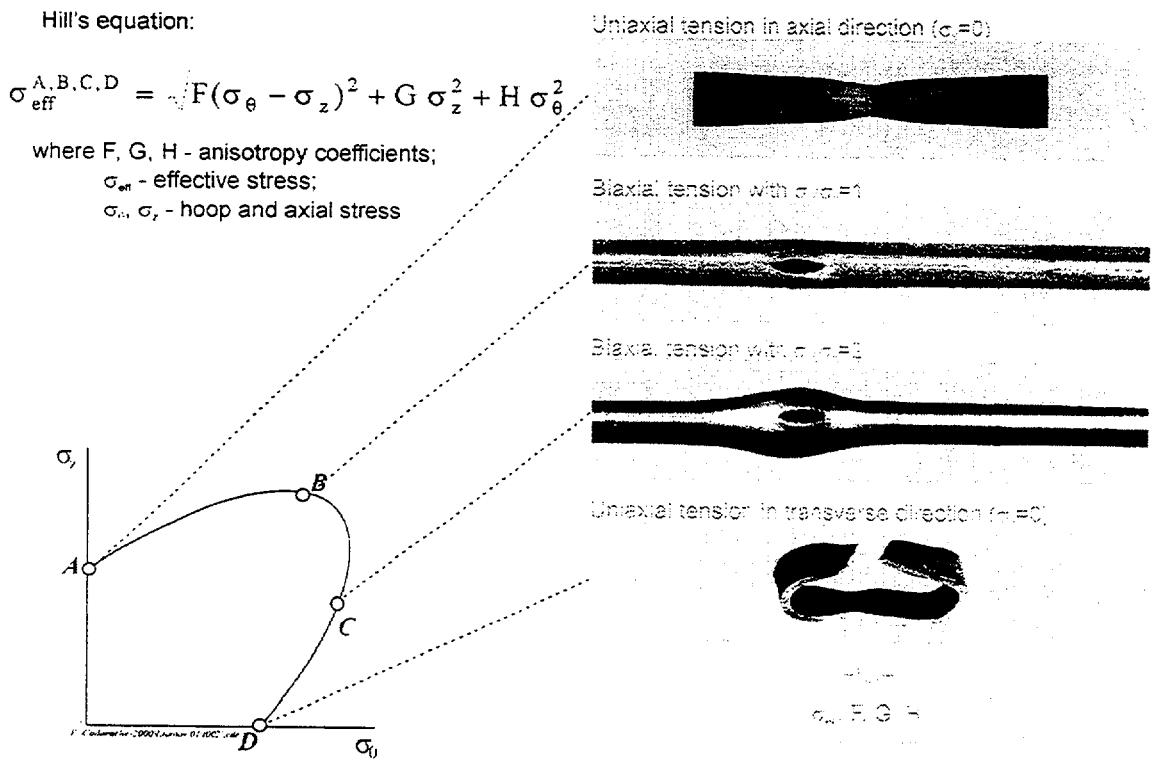

Fig. 7. Input data base to estimate anisotropy coefficients of irradiated Zr-1%Nb cladding.

Major provisions of the used approach can be formulated in the following way:

- graphic view of Hill's equation is the ellipse in σ_θ, σ_z coordinates;
- four types of mechanical tests allow to determine the fixed coordinates of four experimental points belonging to this ellipse.

The illustration of the approach in more detail is presented in Fig. 8. This figure shows the experimental points A, B, C, D and the ellipse reconstructed by the least-square method. The ellipse characterizing the isotropic case is also presented for the comparison.

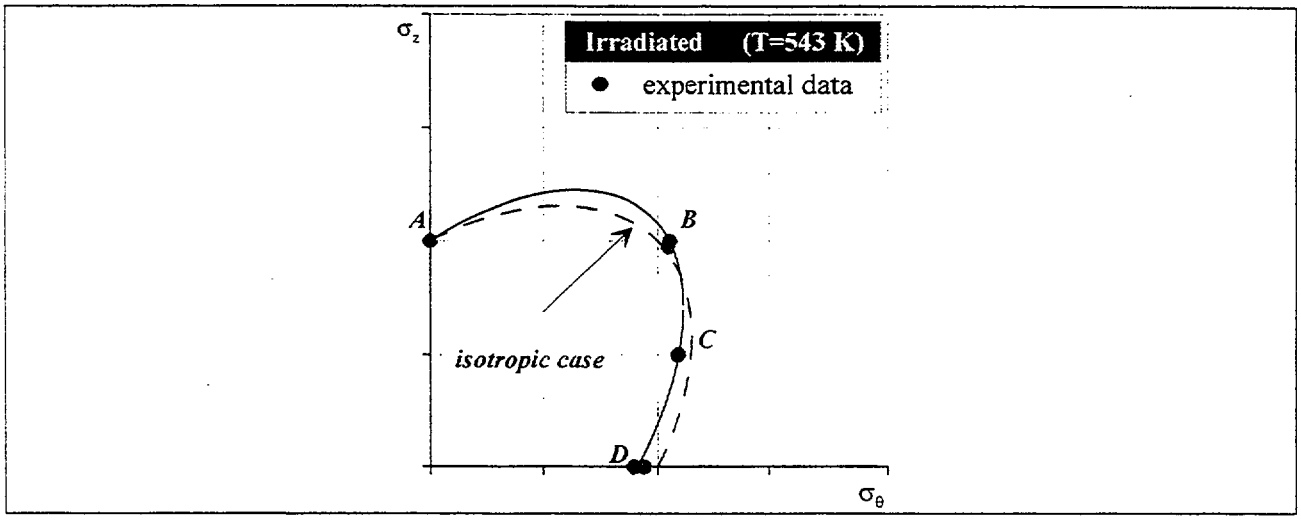

Fig. 8. Interpretation of the test data by Hill's equation.

The application of this procedure to the test data obtained at different temperatures allowed to estimate the anisotropy coefficients of the irradiated Zr-1%Nb cladding (see Table 1).

Table 1. Anisotropy coefficients of irradiated Zr-1%Nb cladding.

Type of coefficient	Temperature (K)		
	423	543	723
F	0.78	0.60	0.55
G	0.32	0.35	0.53
H	0.40	0.55	0.42

The anisotropy coefficients became the last elements of the data base for the development of power laws for thermal mechanical codes in the MATPRO standard. The major provisions of this procedure and graphic view of obtained deformation laws for unirradiated and irradiated Zr-1%Nb cladding are presented in Fig. 9.

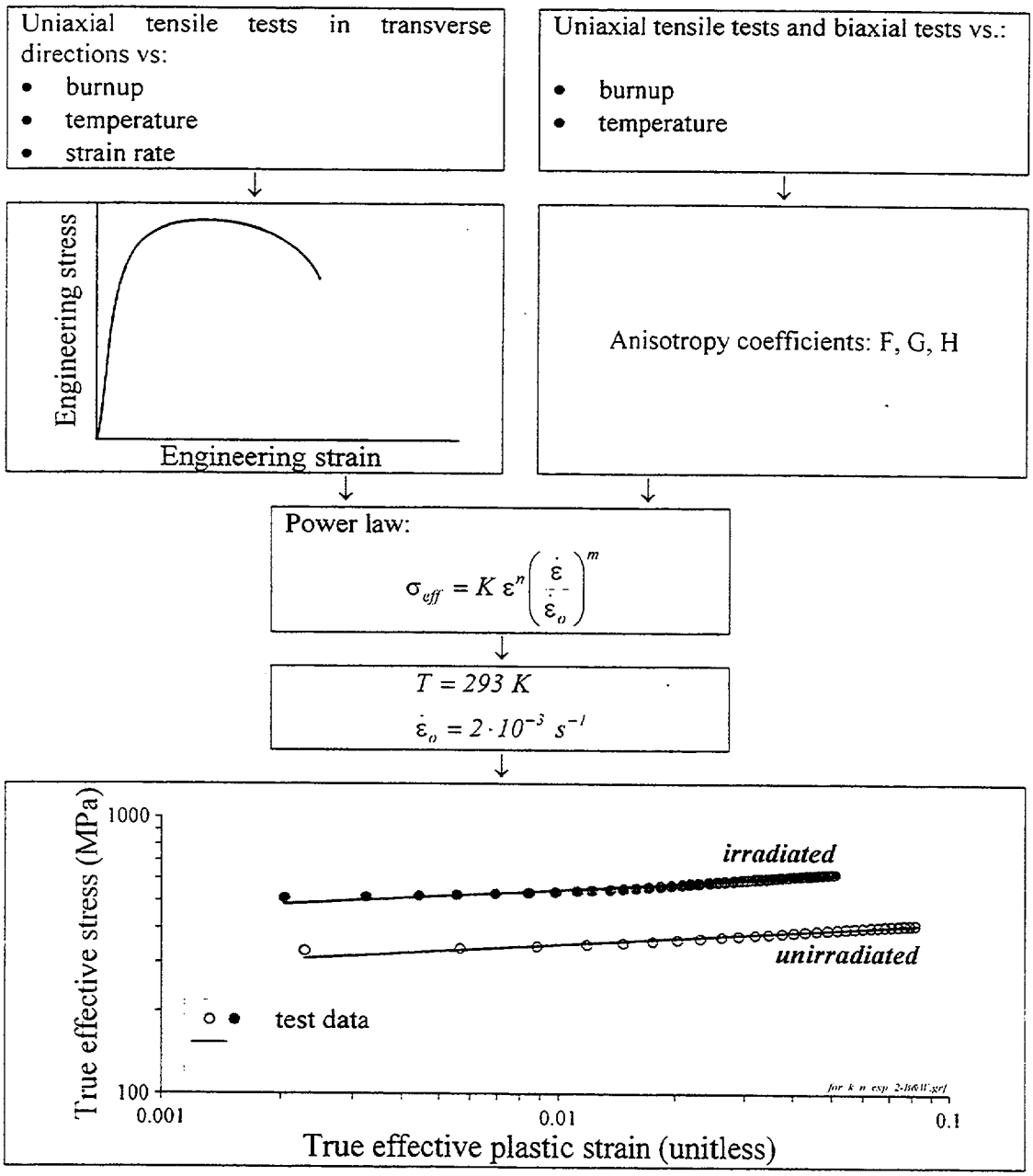

Fig. 9. Major provisions for the procedure of the stress-strain law development for unirradiated and irradiated Zr-1%Nb cladding.

Within the bounds of this work the final efforts were applied to use the results of these mechanical tests for the development of cladding failure correlations under low temperature and high temperature conditions. These investigations performed in accordance with the requirements of computer codes allowed to obtain reasonable correlations for the true hoop stress at rupture versus the temperature (see Fig. 10).

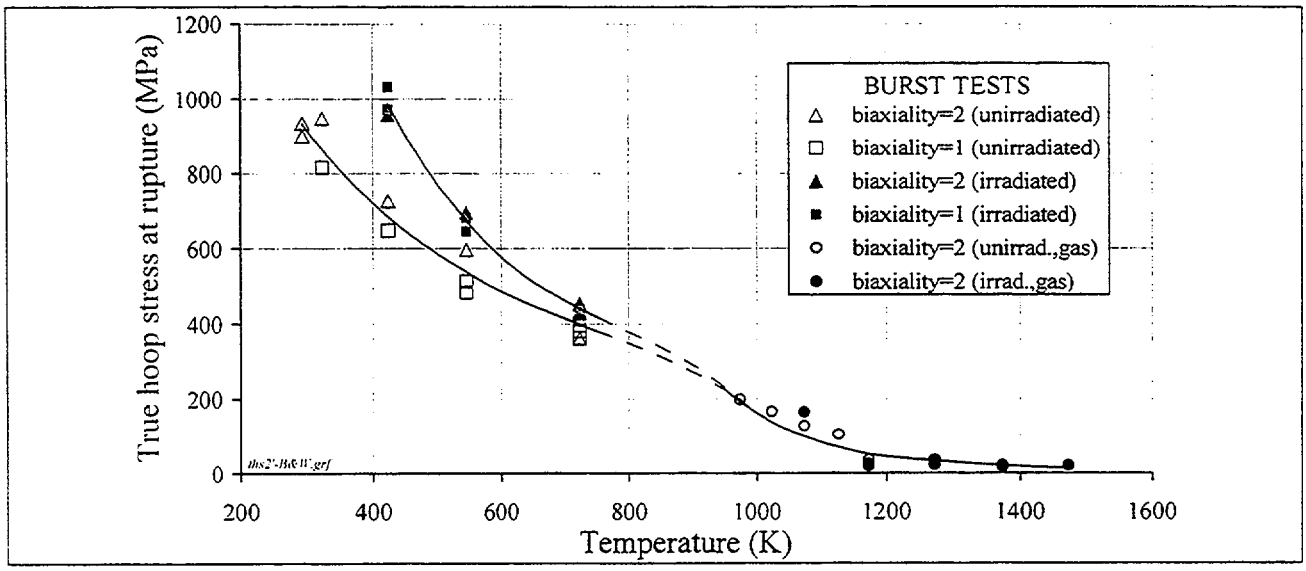

Fig. 10. Rupture parameters for the unirradiated and irradiated cladding vs. the temperature.

Conclusions

The program of mechanical tests with the unirradiated and irradiated Zr-1%Nb (E110 alloy) cladding was performed during 1997–2000. The goal of this program was to reveal specific features of the mechanical behavior of the irradiated cladding under accident conditions (RIA and early stage of LOCA). The results of tests showed that:

- irradiation of Zr-1%Nb cladding leads to an increase in cladding strength and to a decrease in the cladding ductility in the low temperature range;
- the difference between mechanical properties of unirradiated and irradiated cladding disappears completely at temperatures higher than 860 K;
- the peak value of the cladding strain (up to 100%) is observed at the temperature of 1000 K for irradiated and unirradiated cladding (at basic strain rate);
- the anisotropy effect is insignificant for the irradiated cladding within the temperature range 293–1400 K and for the unirradiated cladding at temperatures higher than 800 K;
- the strength parameters for the unirradiated and irradiated cladding are practically independent of the biaxiality ratio (1 or 2);
- a high sensitivity of the circumferential elongation to the biaxiality ratio was revealed for the unirradiated cladding within the low temperature range 293–723 K;
- the circumferential elongation of the irradiated cladding within the temperature range 293–1400 K is independent of the biaxiality ratio.

The obtained data base with mechanical properties for two types of the cladding was used to estimate anisotropy coefficients of the irradiated cladding, to determine the correlations for the cladding failure conditions, and to develop the stress-strain laws in accordance with the computer code standards.

References

1 V.Asmolov, L.Yegorova "The Russian RIA Research Program: Motivation, Definition, Execution, and Results", *Nuclear Safety*, Vol.37, No.4, 1996.

2 J.Papin, M.Balourdet, F.Lemoine, F.Lamare, J.Frizonnet, and F.Schmitz "French Studies on High Burnup Fuel Transient Behavior under RIA Conditions", *Nuclear Safety*, Vol.37, No.4, 1996.

3 T.Fuketa, F.Nagase, K.Ishijima, and T.Fujishiro "NSRR/RIA Experiments with High-Burnup PWR Fuels", *Nuclear Safety*, Vol.37, No.4, 1996.

4 D.L.Hagrman, G.A.Reymann, R.E.Mason "MATPRO-Version 11 (revision 1): Handbook of Material Properties for Use in the Analysis of Light Water Reactor Fuel Rod Behavior", *NUREG/CR-0497 TREE-1280*, Rev 1, February 1980.

5 V.Asmolov, L.Yegorova, E.Kaplar, K.Lioutov, V.Smirnov, V.Prokhorov, A.Goryachev "Development of Data Base with Mechanical Properties of Un- and Preirradiated VVER Cladding", *Proceedings of the Twenty-Fifth Water Reactor Safety Information Meeting, NUREG/CP-0162*, Vol.1, 1998.

6 L.Yegorova, V.Asmolov, G.Abyshov, V.Malofeev, A.Avvakumov, E.Kaplar, K.Lioutov, A.Shestopalov, A.Bortash, L.Maiorov, K.Mikitiouk, V.Polvanov, V.Smirnov, A.Goryachev, V.Prokhorov, and A.Vurim "Data Base on the Behavior of High Burnup Fuel Rods with Zr-1%Nb Cladding and UO_2 Fuel (VVER Type) under Reactivity Accident Conditions", *NUREG/IA-0156 (IPSN99/08-02, NSI/RRC KI 2179)*, Vol.1-3, 1999.

7 K.Lioutov, L.Yegorova, E.Kaplar, A.Konobeyev, V.Smirnov, A.Goryachev, V.Prokhorov, S.Yeremin "Mechanical Properties of Unirradiated and Irradiated Zr-1%Nb Cladding under Accident Conditions", *Proceedings of the Twenty-Seventh Water Reactor Safety Information Meeting, NUREG/CP-0169*, 2000.

8 E.Kaplar, L.Yegorova, K.Lioutov, A.Konobeyev, N.Jouravkova, V.Smirnov, A.Goryachev, V.Prokhorov, O.Makarov, S.Yeremin, A.Svyatkin "Mechanical properties of unirradiated and irradiated Zr-1%Nb cladding", *NUREG/IA-0199 (IPSN 01-16, NSI RRC KI 2241) report*, 2001.

9 R.Hill "Mathematical Theory of Plasticity" (Translation from English), Moscow, 1956 (rus.).

HIGH TEMPERATURE OXIDATION OF IRRADIATED LIMERICK BWR CLADDING

Y. Yan, R. V. Strain, T. S. Bray, and M. C. Billone

Argonne National Laboratory (ANL)
Argonne, Illinois, USA

Abstract

High-temperature steam-oxidation studies have been conducted using Zircaloy (Zry) cladding samples as part of the High Burnup Cladding Performance program. These data will be used to support modeling and experimental efforts to assess licensing criteria for high-burnup-fuel Loss of Coolant Accidents. Limerick BWR fuel rods (≈57 GWd/MTU) and H. B. Robinson PWR fuel rods (≈67 GWd/MTU) are being used for these studies. Steam-oxidation tests have been completed on archival and irradiated Limerick Zry-2 cladding at 1000-1204°C for test times ranging from 5-100 minutes. Based on total sample weight gain, no significant difference in oxidation kinetics has been observed between irradiated and unirradiated Zry-2 samples. Both sets of results are in good agreement with the Cathcart-Pawel best-estimate model predictions, as well as data from irradiated (≈49 GWd/MTU) TMI-1 Zry-4 tests at ≈1200°C. Metallographic analysis, which is more accurate than direct sample weight gain, has been used to determine the oxide, alpha and beta layer thicknesses, along with the weight gain, for Zry-2 samples tested at ≈1200°C. These data are in excellent agreement with the model predictions. The primary high burnup effects observed from these studies are the non-uniformity of the alpha/beta interface, the enhanced growth rate of the oxygen-stabilized alpha layer formed at high temperature and the alpha-prime islands precipitated within the prior-beta layer during cooling. Although these have little impact on weight gain, they result in a reduction in the effective beta layer thickness for irradiated cladding. Metallographic analysis is in progress for samples tested at 1000-1100°C. Future tests will be conducted using high burnup PWR cladding with in-reactor-formed oxide layers of 40-100 μm. The pre-test oxide layers are ≈10 μm for Limerick and ≈30 μm for TMI-1.

Introduction

The High Burnup Cladding Performance program is being conducted at Argonne National Laboratory (ANL) to provide data that support modeling efforts and that assess licensing criteria for Loss-of-Coolant Accident (LOCA) and Reactivity-Initiated Accident (RIA) events involving high burnup fuel rods. The program is sponsored by the USNRC Office of Nuclear Regulatory Research. The Electric Power Research Institute (EPRI) also plays a major role in the program planning and conduct and by supplying the high burnup BWR and PWR fuel rods: seven Limerick BWR fuel rods (≈57 GWd/MTU) and seven H. B. Robinson PWR fuel rods (≈67 GWd/MTU). In addition, two TMI-1 fuel rods (≈49 GWd/MTU) have been provided by EPRI for validation of test methodologies. The major tasks of the program include: fuel and cladding characterization, cladding high temperature steam oxidation kinetics studies, LOCA Integral Tests, and mechanical properties tests. The focus of this paper is on the results of the oxidation kinetics studies and their impact on LOCA Integral Test planning and interpretation of results.

The current LOCA licensing criteria (10 CFR50.46) limit peak cladding temperature to 2200°F (1204°C) and maximum Equivalent Cladding Reacted (ECR) to 17% during high temperature steam oxidation to ensure adequate ductility during the Emergency Core Cooling System (ECCS) quench and during possible post-LOCA seismic events. In addition, NRC Information Notice 98-29 specifies that the ECR should be based on the total oxidation, including oxide layers formed during normal reactor operation. For PWR cladding, high burnup operation may induce coolant-side oxidation thicknesses of ≈100 μm, corresponding to 10-14% ECR. This would leave very little margin for the LOCA transient oxidation. The primary high burnup phenomena that may affect cladding response during ballooning and burst, steam oxidation, quench and post-quench are: loss of load-bearing base metal thickness due to oxidation, hydrogen pickup (≈500 wppm at ≈100 μm oxide thickness) and formation of an inner-surface oxide layer, all during normal operation; the effective thickness and chemistry (i.e., H_2 and O_2 content) of the prior-beta phase layer following steam oxidation and quench; and decreased fuel permeability and the tightness of the fuel-cladding bond. The LOCA Integral Tests will be conducted with high burnup fueled cladding segments in order to include all the phenomena highlighted. However, it is essential that oxidation studies be performed with cladding samples from the high burnup rods to plan the LOCA Integral Test experimental times that will test the adequacy of the current criteria and will determine the failure threshold for fragmentation during quench and/or the nil-ductility threshold following ECCS quench.

The test plan for oxidation studies of high burnup BWR and PWR cladding specifies ranges of temperature (900-1300°C) and test times (0-300 minutes). The two main purposes for these tests are: to provide adequate oxidation data at 1204°C (0-20 minutes) for planning LOCA Integral Test times to achieve ECR values ≤ 30%; and to develop fundamental data for modeling codes on the effects of high burnup operation on high temperature (900-1300°C) steam oxidation kinetics. Of particular interest is the influence of the in-reactor-formed, coolant-side oxide layer, and associated hydrogen pickup, on the oxidation kinetics and phase boundary evolution during steam oxidation. In order to determine the effects of these parameters on oxidation kinetics, unirradiated archival cladding samples are tested in the same apparatus used to test the high burnup samples. One-sided, outer-surface oxidation tests are conducted to determine directly the effects of the in-reactor-formed oxide layer on the oxidation kinetics.

At the 28th Water Reactor Safety Information Meeting (WRSM), weight gain results were presented for unirradiated Limerick archival Zircaloy-2 tested in steam at 1204°C for 5-40 minutes [1]. Three independent methods were used to determine weight gain: change in total sample weight normalized to the oxidation surface area, oxygen content determined from metallography and assumed equilibrium oxygen concentrations at the phase boundaries, and change in oxygen content determined from direct LECO measurements. These results were compared to predictions of the Cathcart-Pawel [2] best-estimate model, which includes rate equations for sample weight gain due to oxygen pickup and for increases in oxide, alpha and oxide-plus-alpha layer thicknesses. The models are based on parabolic kinetics due to diffusion. The model rate constants were determined from tests conducted with unirradiated Zry-4 samples with no pre-test oxide layer. Relative to model predictions, the total sample weight gain data were high due to end effects and local regions of non-uniform oxide growth at the cladding outer surface; the weight gains deduced from the metallography at the midplane were in excellent agreement with model predictions; and the weight gains determined from the direct measurement of oxygen concentration near the sample midplane were low due to oxide/alpha material loss during sample preparation. The oxide layer thickness data from the metallography were also in excellent agreement with the Cathcart-Pawel predictions. The presence of non-uniform regions of enhanced oxidation at the cladding outer surface suggested inadequate control of the steam flow rate and the test chamber environment.

Following the 28th WRSM, the oxidation apparatus was redesigned to provide: better control of the test chamber environment and steam flow, as well as higher steam flow rates. With the new apparatus, extensive out-of-cell thermal and oxidation-kinetics benchmark tests were conducted using unirradiated Zircaloy-2 (Zry-2) and Zircaloy-4 (Zry-4) samples. Test temperatures and times ranged from 1000-1204°C and 5-20 minutes, respectively. Based on the excellent out-of-cell results, the new oxidation apparatus was installed into a hot cell workstation and tests were conducted on irradiated and unirradiated Limerick Zry-2 cladding samples at 1204°C (5-20 minutes), 1100°C (10-50 minutes) and 1000°C (20-100 minutes). Several test were also run at 1204°C with irradiated TMI-1 Zry-4 cladding.

Cladding Characterization

The archival Limerick tubing has dimensions typical of the GE-11 (9-by-9 fuel rod array) design: outer diameter (OD) of 11.18 mm and thickness of 0.71 mm. The inner ≈0.1 mm of the tubing is a zirconium barrier and the remaining ≈0.6-mm thickness is recrystallized-annealed Zry-2. The oxygen content has been measured to be ≈0.11 wt.%.

The irradiated Limerick BWR cladding samples have been taken from grid span 4 of a fuel rod (F9) irradiated to an axially averaged burnup of 56 GWd/MTU. Based on metallographic examinations, the inner-surface oxide layer is about 10-15 μm. The outer-surface oxide layer varies circumferentially from about 3 μm to 18 μm, with an average value of ≈10 μm. In the regions where the oxide layer is thin, tenacious crud deposits of 5-10 μm are observed. Based on Leco determinator measurements, the oxygen content of the irradiated cladding is 0.70±0.09 wt.% and the hydrogen content is 72±7 wppm. These values include O_2 and H_2 in crud, outer and inner surface oxide layers and the base metal. At room temperature, the hydrogen is in the form of hydrides concentrated at the outer surface (radial), the inner barrier surface (radial) and in the central region of the cladding ("X-shaped" patterns).

Experimental Apparatus

The schematic of the improved experimental apparatus is shown in Fig. 1. All components, except for the control and monitoring system and the furnace power source, are located in one of the Alpha-Gamma Hot Cells. The cell atmosphere is N_2 with a low, controlled O_2 level. The furnace is a 250-mm-long quad-elliptic, focused radiant heater. With the test train positioned within the furnace, the uniform temperature zone is >100 mm. The furnace is centered with respect to the 52.6-mm-ID quartz tube, which contains the test train and the flowing steam. The test train, which holds the sample, is centered relative to the quartz tube by perforated spacer discs. The test train within the quartz tube is purged with an inert gas (Ar) prior to the introduction of steam. The steam flows from the boiler into the quartz tube, which is sealed at the boiler-tube interface, and exits out the top of the system into the cell. Tests were conducted with average steam flow rates of ≈120-140 mg/s (deduced from water consumption). The system is designed to produce one-sided (outer-surface) oxidation of the sample. It is compatible with the LOCA Integral Test Apparatus, which also includes a line to internally pressurize the sample and a line for the water quench. In order to achieve good reproducibility, the quartz tube remains centered in the furnace and the test train is lowered into the tube. The test train is shown in Fig. 2. The 25-mm-long sample is protected from eutectic interaction with the Inconel holder by alumina spacers and zirconia washers. The Inconel test train is threaded inside the sample area to allow compression to be exerted on the washers. It is also perforated to allow an overpressure of near-stagnant Ar within the sample to further inhibit steam ingress. Three Type-S thermocouples (120° apart) are welded onto the Inconel outer surface about 13 mm above the sample. One of these is used for furnace control. The remaining two TCs are used to assess the circumferential temperature variation. A fourth thermocouple (not seen in Fig. 2) is suspended within the sample at the sample midplane. This internal thermocouple is used for data analysis.

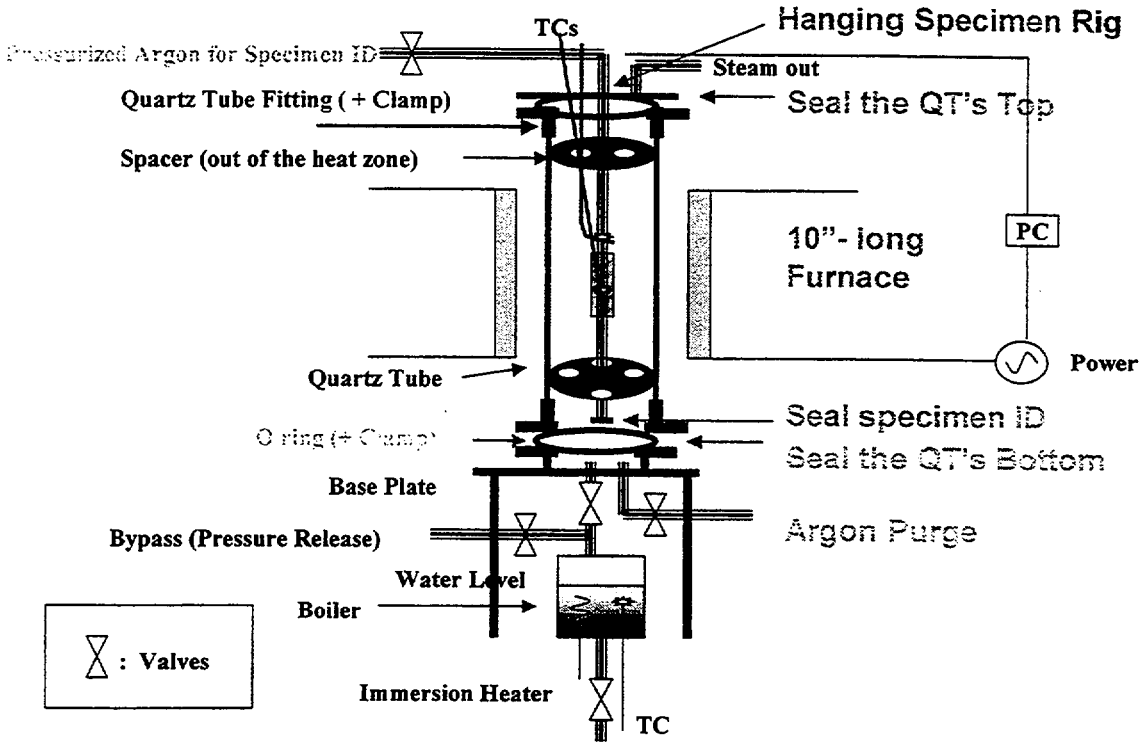

Fig. 1. Schematic of the in-cell steam-oxidation kinetics test apparatus.

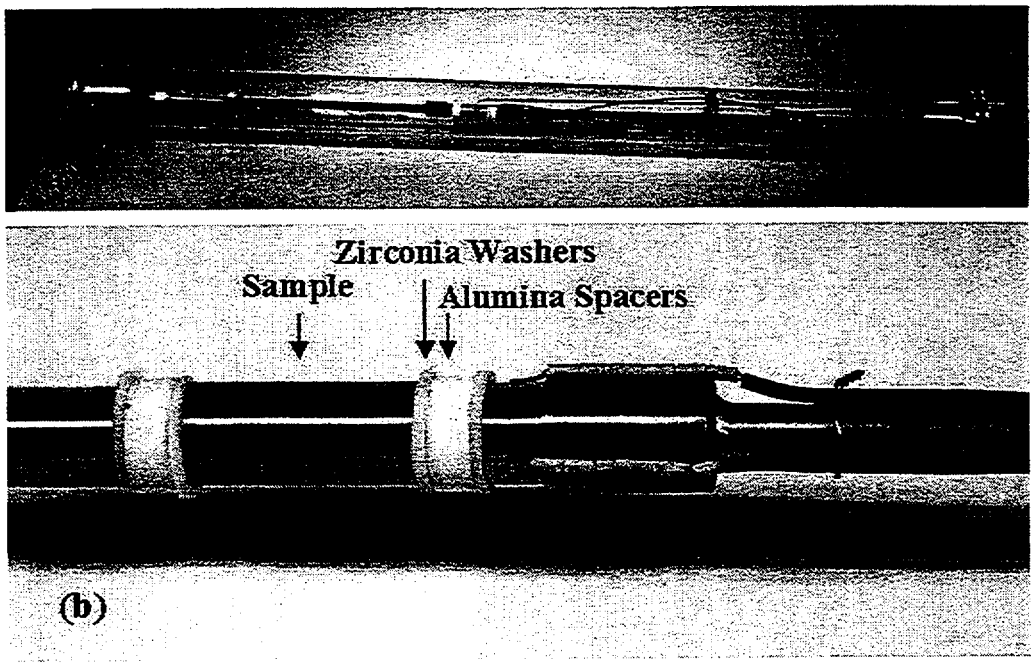

Fig. 2. Test train for in-cell steam-oxidation kinetics studies of Zircaloy cladding: a) test train within quartz tube; b) enlarged view of sample region within the test train.

Test Conditions

Extensive out-of-cell benchmark tests were conducted to ensure adequate temperature control in terms of time history and uniformity of temperature in the circumferential direction. During the course of the benchmark testing, modifications were made to the thermocouple (TC) attachment method and geometry. It was found that excellent reproducibility of results and agreement in readings among the furnace-control TC attached to the Inconel holder, the other two TCs attached to the holder for monitoring temperature variations in the circumferential direction and the internal TC suspended within the sample for data analysis were obtained by: welding the three external TCs to the Inconel and by laying the TC leads as close as practical to the Inconel holder to minimize fin-cooling effects. The design shown in Fig. 2b resulted in reasonably small temperature variations in the circumferential direction and an internal TC reading approximately equal to the average reading of the three external TCs. Additional thermal benchmarking tests were conducted with TCs welded directly onto the outer surface of the sample. Again, the inner TC readings were in excellent agreement with the average of the readings from the TCs welded to the sample. Figure 3 shows the temperature history of the four TCs for the in-cell test LOI-6 with an irradiated Limerick Zry-2 sample at an average hold temperature of 1203°C for 10 minutes in steam. The response of the internal TC (TC4) lags the control TC (TC2) during the temperature ramp, shows slower cooling after the furnace power is set to zero at the end of the test, but is in very good agreement with the average of the three external TC readings during the hold period.

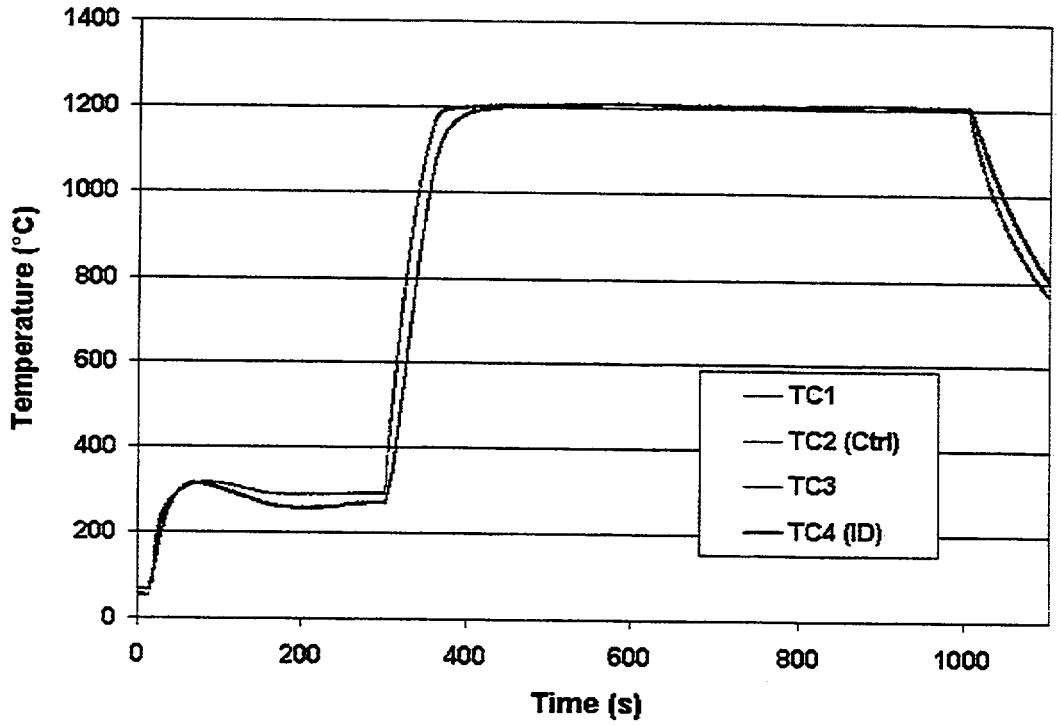

Fig. 3. Thermal response of the four thermocouples during the 10-minute test of an irradiated Limerick Zry-2 sample. The control TC (2) reads 1204°C during the hold period as programmed. The internal TC (4) reading (1203°C) agrees well with the average of the 3 external TC readings during the hold time.

The sample identification numbers and test conditions for the in-cell tests are summarized in Table 1. The samples include: unirradiated (archival) Zry-2, irradiated (Limerick) Zry-2 and irradiated (TMI-1) Zry-4. Also shown in Table 1 are the Cathcart-Pawel model-predicted values for weight gain (Δw_p) and the equivalent test time (t_{eq}). The model is integrated over the temperature history recorded by the interior TC (#4 in Fig. 3) to give the predicted weight gain normalized to the exposed surface area (Δw_p). Thus, the ramp-up and ramp-down in temperature are included in the model prediction. The model is used a second time to determine the equivalent time that would give the same weight gain at the steady temperature (T_s). This equivalent time is longer than the hold time because it includes the effects of the temperature ramps. It is a better measure of the time at temperature than the nominal hold time. The degree to which this time is relevant for tests on irradiated cladding with in-reactor-formed oxide layers is determined by the degree to which the weight gain data and oxidation-layer-increase data agree with the model predictions. The measured weight gains (Δw_w) listed in Table 1 were determined by the change (after-test minus before-test) in sample weight normalized to the sample outer surface area exposed directly to the steam. As will be discussed in the next section, these values tend to be higher than predicted because of end effects. Not included in the table are the conditions for, and the results of, the many out-of-cell tests conducted. These tests were conducted in the out-of-cell LOCA Integral Test Mock-up Apparatus (Zry-2 at ≈1204°C for 10 minutes) and in the out-of-cell Oxidation Test Apparatus (Zry-2 at ≈1204°C for 5-20 minutes and Zry-4 at 1000-1204°C for 10 minutes) with and without TCs welded directly onto the sample outer surface. As all the results for unirradiated Zry-2 and Zry-4 have been in good agreement with the Cathcart-Pawel model predictions, especially when the experimental weight gains are determined from detailed metallographic analysis, the emphasis of the in-cell testing has been on the oxidation kinetics of irradiated, high burnup cladding.

Experimental Results

As discussed in Ref. 1, three independent experimental methods are used to assess the sample weight gain and oxygen pickup during high temperature steam oxidation: gross sample weight gain normalized to the sample outer surface area directly exposed to the steam (Δw_w), normalized weight gain based on the increase in oxygen content as determined by the LECO apparatus (Δw_o), and weight gain based on the detailed calculations of the oxygen content within the oxide, alpha and beta layers, whose effective thicknesses are determined though metallographic analysis (Δw_m). In general, the Δw_w values tend to be high because of end effects, the Δw_o tend to be low because some brittle oxide is lost during sample preparation for LECO oxygen determination, and the Δw_m values are the most reliable and accurate.

1. Normalized gross sample weight gain (Δw_w) results

Table 1 lists the Δw_w values determined for the in-cell oxidation tests. These values, along with the values obtained out-of-cell, are plotted vs. the Cathcart-Pawel model predictions (Δw_p) in Fig. 4 (results at ≈1200°C), Fig. 5 (results at ≈1100°C) and Fig. 6 (results at ≈1000°C). Also shown in these figures are the Cathcart-Pawel data (determined from metallographic analysis) used to derive the model. In order to interpret these graphs, points that lie along the 45° line would indicate perfect agreement between data and model predictions. Points lying above the 45° line indicate that the data are higher than the model predictions, which is the case for the ANL data set. As end effects, including partial oxidation of the sample inner surface, are not included in the surface area used to normalize the ANL data, it is not surprising that the Δw_w results are higher than the model predictions. Metallographic analysis of the extent of the end effects would be needed to adjust the surface area to determine the effective surface area for the normalization. Figure 5 shows these end effects for tests LOI-7 (irradiated Zry-2 in 1204°C steam for 5 minutes) and LOU-11 (unirradiated Zry-2 in 1204°C steam for 10 minutes). Although detailed metallographic examinations can be used to correct the data in Table 1 and Figs. 4-6, such examinations

Table 1 Experimental Conditions for the In-Cell Steam Oxidation Tests; unirradiated (U) Zry-2 is archival cladding (11.18-mm OD/9.75-mm ID), irradiated (I) Zry-2 is from Limerick rod F9, and irradiated (I) Zry-4 is from TMI-1 PWR rod H6. Steam flow rate is ≈140 mg/s. "TBC" = To Be Conducted.

Test ID#	Material	Nominal Time minutes	Steady Temperature T_s, °C	Equiv. Time* t_{eq}, s	Predicted (CP-Model) Weight Gain, Δw_p, mg/cm^2	Measured Weight Gain Δw_w, mg/cm^2
LOU-12	Zry-2 (U)	5	1203	343	12.3	14.9
LOU-11	Zry-2 (U)	10	1202	631	16.6	19.9
LOU-13	Zry-2 (U)	20	1205	1250	23.7	26.1
TBC	Zry-2 (U)	10	≈1100	---	---	---
LOU-14	Zry-2 (U)	30	1100	1820	17.0	20.4
TBC	Zry-2 (U)	50	≈1100	---	---	---
TBC	Zry-2 (U)	20	≈1000	---	---	---
TBC	Zry-2 (U)	60	≈1000	---	---	---
TBC	Zry-2 (U)	100	≈1000	---	---	---
LOI-7	Zry-2 (I)	5	1201	373	12.7	14.1
LOI-16	Zry-2 (I)	5	1210	393	13.6	14.0
LOI-6	Zry-2 (I)	10	1203	648	16.9	17.8
LOI-18	Zry-2 (I)	10	1211	631	17.3	17.0
LOI-8	Zry-2 (I)	20	1203	1263	23.6	24.3
LOI-17	Zry-2 (I)	20	1210	1194	23.7	28.1
LOI-9	Zry-2 (I)	10	1098	669	10.2	9.7
LOI-10	Zry-2 (I)	30	1101	1865	17.3	19.8
LOI-11	Zry-2 (I)	50	1100	3076	22.1	24.6
LOI-12	Zry-2 (I)	20	1005	1227	8.1	8.5
LOI-13	Zry-2 (I)	60	1001	3634	13.6	12.9
LOI-15	Zry-2 (I)	100	1000	6092	17.5	21.8
TMI-2	Zry-4 (I)	5	1203	371	12.8	13.2
TMI-1	Zry-4 (I)	10	1201	683	17.2	18.0
TMI-3	Zry-4 (I)	20	1203	1263	23.6	31.1

*$t_{eq} = \exp\,[20101/(T_s + 273) - 12.8]\,(\Delta w_p)^2$

would be costly and defeat the main advantages of the sample weight gain approach: data obtained in a simple, fast and reliable manner at very low cost. Given that detailed metallography would be needed to "correct" the sample weight gain data, it would be more useful to do the metallography at the midplane of the sample where the oxide, alpha and beta layers are relatively uniform and representative of the results for these test conditions. For one-sided oxidation tests, such as the ones performed in this study, Δw_w data are used more for screening purposes: excessive weight gains (e.g., factor of 2) may indicate that the test should be repeated rather than be subjected to the more time-consuming techniques of metallographic analysis and/or LECO oxygen determination; and weight gains that are 20-30% higher than model predictions suggest that the mid-planes of the samples should be examined by detailed metallographic analysis to determine weight gains that are independent of end effects. Also, a judgment can be made from the direct sample weight gain data as to whether or not there appears to be significant differences between the oxidation kinetics of irradiated vs. unirradiated cladding. Within the uncertainty of the sample weight gain data in Table 1 and Figs. 4-6, there appears to be no significant difference.

The extent of the "end effects" is dependent on the degree of compression. Zero compression (loose fitting zirconia washers) can result in extensive inner-surface oxidation due to steam ingress. Excessive compression can result in flaring, splitting and heavy oxidation of the ends of the over-constrained sample. Through experience, the pre-test compression can be set within a range that leaves more than ≈80% of the sample free of end effects, particularly those associated with inner-surface oxidation. The experience to date indicates that the end effects extend ≤2 mm from each end of the 25-mm-long sample. Within the remaining 21 mm of the sample, the oxide layers are very uniform, displaying even less thickness variation axially than observed circumferentially at the midplane.

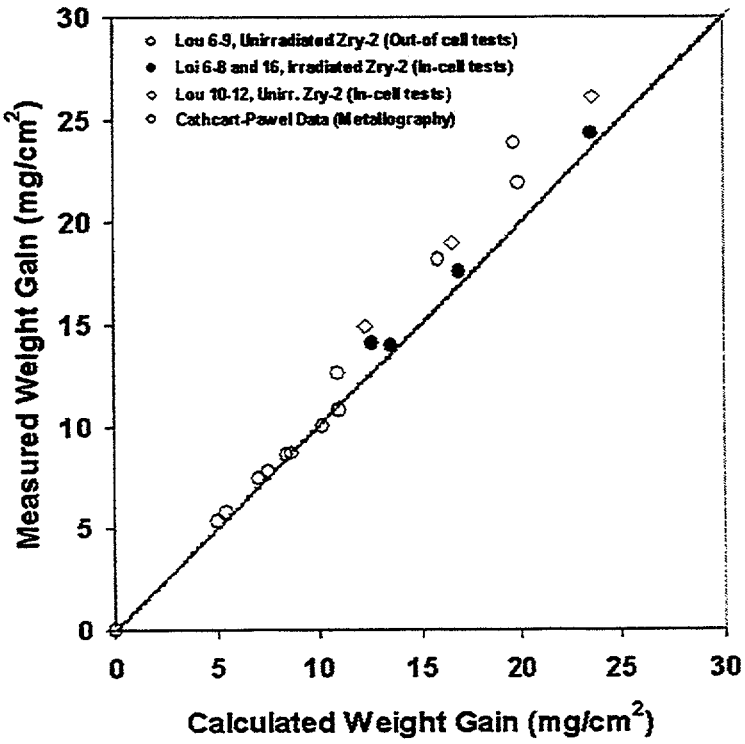

Fig. 4. Comparison of Cathcart-Pawel model predictions (Δw_p) and sample weight gain data (Δw_w) for irradiated (Limerick) Zry-2 and unirradiated (archival) Zry-2 after steam oxidation at ≈1200°C.

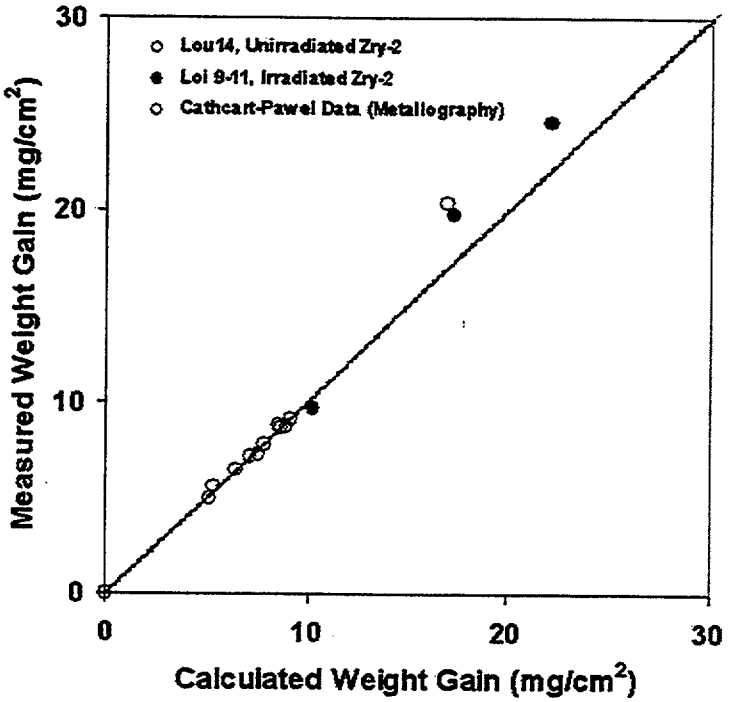

Fig. 5. Comparison of Cathcart-Pawel model predictions (Δw_p) and sample weight gain data (Δw_w) for irradiated (Limerick) Zry-2 and unirradiated (archival) Zry-2 after steam oxidation at ≈1100°C.

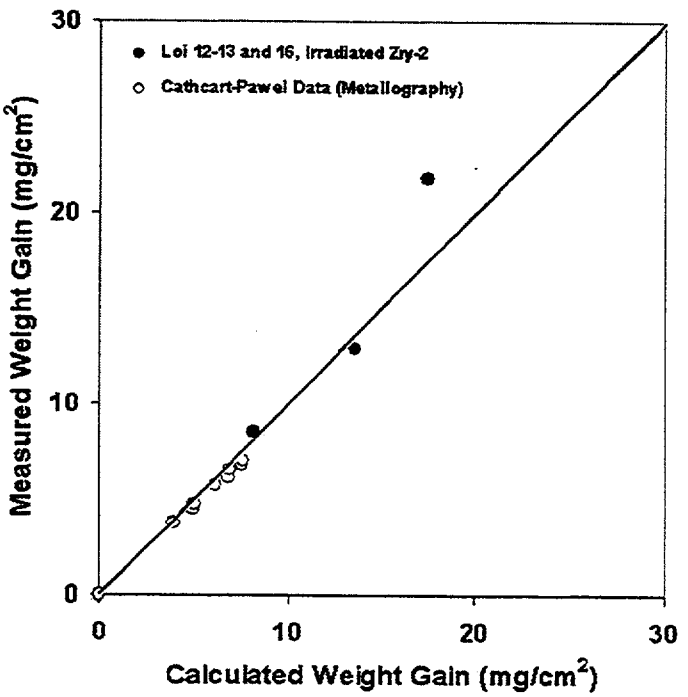

Fig. 6. Comparison of Cathcart-Pawel model predictions (Δw_p) and sample weight gain data (Δw_w) for irradiated (Limerick) Zry-2 after steam oxidation at ≈1000°C.

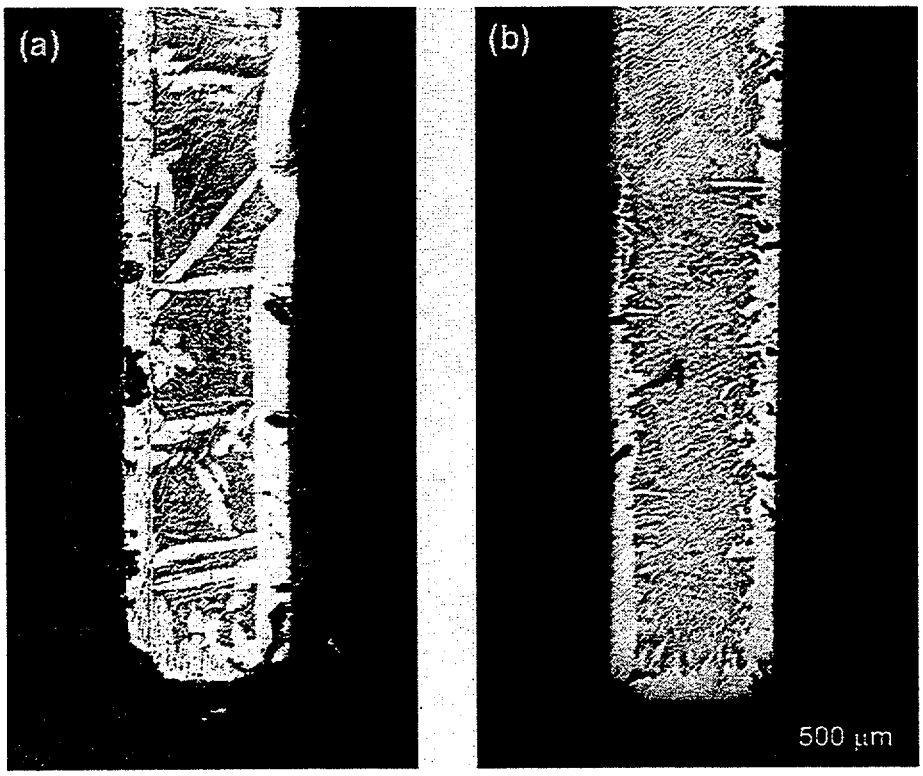

Fig. 7. Oxidation of sample end and partial (<2 mm) oxidation of sample inner surface for (a) LOU-11 test (unirradiated Zry-2 exposed to steam at 1202°C for 10 minutes) and (b) LOI-7 test (irradiated Zry-2 exposed steam at 1201°C for 5 minutes).

2. Weight gain determined from LECO oxygen analysis before and after steam oxidation (Δw_o)

Because of the saturation limit of the LECO oxygen determinator, specimens need to be < ≈0.1 g. Specimen preparation involves cutting out a ring ≈3-mm long from near the mid-plane of the 25-mm-long oxidation sample with a wet diamond saw and sectioning it into 4-6 arc lengths. As discussed in Ref. 1, the weight gain deduced from direct measurements of oxygen before and after steam testing tends to fall below the expected value due to partial loss of brittle oxide during specimen preparation. Improvements have been made to both steps in the preparation process to minimize the loss of oxide. In the improved method, the ends of the specimen are ground down to a depth at which the oxide layer is uniform. A wire saw is then used to subdivide the polished ring into ≈0.1-g specimens. These improved specimen preparation techniques have been demonstrated out-of-cell with unirradiated specimens. The results of the LECO oxygen analysis for the better-prepared specimens are compared in Fig. 8 to both the Cathcart-Pawel model prediction and the weight gain determined from metallography for LOCA Test #6 (≈1209°C for 10 minutes) and LOU-7 (≈1192°C for 10 minutes). The weight gains deduced from the change in oxygen content (as determined by LECO analysis) are ≈10% lower than the weight gains determined from the metallography. It should be noted that using the previous Ref. 1 techniques for sample preparation gives results ≈25% lower than those deduced from metallography.

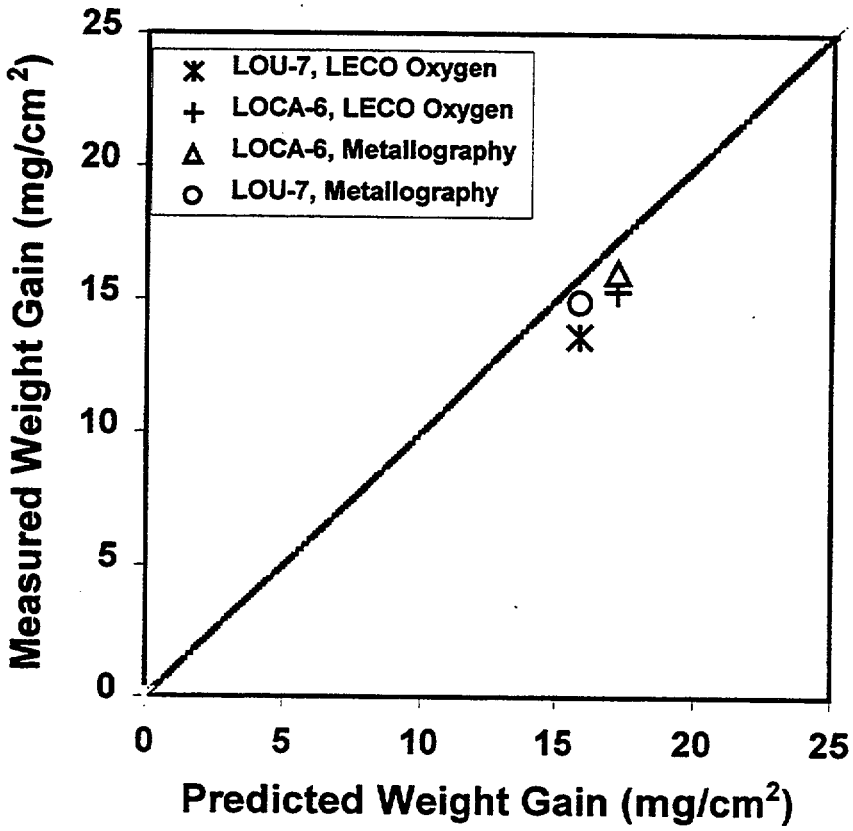

Fig. 8. Comparison of Cathcart-Pawel model predictions for weight gain (Δw_p) with weight gains determined from metallographic analysis (Δw_m) and from the LECO oxygen analysis (Δw_o) after careful specimen preparation to minimize oxide loss. The samples for both LOCA-6 (10 min. in steam at 1209°C) and LOU-7 (10 min. in steam at 1192°C) tests are unirradiated (archival) Zry-2.

3. Weight gain determined from metallographic analysis (Δw_m)

This procedure involves metallographic analysis to determine the effective thicknesses of the oxide, alpha and prior-beta layer following steam oxidation of the Zircaloy samples. The thickness of these layers can be compared directly to Cathcart-Pawel model predictions. By assuming "equilibrium" oxygen concentrations at the oxide outer surface (26 wt.% at 1204°C), at the oxide/alpha interface (24-wt.%/6.7-wt.% at 1204°C) and at the alpha/beta interface (2.4-wt.%/0.6-wt.% at 1204°C), as well as a time-dependent diffusion model for the oxide distribution within the layers, the total oxygen increase can be determined. The corresponding weight gain can then be determined and compared to the predicted value. The procedure is straightforward for unirradiated Zircaloy, which is characterized by a negligible outer surface oxide layer and tends to exhibit uniform layer interfaces following high-temperature steam oxidation. More judgment is required in the analysis of irradiated cladding as the in-reactor-formed oxide

layer needs to be defined and subtracted from the total oxide layer observed in the metallographs, and the alpha/beta interface tends to be highly non-uniform due to local regions of enhanced alpha-phase growth.

Based on numerous out-of-cell test results obtained with unirradiated (archival) Zry-2 samples and the more limited test results obtained with unirradiated Zry-4 samples, both the measured oxide layer thickness and the weight gain deduced from the metallographic analysis of oxide/alpha/beta layer thicknesses are in excellent agreement with the Cathcart-Pawel model predictions for steam oxidation tests at ≈1200°C. Limited data analyzed for specimens tested at 1000°C and 1100°C are also in good agreement with the Cathcart-Pawel model predictions. However, more tests at these lower temperatures and more data analyses need to be completed before conclusions for these lower temperatures can be made with confidence. As the focus of this paper is on the test results for irradiated cladding, the results for the unirradiated cladding will be incorporated into the data plots for irradiated cladding.

Figures 9 and 10 show the overview of specimen selection and preparation for metallographic analysis. The midplane cross-section of the sample (25-mm-long, irradiated Limerick Zry-2) for test LOI-6 (10 minutes in steam at 1203°C) was prepared (e.g., cut, polished, etched) for metallographic imaging. Although the whole cross-section is viewed on the metallograph, eight locations covering ≈45% of the cladding circumference are chosen for detailed analysis. Figure 9 shows the circumferential locations for the eight specimens. Figure 10 represents an enlargement of these metallographic images to highlight the oxide layer at the cladding outer surface. For analysis purposes, each of these images is further enlarged (see Fig. 11) and analyzed using a linear-intercept method and ImagePro Plus software. Three readings of the oxide thickness are taken for each of the eight micrographs. The 24 readings are used to determine the average oxide layer thickness and the standard deviation. For unirradiated material (Fig. 12), the same procedure is used to determine the alpha and beta layer thicknesses because the alpha/beta interface is uniform for unirradiated Zircaloy after high temperature steam oxidation. As can be seen in Fig. 11, this is not the case for irradiated material. Both non-uniformity of the alpha/beta boundary and islands of alpha-prime are observed in Fig. 11. The islands of alpha-prime are formed during cooling and are not important in calculating weight gain as they draw oxygen from the beta layer during cooling. However, the local regions of enhanced oxygen-stabilized alpha phase observed in Fig. 11 are formed during high temperature steam oxidation. Thus, these regions need to be included in the calculation of the effective alpha and beta layer thicknesses for weight gain analysis. Image-Pro Plus software is used to determine the area fractions of alpha and beta in the metallographic images, such as the one shown in Fig. 11.

Figure 13 compares the measured oxide layer thicknesses for unirradiated and irradiated Zry-2 and unirradiated Zry-4 to the values predicted by the Cathcart-Pawel model. The data are for tests conducted at ≈1200°C in steam for times ranging from 5 to 40 minutes. Included in the figure are the data described in Ref. 1 for unirradiated Zry-2 tested in cell (data points with scatter bars), the out-of-cell data, and the in-cell data. The data plotted in Fig. 13 for irradiated Limerick cladding represents the change in oxide thickness during the steam oxidation. As can be seen in Fig. 14, this requires some judgment. The loose oxide islands that appear disconnected from the main oxide layer are not included in the total oxide. It is assumed that these are oxidized crud. A nominal 10 μm of in-reactor-formed oxide thickness is subtracted from the total oxide layer thickness readings (excluding the loose oxide) deduced from the metallographic image in Fig. 14. Considering that the Cathcart-Pawel model is based on data for unirradiated Zry-4 exposed to ≈1200°C steam for <5 minutes, the agreement between the extrapolated model predictions and the ≈1200°C data generated within the ANL program is excellent. As most of the weight gain is contained within the oxide layer, one can expect excellent agreement between the model predictions and the weight gain deduced from the metallography.

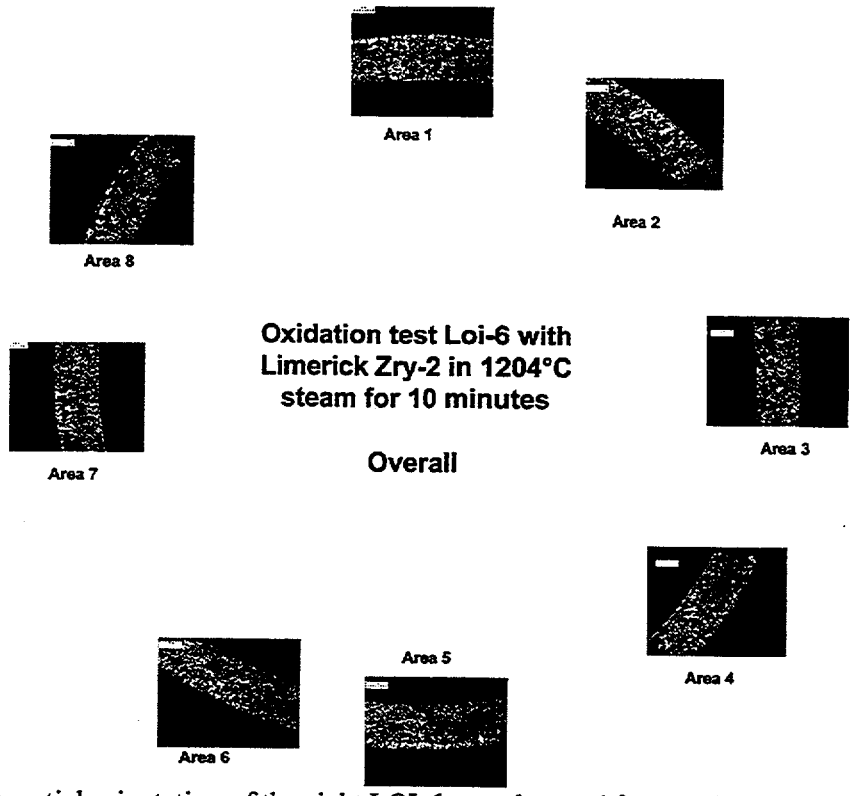

Fig. 9. Circumferential orientation of the eight LOI-6 samples used for metallographic analysis.

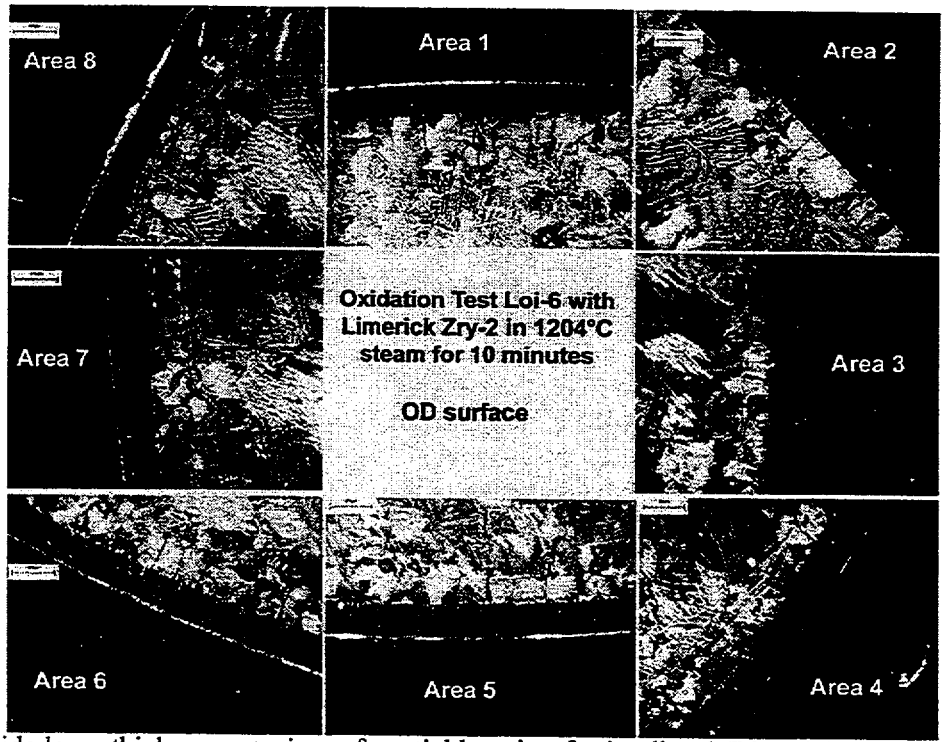

Fig. 10. Oxide layer thickness vs. circumferential location for irradiated (Limerick) Zry-2 LOI-6 test sample.

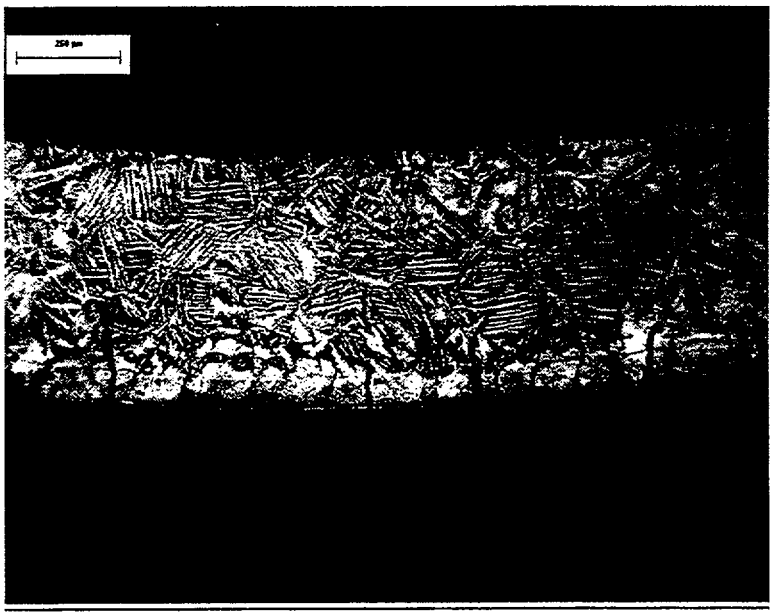

Fig. 11. Etched specimen of irradiated Limerick Zry-2 after 10 minutes exposure to 1204°C steam. Local regions of enhanced growth of the oxygen-stabilized alpha phase are clearly visible.

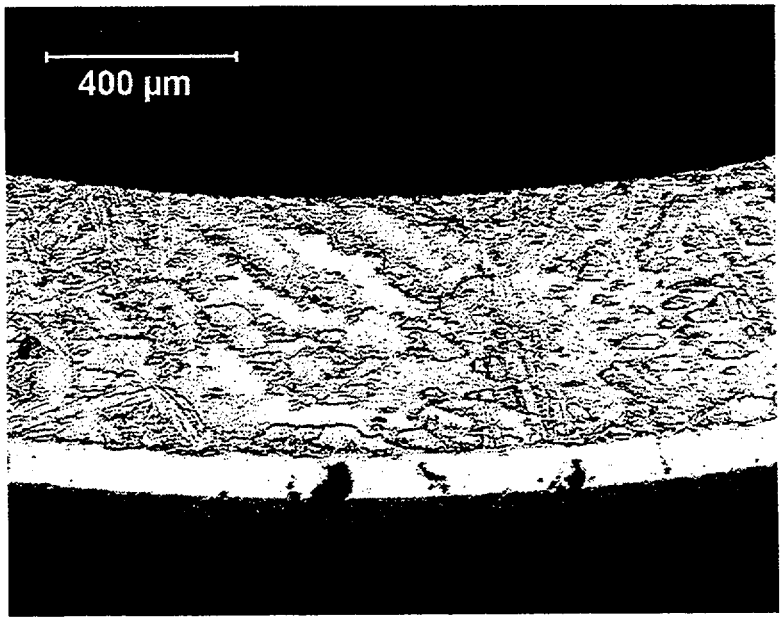

Fig. 12. As-polished specimen of unirradiated archival Zry-2 after 10 minutes exposure to 1192°C steam. Uniformity of oxide/alpha and alpha/beta interfaces is clearly visible in the unirradiated material.

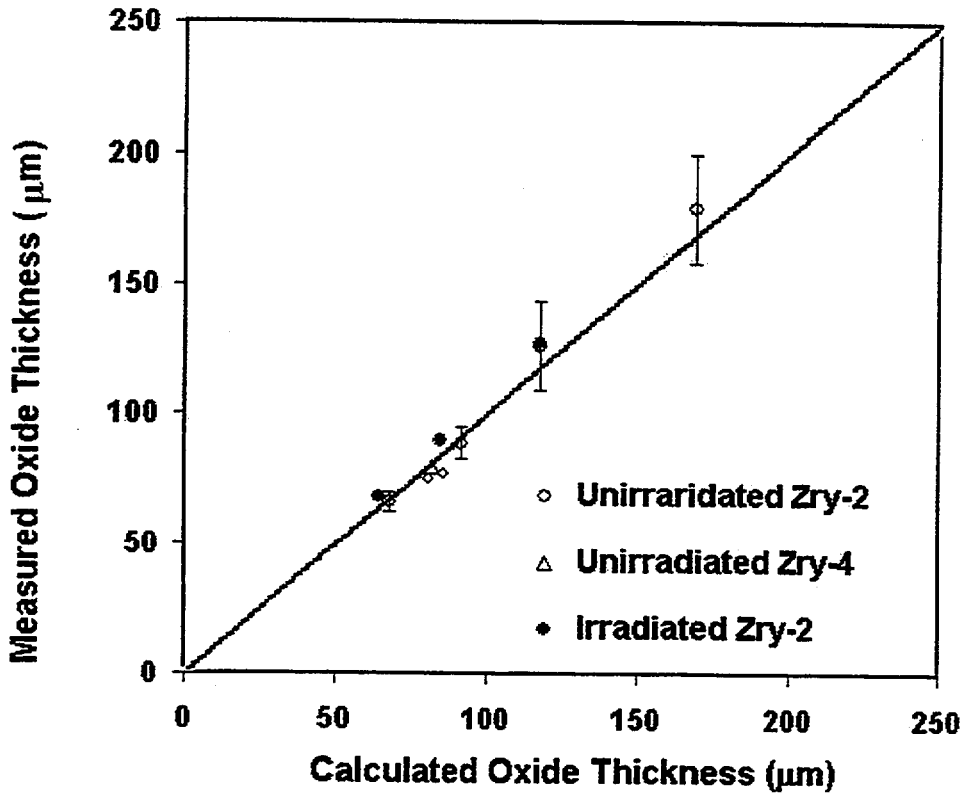

Fig. 13. Comparison of Cathcart-Pawel model predictions and metallographic data for oxide-layer thickness for Zry-2 and unirradiated Zry-4 after ≈1200°C steam oxidation for 5 to 40 minutes.

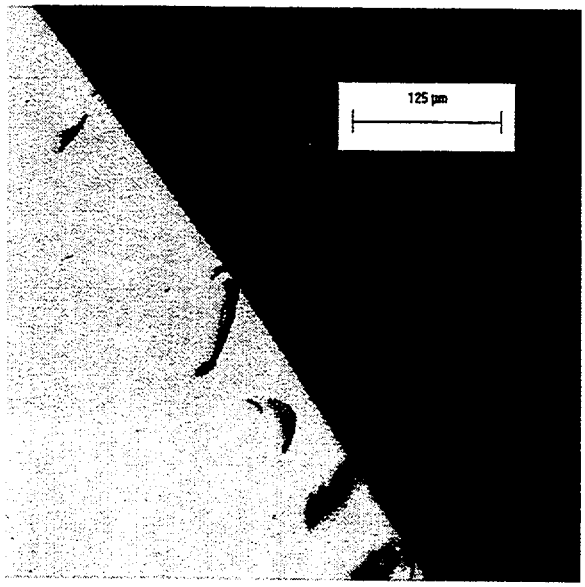

Fig. 14. Enlarged view of the outer-surface oxide layer of irradiated Limerick Zry-2 after exposure to 1204°C steam for 10 minutes.

Weight gain at ≈1200°C has been determined from the metallographic images of the unirradiated samples exposed to steam for 5 to 40 minutes and the irradiated (Limerick) samples exposed to steam for 5 to 20 minutes. As shown in Fig.12, the smooth boundaries between the oxide, alpha and beta layers for unirradiated Zircaloy allow for the use of the linear-intercept method for determining oxide, alpha and beta layer thicknesses. The results are shown in Fig. 15 for the Ref. 1 in-cell tests (LOU 1-4) and for out-of-cell tests (LOCA#6, LOU 7-9, and OC#7 Zry-4). Based on the results shown in Fig. 15, excellent agreement is observed between the model predictions and the weight gain data determined from metallographic analysis of unirradiated Zry-2 and Zry-4 and irradiated Zry-2 oxidized in steam at ≈1200°C. The same good agreement is expected from the in-cell tests conducted on unirradiated Zry-2 samples oxidized in steam at 1000-1200°C and on irradiated Zry-2 at 1000-1100°C. These metallographic analyses are in progress

The weight gains determined by metallographic analysis for in-cell ≈1200°C tests LOI-7 (13.8 mg/cm^2 after 5 min.), LOI-6 (17.8 mg/cm^2 after 10 min.) and LOU-8 (24.4 mg/cm^2 after 20 min.) are only ≈6% higher than the Cathcart-Pawel model predictions and ≈9% higher than the average results for the ≈1200°C data set for unirradiated samples. The data sets for both the irradiated and unirradiated samples are within the uncertainty band for the model. From a weight gain perspective, the difference of ≈9% between the unirradiated and irradiated samples is not significant. However, as explained in the next section, there are interesting differences in the effective alpha and beta layer thicknesses.

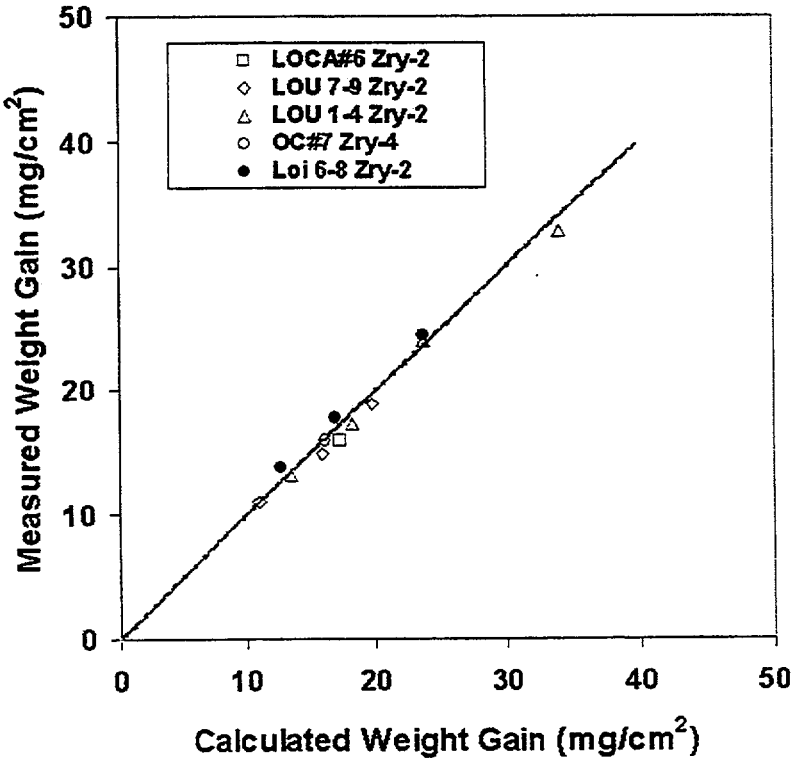

Fig. 15. Comparison of Cathcart-Pawel model predictions (Δw_p) and weight gain data deduced from metallographic analysis (Δw_m) of unirradiated Zry-2 (LOCA#6 and LOU) and Zry-4 (OC#7) and irradiated Limerick Zry-2 (Loi 6-8) samples exposed to steam for 5-40 minutes at ≈1200°C.

Discussion

One-sided (outer-surface) oxidation tests have been conducted on unirradiated Zry-2 (archival) and Zry-4 and on irradiated Zry-2 (Limerick at 56 GWd/MTU) and Zry-4 (TMI-1 at 49 GWd/MTU) cladding samples. In addition to the many tests conducted out-of-cell on archival Zry-2 and low-tin Zry-4, Table 1 lists the tests that have been completed in cell on unirradiated and irradiated Zry-2 and irradiated Zry-4, as well as the few remaining tests to be completed on unirradiated Zry-2 at 1000°C and 1100°C. The decision to use the one-sided oxidation approach, rather than the two-sided approach, was based on several factors: Cathcart and Pawel [2] used this approach to develop the database for their best-estimate model that is used throughout the current work as a basis for comparison; the approach allows for temperature monitoring by means of a thermocouple suspended within the sample; by oxidizing the outer surface, the effects on the oxidation kinetics of the in-reactor-formed, coolant-side oxide layer can easily be isolated and studied; and for the LOCA Integral Tests, most of the 300-mm-long high burnup sample will be exposed only to outer-surface steam oxidation.

Weight gain has been determined by three independent means. Direct measurement of the sample weight before and after the test gives the total weight gain, which is divided by the sample outer surface area, to give the normalized weight gain (Δw_w). These data are ≈5-20% higher than predicted by the Cathcart-Pawel model because end effects result in additional oxidation. This additional oxidation near sample ends has been confirmed by metallography. A better value for the effective surface area that undergoes oxidation could be determined through extensive metallography near the samples ends, but it would not be worth the effort. The simply-obtained Δw_w values are used for: screening purposes to assess the quality of the tests; for comparing the behavior of unirradiated to irradiated Zircaloys; and for demonstrating that the data are more in agreement with the Cathcart-Pawel best-estimate model than with the conservative Baker-Just correlation [3]. The last test in Table 1 (irradiated TMI-1 Zry-4 in steam at 1203°C for 20 minutes) has an unexpectedly high weight gain (32% higher than model predictions). The metallography at the midplane will be examined very closely to determine whether or not the weight gain deduced from midplane metallographic analysis is also high and, if so, why it is high. The Δw_w data in Table 1 indicate no difference (within the uncertainties of this simplistic approach) between unirradiated and irradiated Zircaloy oxidation kinetics. At 1200°C the Baker-Just predictions are ≈34% higher than the Cathcart-Pawel predictions. Even though the Δw_w data are artificially high due to end effects, they are lower than the Baker-Just predictions. For irradiated Limerick Zry-2 tests conducted at ≈1200°C, the average of the weight gains after 5 to 20 minute exposure to steam are only ≈7% higher than the Cathcart-Pawel predictions.

The second method for determining weight gain (Δw_o) is to measure the oxygen content of a sibling sample before the steam-oxidation test and the oxygen content of the test sample after the steam-oxidation test. This approach involves careful preparation of the oxidized specimens for LECO oxygen analysis, as some brittle oxide is lost during the preparation process. To date, significant progress has been made in this area for unirradiated Zry-2. The oxygen content of the as-fabricated cladding is relatively low (≈1100 wppm) and uniform and the cutting and polishing of specimens for LECO analysis can be done carefully out-of-cell. In comparing the weight gains (Δw_o) derived from this approach for unirradiated Zry-2 to those determined from metallographic analysis and from the Cathcart-Pawel model predictions, the values tend to be ≈10% low because some oxide is still lost during the preparation process. However, this is a vast improvement as compared to the techniques and results given in Ref. 1. The old procedure resulted in values that were as much as 25% too low. Work is in progress to apply the new specimen-preparation techniques to irradiated cladding samples.

The third method for determining weight gain (Δw_m) is through metallographic analysis, which is used to measure the effective thicknesses of the oxide, alpha and beta layers after steam oxidation. Using equilibrium assumptions for oxygen content at the oxide outer surface and at the interfaces, along with a time-dependent diffusion model, the oxygen pickup can be determined. This approach is straightforward for unirradiated material, which exhibits smooth interfaces after steam oxidation. For unirradiated Zry-2 tested at ≈1200°C, the Δw_m values agree with the model predictions to within ≈3%. For irradiated Zircaloy, the procedure is complicated by three factors. A judgment must be made with regard to the outer boundary of the oxide layer, an average in-reactor-formed oxide layer measured from a sibling sample must be subtracted from the total oxide layer thickness observed, and the effective alpha and beta layer thicknesses must be determined from an area averaging approach due to the non-uniformity of the alpha/beta interface. These factors do not have a significant impact on the weight-gain results for irradiated Limerick cladding exposed to steam at ≈1200°C. The in-reactor-formed oxide layers are small (≈10 μm), and the enhancement in the growth of the alpha region contributes <10% to the overall weight gain. Based on detailed metallographic analysis of the tests conducted on irradiated Zry-2 at ≈1200°C, the measured oxide layer increases with time are ≈7% higher, the alpha layers are ≈45% thicker and the beta layers are ≈8% thinner than predicted by the Cathcart-Pawel model. Metallographic analysis is in progress to determine the behavior of irradiated Limerick Zry-2 oxidized at 1100°C and 1000°C and irradiated TMI-1 Zry-4 oxidized at ≈1200°C.

Future work is planned to determine the oxidation kinetics of high burnup PWR (H. B. Robinson) Zry-4 cladding under the same test conditions listed in Table 1. The tests will be performed on samples taken from grid span 2 with an in-reactor-formed oxide layer of ≈50 μm and on samples taken from grid span 4 with an in-reactor-formed oxide layer of ≈100 μm. Thus, the full oxidation test matrix includes pre-oxide layers ranging from 10 to 100 μm and hydrogen contents ranging from 70 to ≈500 wppm.

The primary purpose of generating oxidation kinetics data at ≈1200°C for high burnup cladding is to help plan and interpret the results of the Integral LOCA Tests, which will be conducted with fueled cladding samples at this oxidation temperature. The data obtained to date indicate that exposure times to generate a desired effective cladding reacted (ECR) can be adequately predicted by using the Cathcart-Pawel model. However, weight gain and the associated ECR are not very sensitive measures to determine what is important in ensuring adequate ductility to survive ECCS quench and post-quench events. The effective thickness of the beta layer, its oxygen content and its hydrogen content are the critical factors in determining quench and post-quench ductility. The main difference observed between unirradiated and high burnup Zry-2 behavior is the enhanced growth of the oxygen-stabilized alpha phase in steam-oxidized irradiated cladding. Although this enhancement has little impact on weight gain and ECR, it does result in a reduction in the effective thickness of the ductile beta layer. This assessment requires the use of metallographic analysis and cannot be determined from change in either sample weight or oxygen content. Thus, metallography has two major advantages over the other approaches: it produces the most reliable data for weight gain kinetics and it allows a quantitative determination of the effective beta layer thickness. Work is in progress to determine further reductions in the effective beta layer thickness due to the alpha-prime islands observed within the prior-beta layer.

The effective beta layer thickness following high temperature oxidation in steam is dependent on the cooling rate. Slower cooling will result in a higher fraction of brittle-alpha formation within the prior beta layer and lower ductility of that layer. Based on Fig. 3, the average cooling rate from 1200 to 800°C is ≈5°C/s, within the 4-7°C/s ramp planned for the LOCA Integral Tests. The LOCA tests will have much faster cooling from 800°C to room temperature than the oxidation tests. However, no significant diffusion and phase changes are expected below ≈800°C.

Conclusions

High temperature steam oxidation tests have been conducted to determine the oxidation kinetics of high burnup Zircaloy cladding. The tests conducted at ≈1200°C provide data that will be used to help plan the test times for, and to interpret the data from, the Integral LOCA Tests. The broader range of temperatures in the test matrix (900°C-1300°C) will provide data that are important in the analysis of small-to-large break BWR and PWR LOCA events at high burnup. The oxidation tests and post-test analyses completed to date have focused on high burnup Zircaloy-2 (Zry-2) cladding from Limerick BWR rods (56 GWd/MTU), as well as unirradiated (archival) Zry-2 cladding, in the temperature range of 1000°C-1200°C. Limited testing has also been completed on irradiated PWR (TMI-1) Zircaloy-4 (Zry-4) cladding, as well as on unirradiated Zry-4, at ≈1200°C. Additional tests are planned to determine the oxidation kinetics of high burnup PWR (H. B. Robinson at 67 GWd/MTU) Zry-4 cladding.

The results obtained thus far indicate that there are no significant high burnup effects on the weight-gain kinetics of high burnup Zry-2 exposed to steam at 1000-1200°C. The results are in good agreement with the results for unirradiated Zry-2 (archival) and Zry-4, as well as those predicted by the Cathcart-Pawel model. Detailed metallographic analyses of unirradiated and irradiated (Zry-2) samples tested at ≈1200°C give oxide layer thicknesses (Zry-2 and Zry-4) and weight gains (Zry-2) determined from the metallography that are in excellent agreement with the Cathcart-Pawel model predictions. Determination of weight gain from metallographic analysis of the irradiated samples tested at ≈1000°C and ≈1100°C is in progress. Based on preliminary analyses, the weight gain determined from metallography of the high burnup Zry-2 tested at ≈1200°C is within 10% of the Cathcart-Pawel model predictions. The main difference observed between the characteristics of unirradiated and irradiated samples oxidized at ≈1200°C is the presence of non-uniform alpha/beta interfaces in irradiated cladding leading to larger (≈45%) oxygen-stabilized alpha regions formed at high temperature and the presence of alpha-prime islands formed within the beta layer during cooling. Although the increased thickness of the brittle oxygen-stabilized alpha and alpha-prime regions has little impact on weight gain, it may have a detrimental effect on ECCS quench and post-quench performance by reducing the thickness of the ductile beta layer.

The oxidation tests completed thus far with irradiated cladding are with samples having pre-test outer-surface oxide layers of ≈10 μm (Limerick) and ≈30 μm (TMI-1) and corresponding hydrogen levels of ≈70 wppm and ≈150 wppm. Completion of the high burnup PWR cladding tests will broaden this range to in-reactor-formed oxide layers of ≤100 μm and hydrogen contents of ≤500 wppm. This range is more than adequate to characterize the oxidation kinetics of high burnup BWR and PWR Zircaloy cladding.

References

1. Y. Yan, T. S. Bray, H. C. Tsai and M. C. Billone, "High temperature Steam Oxidation of Zircaloy Cladding from High Burnup Fuel Rods," Proc. 28th WRSM, Oct. 23-25, 2000, Bethesda, MD, NUREG/CP-0172 (2001) 239-250

2. J. V. Cathcart, R. E. Pawel, R. A. McKee, R. E. Druscel, G. J. Yurek, J. J. Cambell and S. H. Jury, "Zirconium Metal-Water Oxidation Kinetics IV. Reaction Rate Studies", ORNL/NUREG-17, Aug. 1977.

3. L. Baker and L.C. Just, "Studies of Metal-Water Reactions at High Temperatures; III. Experimental and Theoretical Studies of the Zirconium-Water Reaction," ANL-6548, May 1962.

Status of the CABRI International Program and Preparation of the CIP0 Series

J. Papin, C.Marquié, F.Lemoine, M.Faury, J.C. Melis

Département de Recherches en Sécurité
Institut de Protection et de Sûreté Nucléaire
CE Cadarache 13108 St Paul lez Durance
France

Abstract

The CABRI International Programme (CIP) is devoted to the study of reactivity initiated accidents of pressurized water reactors (PWRs) and is now being launched by the "Institut de Protection et de Sûreté Nucléaire" (IPSN)" with the collaboration of Electricité de France (EDF) in the frame of a broad international cooperation under the auspices of the OECD .Its main objectives are to provide under typical PWR conditions, bases for the assessment of new safety criteria and evaluation of safety margins relatively to the use of advanced alloys (Zirlo, M5, Duplex...), high burnup fuels and future fuel conceptions including MOX fuel.

A special focus has been given to the preparation of the two tests of the CIP0 series to be performed in the CABRI sodium loop in 2002 with the specific objectives of giving a first answer on the behaviour of UO_2 advanced fuel rods at higher burnup (75 GWd/tU) than the current values and providing a link between sodium loop and water loop tests (CIP-1).

The CIP is now entering in its first experimental phase and will soon provide first results on advanced fuel behaviour under RIA .

1. Introduction

The CABRI International Programme (CIP) is now being launched by the "Institut de Protection et de Sûreté Nucléaire" (IPSN)" with the collaboration of Electricité de France (EDF) in the frame of a broad international cooperation under the auspices of the OECD [1].

It has been initiated in the context of the world-wide evolution of the fuel management strategy with the further increase of the UO_2 fuel discharge burnup and the introduction of the MOX fuel which created the need for qualification of the advanced fuels under reactivity initiated accidents (RIAs) as resulting from control rod ejection.

The main objectives of the CIP are to provide under typical PWR conditions, bases for the assessment of new safety criteria and evaluation of safety margins relatively to the use of advanced alloys (Zirlo, M5, Duplex...), high burnup fuels and future fuel conceptions including MOX fuel.

The basic test matrix is composed of twelve tests included into different series with the following general objectives :

CIP-0: two reference tests in the sodium loop with high burnup fuel and advanced cladding material (Zirlo and M5)
CIP-Q: Qualification test of the Water Loop
CIP-1: two reference tests in the water loop , similar to CIP0 tests
CIP-2: very high burnup fuel (80-100 GWd/t, one test with Duplex rod)
CIP-3: improvement of physical understanding of RIA
CIP-4: tests with MOX fuel
CIP-5: complementary tests (open)

The test matrix is elaborated through the work of the Technical Advisory Group (TAG) of the CABRI programme.

2. Preparation of the CIP-0 series

A special focus has been given to the preparation of the two tests of the CIP0 series to be performed in the CABRI sodium loop in 2002 with the specific objectives of giving a first answer on the behaviour of UO_2 advanced fuel rods at higher burnup than the current values and providing a link between sodium loop and water loop tests (CIP-1).

The CIP0-1 experiment, first test of the CIP, has been prepared with the span 5 of an UO_2 ENUSA rod irradiated in Vandellos reactor up to 68 GWd/tU (rod average) with Zirlo cladding.The rod has been reconditioned and characterized in Studsvik laboratories and will be shipped to France during the first trimester 2002 and loaded in the test device to be tested in CABRI in April 2002.

Detailed pre-calculations of the CIP0-1 test have been performed with study of the influence of the pulse width on the rod behaviour. From the non destructive examinations performed in Studsvik and from the calculation of the irradiation campaign performed with the IPSN TOSUREP code, the main characteristics of the rodlet before test were derived: maximum local burnup of 74,75 GWd/t (see figure 1), average corrosion thickness of 75 µm at span 5, without spalling.

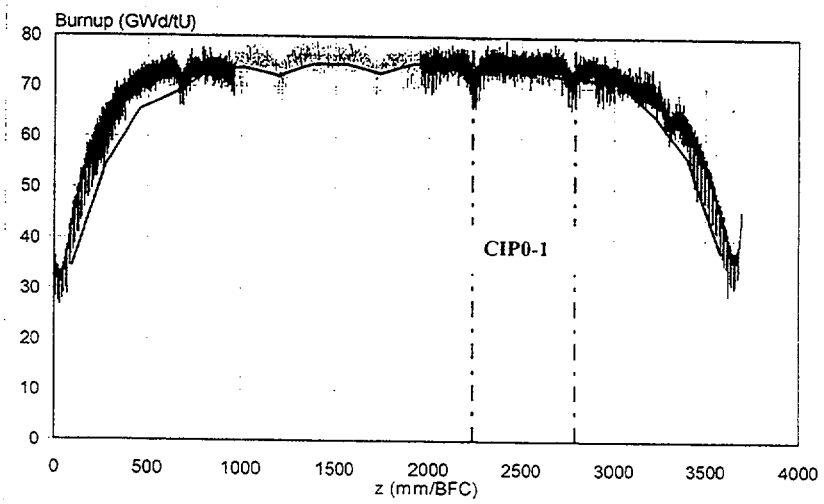

FIG 1: burnup axial profile of the ENUSA rod (measured and TOSUREP calculation)

The rim width has been evaluated to be around 330 μm (15% of fuel mass, based on Siemens high burnup fuel data from reference [2], figure 2)

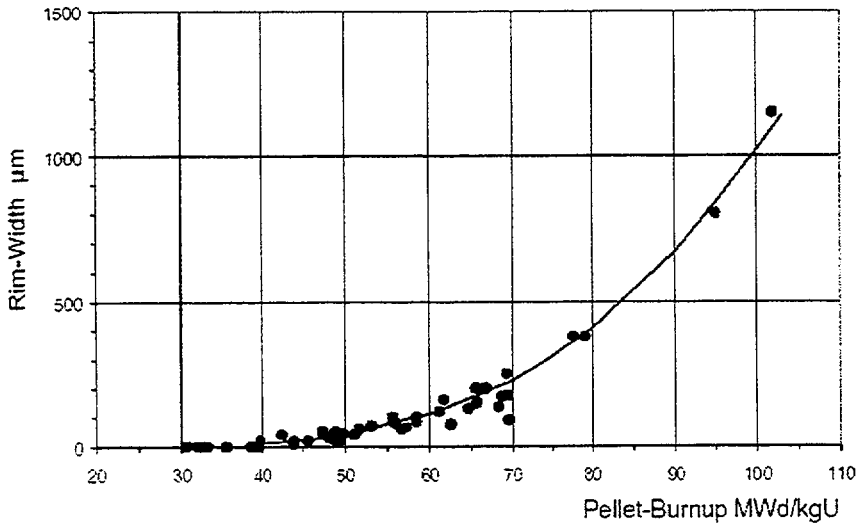

FIG 2: Rim width versus pellet burnup for UO_2 fuel from reference [2]

The interpretation of the previous REP Na tests has underlined the important role of fission gases behaviour during RIA transients [3] with possible contribution on clad loading in addition to the classical fuel thermal expansion effect. Indeed, extensive fuel fragmentation (grains separation) has been observed in most of the REP Na tests. This phenomenon is attributed to the high overpressure which is developed in the small inter-granular bubbles during fast heating rates and which induces high stress fields between the grains, leading to the grain boundaries cracking. Subsequent grains separation depends on the respective influences of gas pressure and external fuel constraint. Largely observed in UO_2 fuel, it appears also clearly in the fuel matrix with MOX tests, in spite of the relatively low burnup level. The main consequences of this phenomenon are a degradation of fuel mechanical properties, the fast availability of all the grain boundary gases with associated driving pressure leading to solid fuel pressurization and swelling, clad loading with risk of failure and finally to gas release.

So, for the CIP0-1 rod, at such a high burnup level and with the associated wide rim zone, the average grain boundary gas content (from inter-granular and porosity bubbles) is expected to be important as deduced from the figure 3 showing the grain boundary gas concentration increasing with burnup for both UO_2 and MOX fuels. An evaluation based on the micro-probe examination analysis of Siemens fuel at 75 GWd/t shows that the estimated value for the CIP0-1 rod is in the range of the one determined for the REP Na 7 rod (MOX fuel at 55GWd/t) in which rod failure suggested a possible contribution of gas pressure for clad loading due to grain boundary failure leading to grain boundary fission gas availability and fuel pressurisation during the fast heating of the fuel [3]. This result indicates that such mechanism may be considered as a possible failure mechanism for the CIP0-1 high burnup UO_2 rod.

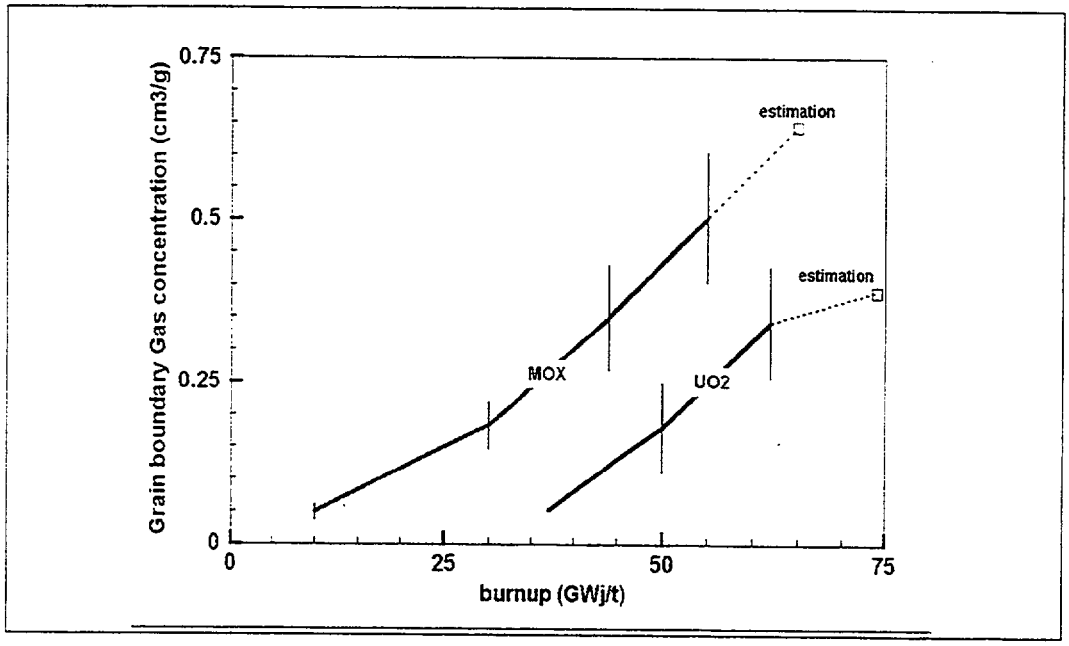

FIG 3: grain boundary gas content versus burnup for UO_2 and MOX fuel

The transient calculations have been performed with the SCANAIR code assuming mechanical properties of the Zirlo cladding similar to those of Zr-4 and transient oxide spalling (based on the high initial corrosion level).

Two power pulses were considered:

- 30 ms half width, 92 cal/g injected leading to a maximum enthalpy of 94 cal/g and to a maximum clad plastic hoop strain of 0.44%,
- - 10 ms half width, 100 cal/g injected leading to a maximum enthalpy of 108 cal/g and to a maximum clad plastic hoop strain of 0.83%.

The rod failure risk has been evaluated on the basis of the PROMETRA database taking into account the uncertainty range. The low level of clad plastic straining which is far below the total elongation data, clearly indicates for both pulses, a low ductile failure risk in case of imposed deformation resulting from pure pellet-clad mechanical interaction. In case of gas pressure loading associated to fast heat-up phase of the fuel, a ductile failure risk has been found on the basis of the cumulated plastic strain compared to the uniform elongation data; such failure risk is increased with a 10 ms half width pulse. In addition, considering the high corrosion level of the CIP0-1 rod, a high risk of brittle failure is estimated and increased with a narrow pulse

As a result of the TAG discussions, the proposed test conditions are a power pulse of 30 ms half width with the maximum energy injection estimated to be around 92 cal/g at peak power node (PPN).

A guide criterion based on the fuel enthalpy at failure, if any, has been defined for CIP0-1 and CIP0-2: if the rod failure occurs below 60 cal/g (maximum enthalpy) with fuel dispersal, the need of doing a third test in the Na loop should be considered carefully (use of the span 3 of the Spanish rod or the span 5 of a Westinghouse-North Anna rod at similar burnup).

The CIP0-2 test is foreseen using the span 5 of an UO_2 EDF rod irradiated up to 69 GWd/tU (rod average) in the Gravelines 5 reactor, with a M5 cladding (expected corrosion thickness about 30μm). Rod characterization and reconditioning are scheduled during first semester 2002 for a test planned in autumn 2002.

3. Other studies for CIP preparation

The need of a qualification test for the water loop has been underlined and led to propose the CIP-Q test as the first test to be performed in water conditions. Its specific objectives are to validate the facility operation throughout the whole transient including possible rod failure and check the instrumentation response. The use of a UO_2 rod with Zr-4 cladding and moderate burnup (≈50 GWd/tU) is envisaged and prospective studies are underway at IPSN in relation with the evaluation of the representativity of the test channel as compared to reactor case (influence of annular/reactor geometry, spacer system with thermocouples). In case of success, such test addressing the RIA phenomenology will be part of the CIP3 series.

The CIP1 series will be performed in the water loop using twin rods of the CIP0 ones.

The detailed definition of the other tests series is in an early stage. However, beyond the impact of fuel burnup, fuel and cladding types, objectives for various fields of investigation have been identified such as effects of initial power level, fuel duty under operation, power pulse width, an understanding of failure mechanism and study of consequence of rod failure. In addition, the partners have proposed several fuel rod candidates, and a choice will be made on the basis of detailed objectives, common interest and availability.

As a general concern for the understanding and interpretation of the results, a standard pre- and post-test examinations programme has been elaborated; the importance of the initial characterization of the father rods (to be provided with the test rods) has been underlined.

In parallel to the test matrix definition, a programme for mechanical characterization of the advanced claddings has been elaborated and optimised taking into account the future availability of a new facility for mechanical testing of irradiated materials in 2003 in CEA/Saclay, with well instrumented burst tests (axial, radial extensometry).

The objectives of the proposed programme are to provide:

- clad mechanical constitutive laws with hoop tensile tests associated to FEM analysis,
- data for failure criteria based on plain strain and burst tests,
- evaluation of anisotropy and mean hydrogen content.

Such a mechanical characterization programme is foreseen for each new cladding material experimented in the CABRI programme and for a same material at different burnup levels if tests with significantly different burnup levels are realized.
One corrosion level is foreseen to be tested (from samples close to the CABRI rodlet) unless significant differences appear in the tests results in comparison to those of one already well-characterized material. In such a case, an additional testing campaign could be defined.

Depending on the database, this programme may be undertaken in two steps and may be reduced if the first step leads to the same results as those obtained from a similar cladding type.

The following test matrix is defined for the tests in 2002:

		$\dot{\varepsilon} = 1s^{-1}$			$\dot{\varepsilon} = 0.01\ s^{-1}$
			T (°C)		
	280	**480**	**600**	**800**	**600**
Hoop tensile Tests (10)	X X	X X	X X	X X	X X
Axial tensile Tests (2)	X X				
Plain-strain Tests (8)	X X	X X	X X	X X	
Burst Tests (2	X X				

First step to be analysed before decision of launching the second step of the programme.

For the Zirlo and M5 materials related to CIP0-1 and CIP0-2 tests, hoop tensile tests and FEM analysis are scheduled in 2002 after defueling of the samples and the following part of the programme is planned in 2003.

On the other hand, important research and development work is launched in the field of instrumentation in order to implement high quality measurement needed for reliable quantification of the phenomena. An associated qualification programme is elaborated and concerns sensors in pile capability with fast transient response under high temperature and pressure conditions and with limited space available.

4. General planning and conclusion

The CABRI facility is now shut down for a first phase of renewal; the work needed for additional renewal will be fixed in first trimester 2002. The water loop detailed studies have been completed and the implementation is scheduled in mid 2003-2004 with first acceptance tests in first trimester 2005. Such schedule has to be confirmed according to the expertise for renewal work and to safety authorizations based on a decree expected in mid 2003 and on an operating license in early 2005.

Following the CABRI REP Na experiments, the CABRI International Programme has now entered active phases. Fruitful international cooperation and discussions inside the CIP working group (TAG) led to define the first tests series CIP0 and CIP1. General matters relative to the programme were also discussed and defined (mechanical characterization, pre and post test examinations, channel representativity ...).

Definition of the further tests series is underway with intense participation of the partners including test rods proposals.

The CIP is now entering in its first experimental phase and will soon provide first results on advanced fuel behaviour under RIA .

References

[1] J. Papin, J.C. Melis, C. Lecomte
Definition and Status of the CABRI International Program for High Burnup Fuel Studies, WRSM 28th, Bethesda, USA, October 2000.

[2] R. Manzel, C.T. Walker
High Burnup Fuel Micro-Structure and its Effects on Fuel Rod Performance, International Topical Meeting on LWR fuel performance, Park City, Utah, USA, April 2000.

[3] F. Lemoine, B. Cazalis, H. Rigat
The Role of Fission Gases on High Burn-Up Fuel Behaviour in Reactivity Initiated Accident Conditions, 10th STNM, Halifax, August 2000.

FRAPTRAN Fuel Rod Code and its Coupled Transient Analysis with the GENFLO Thermal-Hydraulic Code

Keijo Valtonen[1], Anitta Hämäläinen[2], Mitchel E .Cunningham[3]

[1]Radiation and Nuclear Safety Authority, STUK, P.O. Box 14, FIN-00881 Helsinki, Finland
[2] VTT ENERGY, P.O. Box 1604, FIN-02044 VTT, Finland
[3]Pacific Northwest National Laboratory, P.O. Box 999, Richland, WA

ABSTRACT

The FRAPTRAN computer code has been developed for the U.S. Nuclear Regulatory Commission (NRC) to calculate fuel behavior during power and/or cooling transients at burnup levels up to 65 GWd/MTU. FRAPTRAN has now been assessed and peer reviewed. STUK/VTT have coupled GENFLO to FRAPTRAN for calculations with improved coolant boundary conditions and prepared example calculations to show the effect of improving the coolant boundary conditions.

INTRODUCTION

Plans to increase the burnup of nuclear fuel, to utilize new fuel designs, and in some countries to include additional transients such as the anticipated transient without scram (ATWS) in safety evaluations, require that new or updated models be used in safety analyses. Addressing these issues requires improving the fuel models in reactor dynamics codes or incorporating more advanced thermal-hydraulic models in fuel behavior codes. An example of the latter approach involves coupling the Finnish thermal-hydraulic model GENFLO (GENeral FLOw) with the new US Nuclear Regulatory Commission (NRC) FRAPTRAN code. Provided in this paper are a summary of the recent code assessment and peer review of FRAPTRAN, a description of GENFLO and its coupling with FRAPTRAN, and the results of two example calculations using FRAPTRAN-GENFLO.

FRAPTRAN ASSESSMENT AND PEER REVIEW

FRAPTRAN (Fuel Rod Analysis Program TRANsient) is being developed and maintained for the NRC to calculate fuel behavior during power and cooling transients at burnup levels up to at least 65 GWd/MTU (Cunningham et al. 2001a). This FORTRAN-language code will be applied for the evaluation of fuel behavior during transients such as reactivity accidents, loss-of-coolant-accidents, and boiling-water reactor power oscillations without scram. FRAPTRAN uses a finite difference heat conduction model for the transient thermal solution, the FRACAS-I mechanical model, and the MATPRO material properties package. To account for the effects of high burnup, FRAPTRAN uses a UO_2 thermal conductivity model that incorporates the degradation effects of burnup and a revised model for Zircaloy mechanical properties that accounts for the effect of oxidation and hydrides in addition to irradiation damage. Burnup dependent fuel rod initial conditions can be obtained from the companion FRAPCON-3 steady-state fuel rod performance code (Berna et al. 1997).

FRAPTRAN has been assessed (Cunningham et al. 2001b) using a data base that emphasized experiments investigating the effects of burnup on fuel rod behavior during reactivity-initiated accidents (RIAs) and loss-of-coolant-accidents (LOCAs). FRAPTRAN generally performed well in the comparisons to data. Principal conclusions for the code-data assessment include:

- Comparison of code predictions with data have provided assurance that the basic models are working satisfactorily; i.e., temperature, gap conductance, gas pressure, and thermal expansion.

- Comparisons of predicted and measured fuel centerline temperature during scrams show that the code consistently calculates faster temperature decreases than were measured. This is likely due to FRAPTRAN calculating lower thermal resistances in the fuel or fuel-cladding gap than are operating in the rods.

- Rod internal gas pressure is correctly calculated when other paramters that determine gas pressure, such as available volume and corresponding coolant temperatures, are correctly input. In addition, when gas pressure is correctly calculated for the LOCA cases, then reasonable agreement between predicted and measured time to failure is obtained; this is illustrated in Figure 1 for the MT-4 experiment (Wilson et al. 1983). The initial decreases in pressure are due to cladding ballooning increasing the rod volume and rod failure is indicated by rod pressure decreasing to system pressure (i.e., 0.28 MPa).

- FRAPTRAN provides reasonable predictions of cladding axial elongation for fast transients but, as expected because the code does not include a fuel creep model, does not follow the fuel and cladding relaxation when steady-state power conditions are achieved; this is illustrated in Figure 2 where measured and predicted cladding elongation are compared for the IFA-508 test in the Halden Boiling Water Reactor (Uchida and Ichikawa 1980). For this experiment, power was held constant after each power increase, and cladding elongation could be seen to decrease. FRAPTRAN compared well to the rate of cladding elongation for each power increase, but does not calculate the relaxation during the power hold.

- FRAPTRAN consistently underpredicts permanent cladding hoop strain for the RIA tests recently conducted in the NSRR and CABRI facilities. This is indicative of fuel-cladding mechanical interaction occurring in these tests that is not modeled by the code. This underprediction of permanent hoop strain is illustrated in Figure 3 by comparing predicted hoop strain to measured hoop strain for tests conducted in the NSRR (Fuketa, Nakamura, and Ishigima 1998) and the CABRI test facilities (Papin and Schmitz 1998).

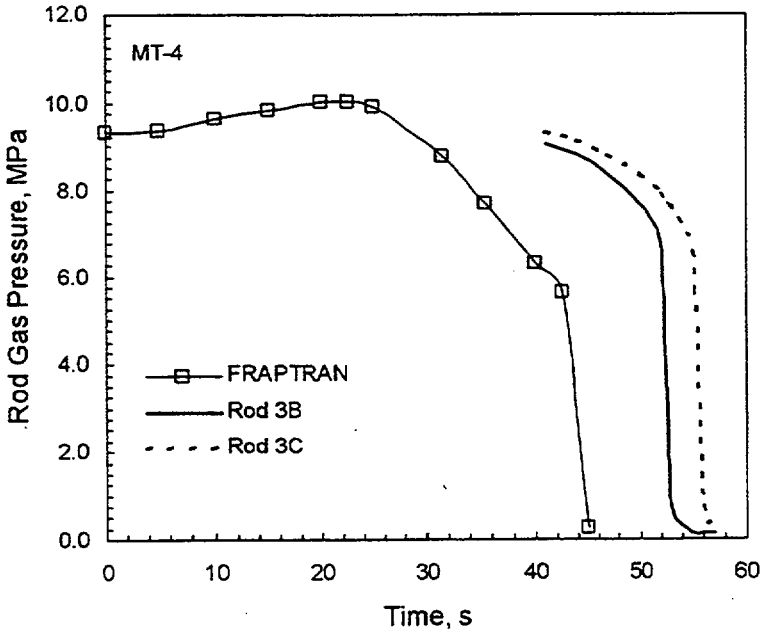

FIGURE 1. Measured and Predicted Rod Gas Pressure for MT-4 LOCA Test

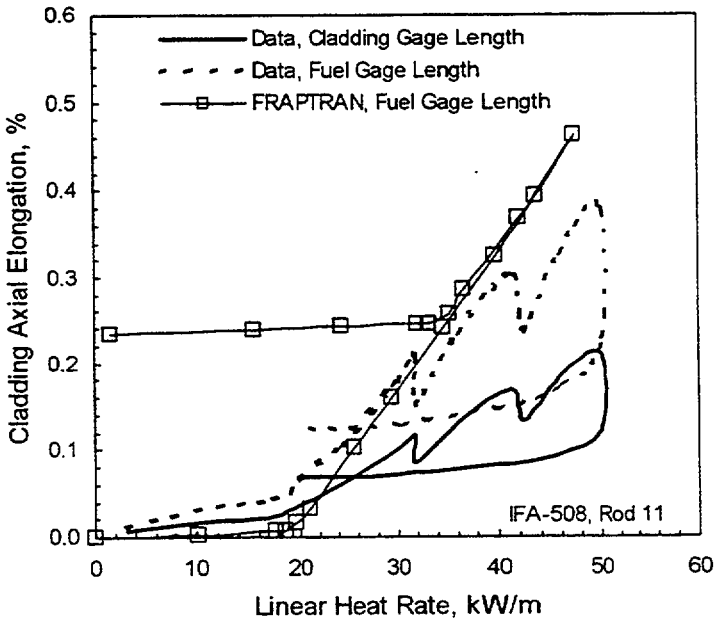

FIGURE 2. Comparison of Predicted and Measured Cladding Elongation for IFA-508, Rod 11

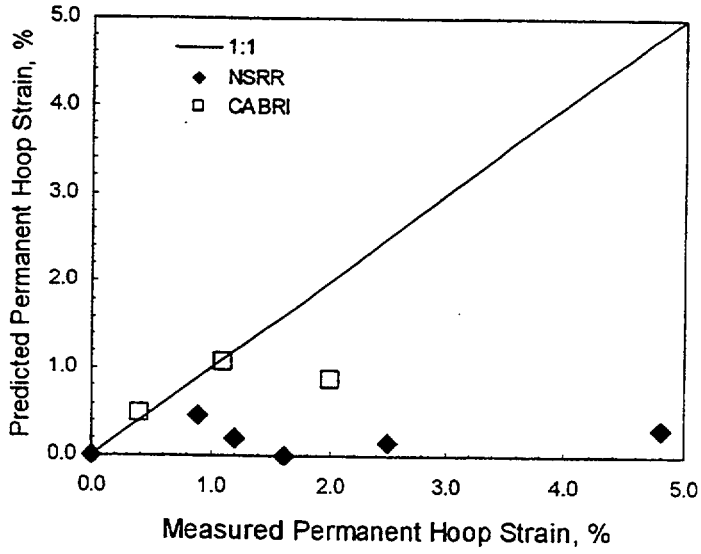

FIGURE 3. Comparison of Measured and Predicted Permanent Cladding Hoop Strains for RIA Experiments Conducted in the NSRR and CABRI Facilities

In addition to the code assessment, an independent peer review of FRAPTRAN was conducted using peer reviewers representing a broad background of code developers, code users, and experimentalists. Each reviewer had greater than 20 years of experience. After reviewing the draft description and assessment documents, and meeting and discussing their comments with FRAPTRAN's developers, many useful recommendations were made and implemented. Principal conclusions from the peer review process include: the FRAPTRAN fuel and cladding models are reasonable, FRAPTRAN is able to predict the trends in the transient experimental data, and the assessment data base adequately covered the intended applications for the code. Recognizing that development work will continue on FRAPTRAN, the reviewers recommended that priority be given to adding models for transient fission gas release and transient fuel swelling/creep.

FRAPTRAN is being released though the FRAPCON-3 and FRAPTRAN users group managed by Pacific Northwest National Laboratory for the NRC. Members of the users group will be supplied the documentation, the code, and a selected set of sample problems. Information about the users group can be found on the FRAPCON3 website (www.pnl.gov/frapcon3).

THE GENFLO MODEL AND COUPLING WITH FRAPTRAN

The thermal-hydraulic models provided in FRAPTRAN are applicable for homogeneous, slowly changing thermal-hydraulic conditions and for many transients it is necessary to use a thermal-hydraulic code to calculate coolant boundary conditions. Especially during the ATWS in boiling-water reactor (BWR) plants, the hot channel and the whole core may experience rapid transitions between the wetted and dry states. Because of this, a dynamic exchange of detailed local data between the fuel performance and thermal-hydraulic models is needed.

The thermal-hydraulic model GENFLO (GENeral FLOw) has been developed by VTT Energy (VTT) and, under the sponsorship of the Finnish Radiation and Nuclear Safety Authority (STUK), the code is coupled with the FRAPTRAN code. The thermal-hydraulic solution principles of GENFLO are based on the models developed for the SMABRE model (Miettinen and Hämäläinen 2000). GENFLO is a fast running, five-equation model, where the wetted wall heat transfer, dryout, post-dryout heat transfer and quenching models are included. The flow modes covered by GENFLO are depicted in Figure 4. The geometry described by GENFLO comprises one or several parallel fluid flow channels and an optional fuel structure. The lower and upper plena are always included but the core bypass and the downcomer may be zeroed, as is done in subchannel applications.

GENFLO solves the coolant mass, momentum, and energy conservation equations, including the calculation of the axial distributions of the fluid temperature and the void fraction. As a result, the fluid temperatures and heat transfer coefficients for each axial level at each time step are supplied for FRAPTRAN. The temperatures in the fuel rod, and the deformation of fuel pellets and cladding, including possible ballooning, are calculated in FRAPTRAN using burnup dependent models. At this stage GENFLO and FRAPTRAN use their own models, i.e., for fuel and cladding temperatures including cladding oxidation and hydrogen generation, though FRAPTRAN supplies the local gas gap heat transfer coefficient for GENFLO. The axial power profile used by both FRAPTRAN and GENFLO comes from the system code. In the future, models now performing in parallel will be unified.

In the coupled code, FRAPTRAN is the master code calling GENFLO which provides the thermal-hydraulic conditions for the whole channel. This calculation is performed only once for each time step, even if a number of iterations would be done in FRAPTRAN during the time step. In the beginning, there is a need from GENFLO for a steady state calculation before any coupled code calculation. In the coupled code calculation, the FRAPTRAN code dictates the length of the time step. A typical time step is short, 0.01 to 0.05 seconds. Even with such short steps, the actual FRAPTRAN-GENFLO calculation is not time-consuming because of the non-iterative feature and effective numerical methods for the fast running thermal-hydraulics module.

The system behavior and boundary conditions needed for detailed core simulation and studying the fuel rod behavior with FRAPTRAN-GENFLO may be calculated with various system codes such as RELAP5 or others. The results of the analyses of the three-dimensional pressurized-water reactor (PWR) or BWR reactor dynamics codes TRAB-3D and the simulator APROS have been used by STUK/VTT. The data exchange between a system code, GENFLO, and FRAPTRAN is illustrated in Figure 5. At present, the boundary conditions for GENFLO from the system code are the mass flow and enthalpy at the channel inlet, the coolant pressure at the top of the channel, and the total power and power profile of the fuel rod.

The GENFLO model is being evaluated to supplement the selection of transient heat transfer models available to FRAPTRAN. Although GENFLO has been tested in different surroundings,[a] the coupled FRAPTRAN-GENFLO code will need some verification, including comparisons against the existing thermal-hydraulic models used by FRAPTRAN.

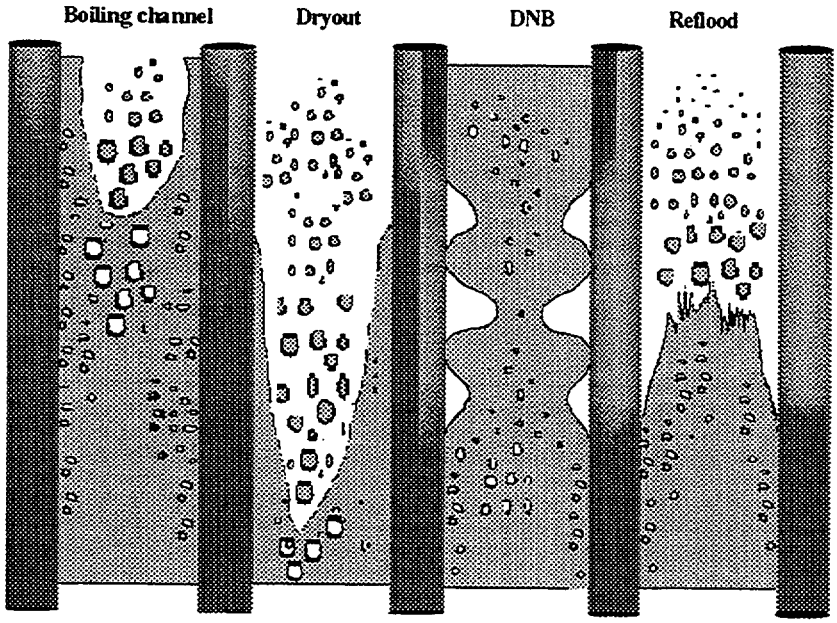

FIGURE 4. The channel flow modes in GENFLO

a) The GENFLO code is being used in two other applications in addition to FRAPTRAN. First, in the code RECRIT (Miettinen et al. 2000), GENFLO is coupled with the two-dimensional transient neutronics model TWODIN. RECRIT has been used for analysing recriticality incidents for BWRs under conditions where the control rods have melted at high temperatures but after core cooling has been recovered. Because the thermal-hydraulic solution of GENFLO has been included in the RECRIT code, the validation of RECRIT also supports the GENFLO thermal-hydraulics. The validation cases for the RECRIT code include ERSEC, ACHILLES, REWET-II, GÖTA, FLECHT and QUENCH experiments. For this case, a whole BWR vessel has been modelled for GENFLO. Second, in the APROS-SA application, GENFLO is used to calculate the PWR pressure vessel thermal-hydraulics during a severe accident until core melting, relocation, and pool generation at the bottom of the reactor vessel is simulated.

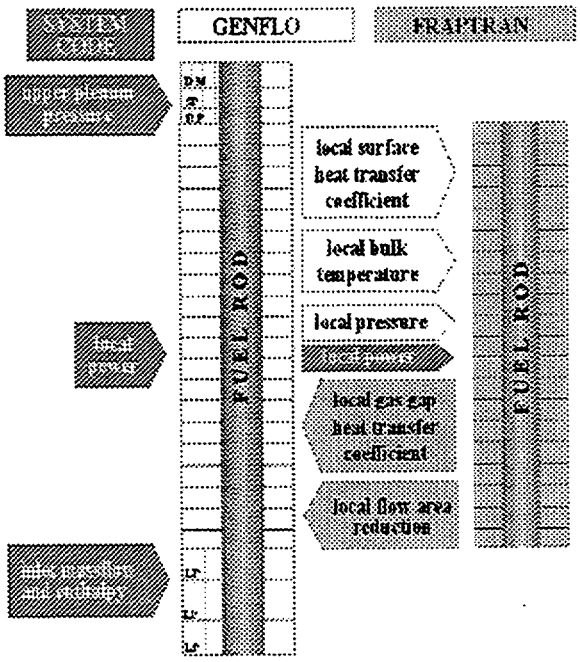

FIGURE 5. Data exchange between the system code, GENFLO and FRAPTRAN.

TWO EXAMPLE CALCULATIONS USING FRAPTRAN-GENFLO

The first example using FRAPTRAN-GENFLO is for fuel behavior during a hypothetical large break LOCA (LBLOCA) at the Loviisa VVER-440 power plant. The engineering simulator APROS has been used to generate LBLOCA analyses. The thermal-hydraulic boundary conditions, as well as geometry and safety factors used in hot channel analyses of the LBLOCA have been averaged for one sub-channel and then used as input for FRAPTRAN-GENFLO. The initiating event for the transient is a double-ended break between the pressure vessel and the reactor coolant pump in one of the six cold legs. The LBLOCA transient is assumed to occur at beginning-of-life when the fuel has no significant burnup. As a comparison to the effects of using GENFLO thermal-hydraulics with FRAPTRAN, the same case was calculated by FRAPTRAN using a simple built-in coolant model ("separate" calculation).

In the transient, the fuel rod temperatures increase in the nearly dry core until injection from the emergency core cooling system quenches the core. Besides the high and low pressure safety injection, as simulated in the APROS calculation, two hydro accumulators start an injection to the downcomer. The other two accumulators, injecting to the upper plenum, are not operating in this transient.

A reactor trip immediately follows the pipe break. Due to the large break flow, coolant pressure decreases quickly and the core is uncovered. In this situation, the small flow to the hot channel is voided and is occasionally reversed. The real physical oscillation of inlet flow is difficult to separate from the numerical

one calculated by APROS. To eliminate the fastest numerical frequencies, the channel inlet mass flow and enthalpy results have been filtered to provide a simpler history for GENFLO. The effects of filtering are seen in differences in the inlet liquid mass flow in Figure 6 between the GENFLO and APROS curves. Another reason for using filtering was the decision to calculate the same transient with the standard FRAPTRAN, which does not accept reversed flow.[b]

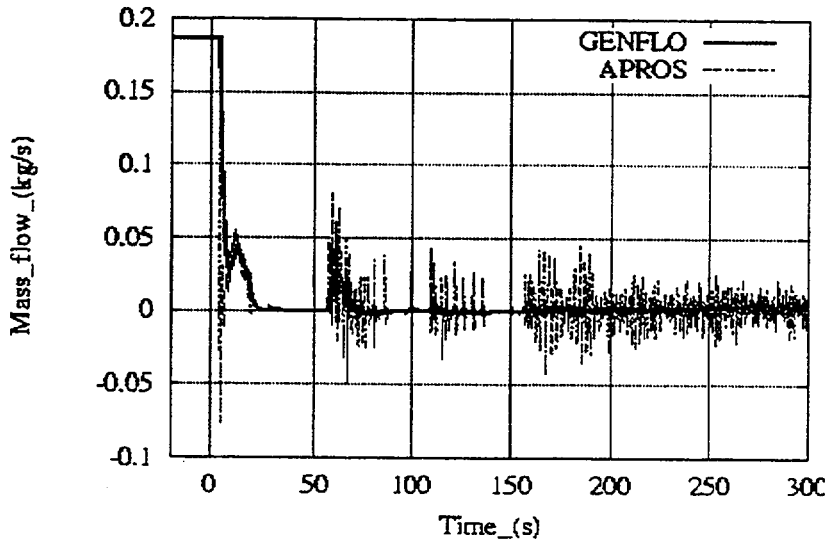

FIGURE 6. Inlet liquid flow at bottom of channel for LOCA example

At the beginning of the transient, the fuel temperature quickly drops because of the power decrease, as shown in Figure 7 (0-10s). Later, due to the loss of coolant inventory, the fuel temperature starts increasing (~25s). The coupled code suggests that even a small amount of water in the channel inlet after 60s is sufficient to first stop the temperature increase and then to temporarily decrease the temperatures.

At about 150s into the transient, the average void fraction is at its maximum with the water level at its minimum. The fuel temperatures increase and the quench front of the hydraulic channel drops until 200s at which time the quench front starts to rise again. At the time of maximum temperature, there is a quite sharp transition from one flow regime to another.

The FRAPTRAN-GENFLO and FRAPTRAN calculations assume similar enthalpy values, even though for the separate FRAPTRAN calculation the enthalpy of the inlet flow may be unrealistic at the time of flow reversal.

---

b) The coolant enthalpy model of FRAPTRAN was considered able to give the best possibility for a comparison with results not strongly dependent on the properties of an external thermal-hydraulic code. The raw transient data has to be slightly modified by filtering in order to avoid possible instantaneous coolant reverse flow, which could not be handled by the FRAPTRAN coolant enthalpy model. Hence, the comparison case is not completely realistic in all details, but it is a test and an indication of the capabilities of the models and also serves as a tool for revealing deficiencies or necessary improvements in the models.

The results from the separate FRAPTRAN and FRAPTRAN-GENFLO calculations are quite similar until the steam supply starts. The bulk coolant temperature significantly increases due to high enthalpy values in the separate FRAPTRAN calculation. There are also corresponding differences in the heat transfer coefficients, rod temperatures and cladding deformation. Used separately, FRAPTRAN predicts that the clad starts ballooning at the time of the highest cladding temperatures. This is shown in Figure 8 by the decreasing plenum gas pressure at 150s. The internal pressure of the rod is seen to undergo rapid changes and then equals the channel pressure when the rod fails at about 250s (Figure 8). In contrast, no cladding ballooning or rod failure is predicted to occur by FRAPTRAN-GENFLO.

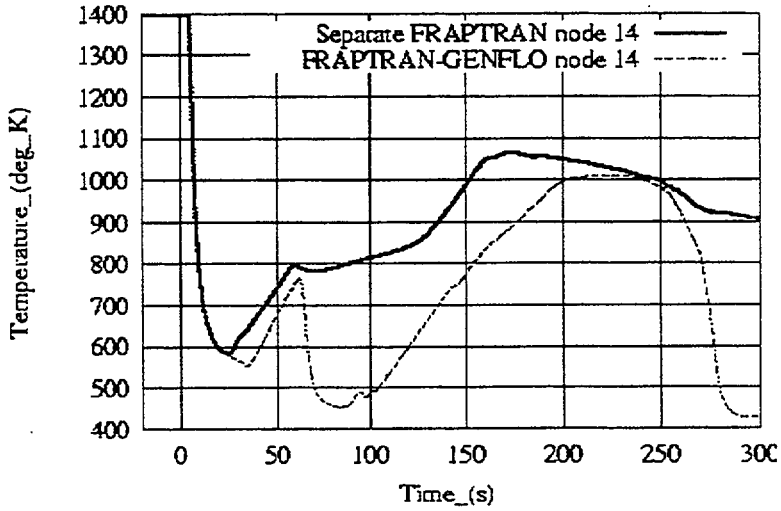

FIGURE 7. Fuel centerline temperature at level 14 / 20.

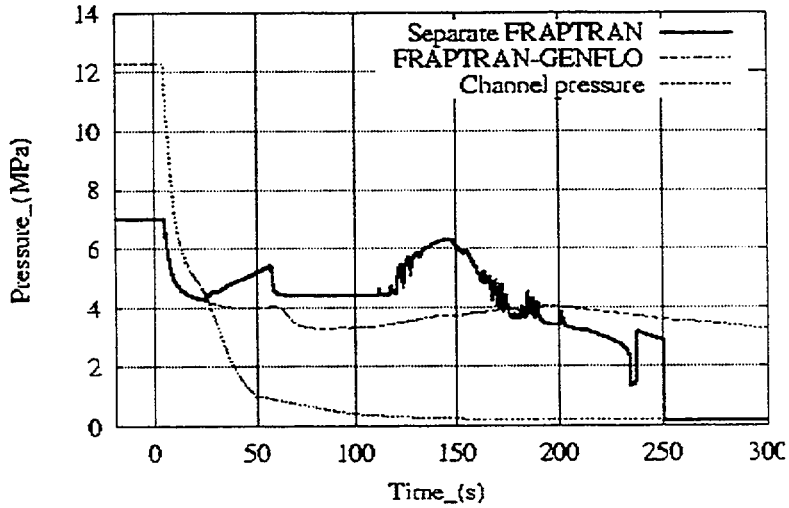

FIGURE 8. Channel pressure and rod plenum gas pressure

The second example calculation for FRAPTRAN-GENFLO is for an ATWS at a BWR plant. The basis for the analysis is an oscillation incident in the Finnish Olkiluoto 1 BWR during reactor startup on February 22, 1987. The incident was safely terminated by normal operation of the reactor safety systems. The incident was analyzed by STUK (Valtonen 1989) and simulated with the Finnish TRAB-3D code (Daavittila et al. 2000). The results of the TRAB-3D calculation agree with measurements and earlier analyses. The oscillation frequency and the phase shift between the inlet and outlet flows in a channel of high relative power show good consistency, as do the out-of-phase oscillation of mass flows between high power channels and the core by-pass channel.

To test the performance of the new model combination, the case was hypothetically extended assuming no actions of the safety system. The transient was recalculated with TRAB-3D as an ATWS case. The escalating oscillation phase of this calculation was chosen as a subject of further study in this FRAPTRAN-GENFLO analysis. The oscillations of boundary conditions were artificially continued in time and amplified. The total power in the hot assembly calculations with TRAB was multiplied by a factor of 1.3 for the hot rod analysis with FRAPTRAN-GENFLO. Also, the oscillating power was given a minimum value. Shown in Figure 9 is the boundary condition of the channel inlet mass flow. The flow rate oscillation finally leads to temporary flow reversals (negative mass flow).

A continuously changing axial power profile was created to match the TRAB-3D calculations. The axial power profile was dynamically changed in GENFLO. For FRAPTRAN, an average profile was used. Contrary to the original TRAB-3D calculation, high burnup fuel was assumed with a value of 62.3 MWd/kgU. The frequencies of oscillations of boundary conditions were according to the TRAB-3D calculations.

The results of the FRAPTRAN-GENFLO calculations for this BWR instability case show that with a power cycle period of about 2s the fuel rod remains covered with water until the time of flow reversal. Then the quench front starts dropping in the channel. Before the flow reversal, only local or temporary dryout or DNB conditions may be achieved. The flow reversal soon leads to high cladding temperatures at the upper part of the fuel rod (1682K). On the other hand, the highest fuel temperatures occur at the lower part of the rod (2729K), where the linear power is higher. The temperature profiles are shown in Figures 10, 11, and 12. At the end of the calculation the cladding is quite soft and in contact with the fuel pellet (PCMI, pellet-to-cladding mechanical interaction). The plenum gas pressure remains below the fluid channel pressure during the whole transient, and no rod failure is predicted in spite of the fast deformation of the fuel rod (Figure 13). This result may be partially due to FRAPTRAN not having a transient fission gas release model.

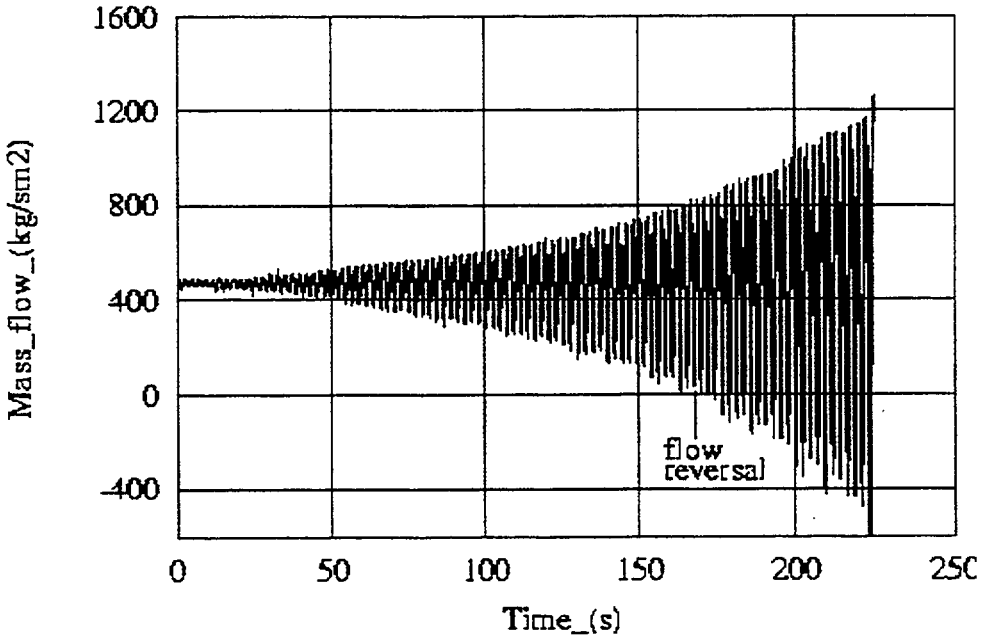

FIGURE 9. The mass flow rate boundary condition at channel inlet in hypothetical BWR instability case

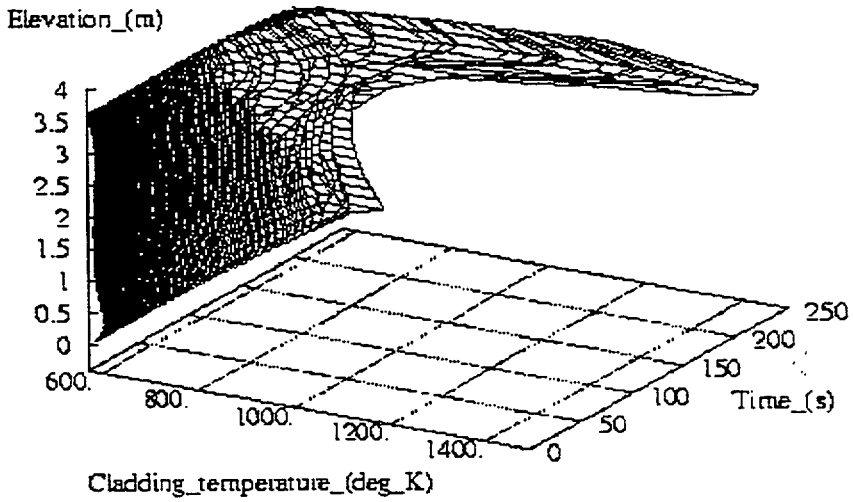

FIGURE 10. Cladding surface temperature profile in hypothetical BWR instability case

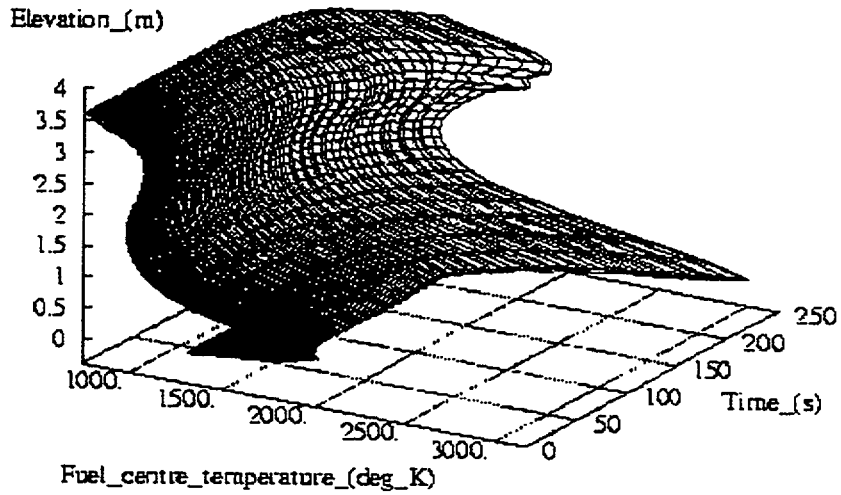

FIGURE 11. Fuel center temperature profile in hypothetical BWR instability case

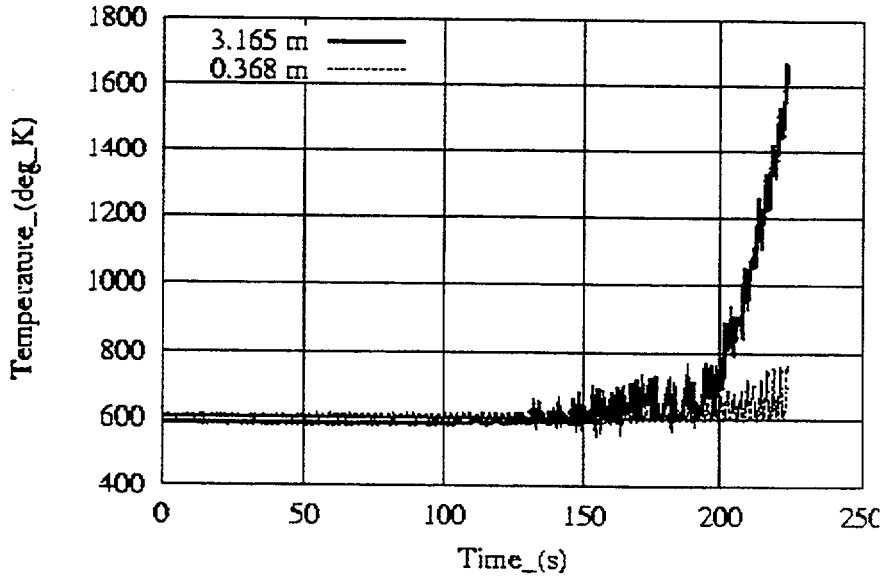

FIGURE 12. Cladding temperature in BWR instability case

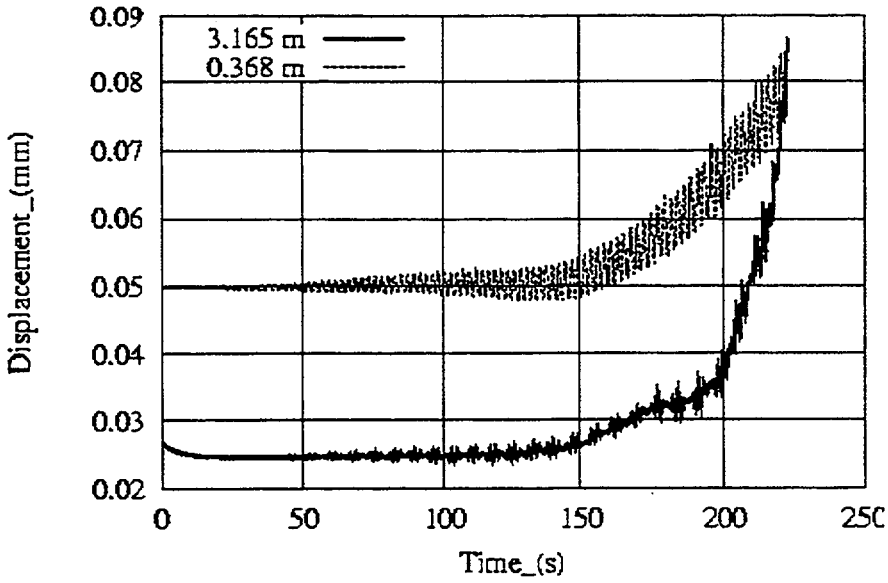

FIGURE 13. Displacement of cladding outer surface in BWR instability case

FRAPTRAN-GENFLO is proving to be a proper tool for studying oscillation phenomena in a single subchannel, although continuation of the oscillation in real geometry may be very different from the oscillations assumed for this example. Another result from this study is that the critical heat flux correlations in GENFLO need further review.

DISCUSSION

The coupling of the FRAPTRAN and GENFLO codes demonstrates a direction to proceed with more detailed thermal-hydraulic description in fuel transient analyses where coupling of coolant and fuel rod mechanical behavior is important. The results of the two examples illustrate that the coupling is successful and can result in different predicted fuel behavior than using FRAPTRAN alone. To build on this preliminary work, modifications and improvements to both codes have been identified and are being planned.

In order to benefit from the more detailed thermal-hydraulic input available from GENFLO, FRAPTRAN needs modifications to enable it to take advantage of accepting dynamic axial power and pressure profiles. Also, an increasing number of the system code calculations are now providing dynamic power profiles from 1 and 3-dimensional neutronics calculations in the core.

Some features already present in GENFLO are not enabled in the FRAPTRAN-GENFLO application. Examples include the flexible hydraulic channel geometry in GENFLO due to ballooning and an option to use more than one subchannel in a single run. Further, some GENFLO models, like departure from nucleate boiling (DNB) and critical power ratio (CPR) correlations, that are suitable for a single hot rod and for BWR instability cases, need additional attention. Presently when using GENFLO, it is necessary to

use the material properties within GENFLO. For consistency, the same material properties, valid to high burnups levels, should be used in both codes.

SUMMARY AND CONCLUSIONS

The FRAPTRAN transient fuel analysis code has been developed by the NRC and is now being made available to the FRAPCON-3 users group. This code has been assessed against a data base that emphasized experiments investigating the effect of burnup on fuel rod behavior during RIA and LOCA transients. FRAPTRAN has been shown to generally perform well in the comparisons to data. An independent peer review of FRAPTRAN also concluded that FRAPTRAN was able to predict the trends in the experimental data and that the code has been assessed against data appropriate for the intended uses of the code.

GENFLO, a thermal-hydraulic subchannel code, has been developed by VTT and has been coupled with FRAPTRAN. Two example cases, a Loviisa LBLOCA and a BWR instability case, have shown that coupling FRAPTRAN with GENFLO can work successfully. The coupling of the codes enables the evaluation and studying of the improvements and changes necessary in both FRAPTRAN and GENFLO, and further features may be inserted easily. Several improvements for both codes have been introduced.

For the LBLOCA case, no cladding ballooning was predicted with the coupled code. In contrast, the separate FRAPTRAN calculation predicted cladding ballooning and rod failure because of unrealistic calculated coolant boundary conditions. For the BWR instability case, the calculation shows that with small cycle times the channel is wetted and rod failure does not occur until flow reversal. More analyses using variations in assumed rod design, power, and boundary conditions are needed for greater understanding of both example cases.

The results of the example cases show that GENFLO can be used as a thermal-hydraulic model for FRAPTRAN. From these two cases, it may be concluded that FRAPTRAN-GENFLO may be effectively used for single fuel rod and subchannel analyses where coupling of coolant and fuel rod mechanical behavior is important. The results of this first version of the coupled code are encouraging and support further development in conjunction with careful validation against experimental data.

REFERENCES

Berna, G.A., et al. 1997. *FRAPCON-3: A Computer Code for the Calculation of Steady-State, Thermal-Mechanical Behavior of Oxide Fuel Rods for High Burnup.* NUREG/CR-6534 (PNNL-11513), Vol. 2, Pacific Northwest National Laboratory, Richland, Washington.

Cunningham, M.E., et al. 2001a. *FRAPTRAN: A Computer Code for the Transient Analysis of Oxide Fuel Rods.* NUREG/CR-6739 (PNNL-13576), Vol. 1. Pacific Northwest National Laboratory, Richland, Washington.

Cunningham, M.E., et al. 2001b. *FRAPTRAN: Integral Assessment.* NUREG/CR-6739 (PNNL-13576), Vol. 2. Pacific Northwest National Laboratory, Richland, Washington.

Daavittila, A, E. Kaloinen, R. Kyrki-Rajamäki, and H. Räty. 2000. *Validation of TRAB-3D Against Real BWR Plant Transients*. Proceedings of International Meeting on "Best-Estimate" Methods in Nuclear Installation Safety Analysis (BE-2000), November 2000, Washington, DC.

Fuketa, T., T. Nakamura, and K. Ishigima. 1998. "The Status of the RIA Test Program in the NSRR," in Proceedings of *Twenty-Fifth Water Reactor Safety Information Meeting,* NUREG/CP-0162, Volume 2. U.S. Nuclear Regulatory Commission, Washington, D.C.

Miettinen, J., and A. Hämäläinen. 2000. *Development and Validation of the Fast Running Thermohydraulic Model SMABRE for Simulator Purposes.* Proceedings of ICONE 8, 8th International Conference on Nuclear Engineering, 2-6 April 2000, Baltimore, MD USA.

Miettinen, J., F. Hoejerub, W. Frid, and I. Lindholm. 2000. *RECRIT Code for BWR Recriticality Analysis*. Proceedings of ICONE 8, 8th International Conference on Nuclear Engineering. 2-6 April 2000. Baltimore, MD USA.

Papin, J., and F. Schmitz. 1998. "The Status of the CABRI REP-Na Test Programme: Present Understanding and Still Pending Questions," in Proceedings of *Twenty-Fifth Water Reactor Safety Information Meeting,* NUREG/CP-0162, Volume 2. U.S. Nuclear Regulatory Commission, Washington, D.C.

Uchida, M., and M. Ichikawa. 1980. "In-Pile Diameter Measurement of Light Water Reactor Test Fuel Rods for Assessment of Pellet-Cladding Mechanical Interaction." *Nuclear Technology,* 51(1980)33-44.

Valtonen, K. , 1989. *BWR stability analysis*. Finnish Centre for Radiation and Nuclear Safety STUK-A-88, Helsinki, Finland.

Wilson, C.L., et al. 1983. *LOCA Simulation in NRU Program: Data Report for the Fourth Materials Experiment (MT-4).* NUREG/CR-3272 (PNL-4669), Pacific Northwest National Laboratory, Richland, Washington.

PULSE WIDTH DURING A PWR ROD EJECTION ACCIDENT

D.J. Diamond, B. Bromley, and A. Aronson
Brookhaven National Laboratory

ABSTRACT

An analysis of pulse width during a rod ejection accident was carried out to help in designing experiments to test fuel behavior under reactivity initiated accident conditions. The analysis primarily used calculations based on a three-dimensional neutron kinetics code, PARCS and a model of a pressurized water reactor at both beginning and end of a fuel cycle. Results showed that pulse width varied inversely with the maximum increase in local fuel enthalpy and this is consistent with simple analytical models. The pulse width ranges from 25 to 100 ms for cases where the energy deposition goes from 30 to 10 cal/g. This is the range expected for the most likely REA as the probability of a particular rod worth increases as one goes to smaller rod worths above prompt-critical. The pulse width is 10-15 ms when the maximum increase in fuel enthalpy is in the range of 60-100 cal/g. It is at these enthalpies, or higher, where fuel failure might be expected. Hence, if tests are to be done to test the limits of a fuel pin, the pulse width in the tests should be in the range 10-15 ms. If the tests instead were done with pulse widths that are greater than 25 ms and fuel enthalpies that are in the range where failure is expected, e.g., 100 cal/g, there is an inconsistency.

INTRODUCTION

This study is part of a U.S. Nuclear Regulatory Commission (NRC) program to understand the consequences of reactivity accidents, especially for fuel with high burnups, and to define new acceptance criteria for these events. The work at Brookhaven National Laboratory (BNL) has focused on analytical studies of the neutronics and thermal-hydraulics during a rod ejection accident (REA) in a pressurized water reactor (PWR). Of particular interest have been: 1) parametric studies to determine what influences the increase in local fuel enthalpy (pellet radial average), 2) the uncertainty in fuel enthalpy, and 3) the characteristics of the power trace during the REA. The parametric studies have considered the ejected rod worth, delayed neutron fraction, fuel specific heat, initial power level, time during the fuel cycle, pellet power distribution, and location of the ejected rod. The study of uncertainty showed that the uncertainty in these parameters leads to a large uncertainty in calculated fuel enthalpy.

In the present study it is the pulse width of the REA power pulse that is of interest to assure that corresponding experimental programs are designed with conditions that come as close as

possible to those expected during the accident. Power pulses can be shaped by varying the pulse height and width (within limits) in the experimental programs in France, at the Cabri test reactor, and in Japan, at the NSRR test reactor.

In the following section, the calculational methodology, both reactor code and reactor model, are explained. The next section contains a discussion of results. It is broken into two subsections; in the first, results of calculations of the REA are explained whereas in the second, the connection to analytical results is explained. At the end, conclusions are given.

CALCULATIONAL METHODOLOGY

The PARCS (Purdue Advanced Reactor Core Simulator) code (Version 1.05) [1] was used with a model of the TMI-1 core [2]. PARCS is a three-dimensional, two-group diffusion theory code using nodal methods. It has been coupled to the thermal-hydraulics codes RELAP5 and TRAC-M but for the present study a stand-alone version was used which incorporates a simpler thermal-hydraulics model. It was confirmed, by doing sample comparisons, that this model provides the same level of accuracy for an REA calculation as use of PARCS/RELAP5. This occurs because the difference in codes is primarily in fluid dynamics models which do not have a strong impact on the REA.

Some of the design and operational parameters of the TMI-1 core model at end-of cycle (EOC), as well as the nodalization in PARCS are given in Table 1. Figure 1 is the core layout showing the 177 fuel assemblies and the positions of Control Banks 1-8. There are four radial neutronic nodes per fuel or reflector assembly, giving a total of 964 radial nodes. There are 28 axial neutronic nodes. There is one thermal-hydraulic channel node per fuel assembly. Banks 1, 2, 3, and 4 are safety banks that are inserted to shut down the reactor in the event of a reactor trip or a planned shutdown. Banks 5, 6, and 7 are regulating banks that are used to adjust the power level. Bank 8 contains axial power-shaping rods (APSRs). For the present analysis of a rod ejection accident (REA), the control rod assembly in the center of the core, 7A, is ejected.

For beginning-of-cycle (BOC) calculations the only parameters in Table 1 that change are the delayed neutron fraction (which becomes 0.006323), the boron concentration (1700 ppm) and the initial position of Bank 8 which is partially inserted to 291.3 steps.

The version of PARCS in use for the analysis of the TMI-1 core makes use of a table look-up method for obtaining macroscopic cross section data in two energy groups at various fuel temperatures, moderator densities, and boron concentrations within fuel assemblies of a specified composition. The core is modeled with 438 different compositions for unrodded fuel assemblies, and a smaller number of compositions for rodded fuel assemblies. Each composition represents the effect of fuel design, burnable poison history, burnup and moderator density history. The cross section data were generated using the CASMO™ lattice physics code. The preparation and format of the cross section data for the macroscopic cross section data file at BOC differ somewhat from that at EOC. The data at EOC is generated for a specific boron concentration (5

ppm), and the assembly discontinuity factors are directly incorporated into the values of the cross sections. The data at BOC is generated for two values of boron concentration (5 ppm and 2000 ppm), and the assembly discontinuity factors are separated from the cross section data providing a more accurate model.

Table 1 Specifications for the PARCS Model for TMI-1

Fuel Cycle	EOC
Full Power Level (FP)	2772 MWth
Hot Zero Power (HZP) Level	1.0E-4 % FP
Number of Fuel Assemblies (FA)	177
Number of Reflector Assemblies	64
Fuel Assembly Size and Pitch	21.8 cm
Active Core Height	357.1 cm
Thickness of Reflector	21.8 cm
Position of Fully Inserted Control Rod Relative to Bottom of Reflector	36.2 cm
Step Size for Control Rods	0.353 cm
Delayed Neutron Fraction (Beta)	0.005211
Number of Delayed Groups	6
Boron Concentration	5 ppm
Inlet Coolant Temperature	278°C
Inlet Coolant Flow per Fuel Assembly	89.5 kg/s
Number of Radial Neutronic Nodes	964
Number of Axial Neutronic Nodes	28 (26 core, 2 reflectors)
Number of Radial TH Nodes	177 (core only)
Number of Axial TH Nodes	26 (core only)
Initial Position for Banks 1 to 4	Withdrawn (971 steps)
Initial Position for Banks 5,6,7	Inserted (0 steps)
Initial Position for Bank 8 (APSR)	Withdrawn (971 steps)

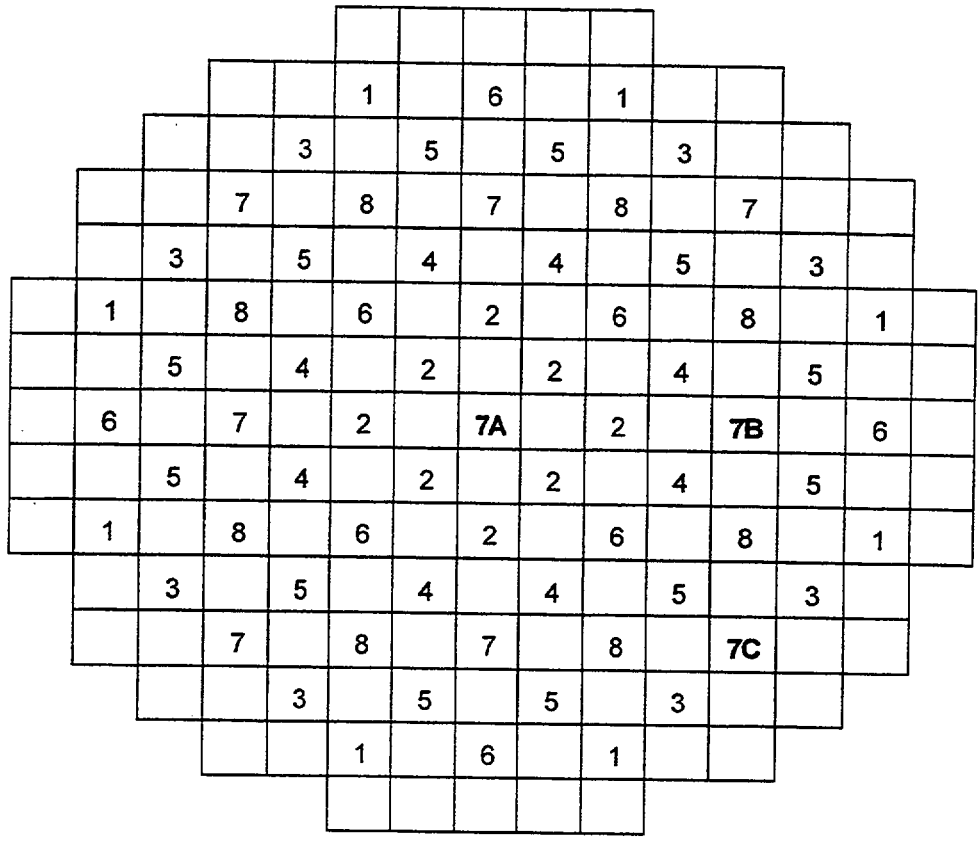

Figure 1 Radial arrangement of control rod banks in TMI-1 PWR core

The REA is calculated assuming the central rod moves out of the core in 100 ms. The reactor is set to trip when it reaches 112% of full power with a delay of 400 ms between the trip signal and the beginning of the insertion of shutdown control banks 1-4. The shutdown banks are inserted at a constant rate, and take 2.2 s to be fully inserted into the core. There is a lower trip setpoint that is set administratively during startup. However, in licensing analysis this trip is ignored since the excore calibration could be from the previous cycle and therefore, inaccurate.

The core configuration at EOC and BOC result in a rod worth for rod 7A of ~\$0.66 and ~\$0.39 respectively at HZP. These control rod worths lead to REAs that are below prompt-critical. The goal is to study REA events above prompt critical (\$1) caused by distorted xenon distributions or non-standard control rod configurations. To allow for high rod worths, the worth of rod 7A is adjusted by changing the macroscopic absorption (Σ_a) and fission yield ($\upsilon\Sigma_f$) cross sections in the central fuel assembly when rod 7A is inserted or removed respectively.

DISCUSSION OF RESULTS

REA Calculations

Before considering pulse widths, consider the general characteristics of the REA. Figure 2 shows the power trace from an REA at both BOC and EOC beginning from HZP. The rod worth is approximately the same ($1.2) in both cases but the traces are different due to the differences in the core in each case. The corresponding reactivity traces are given in Figure 3. The noticeable difference in the period after one second is due to the fact that the different axial power distributions result in different worths for the shutdown banks as a function of distance inserted into the core. The maximum local fuel enthalpy for the two cases is given in Figure 4 and reflects the differences in the power traces and the fact that the BOC core has fuel assemblies with lower burnup and the potential for higher energy deposition during the event.

The maximum local enthalpy depends strongly on the ejected rod worth. This can be seen in Figure 5 which was obtained by doing parametric studies varying the worth of control rod 7A and the delayed neutron fraction. For each transient simulation of a given rod worth and delayed neutron fraction, there would be an associated increase in fuel pellet enthalpy which is plotted on Figure 5 where the rod worth rho (minus delayed neutron fraction beta) is in absolute units. Most values at EOC fall on a single curve almost linear with rod worth. As seen for the single case in Figure 4, the BOC trace is at higher fuel enthalpies relative to the EOC trace.

The variations of the full-width-at-half-maximum (FWHM) power pulse widths for various REA events at EOC and BOC are shown in Figures 6 and 7. The FWHM is based on total reactor power but has been shown to be equal to that found in individual assemblies. The difference between the two figures is the use of $ units for rod worth in Figure 6 and absolute units in Figure 7. According to Figure 6 the pulse width tends to have an inverse relationship with the rod worth, and goes down with increasing delayed neutron fraction. The pulse width is even lower at BOC than at EOC for a given rod worth. According to Figure 7, all the data points at EOC for various rod worths and delayed neutron fractions collapse onto a single curve when the pulse width is plotted against the absolute difference between the rod worth and the delayed neutron fraction. The pulse width has an inverse relationship with the reactivity in excess of prompt critical.

Since the maximum fuel pellet enthalpy rise is proportional to the absolute reactivity (see Figure 5), it is expected that the pulse width also tends to be inversely proportional to the fuel enthalpy rise. This can be seen in Figure 8 which shows pulse width vs the maximum change in fuel enthalpy, i.e., the maximum specific energy depostion. The pulse width for a given enthalpy rise tends to be slightly lower at BOC than at EOC. For an enthalpy rise of more than 40 cal/g, the FWHM pulse width is less than 20 ms.

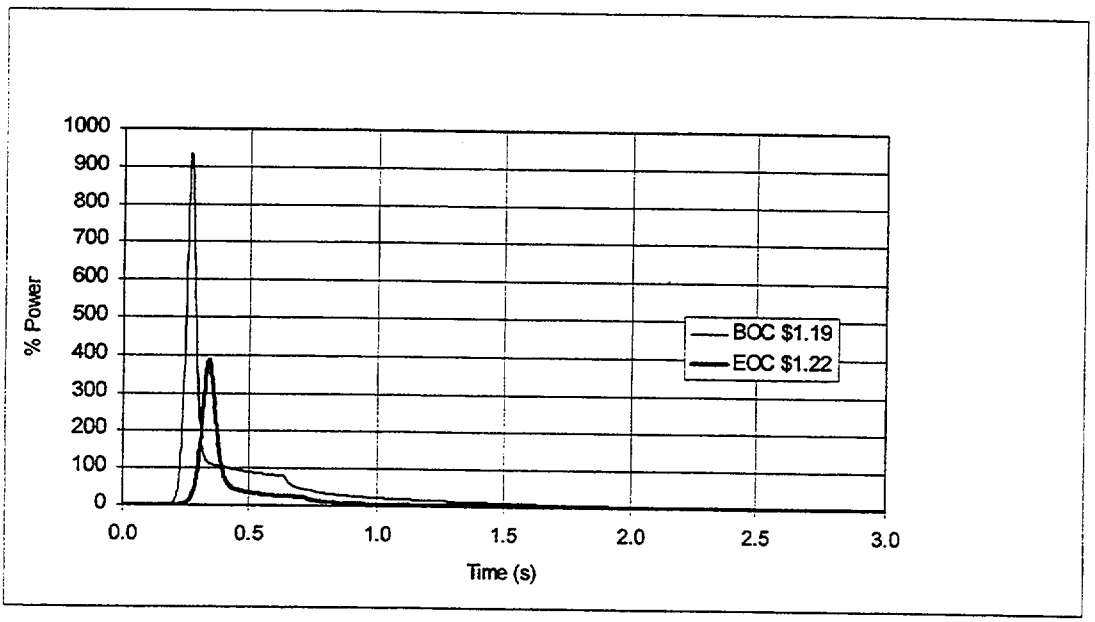

Figure 2 Power Transients for REA from HZP

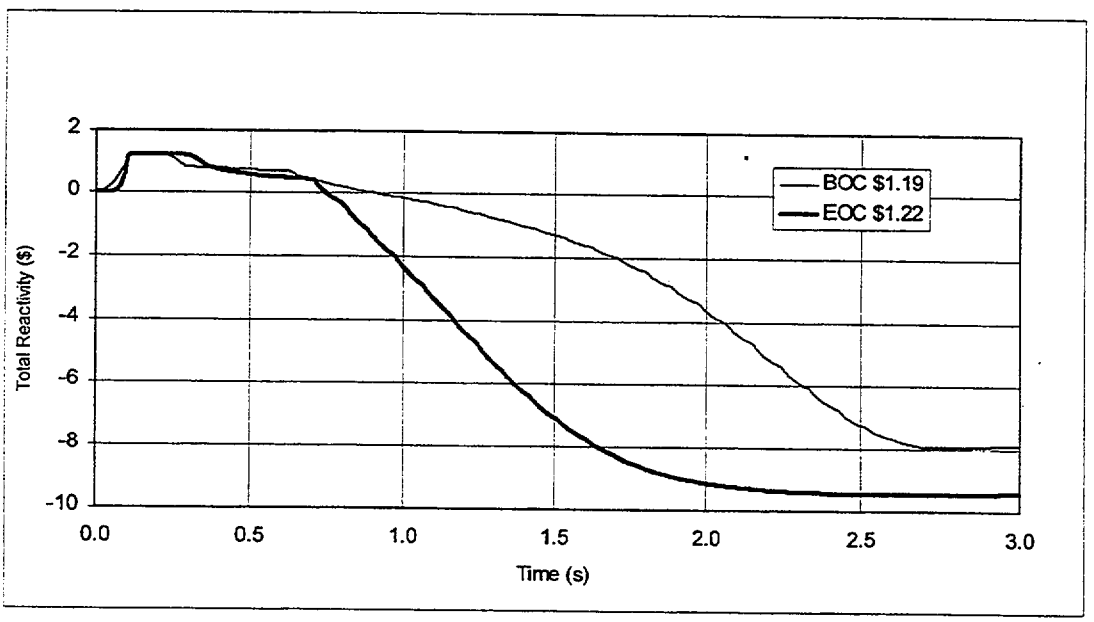

Figure3 Reactivity Transients for REA from HZP

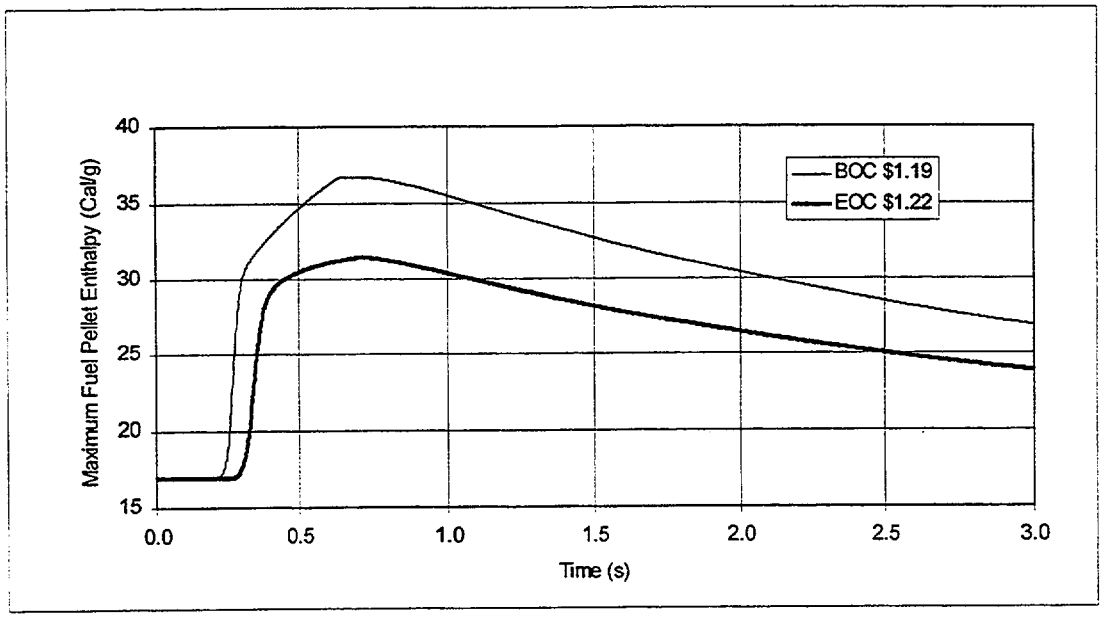

Figure 4 Maximum fuel pellet enthalpy for REA from HZP

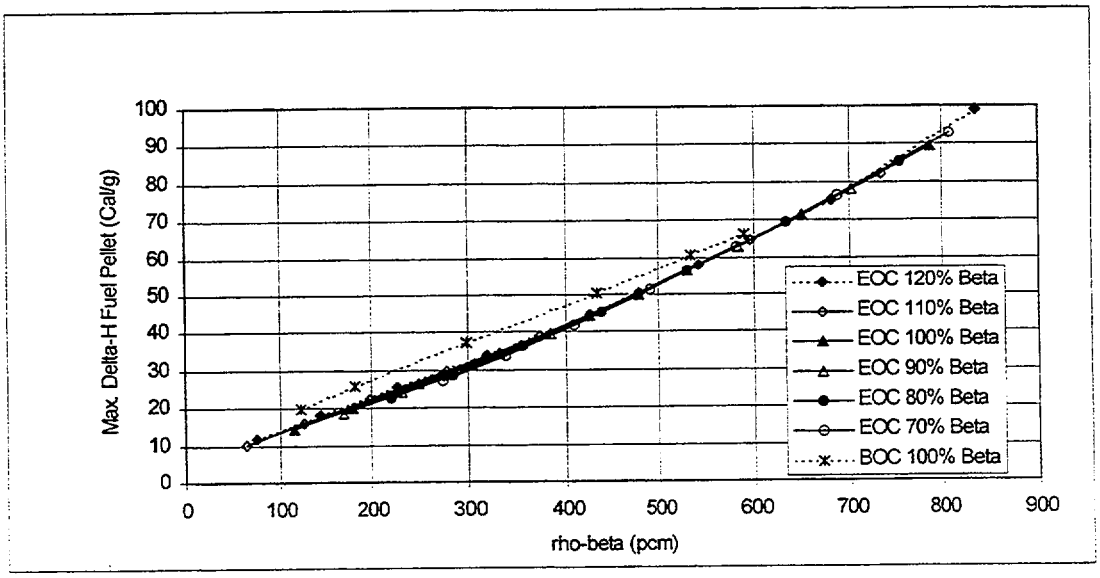

Figure 5 Maximum rise in fuel pellet enthalpy for REA from HZP

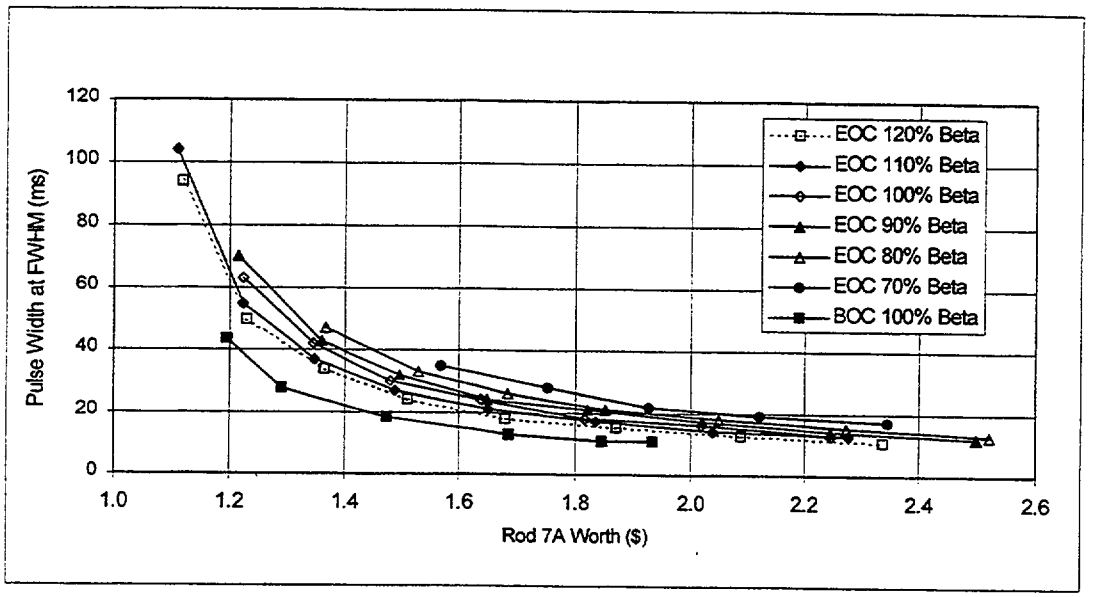

Figure 6 Pulse width at FWHM for REA from HZP

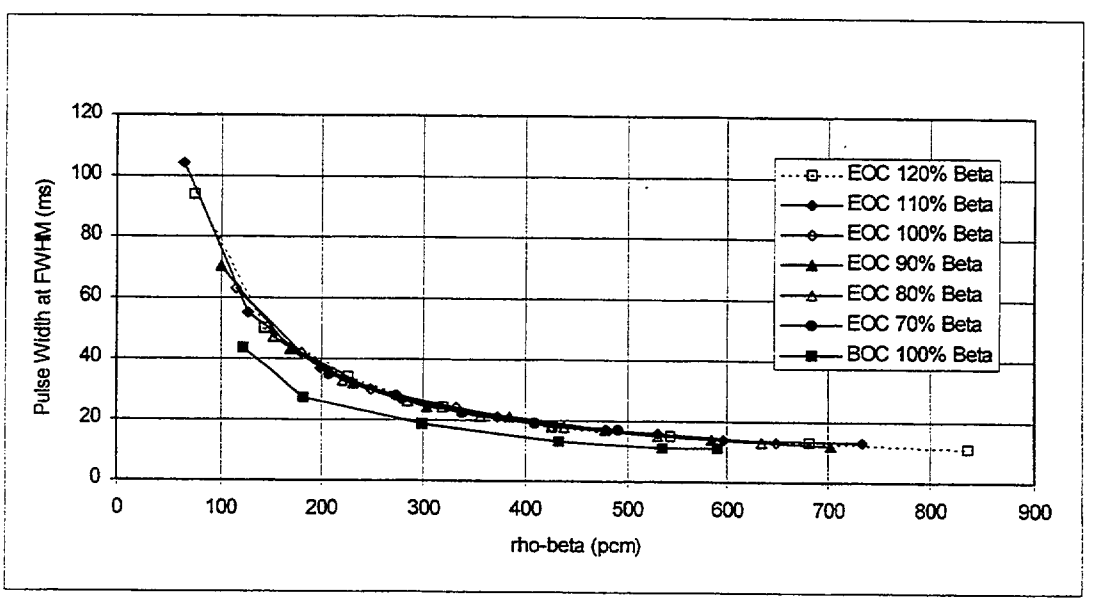

Figure 7 Pulse width at FWHM for REA from HZP

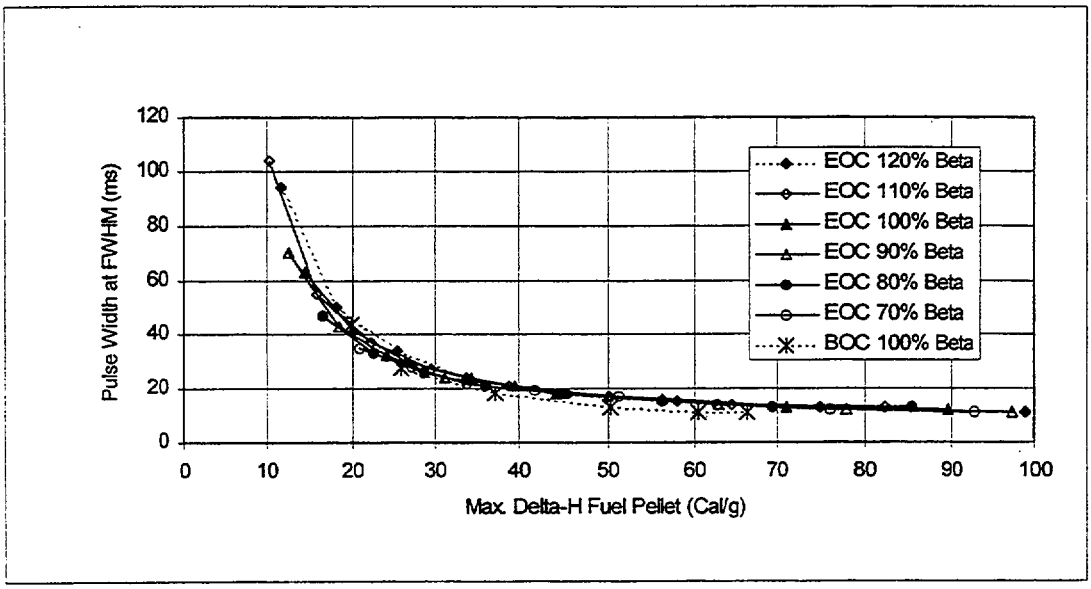

Figure 8 Pulse width versus maximum change in local fuel enthalpy

Analytical Results

The Nordheim-Fuchs zero-dimensional adiabatic model [3] gives an analytical estimate of the results of a super-prompt-critical power excursion. It is based on the point-kinetics model and applicable to a step insertion of reactivity and a linear negative temperature feedback on the reactivity. Although it is a very simple model, it is useful to consider because it can be used to understand results obtained from more sophisticated models such as PARCS.

According to the Nordheim-Fuchs model, the maximum specific power during a super-prompt-critical transient which is terminated by temperature feedback is given by:

$$P_{\max} = \frac{(\rho_0 - \beta)^2 c_p}{2 \alpha \ell} \tag{1}$$

The parameters ρ_o, β, c_p, α, and l are the step reactivity change, the delayed neutron fraction, the fuel heat capacity, the absolute value of the negative reactivity temperature coefficient, and the neutron lifetime respectively.

The specific energy deposition in the fuel during the pulse is given by:

$$E = \frac{2(\rho_0 - \beta) c_p}{\alpha} \tag{2}$$

The pulse width at FWHM is given by either of the following

$$\tau = \frac{3.535\,\ell}{(\rho_0 - \beta)} \tag{3}$$

$$\tau = \frac{7.07\,\ell\,c_p}{E} \tag{4}$$

These relationships are approximately valid when discussing the REA. As can be seen in Figure 5 the energy deposited (the increase in fuel enthalpy) is indeed proportional to (ρ-β) as specified by Equation 3.2). Note that this relationship is valid even though Figure 5 is a plot of the energy deposition at a particular location in the core rather than the total energy deposition as specified in Equation 2. Note too that the simplistic model is approximately valid in spite of the fact that the power pulse in an REA is not completely terminated, i.e., the power has a tail which adds to the energy deposited during the initial pulse.

The previous results for pulse width shown in Figures 7 and 8 also fit with the simple model and Equations 3 and 4, respectively. Note again that these relationships are valid in spite of the fact that the energy deposition plotted is a local rather than global quantity. The global parameters in the simple model (c_p, α, and ℓ) will vary from one reactor core composition and design to the next. Because these parameters at BOC differ from those at EOC, the constants of proportionality relating the pulse width to the energy deposition, and reactivity will change as well.

CONCLUSIONS

The REA analysis done with a sophisticated computer code, PARCS, shows approximately the same trends predicted by simplified analytical models. In particular, with respect to pulse width, it shows that the pulse width is inversely proportional to the maximum energy deposition. Note that this does not mean that you can estimate the energy deposition for an REA from a simple point kinetics model; three-dimensional neutron kinetics are essential for the accurate assessment of local quantities.

From the results of the PARCS calculations, the pulse width ranges from 25 to 100 ms for cases where the energy deposition goes from 30 to 10 cal/g. This is the range expected for the most likely REA as the probability of a particular rod worth increases as one goes to smaller rod worths above prompt-critical. This is because high rod worths require exceptional conditions such as distorted xenon distributions or non-standard control rod patterns.

It is also seen from the results of the PARCS calculations that the pulse width is 10-15 ms when the maximum increase in fuel enthalpy is in the range of 60-100 cal/g. It is at these enthalpies, or higher where fuel failure might be expected. Hence, if tests are to be done to test the limits of a fuel pin, the pulse width in the tests should be in the range 10-15 ms. If the tests instead were done with pulse widths that are greater than 25 ms and fuel enthalpies that are in the range where failure is expected, e.g., 100 cal/g, there is an inconsistency.

REFERENCES

1. H.G. Joo et al., "PARCS: A Multi-Dimensional Two-Group Reactor Kinetics Code Based on the Non-linear Analytic Nodal Method," PU/NE-98-26, Purdue University, School of Nuclear Engineering, September 1998.

2. K.N. Ivanov et al., "PWR Main Steam Line Break (MSLB) Benchmark; Volume I: Final Specifications," NEA/NSC/DOC(99)8, U.S. Nuclear Regulatory Commission and OECD Nuclear Energy Agency, April 1999.

3. David L. Hetrick, Dynamics of Nuclear Reactors, American Nuclear Society, La Grange Park, Illinois, U.S.A., Chapter 5, pp. 164-170, 1993.

Revised RIA Criteria for Burnup Extension Applications

Robert Montgomery, ANATECH Corp.
Nicolas Waeckel, Electricite de France
Rosa Yang, EPRI

Abstract

The US nuclear industry through the Robust Fuel Program Working Group 2 is developing for NRC review a set of revised regulatory acceptance criteria for use in the safety analysis of the hot-zero power (HZP) and hot-full power (HFP) Reactivity Initiated Accidents (RIA) in Pressurized Water Reactors (PWRs) and Boiling Water Reactors (BWRs). For PWRs, the postulated control rod ejection accident (REA) is the primary RIA event considered in the industry evaluation. For BWRs, the postulated control rod drop accident (CRDA) is the primary RIA event considered in the industry evaluation. The development of revised RIA regulatory acceptance criteria are part of the on-going industry effort to extend fuel rod average burnup levels to 75 GWd/MTU for PWRs and 70 GWD/MTU for BWRs.

The approach to develop the revised criteria used an evaluation methodology that combined both experimental data and analytical calculations to understand the influence of burnup on transient fuel rod behavior during RIA events. Experimental data from RIA-simulation tests on UO_2 test specimens with Zircaloy cladding irradiated to 64 GWd/MTU were used in the evaluation. These technical bases were then translated to PWR REA applications using a state-of-the-art fuel rod behavior analysis code as a means to establish the revised regulatory criteria. The advantage of using a combined analytical and experimental data approach to derive the revised regulatory criteria is that the methodology can be applied to other cladding designs and fuel rod analysis tools to determine application specific criteria, if required.

1.0 Introduction

The goal to achieve higher fuel rod burnup levels has produced considerable interest in the transient response of high burnup fuel. Several experimental programs are currently underway to generate data on the behavior of high burnup fuel under transient conditions representative of Loss-of-Coolant Accidents (LOCA's) and Reactivity Initiated Accidents (RIA's) [Chung et al. 1996; Papin et al.1996; Fuketa et al.1996][1]. Such programs include the RIA simulation experiments performed at the CABRI facility in France and the Nuclear Safety Research Reactor (NSRR) in Japan. The purpose of these programs is to provide data that can be used to develop safety criteria for high burnup level applications and to validate analytical codes for high burnup fuel behavior.

The initial results from RIA-simulation tests on fuel rod segments with burnup levels above 50 GWd/tU, namely CABRI REP Na-1 (1993) and NSRR HBO-1 (1994), raised concerns that the

[1] Reference provided in brackets [ ] are entered in alphabetical order in Section 8.

existing licensing criteria defined in NUREG-0800 may be inappropriate beyond a certain level of burnup. As a consequence, EPRI and the nuclear industry conducted an extensive review and assessment of the observed behavior of high burnup fuel under RIA conditions which was summarized in EPRI TR-106387 [Montgomery and Rashid 1996; Ozer et al. 1996; Montgomery et al. 1997a] The objective of this program was to conduct a detailed analysis of the data obtained from RIA-simulation experiments and to evaluate the applicability of the data to commercial LWR fuel behavior during a REA or CRDA. Major conclusions from the industry assessment are:

- RIA-simulation test conditions are not representative of those expected during a postulated in-reactor REA or CRDA.
- In many cases, the conditions under which the test rods were base-irradiated produced cladding corrosion and hydriding features that were not representative of modern commercial LWR fuel.
- Analytical evaluations and separate effects data are required to understand the key mechanisms operative in RIA-simulation tests and to translate the experimental results to LWR conditions and different cladding materials.
- Loss of cladding ductility due to localized hydrides was the major cause of failure for high burnup test rods during the RIA-simulation tests. The primary effect of burnup is to increase PCMI by gap closure effects such as solid fission product swelling.

Since the publication of EPRI TR-106387, the industry has continued the assessment and evaluation of the burnup impact on the behavior of high burnup fuel during a RIA as newer data becomes available. The newer data continue to confirm the major conclusions summarized above. It is becoming apparent that our understanding of high burnup fuel behavior during a RIA event is sufficient and that most experimental results can be explained satisfactorily by analytical codes.

As a logical next step in the process, the Robust Fuel Program, Working Group 2 representing the nuclear industry, has developed a strategy to resolve the RIA licensing issues raised by the RIA-simulation experiments. The Industry strategy consists of: 1) development of revised RIA regulatory acceptance criteria using experimental data and analysis methods, and 2) development of improved neutron kinetics methods to demonstrate compliance to the revised criteria.

The approach employed to develop the revised regulatory acceptance criteria by the Industry combines elements of experimental results and analytical evaluations to establish a fundamental understanding of fuel behavior during RIA events. The approach includes three major components:

1. Establish the transient behavior of intermediate and high burnup fuel rods using well-characterized RIA simulation tests. The RIA-simulation experiments provide a database of in-pile observations and post-test examinations that can be used to evaluate the phenomena and mechanisms that influence the transient performance of the fuel and cladding.

2. Define the cladding mechanical properties using data from separate effects tests. The database of Zircaloy cladding mechanical properties furnishes insights into the influence of

irradiation damage, hydrogen content and distribution, and temperature on the capability of the cladding to accommodate the pellet loading during an RIA event.

3. Develop RIA Licensing criteria for LWR fuel using an analytical approach based on the FALCON transient fuel behavior code benchmarked using experimental data from the database of RIA-simulation tests.

This comprehensive approach has provided some key results: 1) a mechanistic basis for understanding the key phenomena that are operative in RIA-simulation tests and 2) qualified the use of FALCON for the translation of non-prototypical RIA-experimental results to both LWR conditions and different cladding materials. The technical insights gained from this deterministic evaluation form the basis for developing the proposed revisions to the regulatory criteria used in the licensing analysis of RIA events. The revised regulatory criteria are a combination of the best-estimate technical understandings of transient fuel behavior coupled with conservative assumptions to account for the uncertainties associated with high burnup fuel.

Combined with the NRC Phenomena Identification and Ranking (PIRT) review conducted on the PWR REA event, the technical assessment performed by the industry establishes a strong foundation to develop revised licensing criteria for RIA [Meyer 2001]. The development of additional RIA test data will be slow for the next several years as the CABRI facility is modified and upgraded to include a Water Loop [Papin et al. 2000]. The additional RIA-simulation tests on high burnup fuel rods with advanced cladding alloys planned as part of the International CABRI Water-Loop project and the NSRR test program will provide data at extended burnup and with advanced cladding materials that can be used to confirm the proposed regulatory criteria.

2.0 Regulatory Basis for Reactivity Initiated Accidents

Section 4.2 of NUREG-0800 - Standard Review Plan for the Review of Safety Analysis Reports for Nuclear Power Plants (SRP) specifies two licensing criteria applicable to RIA events: a fuel coolability limit and a fuel rod failure threshold [U. S. Nuclear Regulatory Commission, 1981]. The fuel coolability limit was established to restrict the amount of energy deposition into the fuel rod during an RIA event as a means to preclude fuel melting, fragmentation and dispersal. The fuel rod failure threshold was established to meet the requirements of fission product release during postulated accidents. The regulatory and technical bases for these criteria are outlined below.

2.1 Fuel Coolability Limit (Violent Expulsion of Fuel)

The fuel coolability limit was developed to satisfy regulatory requirements contained in General Design Criteria 28 [10 CFR Part 50 Appendix A]. GDC 28 defined in 10 CFR Part 50 Appendix A specifies that reactivity control systems shall be designed to assure that the effects of a postulated reactivity accident neither (1) result in damage to the reactor coolant pressure boundary greater than limited local yielding, nor (2) sufficiently disturb the core, its support structures, or other reactor pressure vessel internals to cause serious impairment of core cooling capability.

Regulatory Guide 1.77, "Assumptions Used for Evaluating a Control Rod Ejection Accident for Pressurized Water Reactors," outlines the acceptable assumptions and analytical methods that may be used in evaluating REAs for PWRs. Furthermore, Regulatory Guide 1.77 states that by using these assumptions and methods it should be shown that:

1. Reactivity excursions will not result in a radial average fuel enthalpy greater than 280 cal/g at any axial location in any fuel rod.
2. Maximum reactor pressure during any portion of the assumed transient will be less than the value that will cause stresses to exceed the Emergency Condition stress limits as defined in Section III of the ASME Boiler and Pressure Vessel Code.

2.2 Fuel Rod Failure Threshold (Excessive Fuel Enthalpy)

The fuel rod failure threshold for RIA events is specified in SRP Section 4.2 (II.A.2.f) and was established to meet the requirements of [10 CFR Part 100.11 and 10CFR50 Appendix A, GDC-19] as these relate to both on-site and off-site dose consequences. The fuel rod failure threshold for PWR and BWR applications is as follows:

PWR

Regulatory Guide 1.77 states "The number of fuel rods experiencing clad failure should be calculated and used to obtain the amount of contained fission product inventory released to the reactor coolant system." Clad failure should be assumed to occur when the calculated heat flux equals or exceeds the departure from nucleate boiling ratio (DNBR) for zero power, low power and full power RIA events in PWRs.

BWR

The fuel rod failure threshold used in BWR's is defined in Standard Review Plan Sections 4.2 (II.A.2.f) and 15.4.9. Cladding failure should be assumed for rods that experience a maximum radially averaged fuel enthalpy greater than 170 cal/g for RDA events initiated from zero or low power. For rated power conditions, fuel rods that experience cladding dryout should be assumed to fail.

3.0 Fuel Rod Failure Mechanisms

RIA-simulation experiments conducted in the 1960's and 1970's using zero or low burnup test rods have shown that cladding failure at low burnup occurs primarily by either thermal quench following excessive cladding temperatures caused by post-DNB operation or by cladding contact with molten fuel [Martison and Johnson 1968; Miller and Lussie 1969; Zimmermann et al. 1979]. These observations formed the basis for the current failure threshold of DNB used for PWR control rod ejection accident analyses or a peak radial average fuel enthalpy of 170 cal/gm used for BWR control rod drop accident analyses. However, a transition from cladding failure dominated by high cladding temperatures to cladding failure by PCMI is observed in recent RIA-simulation tests at burnup levels beyond 30 GWd/tU.

Detailed examination of the results from RIA-simulation experiments on irradiated test rods has revealed that, while the level of PCMI loading from the fuel pellet thermal expansion and fuel matrix fission gas swelling can depend on burnup, the actual mechanisms leading to cladding failure are more related to cladding ductility [Montgomery and Rashid 1996; Yang et al. 2000,

Montgomery et al. 1996]. Mechanical properties tests have shown that the ductility of irradiated cladding is mainly a function of the fast neutron damage, the hydrogen concentration and distribution, the temperature and the loading conditions (strain rate and biaxiality) [Garde 1989, Garde et al. 1996]. As a consequence, the cladding failure response of irradiated fuel during a RIA event is less dependent on burnup and more dependent on the operating environment such as the power level, irradiation time, and coolant temperature and the cladding corrosion characteristics. This is supported by the CABRI database on LWR UO_2 test rods which shows that no cladding failure has occurred up to 64 GWd/tU for rods with non-spalled oxide layers up to 80 microns.

Based on these observations from RIA experiments, the cladding failure mechanisms active during a reactivity-initiated accident can be divided into two main categories;

1). Operation in post-DNB heat transfer for low burnup fuel
2). Pellet-Cladding Mechanical Interaction (PCMI) for high burnup fuel

3.1 Post-DNB Failure

Observations from integral transient tests to simulate power-coolant mismatch conditions leading to DNB [Van Houten 1979], as well as high power RIA-simulation tests [Zimmermann et al. 1979; MacDonald et al. 1980], find that cladding failure by post-DNB operation occurs by two different modes: oxidation-induced embrittlement and ballooning/burst.

For low and intermediate burnup, the potential for cladding failure at fuel enthalpy levels below 200 cal/gm by post-DNB failure modes such as oxidation-induced embrittlement or ballooning and burst is very low in modern fuel designs irradiated under current operating conditions. Therefore, the current maximum radial average enthalpy threshold of 170 cal/gm used for cladding failure for BWR RIA events is also applicable to low and intermediate burnup PWR rods and provides a margin to cladding failure. At maximum radial average fuel enthalpy levels below 170 cal/gmUO_2, the cladding temperatures will remain well below the conditions to produce failure by oxidation-induced embrittlement. For ballooning and burst, the fuel rod internal gas pressure for low to intermediate burnup PWR fuel rods is well below the system pressure at hot standby conditions and is therefore insufficient to produce large cladding deformations that could lead to failure. The restricted axial gas flow and the small fuel-cladding gap limit the amount of gas inventory available to cause ballooning deformations in high burnup fuel rods. As a result, cladding failure by ballooning and burst in high burnup fuel rods is unlikely below a maximum fuel enthalpy of 170 cal/gmUO_2. Based on these observations, it can be concluded that cladding failure of UO_2 fuel below fuel enthalpy levels of 170 cal/ gmUO_2 is only possible by pellet-cladding mechanical interaction.

3.2 Pellet-Cladding Mechanical Interaction

RIA-simulation tests on pre-irradiated test rods conducted in CABRI and NSRR found that cladding failure during the power pulse was caused by PCMI related mechanisms, not by high temperature mechanisms. The process of failure by PCMI is a combination of two main elements: (1) the loading imposed on the cladding by fuel expansion and (2) the ability of the cladding to accommodate the fuel expansion strains. Irradiation influences both of these

components to varying degrees, leading to the apparent burnup dependency of fuel rod failure as exhibited by the RIA-simulation test data.

Cladding failure occurs by PCMI when the displacement controlled loading from fuel thermal expansion and gaseous swelling produced during the power pulse exceed the ductility capacity of the cladding. Therefore, the controlling component in the PCMI failure mechanism is the cladding ductility and how the ductility is influence by irradiation.

PCMI-induced failure is unlikely below 40 GWd/MTU because the wider fuel-cladding gap thickness decreases the PCMI forces and the cladding ductility is sufficient to accommodate the pellet expansion. At higher burnup levels, changes in cladding ductility caused by the effects of hydriding, fast fluence and increased PCMI forces can cause the cladding to fail. Data from RIA-simulation tests show that hydride-induced cladding embrittlement controlled by the cladding temperature and hydride distribution were the main causes of cladding failure by PCMI during an RIA event. The main role of fuel rod burnup is to decrease the fuel-cladding gap and increase the PCMI loading by pellet expansion.

4.0 Fuel Rod Failure Threshold for RIA Events

The following summarizes the methodology used to develop the proposed fuel rod failure threshold defined in terms of radial average fuel enthalpy as a function of rod average burnup. The approach is based on the observations from the RIA-experiments performed on test rods extracted from fuel rods irradiated in commercial reactors as well as fuel rod behavior analyses.

The review of the RIA-simulation experiments on commercial reactor fuel found that the data could not be used directly to define a fuel rod failure threshold as a function of burnup because of the role of cladding ductility. Figure 1 contains the results of the RIA-simulation experiments on both commercial reactor fuel and non-commercial test rods and is a plot of the radial average peak fuel enthalpy as a function of test segment burnup. The rods that developed cladding failure during the power pulse are indicated by the solid symbols. As shown in Figure 1, the rods that experienced cladding failure are interspersed amongst the rods where the cladding remained intact following the power pulse. The fact that the failed and non-failed rods are interspersed when the maximum fuel enthalpy is plotted as a function of burnup indicates that burnup is not the key parameter that influences the cladding integrity, other parameters such as cladding, oxidation level, hydride content and temperature, also have an impact. These factors make it difficult to develop a failure threshold that is a function of burnup using this data directly. Similarly, developing a fuel enthalpy at failure as a function of oxide thickness directly from the data as proposed by some is complicated by variations in the test temperature and oxide spallation that make it difficult to develop a clear trend with oxide thickness [Meyer 2001; Yang 2000; Meyer 1997].

average burnup the fuel rod response during a RIA event representative of a PWR hot-zero power control rod ejection accident.

The approach to develop the fuel rod failure threshold for a PWR control rod ejection event consists of five major steps:

Step 1. Utilize data from mechanical property tests on Zr-4 material to define the cladding ductility (expressed as CSED) as a function of outer surface oxide layer thickness.

Step 2. Utilize cladding corrosion data for low tin Zr-4 to define a conservative upper bound oxide thickness model as a function of burnup.

Step 3. Use results from Step 1 and Step 2 to develop a conservative lower bound cladding ductility as a function of burnup.

Step 4. Use a fuel rod analysis code validated with selected RIA-simulation tests to calculate the increase in cladding stress and strain (expressed as SED) during the power pulse of a control rod ejection accident as a function of burnup and fuel rod radial average fuel enthalpy.

Step 5. Combine the results from Step 3 and Step 4 to develop the fuel enthalpy at cladding failure as a function of burnup.

The fuel rod failure threshold resulting from the aforementioned approach is shown in Figure 2. The threshold is defined in terms of the radial average fuel enthalpy as a function of burnup and is applicable to Zircaloy cladding with oxide thickness layers less then 100 microns and without oxide spallation. The revised fuel rod failure threshold is compared in Figure 2 to the results of RIA experiments using commercial reactor fuel. Included in Figure 2 is the results of the NSRR experiments which have been translated to HZP conditions. The fuel rod failure threshold bounds most of the experiments that survived without cladding failure to a burnup of 64 GWd/tU. Several test rods that exhibited no evidence of cladding failure reside at or above the fuel rod failure threshold using this methodology. This demonstrates the conservative nature of the approach used to develop the failure threshold.

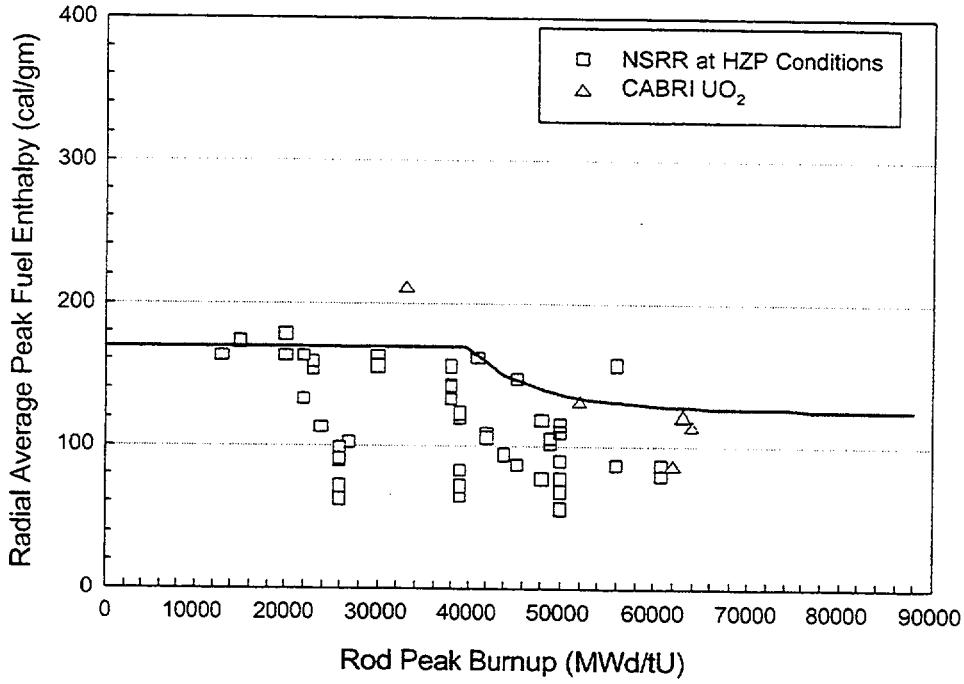

Figure 2. Fuel Rod Failure Threshold as Function of Burnup

5.0 Core Coolability Issues

There are two primary safety concerns raised in connection with the rapid energy deposition and the resulting excessive fuel enthalpy of a reactivity initiated accident: (1) disruption of the core geometry to impair long-term coolability and (2) local yielding of the pressure vessel [AEC 1974]. The main events that can interfere with maintaining a coolable core geometry and ensuring the reactor vessel integrity are the rapid dispersal of fuel material into the coolant and the subsequent fuel-coolant interaction (FCI). The rapid dispersal of high energy fuel material into the coolant may produce coolant pressure pulses that could create destructive forces on the fuel assemblies or reactor vessel, thereby causing changes in the reactor core geometry and deformation of the reactor vessel [Tsuruta et al. 1985; Tompson 1964]. In defining safety limits to preclude core damage, it is important to understand the mechanisms controlling fuel dispersal and FCI under accident conditions. Results from experiments on unirradiated and irradiated test rods show that the factors that influence fuel dispersal and FCI include such mechanisms as the reactivity insertion characteristics, the fuel enthalpy, the coolant conditions, and the fuel rod burnup [Ishikawa and Shiozawa 1980].

5.1 Dispersal of Fuel Material

Early experiments performed in the US and Japan to study transient fuel performance using unirradiated test rods demonstrated that at energy depositions above 250 cal/gm, the fuel enthalpy reached levels that produced molten fuel, energetic dispersal of molten fuel particles, and the conversion of nuclear energy to mechanical energy [Ishikawa and Shiozawa 1980; Martison and Johnson 1968; Miller and Lussie 1969]. Based on these experiments, the NRC established the limit of 280 cal/gmUO_2 on the radial average fuel enthalpy to preclude the potential for the dispersal of molten fuel particles during an RIA event [AEC 1974].

Recently, RIA-simulation experiments on test rods refabricated from previously irradiated commercial fuel rods have shown that a potential exists for the dispersal of non-molten fuel material following cladding failure at energy deposition levels well below that required to produce fuel melting [Sugiyama 2000; Schmitz and Papin 1999]. As has been demonstrated in tests on unirradiated fuel rods, dispersal of fuel pellet material may lead to coolability concerns due to the potential for coolant channel flow blockage, loss of coolable geometry, or pressure pulse generation. However, the question of whether the dispersal of non-molten fuel material leads to coolability concerns depends on the amount, particle size, and the thermal energy of the pellet material dispersed in the coolant, as well as the coolant conditions.

A review of the experimental data shows that the dispersal of non-molten fuel material is a function of the energy deposition after cladding failure, the pellet burnup, and the pulse width of the energy deposition. A plot of energy deposition after cladding failure versus the power pulse width is shown in Figure 3. As can be seen, fuel dispersal occurred only at pulse widths between 4.3 and 9.5 milliseconds. No fuel dispersal was observed for tests with pulse widths above 10 milliseconds and burnup levels above 60 GWd/MTU, even with energy depositions after cladding failure of 69 cal/gmUO_2.

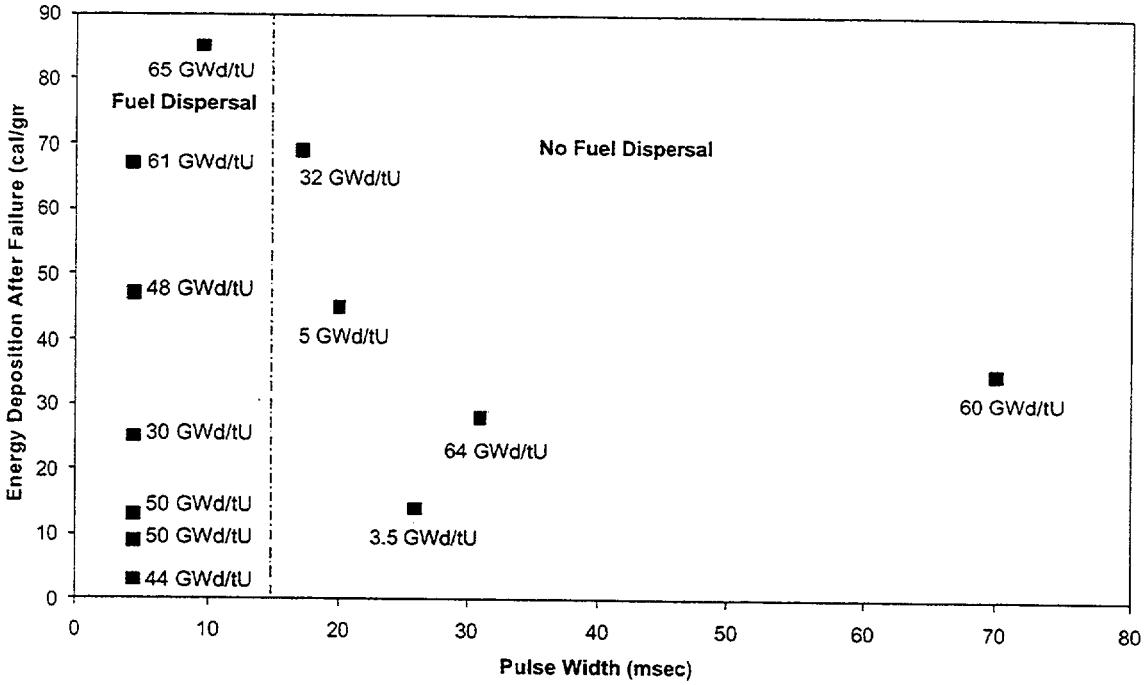

Figure 3. Effect of Pulse Width and Energy Deposition After Cladding Failure on the Dispersal of Non-Molten Fuel Material

The propensity for dispersal of pellet material from fuel irradiated beyond 40 GWd/MTU is related to the development of the pellet rim, and is governed by two main factors: (1) the local temperature and stress peaking in the rim during the rapid energy deposition and (2) the fine-grained structure of the pellet rim material and the tendency of the rim material to fracture into small (<20 micron) particles. Analytical evaluations and post-test examinations have shown that the pulse width of the energy deposition influences the thermal and mechanical behavior of the pellet rim region during the power pulse [Montgomery and Rashid 1996]. For energy deposition with narrow pulse widths, heat conduction from the rim region is low. This leads to higher local temperatures in the rim due to the radial power peaking in the rim region. Energy deposition with wider pulses allows for heat conduction from the pellet to the cladding, thus minimizing the temperature peaking in the pellet rim. The low temperature peaking decreases the potential for fuel particle dispersal.

5.2 Fuel Coolant Interaction

The presence of molten fuel material, both in out-of-pile simulation tests and high energy RIA tests, was shown to be a key element in the FCI process. The rapid ejection of molten fuel through the cladding into the coolant causes the fuel to fragment into fine particles due to the hydrodyamic forces between the molten fuel and the coolant [Fuketa et al. 1993; Vaughan 1979]. This process increases the surface area of the molten fuel and enhances the energy

transfer rate to the coolant. Also, the heat transfer rate from the fuel particles to the coolant increases with the temperature of the fuel [Tsuruta et al. 1985].

The results from both RIA experiments and severe core accident experiments that contained molten fuel indicate that the FCI efficiency as defined by the thermal to mechanical energy conversion ratio is approximately proportional to the inverse of the fuel particle size. RIA experiments resulting in molten fuel dispersal are shown in Figure 4. An inverse dependency on particles is consistent with the theoretical approach proposed by Vaughan which showed that for molten fuel coolant interactions, the efficiency should be proportional to the inverse of the particle diameter [Vaughan 1979].

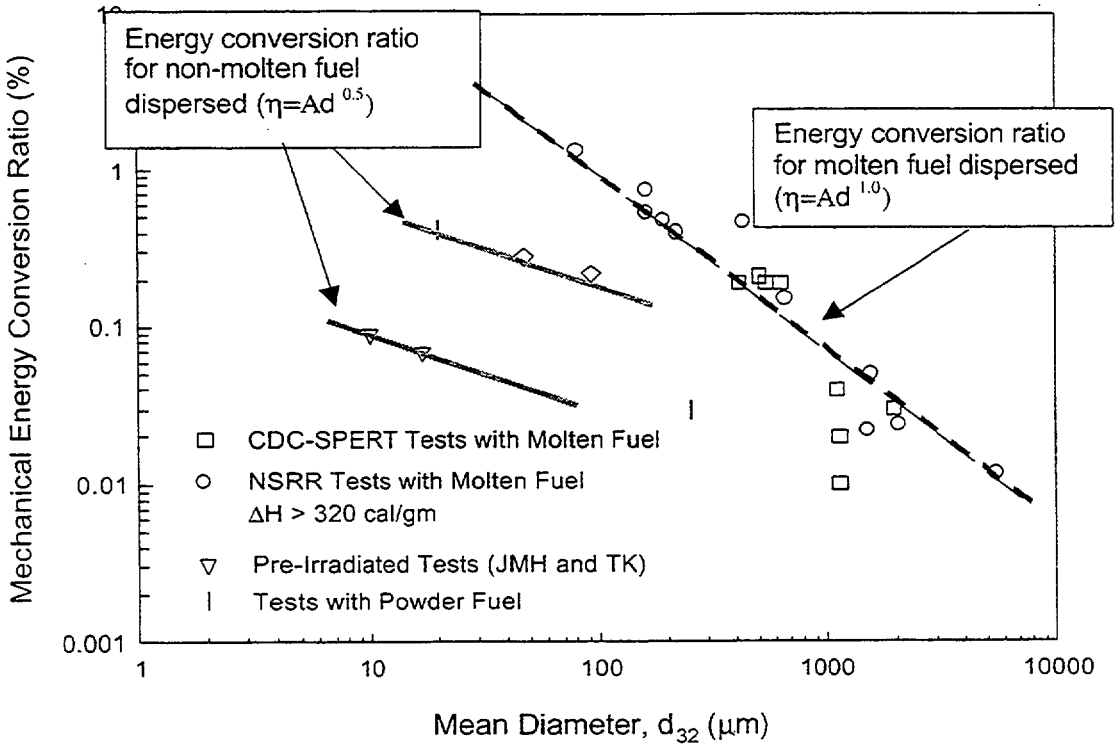

Figure 4. Mechanical Energy Conversion Ratio as a Function of Mean Diameter of Dispered Fuel Material for RIA-Simulation Experiments

As mentioned previously, measurable fuel-coolant interaction has also been observed in four tests in high burnup fuel rods. In these tests, no evidence was found to indicate that the particles were molten prior to dispersal into the coolant. The fuel particles collected from the coolant following the tests were irregularly shaped with faceted surfaces, suggesting fracture [Sugiyama 2000]. Previously molten fuel particles dispersed into the coolant generally have a spherical geometry and a smooth surface finish [Tsuruta et al. 1985].

The mechanical energy conversion ratios for the RIA tests that dispersed highly fragmented non-molten fuel material are also a function of the mean particle diameter. Similar to molten fuel dispersal, the results for these experiments also display an inverse dependency on the mean particle size. However, the mechanical energy conversion ratios are below those for molten fuel and the dependence on particle size is lower. The limited RIA experiments resulting in non-molten fuel dispersal are shown in Figure 4. The exponent n is between 0.4 and 0.5 in the fragmented fuel tests. These results demonstrate that although it may be possible to disperse into the coolant a small fraction of the fuel pellet as finely fragmented particles, the dispersal of non-molten material is less efficient in converting the thermal energy in the fuel particles to mechanical energy in the coolant. The lower energy densities and slower heat transfer rates of the dispersed solid material are the main reasons that the mechanical energy conversion ratios are less than for the dispersal of molten fuel particles.

6.0 Development of Core Coolability Limit

The core coolability limit for RIA represents the ultimate safety limit to ensure that the consequences of the accident do not lead to impairment of the long-term capability to cool the core or threaten the integrity of the reactor vessel. The core coolability limit represents a "no-go" condition and as a result should not be exceeded. The consequences of high energy depositions and high fuel enthalpy levels during a reactivity accident are the potential for loss of fuel rod geometry and the generation of coolant pressure pulses by fuel-coolant interaction.

The potential for zero or low burnup fuel to develop loss of rod geometry or dispersal of fuel material is controlled by the melting response of the fuel pellet and cladding. Gross clad melting may lead to loss of fuel rod geometry since the cladding provides the fuel rod structural support. Melting of the fuel pellet may lead to rapid fuel dispersal and molten fuel coolant interactions. The propensity to generate mechanical energy after dispersal of fuel particles is increased for molten fuel.

The data from zero or low burnup tests indicate that by restricting the fuel enthalpy level to values below that necessary to produce fuel pellet melting would ensure that the fuel rod would maintain a rod geometry throughout an RIA evident. This has been confirmed by recent tests on fuel rods with burnup levels between 30 and 40 GWd/MTU. Both the CABRI REP Na-2 (33 GWd/MTU) and NSRR JMH-5 (30 GWd/MTU) rods reached peak fuel enthalpy levels above 200 cal/gmUO_2 without loss of rod geometry at the completion of the tests [Papin et al. 1996; Sugiyama 2000]. Furthermore, test rod JMH-5 maintained a geometry amenable to long-term cooling that contained more the 80% of the UO_2 material within the cladding, even though the cladding failed by a long PCMI-induced axial crack and dispersed a small amount of solid fuel material into the coolant.

Beyond 40 GWd/tU, the experimental data indicate that dispersal of finely fragmented solid fuel material may occur after cladding failure depending on the pulse width, fuel rod burnup and energy deposition after failure. However, the experimental data also shows that the dispersal of a small quantity of finely fragment fuel particles into the coolant does not lead to loss of rod geometry or the generation of forces that could damage the reactor core or pressure vessel.

The dispersal of finely fragmented non-molten fuel particles from high burnup fuel is not a coolability issue for the following technical reasons:

- No fuel dispersal is expected after cladding failure for pulse widths above 10-15 milliseconds
- The amount of fine-particle material that is available for dispersal is small and limited to the rim:
- The mechanical energy conversion is less efficient for non-molten material

Based on these technical points, it can be stated that the consequence of dispersing a small amount of the fuel pellet as finely fragmented non-molten material into the coolant is a radiological release issue, not a coolability issue. Although limited dispersal of finely fragmented non-molten fuel material has been observed for narrow power pulse tests, the consequences of these tests as defined by the mechanical energy generation are an order of magnitude less than low burnup tests with molten fuel. An appropriate approach to define a core coolability limit for high burnup fuel is to assume that melting of the fuel pellet may lead to unwanted consequences associated with loss of rod geometry, and to therefore limit the peak fuel enthalpy to a level below that to induce fuel melting. Developing a limit based on incipient melting of the fuel pellet is conservative for the following reasons: clad melting is avoided thus ensuring that rod-like geometry is maintained; because of the temperature peaking a majority of the fuel pellet is well below the melting temperature; the mechanical energy conversion ratio is limited well below that required to produce undesirable consequences.

6.1 Approach to Establish Core Coolability Limit

To define the core coolability limit, the radial average peak fuel enthalpy to initiate incipient fuel pellet melting was determined as a function of rod average burnup. The radial average peak fuel enthalpy to induce melting was identified by performing fuel rod calculations for a 20 millisecond pulse width at increasingly larger energy deposition levels until a single radial location in the fuel pellet reached the melting temperature.

The FALCON transient fuel behavior code was used to calculate the temperature response of the fuel pellet during the power deposition. RIA events at both zero and full power were included in the analysis to assess the effect of at power operation on the fuel pellet melting response. Since the cladding to coolant heat transfer can influence the heat conduction from the fuel pellet, cladding-to-coolant heat transfer coefficients representative of nucleate boiling and post-departure from nucleate boiling (DNB) were used in the analysis. The calculation was performed throughout the entire rod average burnup range at increments of 10 GWd/MTU to develop the radial average peak fuel enthalpy as a function of burnup. The effect of burnup on the UO_2 melting temperature and the radial power distribution was also included in the analysis.

6.2 Revised RIA Core Coolability Limit

The maximum radial average fuel peak enthalpy versus rod average burnup curve shown in Figure 5 limits the peak fuel pellet temperature to below the UO_2 melting temperature. As shown in Figure 5, the fuel enthalpy limit bounds the RIA tests conducted above 20 GWd/tU. As indicated, these rods remained a rod-like geometry following completion of the tests.

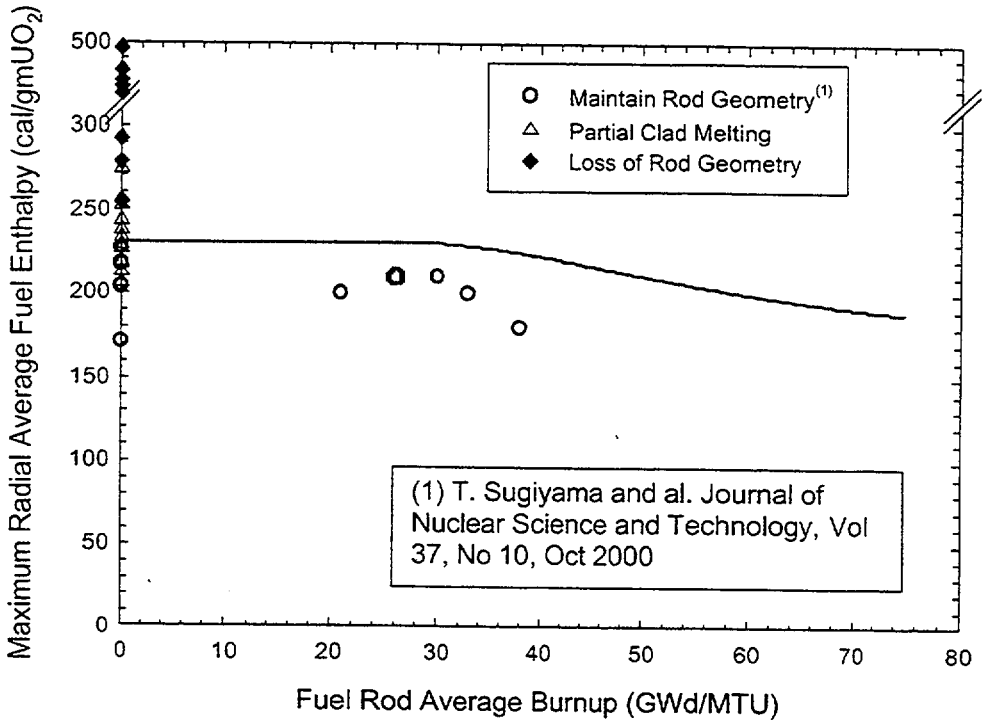

Figure 5. Enthalpy Limit to Preclude Incipient Fuel Pellet Melting as a Function Burnup

A maximum value of 230 cal/gmUO_2 for the radial average fuel enthalpy was used as the basis for establishing the zero burnup limit. This value is below the current regulatory maximum allowable radial average peak fuel enthalpy of 280 cal/gmUO_2. MacDonald, et. al. performed a review and re-assessment of the data used by the NRC to establish the fuel coolability limit of 280 cal/gm for the maximum radially averaged fuel enthalpy as defined in Reg. Guide 1.77 [AEC 1974]. It was found that although the fuel coolability limit is stated in terms of radially average fuel enthalpy, the data used to establish the limit was actually based on the total energy deposition for the tests [MacDonald et al. 1980]. The maximum radial averaged fuel enthalpy is less than the associated total energy deposition by 15-20% due to heat conduction from the fuel and energy deposition from delayed neutrons. Re-evaluation by MacDonald, et. al. of the tests performed in the SPERT and TREAT facilities using the maximum radial average fuel enthalpy shows that a value of 230 cal/gm for the maximum radial average peak fuel enthalpy would provide margin to loss of fuel rod geometry and would be more appropriate for the fuel coolability limit at zero and low burnup.

The maximum radial average fuel enthalpy curve, shown in Figure 5, decreases as a function of rod average burnup. As the rod average burnup increases, the effects of burnup on the UO_2 melting temperature and radial power distribution combine to decrease the radial average fuel

enthalpy to produce incipient melting. These factors lead to the burnup dependency shown in Figure 5.

The revised limit on the radial average fuel enthalpy ensures that fuel melting does not occur during the energy deposition phase of a reactivity-initiated accident. This approach prevents the dispersal of molten fuel that is a precursor for loss of rod geometry and fuel-coolant interaction leading to generation of damaging pressure pulses.

7.0 Conclusions

Two separate criteria have been developed to 1) ensure long-term cooling of the reactor core after the accident and 2) account for radiological release to the environment following cladding failure. To assure core coolability and to preclude damage to the reactor pressure vessel, a core coolability limit is established based on the maximum radial average peak fuel enthalpy that precludes incipient UO_2 pellet melting during the power transient. Second, a threshold on the radial average peak fuel enthalpy is defined that represents the occurrence of fuel rod failure for use in off-site dose calculations. The fuel rod failure threshold below a rod average burnup of 35 GWd/MTU is established to preclude cladding failure by high temperature processes. Beyond a rod average burnup of 35 GWd/MTU, the fuel rod failure threshold is based on cladding failure by PCMI. Both the core coolability limit and the fuel rod failure threshold are defined as a function of fuel rod average burnup to comply with current regulatory practices.

The two criteria shown in Figure 6 are applicable to Zircaloy-clad UO_2 or UO_2-Gd_2O_3 fuel rods operated up to a target lead rod average burnup of 75 GWd/MTU that experiences a HZP or HFP RIA event. In the application of these criteria, the maximum cladding outer surface zirconium oxide layer thickness should not exceed 100 microns and there should be no oxide spallation that significantly impacts the cladding mechanical properties. The RIA fuel rod failure threshold shown in Figure 6 is applicable to advanced cladding designs provided the cladding material exhibits superior or equivalent ductility as Zircaloy cladding with the same outer surface oxide layer thickness and without oxide spallation. Future RIA-simulation experiments with UO_2 fuel rods will provide confirmatory data at high burnup and provide additional characterization of advanced cladding material.

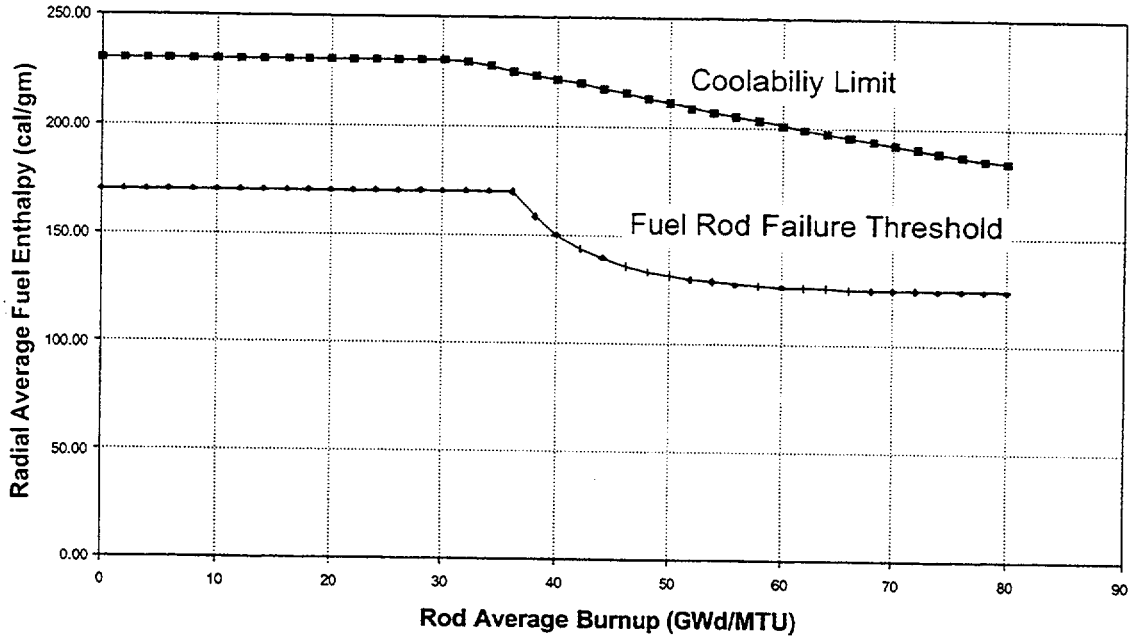

Figure 6. Revised Fuel Rod Failure Threshold and Coolability Limit for RIA Events

8.0 References

10 CFR Part 50 Appendix A, General Design Criteria for Nuclear Power Plants, U.S. Government Printing Office, Washington, 1990.

10 CFR Part 100.11,Determination of Exclusion Area, Low Population Zone, and Population Center Distance, U.S. Government Printing Office, Washington, 1990.

Chung, H. M., L. A. Neimark, and T. F. Kassner, "Test Plan for High-Burnup Fuel Behavior Under Loss-of-Coolant Conditions," *Proceedings of the Twenty-Fourth Water Reactor Safety Meeting*, Vol. 1, Nuclear Regulatory Commission, Bethesda, Maryland, October 21-23, 1996, pp. 173-184.

Cunningham, M., et al., "FRAPTRAN: A Computer Code for the Transient Analysis of Oxide Fuel Rods," NUREG/CR-6739, Volume 1, August 2001.

Federici, E. et al., "Status of Development of the SCANAIR Code for the Description of Fuel Behavior Under Reactivity Initiated Accidents," *Proceedings of the ANS International Topical Meeting on Light Water Reactor Fuel Performance*, Park City, Utah, April 10-13, 2000 pp. 345-358.

Fuketa, T., N. Yamano, and A. Inoue, "Proceedings of the CSNI Specialists Meeting on Fuel-Coolant Interactions," NUREG/CP-0127, NEA/SCNI/R(93)8, Santa Barbara, California, January 5-8, 1993.

Fuketa, T., et al., "NSRR/RIA Experiments with High-Burnup PWR Fuels," *Nuclear Safety*, Vol. 37, No. 4, Nuclear Regulatory Commission, Bethesda, Maryland, October-December, 1996, pp. 328-342.

Garde, A. M., "Effects of Irradiation and Hydriding on the Mechanical Properties of Zircaloy-4 at High Fluences," *Zirconium in the Nuclear Industry: Eighth International Symposium, ASTM STP 1023*, L. F. P. Van Swam and C. M. Eucken Eds., American Society for Testing and Materials, Philadelphia, 1989, pp. 548-569.

Garde, A. M., G. P. Smith, and R. C. Pirek, "Effects of Hydride Precipitate Localization and Neutron Fluence on the Ductility of Irradiated Zircaloy-4," *Zirconium in the Nuclear Industry: Eleventh International Symposium, ASTM STP 1295*, E. R. Bradley and G. P. Sabol Eds., American Society for Testing and Materials, 1996, pp. 407-430.

Ishikawa, M. and S. Shiozawa, "A Study of Fuel Behavior Under Reactivity Initiated Accident Conditions - Review", *Journal of Nuclear Materials*, Volume: 95, 1980, pp. 1-30.

MacDonald, P. E., S. L. Seiffert, Z. R. Martinson, R. K. McCardell, D. E. Owen, and S. W. Fukuda, "Assessment of Light-Water-Reactor Fuel Damage During a Reactivity-Initiated Accident," *Nuclear Safety*, Vol. 21, No. 5, Nuclear Regulatory Commission, Bethesda, Maryland, September-October, 1980, pp. 582-602.

Martinson, Z. R. and R. L. Johnson, "Transient Irradiation of 1/4-Inch OD Zircaloy-2 Clad Oxide Fuel Rods to 590 cal/g UO_2," IDO-ITR-102, Phillips Petroleum Company, Atomic Energy Division, November 1968.

Meyer, R. O., R. K. McCardell, and H. H. Scott, "A Regulatory Assessment of Test Data for Reactivity Accidents," *Proceedings of the ANS International Topical Meeting on Light Water Reactor Fuel Performance*, Portland, Oregon, March 2-6, 1997 pp. 729-744.

Meyer, R. O., "Implications from the Phenomenon Identification and Ranking Tables (PIRTs) and Suggested Research Activities for High Burnup Fuel," Draft, U.S. Nuclear Regulatory Commission, July 2001.

Miller, R. W. and W. G. Lussie, "The Response of UO_2 Fuel Rods to Power Bursts, 5/16-Inch OD, Pellet and Powder Fuel, Zircaloy Clad," IDO-ITR-103, Phillips Petroleum Company, Atomic Energy Division, January 1969.

Montgomery, R. O. and Y. R. Rashid, "Evaluation of Irradiated Fuel During RIA-Simulation Tests", EPRI TR-106387, May 1996.

Montgomery, R. O., Y. R. Rashid, O. Ozer, and R. L. Yang, "Assessment of RIA-Simulation Experiments on Intermediate- and High-Burnup Test Rods," *Nuclear Safety*, Vol. 37, No. 4, Nuclear Regulatory Commission, Bethesda, Maryland, October-December, 1996, pp. 372-387.

Montgomery, R. O., et al., "Review and Analysis of RIA-Simulation Experiments on Intermediate and High Burnup Test Rods," *Proceedings of the ANS International Topical Meeting on Light Water Reactor Fuel Performance*, Portland, Oregon, March 2-6, 1997 pp. 711-720.

Ozer, O., Y. R. Rashid, R. O. Montgomery, R. Yang, "Evaluation of RIA Experiments and Their Impact on High Burnup Fuel Performance," *Proceedings of the CSNI Specialists Meeting on Transient Behavior of High Burnup Fuel*, Cadarache France, September 12-14, 1995, Report NEA/CSNI.R(95) 22, 1996.

Papin, J., et al., "French Studies on High-Burnup Fuel Transient Behavior Under RIA Conditions," *Nuclear Safety*, Vol. 37, No. 4, Nuclear Regulatory Commission, Bethesda, Maryland, October 21-23, 1996, pp. 289-327.

Papin, J., J-C. Melis, and C. Lecomte, "Definition and Status of the CABRI International Program for High Burn-Up Fuel Studies," *Proceedings of the Twenty-Eighth Water Reactor Safety Information Meeting*, NUREG/CP-0172, U.S. Nuclear Regulatory Commission, Bethesda, Maryland, October 23-25, 2000, pp. 185-190.

Schmitz, F. and J. Papin, "High Burnup Effects on Fuel Behavior Under Accident Conditions: The Tests CABRI REP-Na", *Journal of Nuclear Materials*, Volume: 270, 1999, pp. 55-64.

Sugiyama, T., and T. Fuketa, "Mechanical Energy Generation During High Burnup Fuel Failure under Reactivity Initiated Accident Conditions," *Journal of Nuclear Science and Technology*, Volume 37, No. 10, October 2000, pp. 877-886.

Tompson, T. J., and J. G. Beckerley, "The Technology of Nuclear Reactor Safety," Vol. 1, MIT Press, 1964.

Tsuruta, T., M-A. Ochiai, and S. Saito, "Fuel Fragmentation and Mechanical Energy Conversion ratio at Rapid Deposition of High energy LWR Fuels," *Journal of Nuclear Science and Technology*, Volume 22, No. 9, September 1985, pp. 60-72.

U. S. Nuclear Regulatory Commission, Standard Review Plan for the Review of Safety Analysis Reports for Nuclear Power Plants, LWR Edition, NUREG-0800, Office of Nuclear Reactor Regulation, July 1981.

Van Houton, R., "Fuel Rod Failure as a Consequence of Departure from Nucleate Boiling or Dryout," NUREG-0562, U.S. Nuclear Regulatory Commission, Bethesda, Maryland, June 1979.

Vaughan, G. J., "Paper for the Fourth CSNI Specialist Meeting on Fuel-Coolant Interaction in Nuclear Reactor Safety" UKAEA, SRD, Culcheth, England, Bournemouth, UK, April 2-5, 1979.

Yang, R. L., R. O. Montgomery, N. Waeckel, and Y. R. Rashid, "Industry Strategy and Assessment of Existing RIA Data," *Proceedings of the ANS International Topical Meeting on Light Water Reactor Fuel Performance*, Park City, Utah, April 10-13, 2000 pp. 383 - 401.

Zimmermann, C. L., C. E. White, and R. P. Evans, "Experiment Data Report for Test RIA 1-2 (Reactivity Initiated Accident Test Series), NUREG/CR-0765, EG&G Idaho Inc., June 1979.

Need for Experimental Programmes on LOCA Issues Using High Burn-Up and MOX Fuels

Alain MAILLIAT, Michel. SCHWARZ

Institut de Protection et de Sûreté Nucléaire
Département de Recherches en Sécurité
C.E.. Cadarache, France

Safety studies performed in IPSN and elsewhere pointed out that high burn up might induce significant effects, especially those related with fuel relocation during LOCA situations. Uncertainties exist regarding how much the existing safety margins associated with peak clad temperature, clad oxidation, core coolability, clad residual ductility can be reduced by new fuels like the MOX one, burn up increases, the arrival of various alloys for fuel rod cladding. A better knowledge of specific phenomena associated to fuel effects is required in order to estimate the new margins and to resolve the pending uncertainties related to the LOCA criteria. Therefore, in addition to the programmes currently planned in the Halden reactor, IPSN is preparing the so-called "APRP-Irradié" (High Burn up fuel LOCA) programme. One of the important aspects of this programme is In-Pile experiments involving bundle geometries in the PHEBUS facility located at Cadarache, France.

1. INTRODUCTION

In France and in other countries, a permanent evolution of the light water reactors (LWR) is observed since the seventies. The evolution deals with the reactor designs (900 MWe/3 loops, 1300MWe/4 loops, N4, future EPR). It is also related to the fuel management and burnup increase (3 cycles, 4 cycles, 39[1] GWd/tU, 47, 52, 60 GWd/tU in the next future). This evolution affects the fuel itself (UO_2, MOX, Gd fuel), the cladding (Zircaloy, Zirlo, M5) and the control rods (Ag-In-Cd, B_4C). As a consequence of these modifications, there is a permanent need to reassess the reactor safety studies which implies improving the associated knowledge and upgrading the corresponding calculation tools. Such a need is not specific to the French situation. For the studies associated with the continuous evolution of the reactor operation, the safety authorities requirements are both related to the design basis accidents and the severe accidents. They have to appreciate to which extent their analyses and criteria might be modified by the burnup increase and the type of fuel. In France, under safety considerations, it was requested prior to any generic authorisation of discharge burn-up extension, that the high burn-up fuel behaviour be validated, with the support of appropriate R&D tests results, under accidental conditions, particularly under Loss-of-Coolant-Accident (LOCA) conditions.

The current regulatory safety criteria for LOCA, still in use in most countries, are derived from the ECCS acceptance criteria that were issued by USAEC in December 1973 and published in the Code of Federal Regulations (10.CFR50, part 50.46) as "Acceptance Criteria for Emergency Core Cooling Systems for Light-Water-Cooled-Nuclear Power Reactors".

The criteria are stated as 5 requirements, concerning the calculated performance of the cooling system under the most severe loss-of-coolant accident conditions. A summary of these conditions is given on the figure 1 against. These first two requirements address: the peak cladding temperature (PCT) which shall not exceed 1204°C and the maximum cladding oxidation rate, defined through an equivalent cladding reacted (ECR), which shall nowhere exceed 17% of the cladding thickness before oxidation but after cladding swelling with or without rupture.

TYPICAL LOCA TRANSIENT

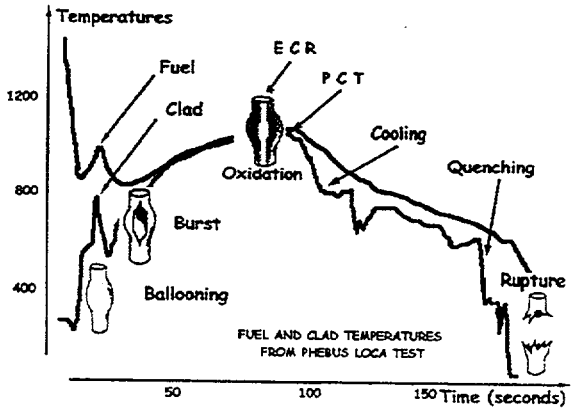

Figure 1

[1] Mean value per assembly

The third request addresses the maximum hydrogen generation, the total amount of which shall not exceed 1% of the hypothetical amount generated by the reaction of all the metal in the cladding surrounding fuel. Finally the last two requirements are related with core cooling. The calculated changes in core geometry shall leave the core amenable to cooling and after any operation of the ECCS, the core temperature shall be maintained at an acceptably low value and decay heat removed for the extended period of time required by long-lived radioactivity.

2. UNCERTAINTIES AND PENDING ISSUES

In the aftermath of the AEC LOCA criteria release, numerous studies were undertaken world-wide in order to improve the basic knowledge of the physical phenomena intervening in LOCA transients, so as to allow a better prediction with realistic models. Beyond the numerous experimental investigations that were conducted on unirradiated rods or cladding, either in-pile or out-of-pile, there exists a few number of available results of such experiments with irradiated material. Following is a very short review of the current knowledge on clad and fuel rod behaviour gained from experiments on irradiated material, that will introduce the pending questions and critical issues for irradiated fuel behaviour in LOCA.

2.1 UNCERTAINTIES

2.1.1 CLAD BEHAVIOUR

An important progress in knowledge relative to irradiated clad behaviour has been obtained from the results of the French EDF/IPSN [1,2] program (TAGCIR and HYDRAZIR tests), addressing the oxidation kinetics and quench bearing capability of irradiated zircaloy. The main outcome concern:

- the protective effect of corrosion oxide scale;
- the oxidation kinetics of irradiated zircaloy;
- the resistance to quench loads of irradiated zircaloy;
- the effect of high hydrogen content, as a result of internal hydriding during LOCA transient.

Relative to oxidation kinetics and quench behaviour, a comprehensive understanding of all involved phenomena and of their inter-related influences is not yet achieved and leaves still pending questions, most of them being not specific to high BU fuel. One important question is the influence on clad quenching resistance of axial constraints that may result from differential contractions upon quench between guide tubes and a fuel rod blocked in spacer grids as a result of ballooning or metallurgical interaction. Such blockage consequences had been evidenced on past tests at JAERI [3] on unirradiated rods and should therefore be expected to some extent on irradiated rods.

2.1.2 ROD BEHAVIOUR

There exists a few number of available results from experiments with irradiated fuel rods under LOCA conditions. The main outcome were found in results from the PBF-LOC tests[4,5] in the USA, the FR2 tests[6] in Germany, and the FLASH5 test[7] in France. They concern the fuel relocation process and an increased cladding deformation.

FUEL RELOCATION

All the available tests performed with irradiated fuel rods experiencing LOCA conditions have shown an accumulation of fuel debris in the swollen region –called balloon- of the burst cladding which resulted from fuel fragments slumping from upper locations (see figures 2 and 3 below from FR2 results).

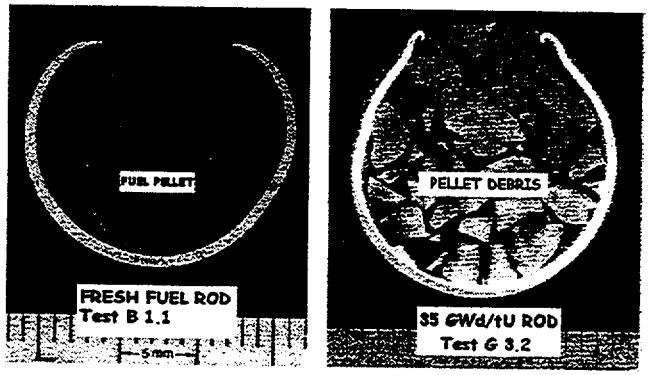

Figure 2

This process, here after called fuel relocation, is initiated at the time of the cladding burst, as demonstrated by the FR2-E3 and E4 tests. It is thought that the driving forces are both gravity and the pressure difference between the rod upper plenum and the channel.

This fuel relocation is not counteracted by the fuel-clad tight bounding, which exists with high burnup fuel.

Indeed, the process was observed in the FLASH-5 test with 50GWd/t fuel in spite of a rather low clad strain (not higher than 16%). It is thought that the cladding temperature increase combined with its ballooning suppress –at less partly- the bounding making possible the fuel relocation.

Finally, fuel relocation process is not specific of high burnup fuel. It was also observed for fuel rod having a burnup as low as 48MWd/t (LOC5-7B test).

AN INCREASED CLADDING DEFORMATION

In PBF-LOC experiments 2 couples of rods (2 unirradiated + 2 irradiated) were simultaneously tested in the same test train. Available data for comparison, although in very limited number due to technical problems, clearly indicate significant differences in the deformation behaviour of irradiated versus unirradiated rods.

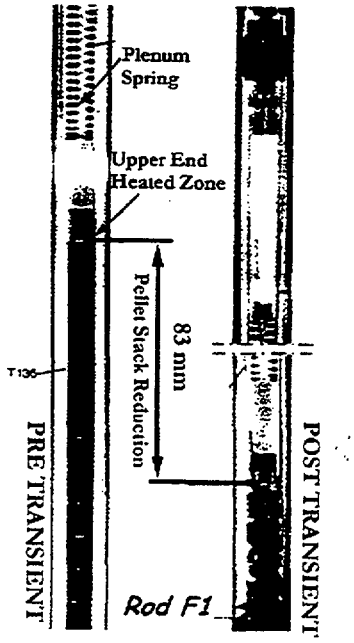

Figure 3

- A higher circumferential rupture strain for irradiated rods (a factor greater than 2 relatively to unirradiated rod strain for maximum values) and more axially extended;
- A wall thinning affecting almost all the circumference of irradiated rods, thus indicating low azimuthal temperature differences as compared to unirradiated rods.

These differences in behaviour have been attributed to the lower temperature differences on the clad of irradiated rods, circumferentially and axially, as a result of the pellet-clad gap reduction due to clad creepdown during rod irradiation.

2.2 THE PENDING ISSUES

A better understanding of the specific phenomena shortly mentionned above leads to raise a list of some complementary questions related with rod behaviour, fuel relocation process and coolability issue during LOCA transients.

2.2.1 ROD BEHAVIOUR

The question mark about rod behaviour is related with the influence of hydrogen pick-up and other irradiation effects on ballooning, burst behaviour and embrittlement during reflooding which were not considered when 10CFR50, part 50.46 was released.

2.2.2 FUEL RELOCATION

Several questions are induced by the relocation process. The first ones concern the process itself. The needed data are the following ones.

- Instant of fuel movement at high burn-up, with possible delay due to fuel-clad bonding.
- Filling ratio of clad balloon at high burn-up, with fragmentation of UO2 rim or MOX clusters
- Impact of the relocated material on steam access inside the balloon and hydrogen uptake rate.

The second set of question marks concerns the consequences of the relocation process.

- Which are the effects on peak clad temperature and final oxidation ratio of the local increase in lineic and surfacic powers and of the local decrease in fuel-clad gap resulting from fuel accumulation?

Note that these last issues are particularly important for end-of-life MOX fuel for which power generation is not reduced, unlike for UO2 fuel.

2.2.3 COOLABILITY

Related questions should be considered additionally, relative to flow blockage behaviour of highly deformed cladding with possibly relocated fuel and the embrittlement potentials associated to fuel fragmentation. The 90% value for flow blockage still coolable, as derived from results of flooding experiments (FEBA, SEFLEX et al) on unirradiated rods arrays is questionable since these experiments did not take account of any fuel relocation and associated effects. The needed information are the following.

- What is the maximum flow blockage ratio that leaves coolable an irradiated rods bundle?
- Does the maximum flow blockage ratio attainable with an irradiated rods array remain below the maximum coolable value indicated above?

There is presently a complete lack of data allowing to answer these questions.

- what flow blockage configuration would be worst coolable with occurrence of fuel relocation?

In other words, is the coplanar flow blockage still the worst coolable case?

3. THE IPSN *APRP IRRADIÉ* PROJECT

For many years, IPSN and several other safety organisations have applied a three-tier method for their reactor safety researches. The first step consists of computer code developments from the existing data bases. The second step involves small-scale, out-of-pile experiments, which provide the additional data bases requested by the code developments and their preliminary assessments. But, as the reactor phenomenology cannot be totally reproduced in such small scale experiments, a third step consisting of integral in-pile experiments using real materials is essential for comprehensive accident analyses. Their results allow the final code assessment in terms of reactor applicability and simulation completeness. This in-pile part of a programme assures that the investments done for code developments and small scale experiments will produce profits in terms of reactor safety. This three-tier method is applied by IPSN for the various research programmes devoted to reactor safety, design basis accidents including RIA and severe accidents programmes.

Regarding the LOCA issue, the current testing programmes dealing with irradiated material only involve out-of-pile experiments : separate effect quench tests on irradiated cladding (TAGCIR tests) in France; tests on irradiated cladding and integral type experiments (ballooning / burst / oxidation / quench) on irradiated rods at ANL (USA) [8] and JAERI (Japan) [9] with the support of an important programme of mechanical tests. In addition, OECD has planned an in-pile programme consisting of some single rod geometry tests with irradiated fuel. The programme should be conducted in the Halden reactor and should provide information about the relocated fuel characteristics.

But these programmes will not solve all the previously mentioned uncertainties because these ones are mainly associated with the combined behaviour of fuel and cladding under representative conditions of the reactor evolution during the LOCA transient. Based on the long fruitful experiences of a three-tier method, the so called *APRP Irradié* programme, providing the in-pile experiments third tier, should provide the missing part of the data bases required for code assessments in terms of reactor applicability and simulation completeness. This programme is prepared in a coherent way with the present international efforts in order to validate, and possibly update, the results obtained from separate effects tests and previous limited in-pile tests.

3.1 THE MAIN EXPERIMENTAL OBJECTIVES

The main objectives of the in-pile experiments will be to investigate the behaviour of fuel and cladding with conditions representative of the reactor during LOCA sequences. The main factors that will be accounted for are:

- the nature of fuel (UO2, MOX, Burn-up),
- the fuel-clad thermomechanical coupling (i.e. fuel relocation)
- thermal azimuthal gradients (main factor affecting cladding strain and blockage ratio)
- thermal-hydraulic aspects (i.e. quenching, coolability of blocked arrays)
-

3.2 TEST DEFINITION RATIONALE

The following analysis provides the rationale for the *APRP-Irradié* programme characteristics. It is shown that the conditions for having representative data for reactor applications are both in-pile tests and bundle geometry.

3.2.1 NEEDS FOR IN-PILE TESTS

The in-pile test need results from three reasons.

Neutron flux provides the unique way to produce the correct heat generation in the fuel fragments, corresponding to the residual power, whatever are the relocations induced by the ballooning and/or the burst of the rod. Both the exact amount of heat generation in the balloon and the heat exchanges with the rod channel depend on the characteristics of the relocated fuel fragments, their size, shapes, and compaction ratio. This heat generation correctness is one of the main conditions for having realistic estimates of the relocation consequences in terms of equivalent clad reacted, peak clad temperature and hydrogen uptake inside the balloon. All

these aspects impact the strength of the rod during the quenching phase and the residual ductility of the rod after the LOCA transient.

During the blowdown phase of the LOCA transient, there is much less heat generation in the fuel and the clad coolant heat transfer is drastically reduced. Therefore, the fuel-stored energy is redistributed in the pellet and the cladding. Simultaneously, within a few seconds, this redistribution produces a decrease of the pellet center-line temperature from 1500°C down to, say, 1000°C and an increase of both the pellet rim and clad temperatures from 300°C up to 1000°C. Due to these temperature transients, the central part of the pellet will experience a contraction while the rim and the clad will undergo an expansion. Fuel mechanical stresses and fragmentation could be induced by these adverse effects. It has to be kept in mind that during usual experiments, for which a blowdown phase is not reproduced, clad and fuel temperatures are simultaneously increased or decreased without producing any comparable thermomechanical transient. In-pile tests including a blowdown phase provide the way to get a definitive answer regarding the additional fuel fragmentation prior to the relocation and how much this refragmentation process affects the amount and the characteristics of the relocated fuel.

Finally, during reflooding and quench process studies, in-pile tests allow to maintain the heat generation in the fuel corresponding to the residual power. By this way, more representative conditions of the thermomechanical loads of the rods are provided. Without such a power during the reflooding phase, steam production and cladding oxidation are reduced; the temperature transients experienced by the rods are less severe. Consequently, under estimates of core embrittling during reflooding could be obtained.

3.2.2 NEEDS FOR BUNDLE GEOMETRY

In addition to the requirement associated to heat generation mentioned above, bundle geometry is a second important condition to produce realistic data. Relocation being closely associated with the volume which is made free by the rod burst, it is clear that a correct amount of relocated fuel will be produced only if the sizes of the balloons are representative of the reactor conditions. Such balloon sizes can be obtained –as explained below- only with bundle geometry. This is the reason why these tests are essential and complementary of single rod tests.

During the early stage of the LOCA transient the fuel rods experience the ballooning and burst processes. For such phenomena, bundle geometry is a necessity to get a correct azimuthal temperature field around the fuel rods since this field is crucial to produce a realistic balloon size. An illustration of the impact of the azimuthal temperature field on the stain at burst is given by the results of single rod tests with heated or non-shroud. A uniformly heated shroud reduces the azimuthal temperature variation around the rod. For such tests a higher rod deformation is obtained. Conversely, an unheated shroud tends to increase the azimuthal gradient and, therefore, leads to small rod deformation at strain (see figure 4 below).

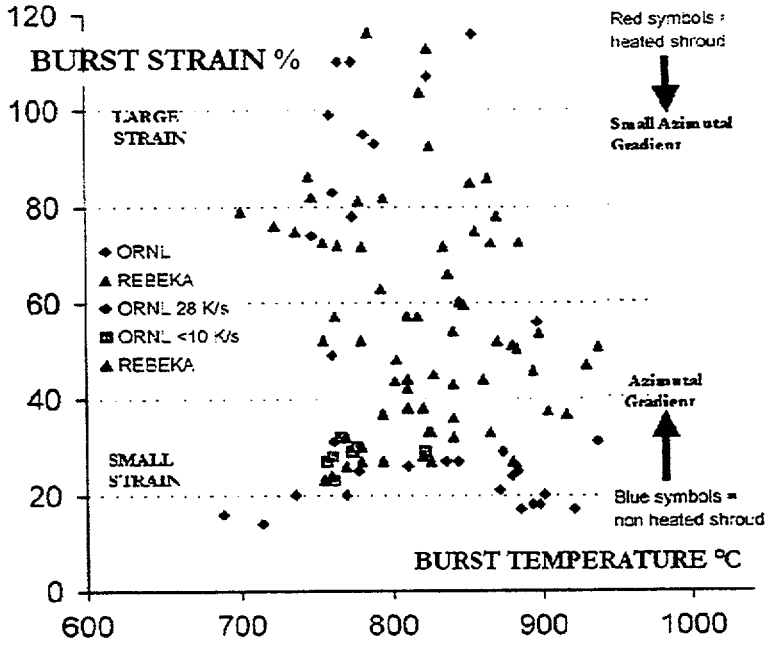

Figure 4

Additional reason for a bundle are the radial interactions between adjacent fuel rods that need to be taken into account because they modify the size and shape of the balloons. Such kind of balloon interactions are clearly illustrated with the side picture (figure 5) from PHEBUS LOCA test 215. Having in mind that the amount of relocated fuel is associated with the size and the shape of the balloon, the picture demonstrates that realistic data will require bundle geometry. This bundle geometry requirement to ensure representative mechanical interactions with neighbour rods was stated in early 80ies – several years ago- in consideration of ORNL MRBT B5/B3 experiments [10].

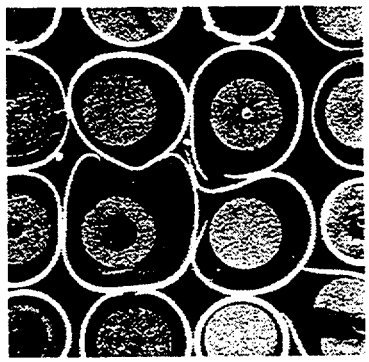

Figure 5

During core reflooding, a bundle is an obvious requirement for reproducing, on one hand, the correct flow blockage induced by the ballooning of the rods and their radial interactions and, on the other hand, the excess of heat generation at the blockage location due to the fuel fragments relocated in the balloons.

Finally, such bundle geometry is also necessary to represent the axial and radial stresses induced by the grids and the adjacent rods, which might restrain the rod contraction during quenching.

3.3 EXPERIMENTAL CONFIGURATIONS

Since it is hardly conceivable to carry out one type of experiments that will address all pending questions with any chance to provide some usable results, it appears more appropriate to perform two kinds of in-pile experiments, namely separate effects tests and integral tests.

3.3.1 SEPARATE EFFECTS TESTS

The objectives of these tests are to address phenomenological aspects, in order to confirm or correct and extent the previous results relative to:

- rod deformation,
- fuel relocation,
- the resulting resistance to thermal shock loads, with or without effect of clad axial constraining.

These tests should be realised with one irradiated rod within a ring of 8 fresh fuel rods, which will provide a representative thermal environment in order to ensure representative strains and subsequent phenomena. In addition, these in-pile separate effects tests should include a blowdown phase. As mentioned before, this phase will provide representative conditions for the temperature transient inside the fuel to study the consequences in terms of thermomechanical pre-fragmentation during blowdown.

3.3.2 3.3.2 INTEGRAL TESTS.

This kind of tests will address the aspects of:

- impact of blowdown phase
- flow blockage
- quenching behaviour and coolability.

These tests should allow to check the absence of unexpected phenomena or unexpected coupling between foreseen processes, and finally provide data for the validation of reactor computational tools.

These tests should be realised with 9 high burn up rods with a ring of 12 or 16 fresh fuel rods which will provide a representative thermal environment in order to ensure representative strains and subsequent phenomena. A blowdown phase will be simulated depending on its importance as observed in the previous studies. Finally, additional axial stress during quenching due to rod blockage in the assembly should be simulated during these tests.

3.3.3 EXPERIMENTAL FACILITY

Such a programme is envisaged by the IPSN in the PHEBUS facility where some twenty LOCA tests were run between 76 and 83 [11,14], see figure 6. By this way IPSN would take advantage of the know-how accumulated when the previous LOCA programme with fresh fuel was run.

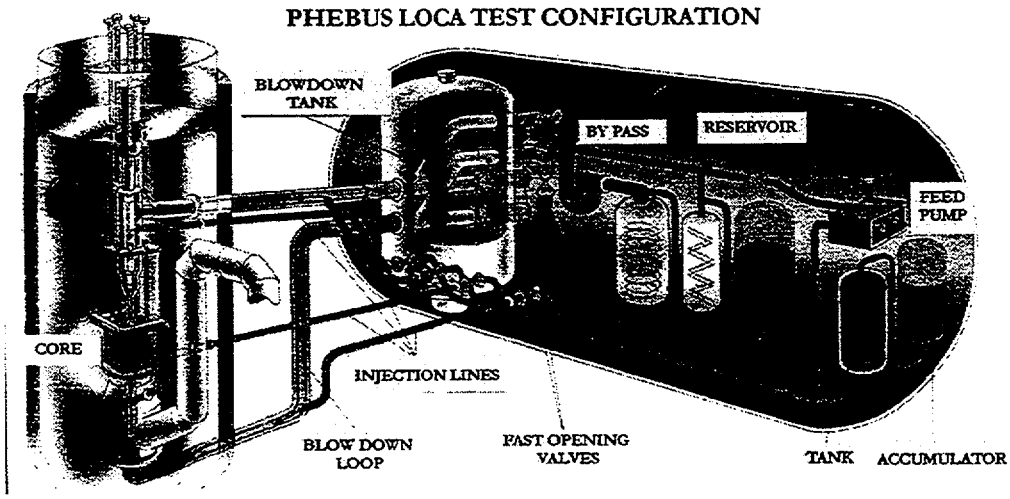

Figure 6

Furthermore, a new LOCA programme in the Phébus facility would take advantage of the R&D efforts made for the subsequent programmes in terms of high activity material measurements

Tomography technique [15,16] is one of the examples, which can be given how such efforts provide practical applications for the new LOCA programme. This technique provides the 3D location and the nature of the material fragments everywhere in a bundle. The exact geometry of the bundle at the end of the test can be reconstructed and explored from the inside. Fuel relocation studies and code validation will be made easier through this technique.

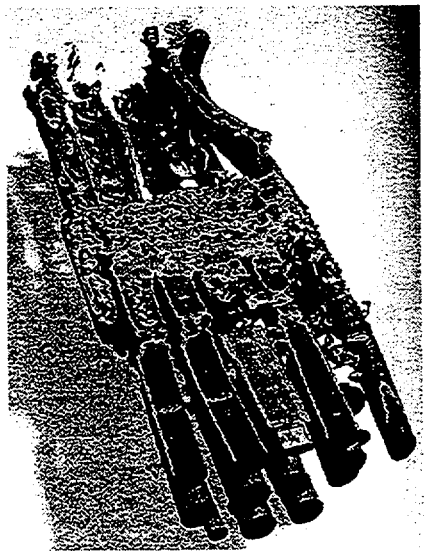

Figure 7

Presently, fragment size less than 500 microns can be located (see figure 7). Further improvement of the existing technique will increase the resolution providing several points inside the clad with an oxide/metal discrimination.

4. CONCLUSIONS

Studies performed in IPSN and elsewhere pointed out that high burnup may induce specific effects under LOCA conditions, especially those related with fuel relocation. Uncertainties exist regarding how much these effects might affect the late evolution of the accident transient and the associated safety issues. IPSN estimates that a better knowledge of specific phenomena is required in order to resolve the pending uncertainties related to LOCA criteria. IPSN is preparing the so-called APRP-Irradié (High Burnup fuel LOCA) programme. One of the important aspects of this programme is in-Pile experiments involving bundle geometries in the PHEBUS facility located at Cadarache, France. A feasibility study for such an experimental programme is underway and should provide soon a finalised project including cost and schedule aspects.

REFERENCES

1. C. Grandjean, R. Cauvin, C. Lebuffe, N. Waeckel, French Investigations of High Burnup Effect on LOCA Thermomechanical Behavior. Part Two : Oxidation and Quenching Experiments under Simulated LOCA conditions with High Burnup Clad Material. 24th Water Reactor Safety Information Meeting, Bethesda, Md, USA, October 21-23, 1996.
2. C. Grandjean, R. Cauvin, P. Jacques, Oxidation and Quenching Experiments with High Burnup Cladding under LOCA conditions. Revision of previous data and main trends of recent tests. 26th Water Reactor Safety Information Meeting, Bethesda, Md, USA, October 26-28, 1998
3. H. Uetsuka, T. Furuta, S. Kawasaki, Failure-Bearing Capability of Oxidized Zircaloy-4 Cladding under Simulated Loss-of-Coolant Condition. J. Nucl. Sc. and Tech., 20 (11), pp 941-950, Nov. 1983.
4. J.M. Broughton et al., PBF LOCA Tests Series. Tests LOC3 and LOC5 Fuel Behavior Report. NUREG/CR 2073, June 1981.
5. J.M. Broughton et al., PBF LOCA Test LOC6 Fuel Behavior Report. NUREG/CR 3184, April 1983.
6. E.H. Karb et al., LWR Fuel Rod Behavior in the FR2 in-pile Tests Simulating the Heat-up Phase of a LOCA. KFK 3346, March 1983
7. M. Bruet et al., High Burnup Fuel Behavior during a LOCA Type Accident : The FLASH5 Experiment. IAEA Technical Committee Meeting Behavior of Core Material and F.P. Release in Accident Conditions in LWRs, Cadarache, France, March 16-20,1992.
8. M.C. Billone et al., Test Plan for the Investigation of High Burnup LWR Cladding under LOCA and other Transient Conditions. IPS-263-Rev. 2, ANL Program Review Meeting, Bethesda, Md, October 29, 1998.
9. H. Uetsuka, Experimental Program on High Burnup Fuel Cladding Behavior under LOCA and other Transient Conditions at JAERI. 22nd NSRR Technical Review Meeting, Tokyo, November 9-10,1998.
10. R. H. Chapman et al. Effect of Bundle Size on Cladding Deformation in Loca Simulation Tests. 6th Int. Symp. Zirc. In the Nucl. Ind. ASM STP824, 1984, pp693-708.
11. J. Duco, M. Réocreux, A. Tattegrain, Ph. Berna, B. Legrand, M. Trotabas, In-pile investigations at the Phebus facility of the behavior of PWR-type fuel bundles in typical L.B. LOCA transients extended to and beyond the limits of ECCS criteria, 5th International meeting on Thermal Reactor Safety, Karlsruhe, Sept. 10-13, 1984.
12. E.F. Scott de Martinville, M.R. Pignard, International Standard Problem No. 19: Behaviour of a fuel rod bundle during a large break LOCA transient with a two peak temperature history, CSNI Report No. 133, (1987).
13. E.F. Scott de Martinville, C.R. Gonnier, Thermomechanics of a nuclear fuel bundle submitted to an L.B. LOCA evaluation transient: lessons drawn from the Phebus LOCA program, 9th SMIRT Conference, Lausanne, August 1987.
14. C. Gonnier, S. Fabréga, E. Scott, G. Geoffroy "In pile investigations at the Phebus facility on the behaviour of PWR-type fuel bundles in severe accident conditions beyond the design criteria" SFEN - NUCSAFE 88 Avignon 2, 7 October 1988.
15. Von der Hardt, P., Jones, A.V., Lecomte, C., Tattegrain, A., "Nuclear Safety Research. The Phebus FP Severe Accident Experimental Programme", Nuclear Safety, Vol. 35(2), July-December; 1994, pp. 187-205
16. M. Schwarz, B. Clément, A.V. Jones "Applicability of Phebus_FP Results to Severe Accident Safety Evaluations and Management Measures", FISA-99, EC-Luxembourg, 29Nov-1Dec 1999

An Overview of NRC Research Activities in Probabilistic Risk Analysis

S. Newberry, P. Baranowsky, M. Cunningham
Division of Risk Analysis and Applications
Office of Nuclear Regulatory Research
U.S. Nuclear Regulatory Commission
Washington, DC, USA

The NRC's Office of Nuclear Regulatory Research (RES) program in probabilistic risk analysis includes a spectrum of activities, from basic research to regulatory applications. NRC's program includes developing probabilistic risk assessment (PRA) methods, such as fire risk analysis methods, and tools, such as the standardized plant analysis risk (SPAR) models; applying these methods and tools to assess regulatory issues, such as the importance of operational events; and using the experience in their application to focus further improvements.

1. Introduction

The NRC's research program in probabilistic risk analysis includes a spectrum of activities, from basic research to regulatory applications. The PRA methods and tools developed in NRC's research program support the NRC's four strategic performance goals of: (1) maintaining safety, (2) improving staff regulatory effectiveness, efficiency and realism, (3) reducing unnecessary burden, and (4) increasing public confidence. This research program includes the following:

- Developing and demonstrating methods that improve existing techniques or fill gaps in the current state of PRA technology. Key activities currently underway within this element are developing methods for human reliability analysis, fire risk analysis, and consideration of aging effects in PRAs.

- Developing and demonstrating advanced models and tools for use by the NRC staff and others performing risk assessments. For the past several years, the staff has been developing its SPAR models for use in a variety of regulatory applications. In concert with this, the staff has been making improvements to its systems analysis program for hands-on integrated reliability (SAPHIRE) computer software to ensure user-friendly interfaces with the SPAR models, as well as with other PRAs available in the SAPHIRE data base.

- Collecting and assessing plant operational data. The staff works closely with the reactor industry to use data from licensee event reports and other sources to assess the reliability of key reactor systems as well as trends in industry performance. These programs include the Accident Sequence Precursor (ASP) program and also the Risk Based Performance Indicator (RBPI) program.

- Reviewing risk assessments performed by licensees or the staff. The key activities in this element have been the reviews of the individual plant examinations of external events (IPEEE) that were performed by licensees of each U.S. nuclear power plant in response to an NRC request in Generic Letter (GL) 88-20.[1] The reviews were completed in 2001.

- Performing risk analyses on NRC-regulated facilities. The staff is performing a risk assessments of dry cask fuel storage devices, as part of a larger office effort supporting the regulation of spent nuclear fuel; circumferential cracking of reactor pressure vessel head penetration nozzles; and assessment of debris accumulation on PWR sump performance (GSI-191[2]).

- Using PRA results and perspectives to identify possible changes to NRC's reactor safety requirements. The staff has been applying PRA methods and tools to assess possible changes to the technical requirements of 10 CFR 50 (including specific work on changes to 50.44,[3] 50.46,[4] and 50.61[5]), to technical issues facing the staff, including the assessment of steam generator performance during severe accidents, and the development of risk-based performance indicators that objectively measure aspects of reactor licensee performance and can be used to enhance the agency's reactor oversight process.

- Using the results of operating experience and regulatory applications to define better PRA methods and tool improvements. The staff has recently completed a review of fires in nuclear power plants. This review focused on the adequacy of current fire PRA methods and identified a limited number of areas where these PRAs may need to be expanded. The results of the review are being incorporated into plans for additional fire PRA research.

While the above list does provide a current overview and highlight of the PRA activities in RES, it is not a comprehensive list of all the current or future programs in RES. Each of the topics listed above is discussed in more detail below.

2. Developing and Demonstrating Methods that Improve Existing Techniques or Fill Gaps in the Current State of PRA Technology

Human Reliability Analysis

Recent research and development work conducted in the area of human reliability analysis (HRA) has focused on the development of A Technique for Human Event Analysis (ATHEANA).[6] ATHEANA is an HRA method aimed at addressing the issue of scenario-specific context and a particularly challenging topic in HRA: the treatment of errors of commission. ATHEANA's underlying premise is that significant human errors occur as a result of a combination of influences associated with plant conditions and specific human-centered factors that trigger error mechanisms in the plant personnel. This premise requires the identification of these combinations of influences, called the "error-forcing contexts," and the assessment of their influence. Recognizing that the ATHEANA development process has made sufficient progress to allow its application in actual regulatory applications (e.g., the analysis of pressurized thermal shock scenarios in support of a potential change to 10 CFR 50.61[5]), and that the NRC has a broad range of HRA research and application needs which need to be addressed, the NRC staff has developed an HRA Research Program Plan to guide its efforts in the next few years.

Continuing research and development work in the HRA program focuses on finalizing the ATHEANA quantification process (including uncertainty); collection and analysis of human reliability data sources; development of HRA guidance for reviewers; the treatment of latent errors in PRA; extension of advanced HRA concepts to include ex-control room activities, low-power and shutdown conditions, long-term recovery actions, and severe accident conditions; and development of formalized HRA methods for screening, cognitive modeling, and crew modeling. Application-oriented tasks in the program provide integration of advanced HRA methods into topics such as pressurized thermal shock, fire risk analysis, steam generator tube failure under severe accident conditions, aging cables in nuclear

power plants, nuclear materials and waste PRA, synergistic effects on safety, and upgraded/advanced control room layouts.

Fire Risk Analysis

RES initiated a research program in 1998 to develop improved fire risk assessment (FRA) methods. The office decided to improve the existing FRAs for two reasons: 1) internal fires are important contributors to the core damage frequency for some plants and 2) disagreements regarding key details of current FRA methods produce variability in the FRA results.

Significant results from four major tasks of the program are presented below.

1) Development of a revised approach for analysis of circuit failures that can occur due to fire-induced contact between one or more energized electric cables ("hot shorts")

Staff reviews of fires at operating plants and experimental fire data found that spurious component operations have occurred (e.g., Browns Ferry Fire and others). However, the significance of these findings for any particular plant situation will vary greatly depending upon many factors (e.g., sequencing and duration of the short(s), circuit design features, reliability of circuit protection features, effects on plant instrumentation and subsequent effects on operator actions).

The staff concluded that the hot short probabilities used in FRAs should be a function of certain identified cable failure modes, circuit design features, and scenario- specific factors and also that the evaluation of fire-related risk should consider possible combinations of cable failure modes and their timing/duration. The staff developed a set of pre-selected base cases that represent relatively simple cable configurations and applications. A distribution for the failure mode of interest is assigned to each base case. These distributions are based either on actual test data or recommendations from a panel of experts.

Once the analyst chooses the best base case for their analysis, the analyst adjusts the base case failure mode likelihood distribution to reflect the influence factors that are characteristic of the specific application of concern. The influence factors impacting each base case are some subset of the influence factors previously identified. For example, for a two-conductor control cable in conduit, the influence factors might include existence of a three-conductor rather than a two-conductor cable, or co-existence of more than one cable in the conduit of interest. For each factor or combination of factors, the analyst modifies the base distribution. The result is a case-specific probability distribution for the specific failure mode of interest.

2) Joint Industry and NRC Fire Experiments

These experiments determined the conditional probability of specific cable failure modes (i.e., hot short, short to ground, open circuit, and electrical insulation resistance degradation) given cable damage due to a fire. The experiments involved placing multiple instrumentation type cables (with one or more conductors per cable) in an open cable tray and then exposing the cables to a fire located several feet below the tray. Energized conductors and other cables were connected to simulated loads which helped to determine the effects on actual loads (e.g., valve actuators) in a nuclear power plant. Insulation resistance between multiple pairs of conductors and cables were also measured using equipment designed specifically for that purpose.

The significant results and conclusions from the test program are the following:

- multi-conductor cables in trays tend to short conductor to conductor first before shorting to ground,
- single conductor cables tend to short to ground first (but not always),
- the insulation resistance test cables routed in conduit fail only by shorting to ground (no other failure modes were detected),
- no open circuit failures detected during any of the tests,
- instrument cables with thermoplastic insulation fail suddenly (with no significant prior degradation), and
- instrument cables with thermoset insulation show noticeable signs of degradation prior to failure.

3) Development of a revised approach for estimating the frequency of challenging fires (sometimes referred to as "severity factors")

This task developed a practical, mechanistic, improved methodology for defining, characterizing, and quantifying the frequency of nuclear plant fire scenarios. The new method provides a mechanistic link between fire initiation and subsequent fire modeling. Current methods embed this link in the "severity factor" and pilot fire assumptions. The mechanistic approach is intended to eliminate or control optimistic and pessimistic assumptions, improve realism, and enhance clarity. The new approach models how ignition occurs and progresses to the burning of a large source of fuel, while inherently treating uncertainties.

This task also defined fire initial phase scenarios (FIPS) that are applicable to certain locations in nuclear power plants and proposed a method for using FIPS in other locations. The FIPS have well-defined characteristics specified by probability distributions that will support subsequent fire modeling. Also included in this task is the development of an approach for adapting current data to the new model using expert judgment. As for future improvements, this task defined a path to improve data collection that would better support the new approach for estimating the frequency of nuclear plant fire scenarios.

4) Development of a revised approach for detection and suppression analysis

This task developed data and tools for modeling the process of fire detection and suppression in a fire PRA. As part of organizing the data and making it more useful for analysis, a preliminary version of a fire events database is currently under development at the NRC. This database will include over 350 nuclear power plant fires occurring between 1986 and 1999. The information in the database will be used to develop fire detection and fire suppression event trees.

Regarding fire detection, the staff developed methods to approximate the fraction of fires typically detected "promptly" as well as by automatic equipment within the context of the fire events database reviewed. The approximations nominally imply that many fires may be detected through delayed manual detection.

Through a review of experience and through the development of representative system fault trees, the staff estimated the availability of the automatic suppression system and their dominant failure modes. Estimates of the fractions of fires suppressed by various means, for both offsite and onsite fires, and for different building locations were developed. Also, automatic and manual suppression time estimates (including uncertainty analyses) were developed for both internal and external onsite fires, for various suppression methods and selected building locations.

Fire detection timing was identified as a specific area of deficiency in the fire events database. In the vast majority of fire events, the time of fire ignition is not known, whereas the time of fire detection is generally specified. Hence, fire durations cited in the fire event reports were interpreted as the time between fire detection and fire suppression.

Considering Aging Effects in PRAs

The incorporation of the effects of the aging of structures, systems, and components (SSCs) is one of the activities in the NRC research program in PRA. The emphasis in this work is on passive SSCs because the aging of these SSCs is expected to dominate the risk from the aging of SSCs. Active components are assumed to be replaced or overhauled before their aging becomes an important contributor to risk. The need for the use of reliability physics models to estimate the failure probability of SSCs arises because of the lack of failure data. A feasibility assessment using reliability physics models has been completed.[7] In this feasibility assessment, the effect of flow accelerated corrosion of piping on the core damage frequency of a nuclear power plant was evaluated. The piping being considered was that of the main feedwater system of a PWR, and pre-heater steam generator piping. Current work involves estimating the risk from in-containment instrumentation and control cables failures in the harsh environment after a loss of coolant accident (LOCA), and how this risk varies with the aging of the cables.

Because the use of reliability physics models is resource-intensive, an important part of the method is the selection of the components whose failure probabilities are to be estimated by reliability physics models. Importance measures are used here. In-containment instrumentation and control cables in redundant trains of a system are exposed to the same or similar environments during normal operation, and may be exposed to the same or similar harsh environments after a LOCA. As a result, the likelihood of failure of the cables in one train of a system after a LOCA, given failure of the cables in another train of the system, may be high. Consequently, it is appropriate to use importance measures for the sets of cables associated with the redundant trains, rather than single component type importance measures. An importance measure consisting of an approximate estimate of the conditional frequency of core damage, given failure of the cables, times an approximate estimate of the probability of failure of the cables, seems appropriate. The reliability physics models for estimating the failure probabilities of the cables are based on existing models of cable aging such as the Arrhenius model for aging due to temperature. Parameters in the model are assigned distributions in order to estimate the failure probability of the cable. The model also includes the random variation in the containment environment after a LOCA, due to randomness in the size and location of the LOCA. Once the failure probabilities as a function of plant age are obtained, they are input into a PRA calculation. Condition monitoring techniques and aging management strategies used throughout the lifetime of the reactor could modify the PRA calculations.

3. Developing and Demonstrating Advanced Models and Tools for Use by the NRC Staff and Others Performing Risk Assessments

Developing Standardized Plant Analysis Risk (SPAR) Models

In order to provide the NRC staff with analytical tools to use in performing risk-informed activities, the RES is developing Standardized Plant Analysis Risk (SPAR) models.

The SPAR models are plant (or plant class)-specific PRA logic models which have been constructed using the agency's SAPHIRE suite of PRA codes for event tree/fault tree analysis and uncertainty calculations. The SPAR models provide the logic, data, and distributions for producing estimates of risk

(including uncertainty). The SAPHIRE codes calculate cut sets and provide frequencies and importance measures by propagating data and distributions through the models.

SPAR model development spans the following areas:

- Level 1 SPAR models for analyzing events/conditions/findings occurring during full power operation.
- Level 1 SPAR models for analyzing events/conditions/findings occurring during shutdown and low power operation.
- Level 2/Large Early Release Frequency (LERF) models for analyzing containment-related events/conditions/ findings under Regulatory Guide 1.174.[8]
- External Events Analysis Capability - for analyzing events/conditions/findings involving external event initiators (fires, floods, seismic events).

The models consist of analytical tools for use by the NRC staff in the following regulatory activities undertaken in pursuit of the NRC's four performance goals:

- To determine the risk significance of inspection findings [Significance Determination Process (SDP) Phase 3] or of events to decide: (a) the allocation and characterization of inspection resources, (b) the initiation of an inspection team, or (c) the need for further analysis or action by other agency organizations.
- To determine the risk significance of events as input to enforcement severity evaluations and temporary enforcement discretion.
- To support risk-informed decisions on plant-specific changes to the licensing basis as proposed by licensees, and provide risk perspectives in support of the agency's reviews of licensees' submittals.
- To perform various studies performed in support of regulatory decisions as requested by the Commission and other Office of Nuclear Reactor Regulation (NRR) branches.
- To estimate the risk significance of events and/or conditions at operating plants so that the agency can analyze and evaluate the implications of plant operating experience in order to: (a) compare the operating experience with the results of the licensees' individual plant examinations/probabilistic risk assessments (IPEs/PRAs), (b) identify risk conditions that need additional regulatory attention, (c) identify risk insignificant conditions that need less regulatory attention, and (d) evaluate the impact of regulatory or licensee programs on risk.
- To provide rigorous and peer reviewed evaluations of operating experience thereby demonstrating the agency's ability to analyze operating experience independently of licensees' risk assessments and enhancing the technical credibility of the agency.
- To screen and analyze operating experience data in a systematic manner in order to identify those events or conditions which are precursors to severe accident sequences.

- To provide the capability for resolution of generic/safety issues, both for screening (or prioritization) and more rigorous analysis to determine if licensees should be required to make a change to their plant or to assess if the agency should modify or eliminate an existing regulatory requirement.

- To assist in the identification of threshold values for performance indicators in the reactor oversight process (ROP) as discussed in the SECY-01-0111 "Development of an Industry Trends Program for Operating Power Reactors."[9]

Thus far, the SPAR Model Development Program has accomplished the following:

- Developed simplified, Level 1, Revision 2QA models for all operating plants that are used in accident sequence precursor (ASP) and other analyses.

- Produced 48 (out of a planned total of 70) Level 1, Revision 3i (where "i" stands for interim) SPAR models for analysis of events/conditions/findings occurring during full power operation.

- Completed the onsite QA review of Revision 3i SPAR models for 12 plants.

- Produced two SPAR models for analysis of events/conditions/findings occurring during low power and shutdown operations that are based on the detailed low power/shutdown probabilistic risk assessments of the Surry pressurized water reactor (PWR) and the Grand Gulf boiling water reactor (BWR).

- Produced preliminary templates and associated guidelines for developing additional low power/shutdown SPAR models for: all PWRs, BWR 5/6s, and BWR 4s.

- Produced preliminary LERF models for 6 PWRs and 2 BWRs.

- Produced preliminary, limited scope, Level 2 models for 8 PWRs and 2 BWRs.

Developing the Systems Analysis Program for Hands-on Integrated Reliability Evaluations (SAPHIRE)

The NRC in conjunction with Idaho National Engineering and Environmental Laboratories (INEEL) developed the SAPHIRE (Systems Analysis Program for Hands-on Integrated Reliability Evaluations) computer code for performing probabilistic risk assessments (PRAs) using a personal computer (PC). INEEL currently maintains the SAPHIRE code. Most of the developmental activity of SAPHIRE took place during the 1990s as a result of the tremendous expansion of software and hardware PC capability, as well as, the NRC's need for risk analysis tools and databases at the onset of the "risk-informed regulation" era.

SAPHIRE is capable of performing Level 1 PRAs (i.e., modeling a nuclear power plant design and operations and estimating core damage frequencies associated with various initiating events) and Level 2 PRAs (i.e., modeling containment performance under severe accident conditions and estimating radioactive releases). SAPHIRE can also estimate the risk associated with internal and external events under full, low, or shutdown power conditions. SAPHIRE has many special features for performing different types of analyses (e.g., seismic events). A most notable SAPHIRE feature is the automated process for performing analyses using the SPAR models. Due to the NRC's need to evaluate events/conditions/findings in a speedy and effective manner, a separate module was developed called

Graphical Evaluation Module (GEM) which provides a highly specialized user interface. With GEM analysts can easily input parameters associated with the under evaluation events/conditions/findings and automatically generate a estimate.

There are three SAPHIRE versions:

- Version 5 - DOS version, used in the early 1990s,
- Version 6 - Windows/NT version, released in 1998; This is the standard version used by the NRC today, and
- Version 7 - Windows/NT version, Capability expanded to handle very large number of cutsets; This version is continually revised to address NRC's needs in different risk-informed initiatives (for example, the development of Level 2 SPAR models).

SAPHIRE was originally documented in NUREG/CR-6116.[10] Up to date documentation of the changes to the SAPHIRE code are now offered in electronic form on-line. SAPHIRE has been extensively tested and validated. The DOS Version 5 was tested through a traditional verification and validation (V&V) process, documented in NUREG/CR-6116 (Vol. 9).[10] For Versions 6 and 7, an automated testing, validation, and verification process (TV&V) was developed to ensure continual, consistent, reliable, and expedited testing of the code. SAPHIRE TV&V is documented in NUREG/CR-6688,[11] also offered as an on-line SAPHIRE feature.

Along with the development and maintenance of the SAPHIRE code, the NRC also created a SAPHIRE library of PRAs by loading NRC and licensee PRAs into SAPHIRE. The databases and SAPHIRE software can be accessed through the SAPHIRE/INEEL web page. Also a direct link of the NRC's network to INEEL is available for the NRC headquarters staff.

SAPHIRE and associated databases have been and are currently used in a variety of regulatory applications. Some examples are:

- Assessing risk implications of plant design, systems operation, and procedures.
- Assessing the significance of existing or proposed regulations, including the potential for retrofitting (i.e., backfits).
- Evaluating the significance of operational occurrences.
- Performing analyses for licensing new reactors (e.g., AP600).
- Performing pilot studies for regulatory guides on risk-informed regulation (e.g. Reg Guide 1.174).
- Performing pilot studies for revising Part 50 rules (e.g., 50.61, Pressurized Thermal Shock).
- Performing analyses for non-USA plants as part of NRC collaborate efforts with primarily Eastern European countries.

It is noted that SAPHIRE is being used extensively by other US government agencies. The Department of Energy (DOE) is using SAPHIRE extensively in its collaborative efforts with Eastern European countries and has sponsored INEEL to add a Russian language capability in Version 7. Also, NASA has established a policy that SAPHIRE is its official code and, during the last year, has undertaken significant efforts in training NASA staff to use SAPHIRE.

4. Collecting and Assessing Plant Operational Data

Accident Sequence Precursor (ASP) Analyses

The Accident Sequence Precursor (ASP) Program provides a safety significance perspective of nuclear plant operational experience. The program uses probabilistic risk assessment techniques to provide estimates of operating event significance in terms of the potential for core damage. The types of events evaluated include initiators, degradation of plant conditions, and safety equipment failures that could increase the probability of postulated accident sequences.

The primary objective of the Accident Sequence Precursor (ASP) Program is to systematically evaluate U.S. nuclear plant operating experience to identify, document, and rank operating events most likely to lead to inadequate core cooling and core damage (precursors). In addition, the secondary objectives of the ASP Program are:

(1) to categorize the precursors by their plant-specific and generic implications,

(2) to provide a measure for trending nuclear plant core damage risk, and

(3) to provide a partial check on probabilistic risk assessment (PRA)-predicted dominant core damage scenarios.

The program is also used to monitor the agency's performance against the following Strategic Plan goals for maintaining safety:[12]

No more than one event per year which is a significant precursor (i.e., CCDP $\geq 1 \times 10^{-3}$) of a nuclear reactor accident.

No statistically significant adverse industry trends in safety performance.

Since its inception, the ASP Program has published 17 reports documenting the results of its review of operational experience for precursors covering the years 1969–1998. These reports have been issued yearly since 1986.

Accident sequences of interest to the ASP Program are those that would have resulted in inadequate core cooling and severe core damage if additional failures had occurred. Events and conditions from licensee event reports, inspection reports, and special requests from NRC staff are reviewed for potential precursors. These potential precursors are analyzed, and a conditional core damage probability (CCDP) is calculated by mapping failures observed during the event onto accident sequences in risk models. An event with a CCDP or a condition with an importance (i.e., ΔCDP) greater than or equal to 1.0×10^{-6} is considered a precursor in the ASP Program.

The NRC staff uses the ASP methodology and models, and results of ASP analyses to do the following:

(1) Promptly assess the risk significance of operational events to support regulatory decisions by senior management.

(2) In Phase 3 of the significance determination process (SDP), evaluate the significance of inspection findings as part of the agency's reactor oversight process.

(3) Evaluate the change in risk associated with licensing amendments submitted by licensees requesting changes in surveillance frequencies or allowed outage times.

(4) Determine the need for generic communications (such as information notices).

(5) Systematically screen, review, and analyze operational experience data for accident sequence precursors.

(6) Evaluate the generic implications of precursors, trend industry performance, and check against PRAs.

(7) Perform regulatory analyses to resolve generic issues.

(8) Evaluate the risk associated with a specific technical issue identified at a specific plant.

(9) Establish plant-specific performance thresholds and performance baselines to support the development of risk-based performance indicators.

Risk-Based Performance Indicator Development

The purpose of the RBPI development is to examine the technical feasibility of providing enhanced performance indicators for potential implementation in the ROP. RBPIs reflect changes in licensee performance that are logically related to risk and associated models. Phase1 of the RBPI development includes performance indicators that are related to the initiating events cornerstone, mitigating systems cornerstone, and the containment portion of the barrier integrity cornerstone. RBPIs potentially provide more comprehensive coverage of significant contributors to plant risk and their performance threshold values are more plant-specific.

The draft report "Risk Based Performance Indicator Results of Phase-1 Development"[13] was published in February 2001. Three initiating event frequency indicators were identified under the initiating events cornerstone of safety. Under the mitigating systems cornerstone of safety, thirteen potential RBPIs for BWRs and eighteen potential RBPIs for PWRs were identified. These involved unreliability and unavailability indicators with plant-specific performance thresholds at the train-level for risk-significant safety systems and cross-system performance of key components. The final Phase-1 RBPI development report will be published in November 2001. Follow-on work in the RBPI development program includes support for a proposed pilot program beginning in 2002 to evaluate potential plant-specific unreliability indicators for the six mitigating systems under the current Reactor Oversight Process (ROP), as well as changes to the current Safety System Unavailability Performance Indicators (SSUPIs).

5. Reviewing Risk Assessments

Review of Individual Plant Examination of External Events (IPEEE)

On June 28, 1991, the NRC issued Supplement 4 to Generic Letter (GL) 88-20, "Individual Plant Examination of External Events (IPEEE) for Severe Accident Vulnerabilities, 10 CFR 50.54(f)."[1] This GL requested that "each licensee perform an individual plant examination of external events to identify

vulnerabilities, if any, to severe accidents and report the results together with any licensee-determined improvements and corrective actions to the Commission." The external events considered in the IPEEE program include seismic events; internal fires; and high winds, floods, and other (HFO) external initiating events involving accidents related to transportation and nearby facilities. Acts of sabotage or terrorism were not included in the set of events considered. The four supporting IPEEE objectives for each licensee were to (1) develop an appreciation of severe accident behavior, (2) understand the most likely severe accident sequences that could occur under full-power operating conditions, (3) gain a qualitative understanding of the overall likelihood of core damage and fission product releases, and (4) reduce, if necessary, the overall likelihood of core damage and radioactive material releases by modifying, where appropriate, hardware and procedures that would help prevent or mitigate severe accidents.

The NRC received 70 IPEEE submittals covering all operating U.S. nuclear reactors and reviewed them for: (1) an overview of the licensee's IPEEE process and insights; (2) the review process employed for evaluation of the seismic, fire, and HFO events; (3) the dominant contributors to core damage frequency (CDF) for fire, seismic, and HFO events; (4) licensee-identified vulnerabilities; (5) plant improvements made or planned as a result of the licensee's IPEEE process; and (6) an overall evaluation of the strengths and weaknesses of the IPEEE submittal.

As a result of the IPEEE program, over 90% of the licensees have identified and implemented or proposed plant improvements. Many of the IPEEE submittals (70%) reported or proposed seismic-related plant improvements. Over 60% of the licensees reported or proposed fire-related plant improvements. About 50% of the licensees reported or proposed improvements pertaining to high winds and external flooding. These improvements include new procedures or procedural changes, hardware modifications, and enhanced training. Many of the licensees found that seismic and fire events are important contributors to CDF. In fact, CDF contribution from seismic or fire events can, in some cases, approach (or even exceed) that from internal events. The most commonly reported dominant contributors to seismic CDF were failures of offsite power, various electrical system components, and block walls located near safety-related equipment. The most commonly reported risk-dominant fire areas were the main control room, switchgear rooms, turbine building, and cable spreading rooms. The staff reviews also concluded that the IPEEE program verified many of the external event-initiated generic safety issues. Because of the significant effort expended in developing their IPEEEs, licensees have acquired relevant knowledge concerning their plants, and have taken meaningful steps to improve plant safety, operations, and configuration.

Comparing the IPEEE results to other analyses (e.g., the IPE program) is somewhat limited for the following reasons: (a) IPEEEs are intended to yield predominantly qualitative perspectives, rather than quantitative findings, such as in the IPEs; (b) IPEEEs address several different types of initiators of varying importance (for a given plant) and, therefore, require different methods of analysis with varying levels of detail and accuracy; and (c) the procedures and methods used by the various licensees to conduct their IPEEEs have also varied considerably, even for the same type of external event initiator. Therefore, factors such as the IPEEE objectives, level of modeling detail, and assumptions needs to be considered when comparing the IPEEE results to results from other analyses.

Based on the reviews of the IPEEE submittals, the NRC staff has concluded that the IPEEE program has been successful in meeting the overall intent of GL 88-20.

6. Performing Risk Assessments

Dry Casks Risk Analysis

The spent fuel pools of commercial nuclear power plants are becoming filled while the search for a permanent repository continues. To avoid having to cease operations when the pools are full, many utilities have been removing fuel from the pools and storing it in dry casks on site. The NRC Office of Nuclear Materials Safety and Safeguards, which licenses these casks, wants to quantify the risk of dry storage of spent nuclear fuel. This quantification will be used for considering options for risk-informing 10 CFR 72[14] regulatory requirements (including inspection programs), considering various options for safety goal development, enhancing public confidence, increasing regulatory efficiency and effectiveness, reducing unnecessary regulatory burden, and assessing the extent to which data on the performance of the casks in the field need to be improved.

RES is performing a pilot PRA of a spent fuel dry cask storage system, the Holtec International HI-STORM 100. This cask is being studied at a specific BWR site where the operations can be observed and modeled. (Although developed for a specific cask at a specific site, the analytical models developed for this preliminary study can be modified and applied to other dry cask systems at other reactor sites.) During its service life, the cask has three operational modes - handling in the reactor building, transfer to the storage pad, and storage for 20 years. In each of these modes, accidents that could result in mechanical and thermal challenges to the cask and that have the potential to cause the release of radioactive material, are postulated. Event tree/fault tree methods are used to develop logic models of plausible accident sequences. Engineering analyses are used to determine the stresses that would be imposed by the postulated events. Fracture mechanics and other engineering disciplines are used to determine the probability of a cask failing when subjected to postulated accident conditions. A human reliability analysis is used to determine the probability of accidents caused by incorrectly performed procedures, such as when the cask is moved while inside the reactor building or while being monitored during storage.

The preliminary results of the PRA suggest that the risk of the HI-STORM cask at the BWR plant is low compared to the risk of accidents involving the core of operating nuclear power plants. Events that have a high conditional probability of failing the cask have a low frequency (on the order of 10^{-6} per year or less). Conversely, events that occur with a high frequency have a low conditional probability (on the order of 10^{-6} or less) of failing the cask. Furthermore, the consequences of most of the postulated events that fracture the cask and the fuel are low because the energy driving the radionuclides from the fuel pellets is low and the inventory of radionuclides in the fuel pellets is relatively low compared to the reactor inventory. Accordingly, the risk, defined as the product of the frequency and consequences of the events, appears to be low.

Circumferential Cracking of Reactor Pressure Vessel Head Penetration Nozzles

Work useful in assessing the risk significance of this issue was performed. In particular, RES estimated the conditional probability of core damage, given various size LOCAs, using both results from the plant IPEs and the SPAR models. These estimates were obtained for a set of ten plants ranked highest with respect to the likelihood of head penetration nozzle cracking within the next few years. For the conditional probability of core damage, given a medium LOCA, estimates in the range from 1E-3 to 1E-2 were obtained.

Generic Safety Issue -191,[3] Assessment of Debris Accumulation on PWR Sump Performance

For this generic issue, the reduction in core damage frequency associated with eliminating PWR sump screen clogging was estimated. These estimates of core damage frequency reduction were obtained for various sets of plants. A given set of plants was characterized by the likelihood of recirculation sump screen failure for the various size LOCAs. For a set of 31 plants which were almost certain to have sump screen clogging (sufficient to fail ECCS recirculation) on medium and large LOCAs, of which 25 were almost certain to have sump screen clogging on small LOCAs as well, the average core damage frequency reduction from fixing the sump screen clogging problem was about 1E-4/yr. In addition, the monetized benefit associated with fixing the sump screen clogging problem was estimated. Additional regulatory action to address the sump screen clogging was found to be cost-beneficial.

7. Using PRA to Identify Needed Changes in Reactor Safety Requirements

Changing 10 CFR 50.44[4]

As part of the staff's program to risk-inform the technical requirements of 10 CFR Part 50 (Option 3 from SECY-98-300[15]), the staff identified 10 CFR 50.44, "Standards for Combustible Gas Control System in Light-Water-Cooled Power Reactors,"[4] as a regulation that warrants prompt revision. Based upon current risk information and research results, the staff believes that little to no risk significance or benefit is associated with some of the combustible gas control requirements of this regulation, potentially resulting in unnecessary burden. Therefore, the staff has recommended the following changes to the requirements of 10 CFR 50.44[4]:

1. Delete the hydrogen recombiner requirement for all containment types (note, the thermal recombiners installed in currently licensed US reactors to meet design basis hydrogen control requirements are different than the passive autocatalytic recombiners for hydrogen control that are slated to be installed in all French PWRs)
2. For facilities where the hydrogen monitors are only necessary for accident assessment purposes, the monitors would no longer be required to be safety grade

Also as part of this effort, the staff has established Generic Issue 189[16, 17] (GI-189) to assess the costs and benefits of possible additional hydrogen control requirements for PWR ice condenser and BWR Mark III containment designs. Analyses indicate that these containments have a high conditional containment failure probability associated with station blackout sequences during which the AC powered igniters are not available. Therefore, removing the dependence on AC power for the combustible gas control systems could be of value for risk-significant accidents. In support of the resolution of GI-189, the staff is developing more realistic hydrogen source terms (with consideration of uncertainties) and assessing the implications of seismic and fire events on the risk from hydrogen combustion in BWR Mark III and PWR ice condenser facilities.

Changing 10 CFR 50.46[5]

As part of the staff's program to risk-inform the technical requirements of 10 CFR Part 50 (Option 3 from SECY-98-300[18]), the staff identified 10 CFR 50.46, "Acceptance criteria for emergency core cooling systems for light-water nuclear power reactors,"[5] Appendix K to 10 CFR Part 50, "ECCS Evaluation Models,"[18] and General Design Criteria (GDC) 35, "Emergency Core Cooling," of Appendix A to 10 CFR Part 50,[19] as regulations that warrant revision. Based on the results of a feasibility assessment, in the near-term the staff has recommended to the Commission voluntary changes

to the technical requirements of the current 50.46 and Appendix K related to acceptance criteria and evaluation model, and voluntary risk-informed changes to the reliability requirements in GDC 35. While the Commission is considering these recommendations, the staff is continuing the technical work and proceeding with preparations for rulemaking. In the longer term, the staff believes that additional changes to 50.46 may also have merit and is continuing to assess the feasibility of making additional changes, potentially including redefinition of the limiting pipe-break size to be considered in design basis LOCA analyses.

The proposed near-term changes to the current 50.46 and Appendix K 5[21] include (1) replacing the current prescriptive ECCS acceptance criteria in 50.46 with a performance-based requirement, and (2) revising the requirements for the ECCS evaluation model to optionally allow the model to be based on more realistic analyses. The proposed risk-informed changes to GDC 35 would include technical requirements to ensure an ECCS reliability that is commensurate with the frequency of challenge to systems. Two options are being considered to accomplish the ECCS system reliability in place of the single failure criterion: (1) a deterministic system reliability requirement based on risk information (e.g., and ECCS design requirement that only one train of ECCS is required for LOCAs larger than a specified size), and (2) an ECCS functional reliability requirement that is commensurate with the LOCA frequency (e.g., a requirement that ECCS design must be such that the core damage frequency [CDF] associated with a specified set of LOCAs is less than an NRC-specified CDF threshold). In addition, consideration is being given to relaxing the coincident loss-of-offsite power (LOOP) assumption for large-break LOCAs.

8. Using Operating Experience and Regulatory Applications to Define Needed Improvements

Reviewing the Adequacy of Fire PRAs[20]

The staff recently completed and published a review of fires in nuclear power plants that was focused on the adequacy of current fire PRA methods. The study was based on 25 fire incidents, 12 of which were in non-U.S. plants. The sequence of events observed in each fire incident was examined and compared to typical assumptions and practices of fire PRA. The review focused on two categories of events: 1) events that illustrate interesting insights regarding factors that fall within the scope of current fire PRA methods and 2) events observed in actual fire incidents that fall outside the scope of current fire PRA methods. (Although not an intended focus of the review, certain observations were also made regarding differences between fire incidents in Western and Soviet-design plants.)

In the first category of events, the incidents demonstrated that smoke propagation can impact the effectiveness of the operators and fire fighters. Current fire PRA methods remain weak in their treatment of smoke effects. Turbine building fires and fires involving non-safety related areas of the plant are generally screened out in the initial stages of a fire PRA. Reviewed incidents indicate that complications from such fires (e.g., smoke propagation and operator error during plant shutdown) may lead into event sequences otherwise considered as very unlikely. There is a potential that such sequences, which are typically screened out in the internal events analysis, may not be picked up in a fire PRA.

In the second category, the incidents have demonstrated that current methods do not address the possibility of multiple initial fires, secondary fires and multiple initiating events. Several fire incidents involved multiple fires ignited at different locations of the plant due to a single root cause (multiple initial fires). In a few cases, additional fires ignited due to damage caused by the original fire (secondary fires). Current fire PRA methodologies do not include an explicit provision for identifying such fire scenarios. Also, a fire incident may be a part of an event involving several distinctly different hazards

(or initiators). For example, several incidents involved a turbine blade ejection incident leading to a fire, and/or involved a fire concurrent with substantial plant flooding. These types of events are not included in the scope of a typical fire PRA.

Thus, the review identified several areas of potential methodological improvement (i.e., the first category above), and it also identified factors that fall outside the scope of current PRAs (i.e., the second category above). However, the review concluded that the overall structure of a typical fire PRA can appropriately capture the dominant factors involved in a fire incident.

Although not in the intended scope of the review, the review also included a substantial number of fire events in U.S. and also in non-U.S. plants. Comparing the U.S. and non-U.S. plants enabled the staff to make observations regarding the substantial differences that appear to exist in the progression and outcome of fire incidents between Western and Soviet-design plants. These differences are likely a reflection of differences in design, construction and maintenance practices and materials selection, particularly as related to cables and electrical systems.

This review identified six fires that have seriously challenged nuclear safety at an operating reactor. In the U.S., the only such fire incident was the 1975 Browns Ferry fire. Since that time, many plant improvements specifically aimed at enhancing the fire safety of U.S. plants have been implemented. These improvements derive primarily from implementation of the 10CFR50 Appendix R requirements that were a direct result of the Browns Ferry fire. The lack of any fires that have significantly challenged nuclear safety at any plant in the U.S. since 1975 is likely a reflection of these fire protection enhancements.

For the Soviet-designed reactors, this review identified four fires occurring between 1978 and 1988 that presented equal or perhaps greater safety challenges than the Browns Ferry incident. The sixth seriously challenging fire occurred at the Narora plant in India, which is substantially different from either U.S. or Soviet designs. In each of these incidents, the post-fire recovery efforts benefitted from reactor design features that allowed a substantial time (several hours) to recover core cooling functions before the onset of core damage. It is also noteworthy that the review did not identify any major fire events in Soviet-designed plants since 1988. Since the mid-1980s substantial effort has been made to upgrade fire safety at plants in Russia and other countries with Soviet-designed reactors. This includes the application of fire retardant coating on cables, upgrading the fire barriers, improved fire suppression systems, and improved protective gear for plant operators and fire fighting personnel. As with the U.S. improvements, the improved safety measures may be a significant contributing factor to the lack of fires leading to a significant nuclear safety challenges since 1988.

9. Conclusions

The NRC's RES program in probabilistic risk analysis continues grow and improve in order to better support agencies goals. The goal of both current and future projects is to improve the safety, efficiency, and effectiveness of regulatory activities. RES intends to accomplish these goals by identifying gaps in and developing new PRA methods and tools. By applying these methods and tools, RES will continue to be an integral part of resolving regulatory and safety issues.

10. References

1. Generic Letter 88-20, "Individual Plant Examination for Severe Accident Vulnerabilities - 10 CFR 50.54(f)." U.S. Nuclear Regulatory Commission, November 23, 1988.

2. NUREG-0933, "A Prioritization of Generic Safety Issues - Generic Safety Issue-191, Assessment of Debris Accumulation on PWR Sump Performance." U.S. Nuclear Regulatory Commission, June 2000.

3. Code of Federal Regulations, *Title 10, Energy*, Part 50.44, "Standards for combustible gas control system in light-water-cooled power reactors."

4. Code of Federal Regulations, *Title 10, Energy*, Part 50.46, "Acceptance criteria for emergency core cooling systems for light-water nuclear power reactors."

5. Code of Federal Regulations, *Title 10, Energy*, Part 50.61, "Fracture toughness requirements for protection against pressurized thermal shock events."

6. USNRC, "Technical Basis and Implementation Guidelines for A Technique for Human Event Analysis (ATHEANA)," NUREG-1624, Revision 1, May 2000.

7. NUREG/CR-5632, "Incorporating Aging Effects into Probabilistic Risk Assessment -- a Feasibility Study Utilizing Reliability Physics Models." U.S. Nuclear Regulatory Commission, August 2001.

8. Regulatory Guide 1.174, "An Approach for using Probabilistic Risk Assessment in Risk-Informed Decisions On Plant-Specific Changes to the Licensing Basis." U.S. Nuclear Regulatory Commission, July 1998.

9. SECY-01-0111, "Development of an Industry Trends Program for Operating Power Reactors." U.S. Nuclear Regulatory Commission, June 2001.

10. NUREG/CR-6116, Vol. 10, "Systems Analysis Programs for Hands-on Integrated Evaluations (SAPHIRE) Version 5.0." U.S. Nuclear Regulatory Commission, April 1995.

11. NUREG/CR-6688, "Testing, Verifying, and Validating SAPHIRE Versions 6.0 and 7.0." U.S. Nuclear Regulatory Commission, October 2000.

12. NUREG-1614, "Strategic Plan, Fiscal Year 2000 - Fiscal Year 2005, Vol. 2, Part 1." U.S. Nuclear Regulatory Commission, February 2000.

13. DRAFT NUREG, "Risk Based Performance Indicator Results of Phase 1 Development." U.S. Nuclear Regulatory Commission, February 2001.

14. Code of Federal Regulations, *Title 10, Energy*, Part 72, "Licensing Requirements for the Independent Storage of Spent Nuclear Fuel and High-Level Radioactive Waste."

15. SECY-98-300, "Options for Risk-informed Revisions to 10 CFR Part 50 - 'Domestic Licensing of Production and Utilization Facilities'." U.S. Nuclear Regulatory Commission, December 1998.

16. Memorandum to John Flack from Mark Cunningham. "Information Concerning Generic Issue on Combustible Gas Control for PWR Ice Condenser and BWR Mark III Containment Designs," U.S. Nuclear Regulatory Commission, August 15, 2001.

17. SECY-01-0162, "Staff plans for proceeding with the risk-informed alternative to the standards for combustible gas control systems in light-water-cooled power reactors in 10 CFR 50.44." U.S. Nuclear Regulatory Commission, August 2001.

18. Code of Federal Regulations, *Title 10, Energy*, Part 50 Appendix K, "ECCS Evaluation Models."

19. Code of Federal Regulations, *Title 10, Energy*, Part 50 Appendix A, " General Design Criteria for Nuclear Power Plants - Criteria Number 35 'Emergency Core Cooling.'"

20. NUREG/CR-6738, "Risk Methods Insights Gained From Fire Incidents." U.S. Nuclear Regulatory Commission, September 2001.

Pressurized Thermal Shock Risk Assessment

Donnie Whitehead and Vince Dandini - Sandia National Laboratories
Alan Kolaczkowski - Science Applications International Corp.
Eric Thornsbury, Nathan Siu, and Roy Woods - US Nuclear Regulatory Commission

ABSTRACT

The U. S. Nuclear Regulatory Commission Office of Nuclear Regulatory Research is developing the technical basis for modifying the Pressurized Thermal Shock (PTS) screening criteria specified in title 10 Part 50.61 of the U. S. Code of Federal Regulations. As part of this effort a probabilistic analysis of the risk posed by PTS in U. S. pressurized water reactors is being performed. This analysis is an update of previous studies that were done in the early to mid 1980's that supported the development of the original (present) version of the rule. The current analysis will incorporate improvements made in probabilistic risk analysis, thermal-hydraulics, and probabilistic fracture mechanics since the original analyses were performed. The overall objective of this effort is to produce realistic risk input to support the re-evaluation of the PTS screening criteria.

1. Overview

The pressurized thermal shock (PTS) phenomenon is a safety concern for pressurized water reactor nuclear power plants. During normal operation, the 6-8 inch-thick steel reactor vessel is maintained at temperatures over 500°F. If a transient occurs which forces colder water near the inner surface of the vessel, a stress due to this thermal shock is created across the vessel wall. There is then a possibility that an existing flaw in the reactor vessel may initiate a crack in the vessel wall. Additional stress due to high pressures in the reactor vessel will increase the overall stress with the possibility of propagating the crack through the vessel wall. If this pressurized thermal shock event progresses to become a "through-wall crack," potentially serious consequences may occur. Another important aspect of the phenomenon occurs as the reactor vessel ages. As the amount of radiation (fast neutron flux) the vessel experiences increases, the fragility of the vessel also increases, raising the likelihood of a through-wall crack.

The objectives of this paper are to provide an overview and summarize the current status of the effort by the U. S. Nuclear Regulatory Commission Office of Nuclear Regulatory Research to re-evaluate the Pressurized Thermal Shock Rule [1]. The PTS rule is located in title 10, Part 50.61 of the U. S. Code of Federal Regulations and is supported by Regulatory Guide 1.154 [2]. The rule consists of a screening criteria based on reactor vessel characteristics and proscribes progressive actions for those nuclear power plants which are projected to exceed the limit. These actions may include neutron flux reduction, plant modifications, thermal annealing of the reactor

vessel, plant specific safety analysis, or closure of the plant. The current version of the rule was created during the early to mid 1980's. Since then, improvements in various technologies have created the need to re-examine the PTS rule.

Motivation for this re-evaluation is driven primarily by improvements in the field of probabilistic fracture mechanics (PFM), though improvements are also evident in probabilistic risk assessment (PRA) and thermal hydraulics (TH). Advances in PFM include a better understanding of the size and distribution of flaws in reactor vessels due to the examination of multiple reactor vessels since the early 1980s. This produces a better understanding of the physical characteristics of real reactor vessels which may indicate the presence of excessive margins in the previous analyses. Therefore, a fresh look at the problem will yield a better understanding of risk due to PTS and enable the agency to maintain safety while potentially reducing unnecessary burden on licensees through more realistic and efficient regulation.

2. Technical Approach

One of the goals of the pressurized thermal shock re-evaluation project is to have an open process including participation from the public and the licensees. The analysis approach will consist of plant-specific PTS risk evaluations of a sample of four US nuclear power plants (pressurized water reactors). Staff from these four plants are voluntarily participating in all aspects of the projects, from providing initial data on plant characteristics and operator behavior to review and comment on the process and results. For the PRA portions of the analysis, two of the plants will be modeled by the NRC and its contractors, while the utilities will provide models for the other two plants. More specific information on the technical approach will be discussed throughout this section.

Challenges

Two significant technical challenges are being faced in the PTS re-evaluation project. This is not to say that these challenges are unique to PTS; on the contrary, any in-depth engineering analysis of risk will likely face similar obstacles. But in this project, these challenges play a vital role in the validity of the outcome. The approach to meeting these challenges, however, is a somewhat innovative approach which may be useful to future engineering analyses.

The first challenge is that of interdisciplinary cooperation. An analysis of this type includes specialists in the areas of probabilistic risk assessment, thermal hydraulics, and probabilistic fracture mechanics. The challenges of cooperation, communication, consistency, and integration among these disciplines are not trivial. The solution imposed upon this challenge for PTS was to create an integrated framework from which all disciplines would work. Details of this framework are discussed below.

The second challenge of significance involves operator actions. PTS transients have the capability to produce conditions which are very challenging to the plant operators. Analysis of these conditions is vital to obtaining a solid understanding of human performance. Identification and quantification of the human actions of concern must be performed in such a way to include

credit for actions which are likely to be taken by the operators, but also must search for vulnerabilities of the operators to take incorrect actions, including so-called "errors of commission." Detailed discussion of the approach to this challenge follows the description of the integrated framework.

Integrated Framework

To meet the challenge of interdisciplinary cooperation, an "Integrated PTS Framework" was created. This framework, which can be seen in Figure 1, serves two important purposes. First, it serves as an outline for the analysis procedure. Second, it provides the structure by which the varying disciplines can be integrated. The framework identifies the places in the analysis where cooperation and interaction are necessary. It points out the needed information feedback and feedforward loops, and it ensures a consistent approach is taken to the treatment of uncertainties. The following paragraphs will walk through the framework and explain each element.

The first box on the left of Figure 1 is labeled "PRA Event Sequence Analysis". The box represents the probabilistic risk assessment discipline. For this project, the PRAs were performed using the SAPHIRE code [3]. The analysis begins by examining a number of initiating events (IE_1, IE_2, ...) such as loss of coolant accidents and steam line breaks. The PRA then models the response of the plant equipment and operators to the initiating event using event trees. Each branch on an event tree represents the performance of a safety function. So a specified path

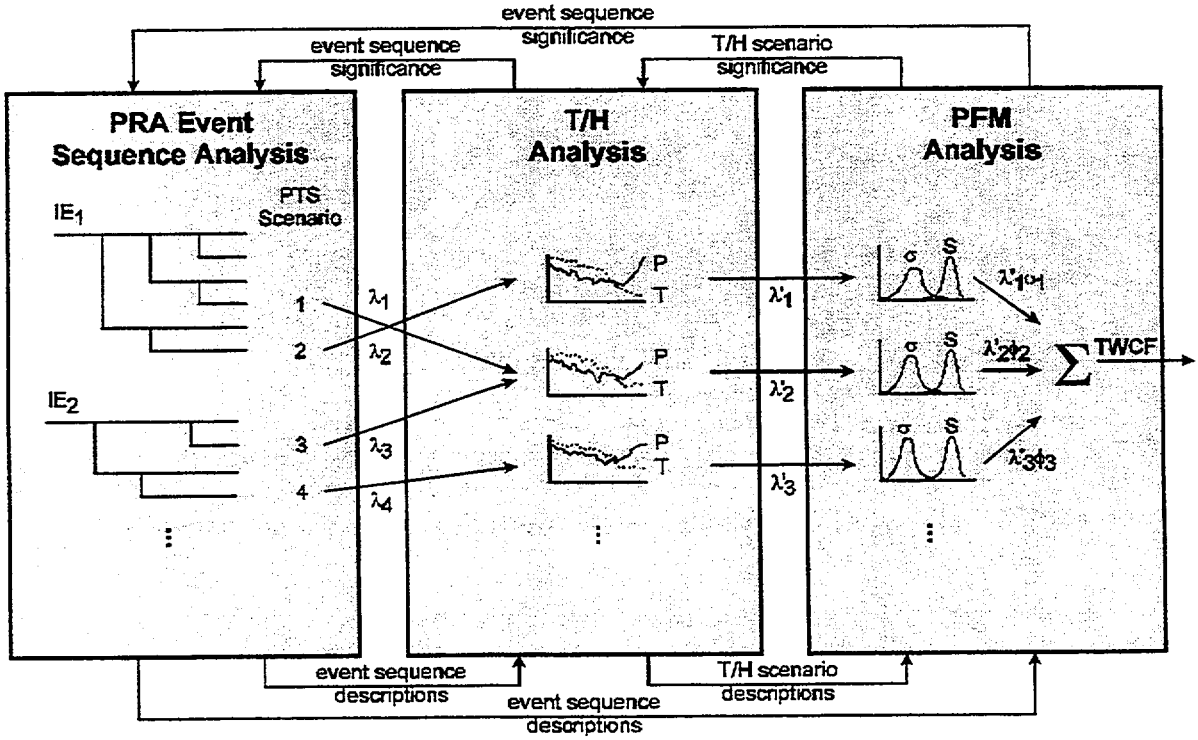

Figure 1. Integrated PTS Framework

through an event tree (called an accident sequence) defines a unique set of plant performance characteristics. Any accident sequence which may produce a temperature and pressure stress on the reactor vessel is identified as "PTS Scenario" (labels 1, 2, 3, 4, ...). The frequency of each PTS scenario is calculated and indicated by λ.

In the interface between the PRA Event Sequence Analysis and the T/H Analysis boxes, a critical step is performed. The PRA model is capable of producing hundreds of thousands of sequences. The thermal hydraulics analysis is not able to individually perform this many calculations. So a process is performed known as "binning." During the binning process, two or more accident sequences which are expected to have similar thermal hydraulic effects are grouped together into one "bin". This is demonstrated in Figure 1 by PTS scenarios 1 and 3. The arrows proceeding from each of these scenarios indicate that they are passed to the same point in the T/H Analysis box. PTS scenarios 2 and 4 are unique enough to warrant individual bins. This processed is performed on the thousands of PRA accident scenarios until the number is reduced to an acceptable level for thermal hydraulic analyses.

The center box on the Integrated PTS Framework is labeled "T/H Analysis," for the thermal hydraulic modeling of the accident sequences. In the PTS re-evaluation project, the TH calculations were performed using RELAP5/MOD3.2.2 gamma [4] with a full plant model (255 nodes). The factor which primarily limits the number of calculations which can be performed is time. A single computer calculation is expected to take approximately six hours, plus considerable time for preparation and post-analysis by the analyst. On the order of 100 TH calculations are expected to be performed for each plant model. The purpose of the TH analysis is to predict the thermal hydraulic characteristics of each bin produced by PRA. The characteristics of interest are temperature at the reactor vessel wall, the pressure on the reactor vessel wall, and the heat transfer coefficient of the reactor vessel wall. Calculations are performed for each bin and the resulting TH information (represented in Figure 1 by plots of P and T) and frequency (λ') are passed to the PFM analysis. Note that where multiple PRA accident scenarios are combined in one bin, the frequencies are added to determine the frequency of the bin ($\lambda_1 + \lambda_3 = \lambda'_2$).

The far-right box in Figure 1 represents the "PFM Analysis." This shows where the probabilistic fracture mechanics calculations are performed. This project is using the FAVOR code [5], a finite element analysis tool which uses linear elastic fracture mechanics to model crack initiation, propagation, and arrest. FAVOR incorporates reactor vessel characteristics such as chemical composition, the neutron fluence history, and distributions of the size and location of flaws. The time, pressure, and heat transfer coefficient data from each TH bin are processed by FAVOR to produce stress/strength (σ/S) comparisons of the reactor vessel to predict the conditional likelihood of vessel failure (ϕ). When these conditional likelihoods are combined with the bin frequencies ($\lambda'_1\phi_1$, $\lambda'_2\phi_2$, ...) and summed (Σ), the frequency of a through-wall crack (TWCF) for a specific plant is produced.

Another aspect of the integrated framework is represented by the arrows above and below the analysis boxes. The top set of arrows show the information feedback processes. The TH and PFM analyses feedback event sequence significance information to the PRA. This provides the PRA with information on the characteristics of significant PTS challenges so that appropriate variation and refinement can be included in the PRA. The PFM analysis also provides similar

feedback to the TH analysis about what types of TH scenario characteristics are important and must be included. Arrows along the bottom of Figure 1 show feedforward information. Descriptions of the event sequences must be passed forward to TH and PFM to ensure realistic modeling. The TH provides further scenario description to the PFM. Though the framework may seem to indicate a serial process, the need for feedback, feedforward, and integration among the disciplines necessitates a somewhat parallel and iterative process.

One additional purpose of the framework is to provide a consistent basis for the treatment of uncertainties. Though nothing is explicitly shown in Figure 1, the integrated nature of the framework is fundamental to a consistent uncertainty analysis. Uncertainties in the PRA event probabilities are propagated through the event trees and into the binning process. The binning step itself introduces additional uncertainty, since each bin may be representable by multiple variations in TH modeling, though only one TH calculation can be performed for each bin. All these uncertainties are carried through to the PFM analysis and those which are quantifiable are included in the final TWCF. Because not all uncertainties in this project can be directly quantified, consideration of the additional uncertainties will be included when the results of the analyses are used for revision of the actual rule.

Operator Actions

The pressurized thermal shock situation creates unique challenges to both the operators and the analysts performing the study. Even in the initial PTS study in the 1980s, it was identified that operator actions have a great impact on the likelihood and progression of PTS scenarios. One particularly difficult aspect of human performance is that in many scenarios, the human operator can decrease the stress on the reactor vessel at any time by controlling the pressure. The specific time at which this action occurs can have drastic effects on the pressure and, therefore, the likelihood of vessel failure.

Another challenging aspect of modeling human actions is related to the uniqueness of the PTS phenomenon. In most nuclear power plant applications, the goal of the operator is to prevent the *overheating* of the reactor core which would lead to core damage. In the case of PTS, the operator is fighting an *overcooling* situation. Actions which may be appropriate to reduce the likelihood of core damage are likely to exacerbate a PTS situation. This phenomenon also introduces a potential source of "errors of commission." Normally, human actions would lead to errors of omission are investigated. For example, an operator may skip a procedure step or fail to actuate a component. An error of commission is one in which an operator takes an action which is inappropriate or unnecessary which places the plant in a more unsafe state. Sometimes, these actions may even be "correct" based on the specific situation. For example, in some accident scenarios, an operator may be directed to initiate a depressurization and cooldown in order to prevent a core damage scenario. From the point of view of PTS, this may increase the likelihood of vessel failure, and therefore be considered an "error" of commission.

For the PTS re-evaluation project, ATHEANA is being applied for the human reliability analysis. ATHEANA (A Technique for Human Event Analysis) is a method developed by the NRC Office of Nuclear Regulatory Research which uses a context-based approach to identify important human events and the conditions which drive them [6]. That is, the context - the combination of

plant conditions and performance shaping factors - of the accident sequence can steer operators into specific actions (both positive and negative). Examination of the context not only provides specific evidence to aid in the quantification of the likelihood of human events, but also provides the necessary detail to use the results of the human reliability analysis to make positive changes to prevent human errors in the future. The PTS re-evaluation project is the first in-depth use of ATHEANA by NRC.

The ATHEANA human reliability analysis for this project uses plant-specific information on operator behavior obtained in coordination with the licensees through plant visits, simulator exercises, examination of procedures, discussions with operators and trainers, and control room tours. The first recently completed analysis produced and quantified approximately 70 human failure events (HFEs). Some of these HFEs were variations of a base case to account for differences in context and timing. One of the human actions which shows a high importance is the throttling of high pressure injection. This action serves to relieve the over-pressure situation which aggravates a PTS scenario. Failure or delay of this action appears to have significant impacts on the severity of a PTS challenge. Another action indicating importance was mentioned earlier as a potential error of commission. A steam generator tube rupture scenario can direct operators to depressurize the reactor in order to limit the leakage through the tubes. This depressurization causes a coincident cooldown, which if not properly controlled, can pose a PTS challenge to the reactor vessel. These actions are evident in the initial results which follow.

3. Initial PRA Results

The work on the four plant-specific analyses is nearing completion. The first plant has completed initial PRA results, binning, and TH calculations and these interim results are in the process of being run through FAVOR. PRA and TH work on the remaining plants is currently scheduled for completion before the end of 2001, with the PFM calculations being wrapped up shortly thereafter. The initial results from the first plant are presented here for discussion purposes, with the caveat that they are not final and remain subject to refinement. Table 1 presents the highest frequency accident sequences from the first plant, the lowest temperature achieved, the pressure at the time the temperature is reached, and an estimate of the severity of the PTS challenge to the reactor vessel. An explanation of each of the accident sequences is also included here. It should be noted that the frequencies appearing here tend to be lower than those calculated in the previous 1980s study [7].

- Stuck-open PZR SV recloses - throttle 1 min

  Following a reactor trip, a safety valve (SV) on the pressurizer (PZR) lifts and sticks open. At some later time during the event, the safety valve recloses due to decreasing pressure in the reactor coolant system. The stuck-open valve causes an overcooling and depressurization, but once the valve recloses, the pressure rapidly increases due to high pressure injection. Once the situation allows, the operators take control of the injection within 1 minute and throttle it according to procedure to control the pressure. For the purposes of this results table, four accident scenarios of this type are consolidated here, including variations on the time the valve recloses and the decay heat in the reactor core.

This event is labeled as a 'medium' challenge to the vessel based on the low temperature obtained and the mild repressurization which occurs.

- Stuck-open PZR Safety Valve

  Following a reactor trip, a safety valve on the pressurizer (PZR) lifts and sticks open. The valve remains open throughout the event since the operators cannot manually close or block the valve. Despite the excessive cooldown, this is considered a 'low' challenge to the reactor vessel because of the continuing low pressure. The frequency includes a variation for decay heat level.

- Small LOCA

  A small loss of coolant accident (LOCA) occurs. For PRA purposes, a small LOCA is defined as one with a diameter from 1.5 - 4 inches. The remainder of the sequence occurs according to expectations. The reactor is significantly cooled, but pressure is also low, leading to an estimate of 'low' PTS challenge. This frequency also includes a variation for decay heat level.

- Stuck-open PZR SV recloses - throttle 10 min

  This set of scenarios is similar to the first set discussed, but the operators take 10 minutes to gain control of the high pressure injection. A similar depressurization and cooldown are experienced, but the repressurization phase goes to a maximum (~2500psia) and remains for approximately 10 minutes. This is labeled as a 'med-high' due to the slow rate of cooling and the limited time spent at high pressure. Variations on reclose time and decay heat are also included.

	Freq (per yr)	Temp/Press	Challenge
Stuck-open PZR SV recloses - throttle 1 min	3E-3	150°F/250psia	medium
Stuck-open PZR Safety Valve	5E-4	85°F/200psia	low
Small LOCA	3E-4	100°F/270psia	low
Stuck-open PZR SV recloses - throttle 10 min	8E-5	150°F/250psia	med-high
SGTR with stuck-open SG Safety Valve	6E-5	400°F/2400psia	low
Stuck-open PZR SV recloses - no throttling	3E-5	150°F/250psia	high
Medium LOCA	3E-5	70°F/200psia	low

Table 1. Initial PRA Results for Plant 1

- SGTR with stuck-open SG Safety Valve

  A steam generator tube rupture (SGTR) initiates the event and a safety valve sticks open on one steam generator (SG). This situation calls for the operators to perform a rapid depressurization and cooldown to limit the leakage through the failed tubes. While this scenario cools down to only about 400°F, the cooldown is rapid and the pressure remains significant. Due to the relatively high minimum temperature, this scenario is being estimated as a 'low' PTS challenge.

- Stuck-open PZR SV recloses - no throttling

  Like the other two similar events in the table, this event begins with a reactor trip with a stuck-open pressurizer safety valve (PZR SV). But in this case, when the valve recloses and the reactor coolant system begins to repressurize, high pressure injection is not throttled. Similarly to the 10 minute throttling case, the repressurization reaches maximum pressure (~2500psia) and remains throughout the calculation, earning a 'high' PTS challenge estimate. A variation on decay heat level is included.

- Medium LOCA

  This event occurs almost identically to the small LOCA, with a slightly faster cooldown and lower pressure. The medium loss of coolant accident (LOCA) accounts for break diameters of 4 - 8 inches in the PRA. With low pressures, it is estimated that the medium LOCA will be a 'low' PTS challenge.

4. Summary and Conclusions

The pressurized thermal shock re-evaluation project currently underway in the Office of Nuclear Regulatory Research faces several challenges. While these challenges are not necessarily unique to the PTS problem, the approaches taken to meet these challenges are somewhat novel and may provide a format for future applications. The integration of the various disciplines involved in the analysis and the effect of human actions on the problem prove to be difficult aspects, but can be accomplished through a structured framework approach to the overall problem.

Indications from initial calculations and improvements in the state of knowledge of the fracture mechanics field point toward a lower calculated risk due to PTS. This decrease can be attributed both to increased realism in the analysis and actual changes in plant operation which lead to fewer initiating events and better operator knowledge of PTS concerns. Final PFM calculations are expected in early 2002 and the technical basis for a possible rule revision is planned for later that year.

5. References

1. U.S. Nuclear Regulatory Commission, "Reevaluation of the Pressurized Thermal Shock Rule (10 CFR 50.61) Screening Criterion," SECY-00-0140, June 23, 2000.

2. U.S. Nuclear Regulatory Commission, "Format and Content of Plant-Specific Pressurized Thermal Shock Safety Analysis Reports for Pressurized Water Reactors," Regulatory Guide 1.154, January 1987.

3. U.S. Nuclear Regulatory Commission, *Systems Analysis Programs for Hands-on Integrated Reliability Evaluations (SAPHIRE) Version 6.0, System Overview Manual*, NUREG/CR-6532, May 1999.

4. U.S. Nuclear Regulatory Commission, *RELAP5/MOD3.3Beta CODE MANUAL Volume 1 to 7*, NUREG/CR-5535, Rev. 1, 2001.

5. U.S. Nuclear Regulatory Commission, *Fracture Analysis of Vessels - Oak Ridge, FAVOR, V01.0, Computer Code: User's Guide*, Oak Ridge National Laboratory, Manuscript Completed: October 9, 2001.

6. U.S. Nuclear Regulatory Commission, *Technical Basis and Implementation Guidelines for A Technique for Human Event Analysis (ATHEANA)*, NUREG-1624, Rev. 1, 2000.

7. T. J. Burns, et al., *Preliminary Development of an Integrated Approach to the Evaluation of Pressurized Thermal Shock Risk as Applied to the Oconee Unit 1 Nuclear Power Plant*, NUREG/CR-3770 (ORNL/TM-9176), Oak Ridge National Laboratory, November 1985.

Risk-Based Performance Indicators and the Inspection Process

Hossein G. Hamzehee

Operating Experience Risk Analysis Branch
Office of Nuclear Regulatory Research
United States Nuclear Regulatory Commission

Abstract

This paper presents the status of Phase-1 of the Nuclear Regulatory Commission's (NRC's) Risk-Based Performance Indicator (RBPI) development program and results. It also provides a summary of planned follow-on activities that will be performed to support the Reactor Oversight Process (ROP).

Status of Phase-1 RBPI Development

The draft Phase-1 RBPI development report was issued in January 2001, after which two public meetings were held in February and April 2001 to discuss it contents. Results of the draft report were presented to the NRC's Advisory Committee on Reactor Safeguards (ACRS) in April 2001. Comments from the ACRS and external stakeholders were received in mid-2001, after which they were resolved and incorporated into a revised report. The final Phase-1 RBPI development report will be issued in November 2001.

Summary of Phase-1 RBPI development Results

Three potential full-power internal initiating event (IE) RBPIs were identified for each plant under the IE cornerstone of safety. For these IE RBPIs, plant-specific threshold values were determined for 44 plants (19 BWRs and 25 PWRs) based on the NRC's Level 1, Revision 3i Standardized Plant Analysis Risk (SPAR) models. The data sources used in selecting the IE RBPIs were NUREG/CR-5750, the NRC's Sequence Coding and Search System (SCSS) Licensee Event Report (LER) database, and the NRC's Monthly Operating Reports (MOR) database.

Under the mitigating systems/components cornerstone of safety, 13 potential full-power internal RBPIs for BWRs and 18 for PWRs were identified. These involved unreliability and unavailability indicators with plant-specific performance thresholds at the train-level for risk-significant safety systems and cross-specific performance of key components. For these mitigating-systems/components RBPIs, plant-specific threshold values were determined for 44 plants (19 BWRs and 25 PWRs) based on the NRC's Level 1, Revision 3i SPAR models. The primary data sources used in selecting the mitigating-systems/components RBPIs were the NRC's system reliability studies (for baseline performance evaluation); the Equipment Performance and Information Exchange (EPIX) database supplied by the Institute of Nuclear Power Operations (INPO) (for reliability data); and the NRC's Reactor Oversight Process (ROP) data (for unavailability data).

Potential containment performance RBPIs were considered. These were unreliability/ unavailability of drywell spray (Mark I BWRs), and unreliability/unavailability of large containment isolation valves (PWRs and Mark III BWRs). Models and data are not currently available for these potential RBPIs to quantify baseline performance values, thresholds, or ongoing performance.

Potential RBPIs during shutdown modes of operation were considered. No IE RBPIs were identified for shutdown modes due to the inability to support timely detection of declining performance. However, four potential RBPIs under the mitigating systems cornerstone of safety for PWRs and BWRs were proposed. They monitor time spent in risk-significant shutdown configurations. The following four shutdown configuration categories were defined based on conditional core damage frequency (CCDF): low, medium, early reduced-inventory (vented), and high. The risk significance of these four shutdown configuration categories were categorized by reactor coolant system (RCS) conditions, time after shutdown, and availability of mitigating system trains. Shutdown RBPIs are being considered for incorporation in the Significance Determination Process (SDP).

No IE RBPIs for fire were identified due to the inability to support timely detection of declining performance. However, mitigating systems/components RBPIs were identified for reliability and availability of the fire suppression system. Data are not currently available for these RBPIs to quantify baseline performance values and thresholds.

The potential Phase-1 RBPIs are summarized in the following table.

Summary of Phase-1 Risk-Based Performance Indicators

Safety Cornerstone	Existing PIs	Proposed RBPIs			
Initiating Event	- Unplanned Scram - LONHR - Unplanned Reactor Power Changes	- General Transient - LOFW - LOHS			
		PWR at Power	**BWR at Power**	**Shutdown**	**Fire**
Mitigating System	- EPS (UA) - RHR (UA) - PWR AFW (UA) HPI (UA) - BWR HPCS/HPCI (UA) RCIC/IC (UA) - Safety system functional failures	- EPS (UR&UA) - AFW-MDP (UR&UA) - AFW-TDP (UR&UA) - HPI (UR&UA) - PORV (UR) - RHR (UR&UA) - SWS (UR&UA) - CCW (UR&UA) - AOV (UR) - MOV (UR) - MDP (UR)	- EPS (UR&UA) - HPCS/HPCI (UR&UA) - RCIC/IC (UR&UA) - RHR (UR&UA) - SWS (UR&UA) - AOV (UR) - MOV (UR) - MDP (UR)	- *Time in High/Medium/Low Risk-Significant Configurations	- *Fire Suppression System (UR&UA)
Barriers	- RCS Specific Activity - RCS Identified Leak Rate	- *CIV (UR&UA)	- *Drywell Spray (MarkI)(UR&UA) - *CIV (Mark III) (UR&UA)	None	None

* Requires data that are not currently reported.

Note: The emergency preparedness, occupational radiation safety, public radiation safety, and physical protection cornerstones of safety are not included in the Phase-1 RBPI scope.

Summary of Planned Follow-on Activities

Follow-on work in the RBPI development program includes support for a proposed pilot program beginning in early 2002 to evaluate potential plant-specific unreliability indicators for the six mitigating systems under the current ROP. The pilot program will also include changes to the current Safety System Unavailability Performance Indicators (SSUPIs), such as inclusion of risk-significant functions versus design-basis functions, resolution of issues related to fault exposure time, credit for simple recovery actions, and the addition of component cooling water (CCW) and service water (SW) support systems.

In addition, performance indicators for containment will be developed; technology of shutdown RBPI methods will be transferred for potential use in the SDP for shutdown modes; and higher-level performance indicators will be developed.

EPRI Strategic Action Plan for Risk Technology

John Gaertner, EPRI
Nuclear Strategic Bridge Plan Project Manager

Jack Haugh, EPRI
Manager of Risk and Reliability

ABSTRACT

EPRI has a strategic plan for Risk Technology R&D with a strong emphasis on support of risk-informed operations and risk-informed regulation. The plan is linked to the *Electricity Technology Roadmap* that identifies opportunities and threats for innovation over the next 25 years and beyond. There is a Nuclear Sector Strategic Bridge Plan with a clear vision and strategic objectives to achieve Roadmap destinations. A strategic action plan has been developed for Nuclear Risk Technology that focuses near-term R&D on these long-term opportunities. EPRI risk technology R&D can support 11 of 17 nuclear strategic objectives. However, the plan identifies 6 significant barriers to success. Five of these barriers inhibit effective use of risk-informed regulations. The plan delineates and critically evaluates all current R&D activities that address these barriers. Most importantly, the plan identifies 5 high priority actions with the greatest potential to break down these barriers. This paper discusses the barriers and high priority actions in detail with emphasis on the impact of these items on risk-informing regulations and operations.

INTRODUCTION

EPRI has a strategic plan for Risk Technology R&D with a strong emphasis on support of risk-informed operations and risk-informed regulation. This paper describes the plan.

The purpose of the Strategic Bridge Plan (SBP) is to evolve the tactical EPRI Nuclear 3-year program plan (see Nuclear Power Program Descriptions, 2002-2005) to support the objectives of the strategic EPRI *Electricity Technology Roadmap* (see EPRI CI-112677, V-1 and V-2) to address mid-term to long-term nuclear industry needs.

The 3-year program plan is large. It is comprised of 25 Targets, multiple Target Solutions within each Target, and specific Solution Elements within each Target Solution. At this time, there are 123 Target Solutions and approximately 500 Solution Elements in the 3-year program plan.

ELECTRICITY TECHNOLOGY ROADMAP

The *Electricity Technology Roadmap* identifies the need to increase nuclear power's value to society and to strengthen the value of R&D investments in EPRI.

The Roadmap is an ongoing collaborative exploration of the opportunities and threats for electricity-based innovation over the next 25 years and beyond. Over 150 organizations have participated with EPRI and its members to shape a comprehensive vision to increase electricity's value to society. This vision is translated into a set of technology development destinations. EPRI will develop R&D pathways to reach these destinations. The SBP is part of the process to identify these pathways.

Early Roadmap destinations are not directly addressed by nuclear power R&D activities. These destinations are, "By 2003, improve power delivery reliability"; and "By 2005, enable customer-managed service networks." The next two destinations are directly addressed by nuclear power R&D activities and are the destinations of the SBP. These destinations are, "By 2010, accelerate economic growth and productivity"; and "By 2015, resolve the energy/carbon conflict." A later destination is also relevant, "By 2025, manage the challenge to global sustainability."

The Roadmap specifically calls for development of certain Limit-Breaking Technologies, including advanced nuclear power and broad use of hydrogen-based fuels, as strategically important to achieving these latter destinations. Considering these destinations naturally leads to two new strategic planning horizons: 5 to 10 years to address mid-term needs for economic growth, and 10 to 20 years to address the long-term challenges of the energy/carbon conflict and global sustainability.

LINKS TO OTHER INDUSTRY STRATEGIC PLANS

In addition to the *Electricity Technology Roadmap*, the SBP Vision and Strategic Objectives have clear links to other industry strategic plans. In particular, the SBP supports the objectives represented in NEI Strategic Directions for the 21st Century. Also, consistency will be sought with strategic objectives of INPO and other industry organizations. Joint planning and resource leveraging with DOE and NRC will help reach industry objectives. EPRI and EDF will collaborate as both organizations undergo parallel strategic planning exercises.

THE VISION

The SBP approach begins with a Vision which is consistent with achieving the Roadmap destinations, but which is more tangible and easier to relate to R&D activities and deliverables. This Vision is consistent with "Vision 2020" of the Nuclear Energy Institute; that is, growth in U. S. nuclear capacity from the current 20% share of nuclear electricity production to a 23% share in 2020. This vision requires current plants to perform well for an extended life and for 50,000 additional megawatts of nuclear generation to be realized through up-rates and the equivalent of 50 new 1000-megawatt plants. The Vision also maintains the current 30% share of generation by emissions-free sources including nuclear, hydroelectric, and other renewable sources.

Clearly, the Vision emphasizes the importance of both existing and new generation. It also calls for expanding an industry that can license, construct, and operate many new plants efficiently and safely, not just one or several, and not as prototypes. Finally, although the Vision is in terms of U. S. needs in the next 20 years, it positions the industry to address diverse global needs and longer-term innovative uses of nuclear power that will surely arise in the long-term time-horizon of the SBP.

STRATEGIC OBJECTIVES

The next step in the approach is the development of Strategic Objectives that support the Vision and will, in total, drive the strategic direction of all nuclear R&D activities. The seventeen high-level Strategic Objectives are intended to completely encompass the EPRI Nuclear Power Sector role in supporting the *Electricity Technology Roadmap* and the other industry objectives:

Safety:
1. Preclude safety event surprises
2. Allay concerns of public safety

Optimal use of existing plants:
3. Achieve maximum plant useful life
4. Improve plant capacity, reliability, and availability
5. Develop technology to address material aging
6. Add cost-effective innovation to existing plants
7. Resolve on-site spent fuel issues

Maximal opportunity for new plants:
8. Evaluate evolutionary and new designs including gas-cooled technology
9. Develop high-utilization fuel cycles to extend resources
10. Resolve technical high level waste issues

Key issues to optimize the nuclear power option:
11. Achieve cost/risk-focused decision-making in regulation, operation, and design
12. Optimize technology transfer and collaboration
13. Employ advances in information technology to design and operations
14. Meet increasing demand for skilled, productive work force
15. Advance the use of high performance fuel
16. Adopt advances in manufacturing and construction technology
17. Provide basis for simplified licensing process

SCENARIO ANALYSIS

Scenario Analysis has been included in the SBP process. The analysis has 4 steps: 1) identify the key external factors that would affect decisions about the future, 2) develop several scenarios that represent potential futures and which include these key factors, 3) evaluate planned R&D in light of each scenario, and 4) continue to use scenarios to answer "What if ..." as the SBP is implemented.

Scenario Analysis is a proven technique to account for the inherent uncertainties in key factors that would affect decisions for the future. Scenarios assist planners to estimate: 1) sensitivity of priorities to externalities, 2) prioritization of activities in light of uncertainties, and 3) R&D gaps relative to likely scenarios. Equally important, scenarios impose a discipline and a consistency in the determination of the strategic importance of an activity.

The strategic content of an activity is first considered in light of the Base Case Scenario. The Base Case Scenario is a reasonable representation of the upcoming five year period, including projections of what are believed to be the key factors in nuclear power's future. Nine factors are specifically considered:

- Nuclear plant performance
- High level waste resolution
- Public perception of nuclear power
- The economy
- Environmental concerns
- Political climate for nuclear growth
- Electricity industry leadership
- Electricity supply infrastructure
- Nuclear industry support organizations
- Regulatory environment

Of course, the Base Case Scenario is not a prediction or an expected future. It is a convention by which we disposition the strategic content of activities and impose structure on our evaluations.

Therefore, it is necessary to consider these same activities in light of alternative scenarios—reasonable variations of the Base Case that would change the strategic content of some activities. The SBP has considered three Alternative Scenarios. An Alternative Scenario can be created at any time to test the sensitivity of activities to perceptions of the future. As a rule, an alternative must be derived from the Base Case and it must be reasonably likely.

MAPPING OF TARGET SOLUTIONS TO STRATEGIC OBJECTIVES

Each Target Solution in the 3-year nuclear program plan was considered for its contribution to addressing each Strategic Objective above. Then, each Target and Target Solution was evaluated as having High, Medium, Low, or no strategic content. This process not only identified the strategic content of the current programs, but it identified "gaps" between current activities and the Strategic Objectives.

The mapping to Strategic Objectives and the Scenario Analysis resulted in 14 Strategic Solution Groups :

1. Material degradation/material aging
2. High performance fuel
3. Radioactive waste and spent fuel management
4. NDE material characterization
5. Plant information management
6. Equipment reliability
7. I&C hardware and systems
8. Asset management/financial risk
9. Safety risk technology and applications
10. New plant design/construction/licensing
11. High level waste repository
12. Workforce knowledge enhancement
13. Assessing/documenting public safety
14. Radiation exposure and effects

NUCLEAR RISK TECHNOLOGY ACTION PLAN

Each Strategic Solution Group will have a "living" Action Plan. The two most significant sections of the Action Plan are 1) Barriers to Strategic Success, and 2) High Priority Actions. Actions are clearly related back to the barriers that they address.

Safety Risk Technology and Applications was one of the first Action Plans to be developed. This strategic technology area directly addresses the following EPRI Nuclear Power Sector Strategic Objectives:

- Preclude safety event surprises
- Achieve cost/risk-focused decision-making in regulation, operation, and design
- Optimize technology transfer and collaboration
- Provide basis for simplified licensing process for new plants

In particular, risk-informing nuclear plant regulations and the corollary, risk-informing nuclear plant operations, is a universal strategic objective of NRC, DOE, and the industry. It is recognized as essential for long-term safe, reliable, and cost-effective operation of current plants. It applies to new plants as well, for all reactor types and power conversion processes.

This strategic technical area indirectly supports the following EPRI Nuclear Power Sector Strategic Objectives; that is, although there is no significant activity directly addressing the objectives there is technology, expertise, opportunity, or secondary benefit:

- Allay concerns of public safety
- Improve plant capacity, reliability, and availability
- Add cost-effective innovation to existing plants
- Resolve on-site spent fuel issues
- Evaluate evolutionary and new reactor designs including gas-cooled technology
- Employ advances in information technology to design and operations
- Provide tools to maintain a skilled, productive work force

BARRIERS TO STRATEGIC SUCCESS

This Action Plan focuses on overcoming significant barriers to successfully achieving the strategic objectives. The following 6 barriers to success have been identified:

1. **Risk assessment tools can yield inconsistent results and decision-makers lack confidence in their accuracy and resolution.** EPRI will evolve and validate PRA and risk assessment tools. These tools include computational software, decision analysis methods, and information management aids. The purpose of these tools should be to improve the accuracy, consistency, and stakeholder acceptance of risk calculations and of risk-informed decisions.

2. **An objective and integrated risk-informed/performance-based decision-making process for risk-informed change at existing plants is lacking.** As a result, many useful and cost-effective changes are not occurring. EPRI will address the technical issues, which are likely to cause objections to cost-effective implementation of such a process. EPRI will also address the related fact that there is a lack of common understanding of the meaning of risk-informed/performance-based concepts. EPRI will interact with NEI and NRC Research. Finally EPRI will continue to support the development and implementation of applications such as Risk-informed In-service Inspection (ISI).

3. **An effective risk management culture does not generally exist in the industry that is strong enough to support widespread risk-informed/performance-based regulation and operations.** EPRI will continue to develop the risk management process and tools (both configuration control and performance monitoring) that plants must employ to support risk-informed and performance-based regulations and operations. The primary emphasis will remain public safety risk; but integration of other financial and performance risk into the decision-making process will be pursued. EPRI will achieve a broader perspective on risk management by evaluating processes and tools in other industries.

4. **A robust, risk-informed regulatory, design, and operating framework does not exist for new plants.** EPRI will significantly contribute to the development and implementation of an objective and integrated framework for new plant regulations, design, and operations that takes full advantage of risk-informed/performance-based decision-making.

5. **EPRI's own program and project planning process does not consider risk/benefits in a consistent and objective way.** As appropriate, EPRI will incorporate risk-informed decision-making into the planning and evaluation of all EPRI nuclear targets. This barrier has two components with distinct solutions. First, EPRI will ensure that projects are appropriately balanced on the issues of public safety and burden reduction to facilitate risk-informed regulation and operation. Second, EPRI will ensure that projects have a business plan to yield the highest practical benefit-to-cost with consideration of risk.

6. **The risk of nuclear power is not objectively and understandably assessed and communicated to stakeholders and the public.** EPRI will develop a comprehensive and continuing assessment capability, knowledge, and effective communication of nuclear plant risk.

SUMMARY OF CURRENT ACTIVITIES RELATIVE TO THE BARRIERS

Strategic planned or ongoing activities overcoming Barrier 1:

- Integration of best-estimate thermal-hydraulics codes and development of models for use in PRAs
- Resolving generic accuracy and consistency issues with at-power PRAs
- Development of ePSA, an information management tool to document the PSA and its applications and to promote efficiency among plants.

Non-strategic planned or ongoing activities overcoming Barrier 1:

- Support of the ASME PRA Standard and the ANS Standard for external events and shutdown risk
- Other activities within the Risk and Reliability Workstation complementary to the strategic items above
- Development of a loss of offsite power risk assessment and management tool for use by nuclear plant operations
- Continuing updates of grid reliability and loss of offsite power frequencies for U.S. nuclear plants
- Collaboration with NRC/RES on probabilistic risk assessment of storage of spent fuel in dry casks
- Development of LPSD human error models and data for use in risk assessment
- Investigating the response of steam generators during severe accidents to address NRC issues related to containment effectiveness
- Support of NEI efforts to resolve spent fuel storage pool issues for decommissioned plants.

Strategic planned or ongoing activities overcoming Barrier 2:

- EPRI participation in industry regulatory initiatives, as appropriate, to justify removing unnecessary conservatism and burdensome technical requirements from risk-informed regulations.

Non-strategic planned or ongoing activities overcoming Barrier 2:

- Application and developments of risk-informed ISI
- Option 2 support for Guidelines development, seismic, EQ and procurement issues.

Strategic planned or ongoing activities overcoming Barrier 3:

- Activities which enable the day-to-day application of configuration risk management in operations, work planning and control, and maintenance
- RIISMS for Risk-informed Tech Specs
- The seismic Risk-informed/Performance-based project
- Fire PRA Re-quantification project.

Non-strategic planned or ongoing activities overcoming Barrier 3:

- Maintenance Rule Users Group (MRUG) activities.

Strategic planned or ongoing activities overcoming Barrier 4:

- Technical participation on industry efforts for new plant regulatory framework.

Strategic planned or ongoing activities overcoming Barrier 5:

- Sustainable Business Initiative commitment to EPRI sponsors which requires all nuclear programs to be risk-informed by 2003.

Strategic planned or ongoing activities overcoming Barrier 6:

- White Paper on the concept of safety risk and the benefits of PRA to the nuclear industry
- Support on defining PRA information submittals to NRC.

High Priority Actions

The preceding section identifies the current activities that are related to the important barriers identified earlier. A critical evaluation of these activities helps identify "gaps" and "opportunities" which will be the focus of overcoming these barriers. EPRI has identified five High Priority Actions in this regard. These actions will be aggressively pursued, monitored, and periodically re-evaluated to assure progress along the strategic path.

These High Priority Actions are:

1. Aggressively pursue funding for integration of best-estimate thermal-hydraulics codes for 2002. Seek cooperation with NRC RES for incorporation of advanced elements into PRA models and calculations. Emphasize enhanced realism and resolution from available computer power. Emphasize the user interface to bring analysis capability to the end-user, who may be an individual other than the engineering analyst. (Addresses Barrier 1.)

2. Define a supplemental collaborative project to build the ePSA product and begin work in 2002. Pursue opportunities with Owners Groups in 2002 and NRC RES to identify projects to seek PRA consistency in key areas identified in this strategic area. (Addresses Barrier 1.)

3. Aggressively pursue funding for the Risk Management Overlay project for 2002. The project will create a conceptual model of a nuclear plant risk management program. The model will identify important functions, processes, and their relationships; and it will be general enough to accommodate a variety of specific tools and methods. It will map the risk management processes at one or two plants onto the conceptual model to produce a "Risk Management Overlay". The result will enable owner/operators to evaluate the effectiveness of their risk management processes, and define enhancements. Opportunities for generic products to improve risk management will be pursued by EPRI. The results will also communicate the power of risk management to facilitate a change to a risk-informed and performance-based safety culture.

   The project will emphasize the importance of performance monitoring. It will coordinate with the Equipment Reliability Action Plan to be certain that this barrier to strategic success is factored into that plan. (Addresses Barrier 3.)

4. Propose a crosscutting team effort to develop an applicable approach to incorporate risk-informed decision-making into the planning and evaluation of all EPRI nuclear targets. Strive for a method transferable to R&D projects in other industries and technologies. (Addresses Barrier 5.)

5. Aggressively pursue the communication of risk concepts and their successful applications to all stakeholders in the pursuit of risk-informed regulations. Begin dialog with NRC RES and NEI on technical issues associated with the risk-informed Option 3 effort and associated with costly or failed risk-informed efforts in the industry. Continue communication until there is a common and appropriate understanding of these issues among stakeholders. (Addresses Barrier 6.)

Conclusions

- EPRI has a strategic plan for Risk Technology R&D with a strong emphasis on support of risk-informed operations and risk-informed regulation.

- The EPRI Nuclear Sector Strategic Bridge Plan process is designed to identify and achieve a well-defined set of industry strategic objectives.

- Specifically, High Priority Actions have been identified to achieve strategic progress using Risk Technology. This Action Plan has strong support among all EPRI stakeholders – sponsors, management, and technical staff.

- EPRI will bring to bear many funding sources and collaboration opportunities to increase the likelihood that these High Priority Actions are successful.

- All of these High Priority Actions would support risk-informed plant operations and risk-informed regulations.

NRC FORM 335
(2-89)
NRCM 1102,
3201, 3202

U.S. NUCLEAR REGULATORY COMMISSION

BIBLIOGRAPHIC DATA SHEET

(See instructions on the reverse)

1. REPORT NUMBER
(Assigned by NRC, Add Vol., Supp., Rev., and Addendum Numbers, if any.)

NUREG/CP- 0176

2. TITLE AND SUBTITLE

Proceedings of the Nuclear Safety Research Conference

3. DATE REPORT PUBLISHED

MONTH	YEAR
May	2002

4. FIN OR GRANT NUMBER

A3988

5. AUTHOR(S)

Conference Papers by various authors;
Compiled by Susan Monteleone, BNL

6. TYPE OF REPORT

7. PERIOD COVERED *(Inclusive Dates)*

October 22-24, 2001

8. PERFORMING ORGANIZATION - NAME AND ADDRESS *(if NRC, provide Division, Office or Region, U.S. Nuclear Regulatory Commission, and mailing address; if contractor, provide name and mailing address.)*

Office of Nuclear Regulatory Research
U.S. Nuclear Regulatory Commission
Washington, DC 20555-0001

9. SPONSORING ORGANIZATION - NAME AND ADDRESS *(if NRC, type "Same as above"; if contractor, provide NRC Division, Office or Region, U.S. Nuclear Regulatory Commission, and mailing address.)*

Same as Item 8 above.

10. SUPPLEMENTARY NOTES

S. Nesmith, NRC Project Manager; Proceedings prepared by Brookhaven National Laboratory

11. ABSTRACT *(200 words or less)*

This contains papers and presentations on reactor safety research made at the Nuclear Safety Research Conference (formerly known as the Water Reactor Safety Information Meeting) held at the Marriott at Metro Center Hotel, Washington, DC, October 22-24, 2001. The papers describe the programs and results of nuclear safety research sponsored by the Office of Nuclear Regulatory Research, U.S. NRC. Also included are invited papers concerning nuclear safety issues from U.S. government laboratories, the electric utilities, the nuclear industry, and from foreign governments and industry.

12 KEY WORDS/DESCRIPTORS *(List words or phrases that will assist researchers in locating the report.)*

reactor safety research
nuclear safety research

13. AVAILABILITY STATEMENT

Unlimited

14. SECURITY CLASSIFICATION

(This Page)
Unclassified

(This Report)
Unclassified

15. NUMBER OF PAGES

16. PRICE

NRC FORM 335 (2-89)

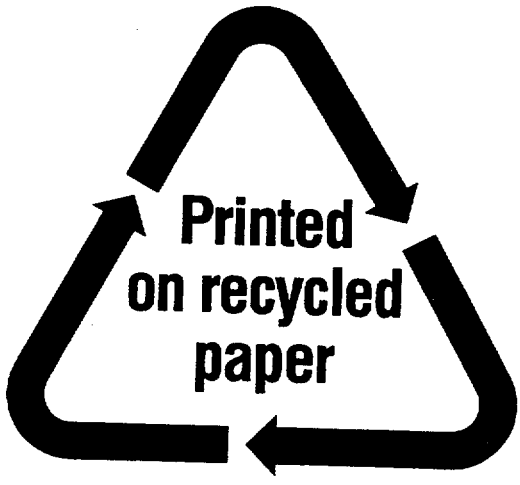

Federal Recycling Program

UNITED STATES
NUCLEAR REGULATORY COMMISSION
WASHINGTON, DC 20555-0001